

UNESCO-IHE DELFT LECTURE NOTE SERIES

A New Approach to Sediment Transport in the Design and Operation of Irrigation Canals



Herman Depeweg
Néstor Méndez V

A NEW APPROACH TO SEDIMENT TRANSPORT IN THE DESIGN
AND OPERATION OF IRRIGATION CANALS

UNESCO-IHE LECTURE NOTE SERIES



BALKEMA – Proceedings and Monographs
in Engineering, Water and Earth Sciences

A New Approach to Sediment Transport in the Design and Operation of Irrigation Canals

HERMAN DEPEWEG

UNESCO-IHE, Delft, The Netherlands

NÉSTOR MÉNDEZ V

Universidad Centro Occidental "Lisandro Alvarado", Barquisimeto, Venezuela



Taylor & Francis

Taylor & Francis Group

LONDON / LEIDEN / NEW YORK / PHILADELPHIA / SINGAPORE

Taylor & Francis is an imprint of the Taylor & Francis Group, an informa business

© 2007 Taylor & Francis Group, London, UK

This edition published in the Taylor & Francis e-Library, 2007.

“To purchase your own copy of this or any of Taylor & Francis or Routledge’s collection of thousands of eBooks please go to www.eBookstore.tandf.co.uk.”

All rights reserved. No part of this publication or the information contained herein may be reproduced, stored in a retrieval system, or transmitted in any form or by any means, electronic, mechanical, by photocopying, recording or otherwise, without written prior permission from the publishers.

Although all care is taken to ensure integrity and the quality of this publication and the information herein, no responsibility is assumed by the publishers nor the author for any damage to the property or persons as a result of operation or use of this publication and/or the information contained herein.

Published by: Taylor & Francis/Balkema
P.O. Box 447, 2300 AK Leiden, The Netherlands
e-mail: Pub.NL@tandf.co.uk
www.balkema.nl, www.taylorandfrancis.co.uk, www.crcpress.com

British Library Cataloguing in Publication Data

A catalogue record for this book is available from the British Library

Library of Congress Cataloging-in-Publication Data

Depeweg, Herman.

A new approach to sediment transport in the design and operation of irrigation canals / Herman Depeweg, Néstor Méndez V.

p. cm.—(UNESCO-IHE lecture note series)

Includes bibliographical references.

ISBN 978-0-415-42693-0 (hardcover : alk. paper) 1. Sediment transport.
2. Irrigation canals and flumes—Design and construction. I. Méndez V., Néstor J., 1954— II. Title.

TC175.2.D47 2007

551.3'53—dc22

2006034650

ISBN 0-203-94581-6 Master e-book ISBN

ISBN13 978-0-415-42693-0 (hardback)

ISBN13 978-0-415-43065-4 (paperback)

ISBN13 978-0-203-94581-0 (e-book)

Table of Contents

LIST OF FIGURES	VIII
LIST OF TABLES	XI
1 INTRODUCTION	1
2 OPEN CHANNEL FLOW	9
2.1 Introduction	9
2.2 Flow types and characteristics	9
2.3 Geometry	14
2.4 Basic hydraulic principles	15
2.5 Velocity distribution	20
2.6 Uniform flow	24
2.7 Non-uniform steady flow	27
2.8 Some general aspects of unsteady flow	32
2.9 Basic differential equations for gradually varied unsteady flow	34
2.10 Solution of the de St. Venant equations	38
2.11 Rectangular channels and the method of characteristics	39
3 SEDIMENT PROPERTIES	49
3.1 Introduction	49
3.2 Density and porosity	49
3.3 Size and size distribution	50
3.4 Shape	53
3.5 Fall velocity	53
3.6 Characteristic dimensionless parameters	56
4 DESIGN CRITERIA FOR IRRIGATION CANALS	59
4.1 Introduction	59
4.2 The role of sediment transport in the design of irrigation canals	60
4.2.1 Regime method	62
4.2.2 Tractive force method	64
4.2.3 Permissible velocity method	68
4.2.4 Rational method	68
4.3 Final comments	71

5	SEDIMENT TRANSPORT CONCEPTS	73
5.1	Introduction	73
5.2	Friction factor predictors	77
5.2.1	Bed form development	78
5.2.2	Effect of bed forms on the flow resistance	82
5.2.3	Determination of the friction factor	84
5.2.4	Composite roughness for non-wide irrigation canals	85
5.2.5	A recommended method for the prediction of composite roughness in trapezoidal canals	90
5.2.6	Comparison of the composite roughness predictors in a trapezoidal canal	92
5.2.7	Prediction of composite roughness in a rectangular canal	95
5.3	Governing equations for sediment transport	98
5.3.1	Sediment transport capacity	103
5.3.2	Comparison of sediment transport capacity	103
5.3.3	Sediment transport computation in non-wide canals	105
5.3.4	Comparison of the procedures for computing the total sediment transport	109
5.3.5	Sediment transport in non-equilibrium conditions	112
5.4	Morphological changes of the bottom level	116
5.5	Conclusions	121
6	SETRIC, A MATHEMATICAL MODEL FOR SEDIMENT TRANSPORT IN IRRIGATION CANALS	123
6.1	Introduction	123
6.2	Water flow equations	123
6.3	Sediment transport equations	124
6.4	General description of the mathematical model	126
6.5	Input and output data	130
6.6	Conclusions	131
7	THE SEDIMENT TRANSPORT MODEL SETRIC AND ITS APPLICATIONS	133
7.1	Introduction	133
7.2	Case 1 – Changes in the discharges	135
7.3	Case 2 – Changes in the incoming sediment load	137
7.4	Case 3 – Controlled sediment deposition	138
7.5	Case 4 – Flow control structures	143
7.6	Case 5 – Operation activities	145
7.7	Conclusions	154
	REFERENCES	155
	SYMBOLS	163

APPENDIX A	METHODS TO ESTIMATE THE TOTAL SEDIMENT TRANSPORT CAPACITY IN IRRIGATION CANALS	169
	A.1 Introduction	169
	A.2 Ackers and White method	170
	A.3 Brownlie method	171
	A.4 Engelund and Hansen method	172
	A.5 Van Rijn method	173
	A.6 Yang method	175
APPENDIX B	METHODS TO PREDICT THE FRICTION FACTOR	177
	B.1 Van Rijn	177
	B.2 Brownlie	182
	B.3 White, Paris and Bettess	182
	B.4 Engelund	183
APPENDIX C	HYDRAULIC DESIGN OF IRRIGATION CANALS	185
	C.1 Introduction	185
	C.2 Alignment of an irrigation canal	186
	C.3 Water levels	187
	C.4 Earthwork	188
	C.5 Design of irrigation canals	189
	C.6 Boundary shear stresses	194
	C.7 Sediment transport criteria	196
	C.8 Transport of the bed material	196
	C.9 Final remarks	197
	C.10 Computer aided design of canals	198
APPENDIX D	DESCRIPTION OF THE MAIN ASPECTS OF THE REGIME THEORY	201
	D.1 Some regime considerations	204
	D.1.1 Sediments	204
	D.1.2 Maturing of canals	204
	D.1.3 Slope adjustments	205
	D.1.4 Diversion of the sediment	205
	D.1.5 Maintenance aspects	206
	D.1.6 Flow capacity	206
	D.1.7 Design considerations	206
APPENDIX E	GLOSSARY RELATED TO SEDIMENT TRANSPORT	209
INDEX		223

List of Figures

Figure 1.1	Classification of sediment transport.	5
Figure 2.1	Classification of flow types.	10
Figure 2.2	Steady and unsteady, uniform flow.	11
Figure 2.3	Unsteady, gradually and rapidly varied flow.	11
Figure 2.4	Examples of gradually and rapidly varied flow (steady conditions).	12
Figure 2.5	Main characteristics of a canal.	15
Figure 2.6	Specific energy as function of the water depth y .	19
Figure 2.7	Distribution of the velocity in a rectangular channel.	21
Figure 2.8	Hydraulically rough and hydraulically smooth boundary layers.	22
Figure 2.9	Tractive force and the distribution of the shear stress in a trapezoidal channel.	25
Figure 2.10	Values of the de Chézy coefficient C as function of the hydraulic radius R , the wall roughness k and the thickness of the laminar sub-layer δ .	26
Figure 2.11	Energy considerations in a channel with unsteady flow.	27
Figure 2.12	Summary of water surface profiles in wide canals ($R = y$ and $q = Q/B$).	30
Figure 2.13	Overview of the most common water surface profiles in wide canals.	31
Figure 2.14	An unsteady flow presented in the x , t and y direction.	34
Figure 2.15	Method of characteristics in the x and t plane, with an explicit solution.	42
Figure 2.16	Characteristics in the x and t plane with an example of the domain of influence and of the domain of dependence.	44
Figure 3.1	Example of particle size distributions.	52
Figure 4.1	Example of a canal with downstream control and a canal with upstream control.	60
Figure 5.1	Hydro-dynamic performance of an irrigation canal with the intended and actual flow at the cross-sections 1 and 2.	75
Figure 5.2	Hydrographs in an irrigation canal: (a) typical, (b) schematised.	76
Figure 5.3	Schematic representation of bed forms for the low flow regime.	78
Figure 5.4	Comparison of theories for predicting bed forms for lower flow regimes.	80
Figure 5.5	Classification of bed forms according to van Rijn (1984c) and expected bed forms in irrigation canals.	82
Figure 5.6	Total shear stress due to skin resistance and bed forms as a function of the mean velocity (Jansen, 1994).	84
Figure 5.7	Accuracy of the methods to predict the friction factor for different error factors f .	86
Figure 5.8	Composite roughness in a trapezoidal canal.	87
Figure 5.9	Comparison of predicted values for various error factors by using the WUR data.	93
Figure 5.10	Comparison of the results of the five prediction methods for composite roughness with the measured WUR data at an error factor of 1.15.	94

Figure 5.11	Comparison of predicted values for various error factors by using the Krüger data.	95
Figure 5.12	Comparison of the results of the five prediction methods for composite roughness with the measured Krüger data at an error factor of 1.15.	96
Figure 5.13	Non-wide rectangular canal schematised as a wide canal.	97
Figure 5.14	Accuracy for several error factors and the predictability at an error factor of 1.075 of the prediction method for composite roughness in rectangular canals.	98
Figure 5.15	Shields' diagram for initiation of motion (after van Rijn, 1993).	101
Figure 5.16	Initiation of motion, initiation of suspension and values of shear stress commonly used in irrigation canals as function of D_* .	102
Figure 5.17	Range of accuracy of the sediment transport predictors for different error factors.	104
Figure 5.18	Schematization of stream tubes in a trapezoidal cross section.	106
Figure 5.19	Velocity distribution in a non-wide canal.	106
Figure 5.20	Velocity distribution in a non-wide trapezoidal canal.	107
Figure 5.21	Relationship between the correction factor α and the exponent N .	109
Figure 5.22	Comparison of procedures to compute sediment transport in non-wide canals.	111
Figure 5.23	Schematization of the 2-D suspended sediment transport model.	113
Figure 5.24	Schematization of a depth-integrated model.	114
Figure 5.25	Schematization of computations of changes on the bottom level.	117
Figure 5.26	Calculation of the change in the bottom level using the modified Lax method.	119
Figure 5.27	Sediment transport for uniform flow.	119
Figure 5.28	Sediment transport for gradually varied flow (backwater effect).	120
Figure 5.29	Sediment transport for gradually varied flow (drawdown effect).	120
Figure 6.1	Flow diagram of SETRIC for calculating the water flow, sediment transport and changes in bottom level in main and/or lateral canals (after Paudel, 2002).	127
Figure 6.2	Flow diagram for SETRIC for calculating the water flow in main and lateral canals during a time step (after Paudel, 2002).	128
Figure 6.3	Flow diagram of SETRIC for calculating the sediment transport in the main canal and lateral canals during a time step.	129
Figure 7.1	Equilibrium and actual concentration at the beginning and at the end of the simulation for a relative discharge of 0.74 and 0.88.	136
Figure 7.2	Sediment deposition and relative sediment deposition along the irrigation canal at the end of the simulation period as a function of the relative discharge.	137
Figure 7.3	Total sediment deposition and relative sediment deposition after 90 days as a function of the variation in the relative sediment load.	139
Figure 7.4	Total sediment deposition and relative sediment deposition after 90 days as a function of the variation in relative median sediment size.	140
Figure 7.5	Relative sediment deposition of the two scenarios for controlling the sediment deposition.	141
Figure 7.6	Sediment transport and sediment deposition in an irrigation canal with controlled deposition (a deepening of 0.50 m of the bottom over the first 1000 m of the canal).	142
Figure 7.7	Sediment transport and sediment deposition in an irrigation canal with controlled deposition (by widening the bottom width over the first 1000 m of the canal).	142

Figure 7.8	Total sediment deposition and relative sediment deposition for the two types of flow control structures.	144
Figure 7.9	Comparison of changes in bottom level for the two types of flow control structures.	145
Figure 7.10	Schematization of an irrigation system and longitudinal profile of the main canal.	146
Figure 7.11	Equilibrium and actual concentration at the end of the irrigation periods 1, 2 and 3 and variation of the bottom level at the end of the simulation (continuous flow).	148
Figure 7.12	Equilibrium and actual concentration at the end of the irrigation periods 1, 2 and 3 during the first turn of irrigation (rotational flow by hour).	149
Figure 7.13	Variation of the equilibrium and actual concentration at the end of each irrigation period during the second turn of irrigation (rotational flow by hour).	149
Figure 7.14	Variation of the bottom level during the simulation period (rotational flow by hour).	150
Figure 7.15	Equilibrium and actual concentration at the end of the irrigation periods 1, 2 and 3 and variation of the bottom level at the end of the simulation period (rotational flow by day).	151
Figure 7.16	Equilibrium and actual concentration at the end of the irrigation periods 1, 2 and 3 and variation of the bottom level at the end of the simulation (rotational flow by week).	152
Figure 7.17	Relative sediment deposition in the reaches and the irrigation canal when compared with the sediment deposition observed in Scenario 1 (continuous flow).	153
Figure B.1	Hydraulic regimes in irrigation canals.	181
Figure C.1	Recommended k_s values for unlined irrigation canals as function of the water depth y for various maintenance conditions.	191
Figure D.1	Example of the design of an earthen canal according to the Lacey method for $m = 2$ and $d = 0.4$ mm.	204
Figure D.2	Example of the design of an earthen canal according to the Lacey method for $m = 2$ and $d = 0.15$ mm.	204

List of Tables

Table 1.1	Characteristics of water flow and sediment transport in rivers and irrigation canals.	4
Table 2.1	Kinematic viscosity of water as a function of the temperature T .	13
Table 2.2	Flow type as a function of the actual water depth.	20
Table 2.3	Type of bottom slope.	28
Table 2.4	Flow types based on the energy line, bottom slope and Froude number.	28
Table 2.5	Summary of water surface profiles.	29
Table 2.6	Summary of the methods for computing gradually varied flow.	32
Table 2.7	Summary of the methods to solve the de St. Venant equations.	39
Table 3.1	The density of fresh water as a function of the temperature T .	51
Table 3.2	Classification of sediment according to their size.	51
Table 3.3	Fall velocity for sediment particles.	55
Table 3.4	Coefficient γ as function of Reynolds number.	55
Table 4.1	Example of the design of earthen canals for two sediment diameters according to the Lacey method.	64
Table 4.2	Recommended critical shear stress (N/m^2) for fine, non-cohesive sediment (Dahmen, 1994).	66
Table 4.3	Limiting boundary shear stress (N/m^2) in cohesive material.	66
Table 4.4	Reduction of the limiting boundary shear stresses in non-straight canals.	66
Table 4.5	Recommended side slope (m) in canals.	67
Table 4.6	Maximum permissible velocity (v) and the corresponding tractive-force value (τ).	68
Table 5.1	Classification parameter used in bed form theories.	79
Table 5.2	D_* parameter for sediment sizes encountered in irrigation canals.	81
Table 5.3	Classification of bed forms according to van Rijn (1984c).	81
Table 5.4	Values of a_i and b_i for $z_a/h = 0.01$ (after Galappatti, 1983).	115
Table 7.1	Geometrical characteristics of main irrigation canal.	146
Table 7.2	Water needs during the irrigation season of the irrigated area.	147
Table B.1	Hydraulic regime types.	178
Table B.2	u_*k_s/ν parameter for plane bed (no motion).	178
Table B.3	u_*k_s/ν parameter for ripples.	180
Table C.1	Smoothness factors as function of maintenance conditions (for earthen canals).	190
Table C.2	Side slopes in canals.	191
Table C.3	Recommended critical boundary shear stress (N/m^2).	195
Table C.4	Reduction of the boundary shear stresses in non-straight canals.	195
Table D.1	Example of the design of earthen canals for two sediment diameters and two side slopes according to the Lacey method.	203

CHAPTER 1

Introduction

The transport of sediment in irrigation canals influences to a great extent the sustainability of an irrigation and drainage system. Unintentional or unwanted erosion or deposition of sediment in canals will not only increase the maintenance costs, but also leads to an unfair and inadequate distribution of irrigation water. Proper knowledge of the behaviour and transport of sediment in these canals will help to plan efficient and reliable water delivery schedules to supply water at the required levels; to have a controlled deposition of sediments, to estimate and arrange the required maintenance activities, and to determine the type of desilting facilities and their efficiency, etc.

The study of sediment transport in irrigation canals is mainly focused on the sediment and erosion processes in canal networks. In view of maintenance activities the head works should be designed in such a way that they prevent or limit the entrance of sediment into canals. In addition, the design of the canal system should be based upon the transport of all the sediment to the fields or to specific places in the canal system, where the deposited sediment can be removed at minimum cost. Sedimentation should be prevented in canals and near structures, as it will hamper and endanger a correct irrigation management, the main objectives of which are to deliver irrigation water in an adequate, reliable, fair and efficient way to all the farmers at the required water level. Inadequate management will result in low efficiency, unnecessary loss of the already scarce water and low yields.

Irrigation canals are usually designed upon the assumption that the water flow is uniform and steady and that the canals are able to carry the water and sediments to the fields. The design supposes that an equilibrium situation exists where the sediments and water entering into the irrigation network will be transported to the fields without deposition or erosion. However, a perfectly uniform and steady flow is seldom found. In the operation of irrigation systems the flow is predominantly non-uniform, with varying discharges and with a constant water level at the regulation points where the water is supplied to the offtakes. The sediment transport capacity of the canals greatly depends on the flow conditions and is variable. Although the water flow can be modelled with a high degree

of accuracy, sediment transport is only understood to a limited extent. The predictability of sediment transport equations and models in view of the quantity of sediment that needs to be removed is still rather poor. Computations of the effects of the non-equilibrium flow conditions on sediment transport are required to determine whether deposition and/or entrainment will occur and to assess the amount and distribution of the sediment deposition and/or entrainment along the canals. Mathematical modelling of sediment transport offers the possibility of estimating the distribution of sediment deposition or entrainment rates for a particular flow and a specific situation.

The main criterion for a canal design is the need to convey different amounts of water at a fixed level during the irrigation season in such a way that the irrigation requirements are met. Furthermore, the design must be compatible with the sediment load of a particular location in order to avoid silting and/or scouring of the canal. The water supply should meet the irrigation requirements and at the same time it should result in the least possible deposition in and/or scouring of the canals. The design process becomes more complicated when canals are unlined and pass through alluvial soils.

The problems of design and maintenance of stable channels in alluvial soils are fundamental to all irrigation schemes (Raudkivi, 1993). Stable or regime canals present ideal conditions for non-scouring and non-silting throughout the irrigation network after one or several seasons of operation. The search for the main characteristics of stable channels started with the work of Kennedy between 1890 and 1894 (Mohammad, 1997). Subsequently, different theories have been developed and are used around the world. All of them assume uniform and steady flow conditions and try to find those canal dimensions that are stable for a given discharge and sediment load.

In the past the irrigation canals used to be designed for protective irrigation, where the government or an irrigation authority ran and maintained the system. The available water was spread over as large an area as possible. The canals carried an almost constant discharge without significant control structures and to some extent the assumption of a uniform and steady flow was realised. In these situations a prediction of the behaviour of the sediment in the canal could be made with some reliability. The growing need for reducing the continually increasing governmental investments in irrigation demand a more economical system, so that the farmers can pay for the operational and maintenance costs with the return that they get from irrigated agriculture. In addition, farmers would like to have a more reliable and flexible water delivery. Flexibility in the delivery system demands more frequent regulation of the water flow, which will create unsteadiness in the flow. This unsteadiness will make all the assumptions made in the original design imprecise and reduces the accuracy of the already poor sediment transport predictors.

Generally three methods for the design of irrigation canals are used: namely Lacey's regime method and the tractive force method for large irrigation schemes, and the permissible velocity method for irrigation systems in hilly areas. Sediment characteristics and coefficients are either simply borrowed from literature or chosen based on the experience of the designer. Hence, there exists a large difference in the design parameters from scheme to scheme and even from canal to canal within the same scheme. Without incentives or obligations for any verification, most designers do not investigate and evaluate the performance of their design in the field.

At the moment, the improvement of the performance of existing schemes is more pressing than the development of new irrigation systems, especially in view of the high investment costs required for the construction and operation of new systems. Appropriate management of sediment in canal networks is one of the major challenges of the improvement works, as a major part of the available maintenance budgets is spent annually on the removal of the sediment deposited. This type of schemes imposes extra conditions on the designer as the canal slope, bed width, structure control, and management practices already exist and in most cases they cannot be changed due to economic resources and/or social considerations. Hence, the selection of an appropriate design philosophy and its applicability for these particular conditions is very important.

The design of irrigation canals is not as simple as normally perceived. It is the final product of a merge of complex and undetermined parameters such as water flows, sediment load, structure control and operation, and management strategies. No design packages are available that deal with all the parameters at the same time. To simplify the design process some parameters are either disregarded or assumed to be constant, which consequently will lead to a less adequate design. Many failures and problems are caused by a design approach that pays insufficient attention to the operational aspects (FAO, 2003). Considering the aforementioned parameters involved in the canal design and their importance in view of the sustainability of the system, a numerical modelling may be one option that can simultaneously simulate all the variables. However, the selection of a model to represent the system and its validity in the proposed environment will have a major influence on the results.

Developments in the knowledge of sediment transport in open canals have mainly been derived from natural channels such as rivers. So far sediment transport theories, the development of bed forms, resistance factors, etc. have been developed under assumptions applicable to the particular conditions encountered in rivers. Even though certain similarities between rivers and irrigation canals exist, the sediment concepts are not entirely applicable to irrigation canals. Most of these irrigation canals are man-made and the irrigation environment presents a number of typical problems that are rarely encountered in rivers. The need to control water

levels and discharges in the upstream and/or downstream direction, the necessity to find an optimal cross section and the large influence of the side banks on the velocity distribution normal to the flow direction create some of the main differences in both kinds of channels. Other differences are the presence of a large number of flow control structures, the occurrence of submerged gate flow, the distinct flow characteristics of inverted siphons and their multiple flow paths. Table 1.1 shows some of the main differences between rivers and irrigation canals.

Irrigation canals are different from natural rivers in terms of hydraulics and sediment characteristics. The computational environment for the modelling of water flows in irrigation canals with sediment transport is much more demanding than for river flows due to the extreme variability and unsteadiness of the flow, the presence of numerous hydraulic structures, dynamic gate movements and pump operations, and the existing topographical complexity. The methods to design stable canals are only useful in very specific flow conditions. For large changes in discharge and sediment inputs they are inadequate to describe the sediment transport

Table 1.1 Characteristics of water flow and sediment transport in rivers and irrigation canals.

Water flow and sediment transport		
Characteristics	Rivers	Irrigation canals
Main function	Conveyance of water and sediment	Diversion, conveyance and distribution of water for agriculture
Discharge	Not controlled; increasing in downstream direction	Controlled by operation rules; Decreasing in downstream direction
Alignment	Rarely straight, bends, sinusoidal meanders and braids	Straight, wide bends
Topology	Convergent	Divergent
Flow control	(Almost) no control structures	Several flow control structures for water level and discharge
Water profiles	Generally without water level control: nearly steady flow	Water level control: gradually varied flow and unsteady flow
Velocity distribution	Nearly uniform velocity distribution in lateral direction	Distribution greatly affected by side walls and side slope
Froude number	Wide range	Restricted by the operation of flow control structures ($Fr < 0.4$)
Width (B)/depth (h)	$B/h > 15$ (wide canals)	$B/h < 7-8$
Lining	Alluvial river bed	Man-made canals: lined or unlined
Sediment concentration	Wide range	Controlled at head works
Sediment size	Wide range of sediment size	Fine sediment
Size distribution	Graded sediment	Nearly uniform distribution
Sediment material	River bed	External sources
Sediment transportation	Suspended and bed load	Mainly suspended load
Bed forms	Mostly dunes	Mostly ripples and mega-ripples
Roughness	Skin and form friction	Form friction

process. Under such conditions the process of sediment transport can best be described by numerical modelling.

Irrigation canals form a complicated hydraulic system as they have to handle the motion of water and sediment as well as the mutual interaction of both motions. The sediment transported by the flowing water causes changes in the bed and sides of the canals and those changes will also influence the water movement. Hence, sediment transport and water flow are interrelated. However, the time scales of the flow of water and the sediment transport are different in canals and therefore, the two processes will be discussed separately to specify their particular properties and characteristics.

The objective of these lecture notes is a description of the sediment transport concepts in irrigation canals and, therefore, only those hydraulic aspects necessary for a better understanding of the sediment transport will be discussed in Chapter 2. This chapter will present a synopsis of the main hydraulic principles in open channels together with a short description of the dimensionless numbers used in the sediment concepts and a classification of flow types including uniform and non-uniform flow theories.

Before discussing the concepts of sediment transport the main properties of sediment will be given. Sediments are fragmented material formed by the physical and chemical disintegration of rocks and they can be divided into cohesive and non-cohesive sediments. Non-cohesive sediments do not have physical-chemical interaction and their size and weight are important in view of their behaviour. The total sediment transport in rivers and canals can be divided in suspended load and bed load (see Figure 1.1).

Chapter 3 will present the main characteristics of sediments including density and porosity; particle size and size distribution; shape and fall velocity and the main dimensionless parameters used in the sediment transport theories.

Dahmen (1994) pointed out that an irrigation network should be designed and operated in such a way that the required flow passes at the design water level; no erosion of the canal bottom and banks occurs and no deposition of sediment in the canal takes place. The design of a canal

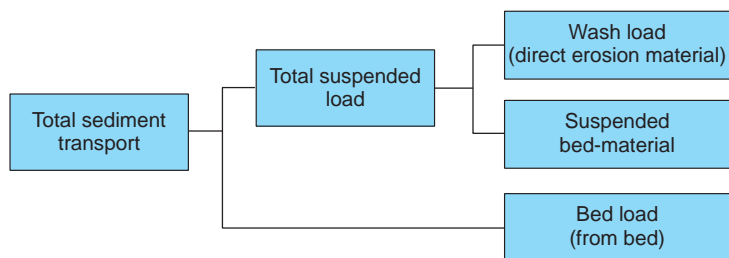


Figure 1.1. Classification of sediment transport.

requires a set of equations related to the water-sediment flow to provide the unknown variables of the bottom slope and cross section. The geometry of an irrigation canal that carries water and sediment will be the end result of a design process in which the flow of water and the transport of sediments interact. Chapter 4 outlines the main aspects of various design methods of irrigation canals.

Mendez (1998) developed the SETRIC model to improve the understanding of sediment transport in irrigation canals under changing flow conditions, sediment load and roughness conditions and for various operation and maintenance scenarios. SETRIC is a one-dimensional model, where the water flow in the canal has been schematised as quasi-steady and gradually varied. The one-dimensional flow equation is solved by the predictor-corrector method and Galappatti's (1983) depth integrated model has been used to predict the actual sediment concentration at any point under non-equilibrium conditions. Galappatti's model is based on the 2-D convection-diffusion equation. The mass balance equation for the total sediment transport is solved by Lax's modified method, assuming steady conditions for the sediment concentration. The model including the various calculation steps are presented in Chapter 6. For the prediction of the equilibrium concentration four predictors have been evaluated and the model uses the Brownlie, Engelund-Hansen, Ackers-White and Modified Ackers-White methods. These sediment transport concepts are extensively discussed in Chapter 5.

The SETRIC model can be applied to evaluate designs of an irrigation network and to analyse the alternatives, but it can also be used as a decision support tool in the operation and maintenance of a system and/or to determine the efficiency of sediment removal facilities in an irrigation system. In addition the model can be helpful for the training of engineers to enhance their understanding of sediment transport in irrigation canals. Some examples of the application of SETRIC for the design and evaluation of irrigation canals are provided in Chapter 7.

In the past few years, SETRIC has been used to evaluate a large irrigation system in Nepal (Paudel, 2002) and to assess its suitability to predict non-equilibrium sediment transport (Ghimire, 2003). A special study analysed the applicability and versatility of the SETRIC model in an irrigation canal for different conditions of operation and sediment inputs (Sherpa, 2005). Also, a one-dimensional convection diffusion module has been developed to calculate the flow and sediment transport in both equilibrium and non-equilibrium conditions (Timilsina, 2005). It transpired from the previous studies that the SETRIC model still has some limitations and the results obtained need careful and thorough verification. At the moment the model is being used for a detailed analysis of field data and updated design processes. The results of the analysis will be used to include necessary modifications and improvements to make the model more compatible with specific field conditions.

A description and analysis of sediment transport concepts under the specific conditions of irrigation canals will contribute to an improved understanding of the behaviour of sediments in irrigation canals. It will also help to decide on improved water delivery plans in view of the operation and maintenance concepts. Finally it will help to evaluate design alternatives re minimal sedimentation and erosion, to maintain a fair, adequate and reliable water supply to the farmers, and to decide on the applicability of these concepts for the simulation of the sediment transport processes under the particular conditions of water flow and sediment inputs.

CHAPTER 2

Open Channel Flow

2.1 INTRODUCTION

Irrigation canals form a complicated hydraulic system as they have to handle the motion of water and sediment as well as the mutual interaction of both motions. Flowing water transports sediment, this sediment causes changes in the bed and on the sides of the canal, which also influences the water movement. Hence, sediment transport and water flow are inter-related and cannot be separated; they influence each other in an implicit manner. The time scales of the two processes in canals are different (see Chapter 4) and therefore, the water flow and sediment transport can, in the first instance, be treated separately to specify their specific properties and characteristics.

However, to predict the topological changes in a canal the two phenomena also have to be considered in conjunction. The objective of these lecture notes is to present a description of the sediment transport concepts in irrigation canals and, therefore, only those hydraulic aspects that are necessary for a better understanding of the sediment transport will be discussed. This chapter will present a short overview of the main hydraulic principles in open channel flow, a short description of the dimensionless numbers used in the sediment concepts and a classification of flow types. In addition, a summary of the uniform and non-uniform theories for steady and unsteady flows is included. For more information on the hydraulic theories, reference will be made to handbooks and lecture notes on hydraulics.

2.2 FLOW TYPES AND CHARACTERISTICS

Phenomena in open channels that convey water may vary considerably in magnitude and also sometimes in direction, both in terms of time and space. This chapter will introduce some main aspects of open channel hydraulics in order to be used as tools in the following chapters, which will deal with the movement of sediments and water together. In some

cases the water flow in canals varies over time and becomes unsteady. For some applications the variation may be considered to be so slow that a steady (or quasi steady) flow can be assumed. Considering the spatial distribution, any flow is essentially three-dimensional, meaning that the magnitude and direction of the flow vary from one point to another. Knowledge of this three-dimensional flow behaviour is still limited; but in many engineering applications it is often sufficient to know particular mean or average values.

The average or mean value can be presented for:

- a two-dimensional flow situation by averaging the value over the canal depth at a certain point; an example is the depth-averaged flow velocity in a vertical;
- a two-dimensional flow condition by averaging the value over the width of the canal (in a lateral direction); the resulting value depends on the longitudinal coordinates; an example is the average water depth in a cross-section;
- a one-dimensional flow situation by averaging the value over the whole cross-section. The resulting values depend on the longitudinal coordinate (the x -values); an example is the average velocity in a cross-section.

It is important to remember that most of the two- and one-dimensional flow problems are simplified by averaging the flow characteristics; some information relating to the ‘un-averaged’ three-dimensional situation and the consequences of the process of averaging should be considered when the mean quantities are interpreted.

Open channel flow can be classified in many ways. A very common classification of open channel (gravity) flow is according to the change of flow depth with respect to time and space and is shown in Figure 2.1. Steady flow means that the main flow variables do not change and are steady with time; the variables at every point remain constant with time. An example is the flow in a channel where the water depth either does not

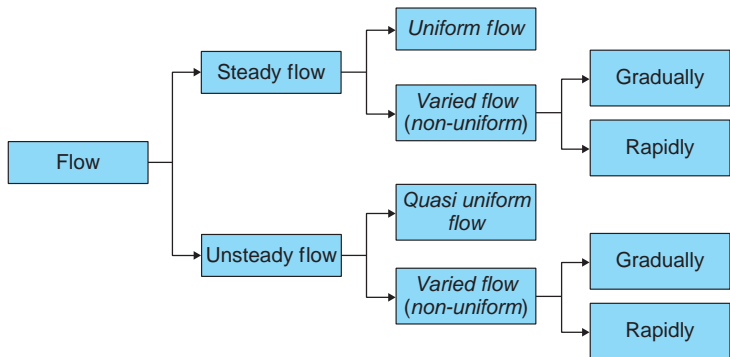


Figure 2.1. Classification of flow types.

change with time or can be assumed to be constant during the time interval under consideration. In unsteady flow the flow variables (magnitude and direction of the velocity, pressure, density, flow path, etc.) vary with time at the spatial points in the flow. Examples are surge waves in irrigation canals after a sudden opening or closing of a gate. In many open-channel problems it is sufficient to study the flow behaviour under steady conditions. However, when the change in flow condition with respect to time is of major concern, the flow should be treated as unsteady. In surges, for instance, the stage of flow will change instantaneously as the waves pass by, and the time element becomes vitally important in the design of control structures.

In uniform flow the cross section (shape, side slope and area) through which water flows remains constant in the flow direction, the flow depth is the same in every section. In addition, the velocity does not change in magnitude and direction with distance. A uniform flow may be steady or unsteady, depending on whether or not the depth changes with time or during the time interval under consideration (see Figure 2.2). Steady uniform flow is the fundamental flow in open channel hydraulics. The establishment of unsteady, uniform flow would require that the water surface fluctuates from time to time while remaining parallel to the channel bottom. Obviously, this is a practically impossible condition.

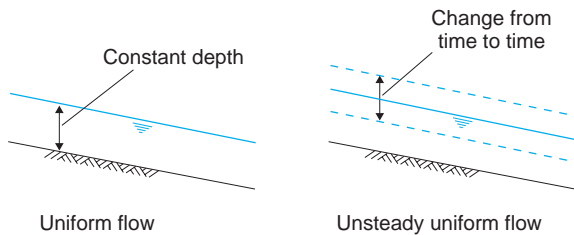


Figure 2.2. Steady and unsteady, uniform flow.

In varied flow, the cross section (shape, side slope and area) changes in the flow direction, the flow depth changes along the channel. Varied flow may be either steady or unsteady. Since unsteady uniform flow is rare, the term 'unsteady flow' is used exclusively for unsteady varied flow. Varied flow may be further classified as either rapidly or gradually varied. The flow varies rapidly if the depth changes abruptly over a relatively short distance; otherwise, it varies gradually. Figure 2.3 shows an example of unsteady, gradually and rapidly varied flow.

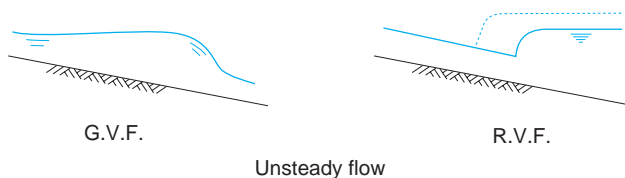


Figure 2.3. Unsteady, gradually and rapidly varied flow.

A rapidly varied flow is also known as a local phenomenon; examples are the hydraulic jump and the hydraulic drop. Spatially constant flow occurs when the average velocity is the same in all points; when the velocity changes along or across the flow, the flow is spatially variable. A clear example of a spatially varied flow is the flow through a gradual contraction or in a canal with a constant slope receiving inflow over the full canal length. Discontinuous or spatially varied flow shows some inflow and/or outflow of water along the reach under consideration; the continuity equation should be adapted to this situation. Examples are side channel spillways, main drainage canals and quaternary canals in irrigation systems. Figure 2.4 gives some typical locations in canals and rivers where gradually and rapidly varied flow might occur.

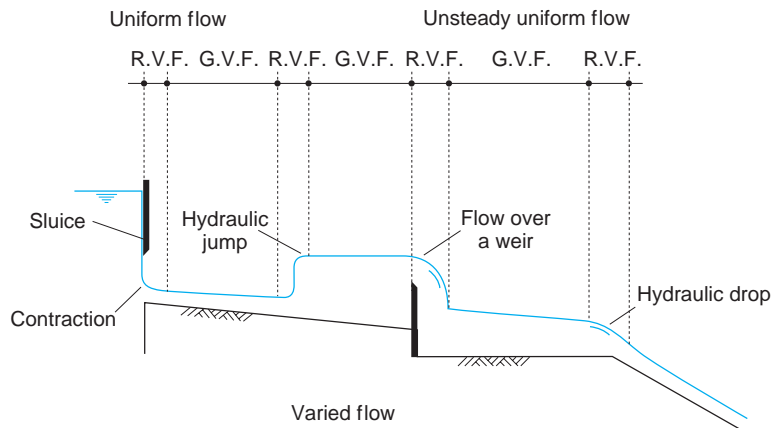


Figure 2.4. Examples of gradually and rapidly varied flow (steady conditions).

R.V.F. = Rapidly varied flow
 G.V.F. = Gradually varied flow

Another flow classification is based on the dimensionless numbers that describe the relative influence of either the force due to viscosity or inertia in relation to the gravitational force. In hydraulics, the force due to viscosity is described as the resistance of a fluid to flow. The resistance acts against the motion of fluid when it passes fixed boundaries (e.g. the canal bottom or walls), but it also acts internally between slower and faster moving adjacent layers. Viscosity is the internal fluid friction that enables the acceleration of one layer relative to the other; it resists the motion of a layer but also makes it possible to accelerate a layer. Viscosity is the principal means by which energy is dissipated in fluid motion, typically as heat.

The difference in velocity between adjacent layers is known as a velocity gradient. To move one layer at a greater velocity than the adjacent layer, a force is necessary; resulting in a shear stress τ . Newton mentioned

Table 2.1. Kinematic viscosity of water as a function of the temperature T .

T (°C)	0	5	10	14	20	25	30
ν (10^{-6} m ² /s)	1.79	1.52	1.31	1.14	1.01	0.90	0.80

that for straight, parallel and uniform flow, the shear stress τ between layers is proportional to the velocity gradient, $\partial u/\partial y$, in the direction perpendicular to the layers.

$$\tau = \mu \frac{\partial u}{\partial y} \quad (2.1)$$

The constant μ is the dynamic viscosity. Fluids, such as water, that satisfy Newton's criterion are known as Newtonian fluids and show linearity between shear stress and velocity gradient. When the viscous forces are related to inertial forces, the ratio is characterized by the kinematic viscosity ν .

$$\nu = \frac{\mu}{\rho} \quad (2.2)$$

The unit of dynamic viscosity is Pa·s (Pascal second) and is identical to 1 N/s m². The unit of kinematic viscosity is m²/s. The viscosity of water decreases with an increase in temperature.

Viscosity is the main factor resisting motion in laminar flow. However, when the velocity has increased to the point at which the flow becomes turbulent, pressure differences resulting from eddy currents rather than viscosity provide the major resistance to motion.

Significant dimensionless numbers in open channels are the Froude number and the Reynolds number. The Froude number gives the ratio between the inertial force and the force due to the gravity and is represented by:

$$\text{Fr}^2 = \frac{\rho L^2 v^2}{\rho g L^3} = \frac{v^2}{gL} \quad (2.3)$$

Where:

v = mean velocity (m/s)

g = acceleration due to gravity (m/s²)

L = a characteristic length, e.g. water depth (m)

ρ = density (kg/m³)

ν = kinematic viscosity (m²/s)

The Froude number differentiates between sub- and supercritical flow. When the Froude number is one, the flow is critical. For numbers larger than one the flow is supercritical.

The Reynolds number gives the ratio between the inertia force and the viscous force and is represented by:

$$\text{Re} = \frac{\rho v^2 L^2}{\mu \nu L} = \frac{vL}{\nu} \quad (2.4)$$

Where:

v = mean velocity (m/s)

L = a characteristic length, e.g. water depth (m)

ν = kinematic viscosity (m^2/s)

For low Reynolds numbers the flow is laminar and for large numbers the flow is turbulent. An additional form of the Reynolds number that is frequently used in the sediment transport theories is the Reynolds number using the shear velocity:

$$\text{Re}_* = \frac{\rho u_* R}{\mu} = \frac{u_* R}{\nu} \quad (2.5)$$

Where:

$u_* = \sqrt{gRS_0}$ = shear velocity (m/s)

g = acceleration due to gravity (m/s^2)

R = hydraulic radius (m)

S_0 = bottom slope (m/m)

ν = kinematic viscosity (m^2/s)

2.3 GEOMETRY

Canals are man-made channels and their cross-section can be prismatic (when A and S_0 are constant) or non-prismatic. Moreover, the cross-section can be either regular (e.g. circular, triangular, rectangular or trapezoidal) or irregular. Figure 2.5 gives the main characteristics within a cross section and a longitudinal section of a canal.

The cross-section is generally defined by the following geometrical measures.

- Water depth y : vertical distance from the bottom to the water surface
- Section depth d : normal (perpendicular) distance from the bottom to the water surface
- Surface or top width B_s : length of the channel width at the water surface
- Area or wetted area A : area normal to the flow direction
- Wetted perimeter P : length of the wetted line of intersection
- Hydraulic radius R : wetted area A /wetted perimeter P
- Hydraulic depth D : wetted area A /top width B_s

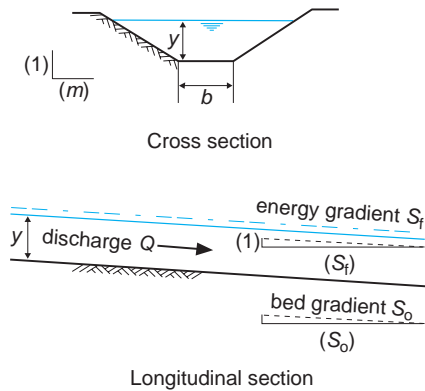


Figure 2.5. Main characteristics of a canal.

Some other quantities that are related to a cross-section include:

- Discharge Q which is the total amount of water flowing through a cross-section during the unit of time t ; the unit of discharge is m^3/s
- The average velocity is by definition: $v = Q/A$
- Total energy: $E = z + d \cos \Theta + \alpha v^2/2g$ (for small slopes $y = d \cos \Theta$; Θ is the bottom slope in radian)
- Specific energy: $E_s = y + \alpha v^2/2g$ (for small slopes $\cos \Theta = 1$)
- Average velocity: $v = Q/A$; where the discharge Q is the amount of water in m^3 flowing through a cross-section during the unit of time
- Velocity head: $\alpha v^2/2g = \alpha Q^2/2g A^2$ (α is the Coriolis coefficient)
- Froude number: $\text{Fr} = \alpha Q^2 B_s/g A^3$

2.4 BASIC HYDRAULIC PRINCIPLES

The motion of water can be described by considering the conservation of mass (continuity) and the conservation of momentum as expressed by Newton's second law. Sometimes the energy equation can also be helpful to describe the motion of water, especially when all the energy losses are known.

Continuity principle

The continuity equation is applicable for all flow types without any restriction. By using an x -, y -, z -coordinate system that is fixed in space and the velocity components u , v and w , respectively, the continuity equation is obtained by considering a small fluid element and the net rate of mass entering that element. The continuity equation for unsteady, compressible, real or ideal (no friction) fluids reads:

$$\frac{\delta \rho u}{\delta x} + \frac{\delta \rho v}{\delta y} + \frac{\delta \rho w}{\delta z} + \frac{\delta \rho}{\delta t} = 0 \quad (2.6)$$

From this general, continuity equation follows the equation for three-dimensional, steady and incompressible flow ($\rho = \text{constant}$):

$$\frac{\delta u}{\delta x} + \frac{\delta v}{\delta y} + \frac{\delta w}{\delta z} = 0 \quad (2.7)$$

In the most common case, namely a two-dimensional flow, the equation becomes:

$$\frac{\delta u}{\delta x} + \frac{\delta v}{\delta y} = 0 \quad (2.8)$$

When $\delta v/\delta y = 0$, the flow is one-dimensional and the equation reads:

$$\frac{\delta u}{\delta x} = 0 \quad (2.9)$$

This equation results in the fact that the velocity u is constant and it represents uniform flow; the direction and magnitude of the velocity in all points are the same. For a steady flow, the discharge Q is constant along the canal and the continuity principle reads:

$$Q = \int^A v \, dA = \bar{v}A = \text{constant}$$

$$Q = \bar{v}_1 A_1 = \bar{v}_2 A_2 \quad (2.10)$$

Where:

A = area of the cross section (m^2)

\bar{v} = mean velocity perpendicular to cross-section (m/s)

When the mean velocity in an open channel is constant ($v_1 = v_2$) then the area $A = Q/v$ of the cross sections is the same; the channel has a prismatic cross section. When the flow is uniform, the water depth will be the same in all sections.

Conservation of momentum

The second law of Newton states that the sum of all external forces P equals the rate of change of momentum. The change of momentum per unit of time is equal to the resultant of all external forces (hydrostatic, friction, weight) acting on the body of flowing water:

$$\sum \vec{P} = \lim_{\Delta t \rightarrow 0} \frac{\Delta(m\vec{v})}{\Delta t} \quad (2.11)$$

$$\sum \vec{P} = \frac{d(m\vec{v})_{\text{out}} - d(m\vec{v})_{\text{in}}}{dt} + \frac{(m_1 \vec{v}_1)_{t+\Delta t} - (m_1 \vec{v}_1)_t}{dt} \quad (2.12)$$

The resultant of the external forces is equal to the rate of change of momentum of that body. P and v represent vectors; hence the change in momentum has the same direction as the resultant. Equation 2.12 states that the forces acting on a fluid mass are equal to the rate of change of the momentum of that mass. The first term on the right side represents the net flow rate of momentum going out of the control volume and the second term represents the rate of accumulation of momentum within the control volume during the time interval Δt .

The direction of ΣP is the same as that of Δv ; ΣP represents the vectorial summation of all forces on the mass, including the gravity forces, shear forces, and pressure forces including those exerted by fluid surrounding the mass as well as the pressure forces exerted by boundaries in contact with the mass. The equation always applies.

In the case of steady flow, the last term in equation 2.10 is equal to zero, the force is equal to the net momentum outflow across the control surface and the equation becomes:

$$\sum \bar{P} = \frac{d(m\bar{v})_{\text{out}}}{dt} - \frac{d(m\bar{v})_{\text{in}}}{dt} = \frac{d(m\bar{v})_{\text{out}}}{dt} - \frac{d(m\bar{v})_{\text{in}}}{dt} \quad (2.13)$$

$$\sum \bar{P} = \rho Q(\beta_2 \bar{v}_2 - \beta_1 \bar{v}_1) \quad (2.14)$$

Where:

$\sum P$ = sum of all external forces acting on the control body (N)

Q = discharge (m^3/s)

A = area of the cross section (m^2)

\bar{v} = mean velocity perpendicular to the cross-section (m/s)

m = mass of water passing a cross section (kg)

$m = \rho v A$

β = Boussinesq coefficient (see Section 2.5)

In this equation, the factor β is the coefficient of Boussinesq, which incorporates the effect of the velocity distribution on the average velocity. When there are no external friction forces, only the conditions at the end sections of the control volume govern the impulse-momentum principle.

Energy principle

The energy equation holds true as long as proper allowance is made for the energy losses. The total energy of a fluid particle per unit of volume is the sum of three types of energy (kinetic, potential and pressure). For an open channel with steady flow, and with straight and parallel streamlines,

the sum of the potential and pressure energy in the z-direction is:

$$\rho gz + p = \text{constant. The kinetic energy of a particle is equal to } \frac{1}{2} \rho v^2$$

The total energy for an entire cross section is equal to the sum of the energy of all the fluid particles. To find the total kinetic energy in this particular cross section, the velocity is expressed by the mean velocity: $v_{\text{mean}} = Q/A$. However, in open channels the velocity is not uniformly distributed over the depth and the width due to the presence of the free water surface and the friction along the boundary (bottom and sides). The true average kinetic energy across the cross-section per unit of volume is: $(\frac{1}{2} \rho v^2)_{\text{average}} = \frac{1}{2} \alpha \rho \bar{v}^2$

For the total energy head this fact is taken into account by multiplying the velocity head ($v^2/2g$) by the coefficient α , the Coriolis coefficient (see Section 2.5).

The total energy E passing through a cross section is:

$$E = \frac{1}{2} \alpha \rho \bar{v}^2 + \rho gz + p \quad (2.15)$$

The total energy divided by the weight results in the energy head, being the total energy per unit weight.

$$E_{\text{tot}} = \frac{\alpha \bar{v}^2}{2g} + \frac{p}{\rho g} + z \quad (2.16)$$

If you assume two cross sections perpendicular to straight and parallel streamlines, and that the energy loss is negligible (the energy principle of Bernoulli), then:

$$E_{\text{tot}} = \frac{\alpha_1 v_1^2}{2g} + \frac{p_1}{\rho g} + z_1 = \frac{\alpha_2 v_2^2}{2g} + \frac{p_2}{\rho g} + z_2 \quad (2.17)$$

Where:

z = height of the channel bottom in a section in m above a datum

$p/\rho g$ = pressure head in a cross-section in m

$\alpha v^2/2g$ = velocity head in a cross-section (kinetic energy) in m

E_{tot} = total energy head in a cross-section in m above a datum

In a *real fluid* (fluid with friction) there are always friction and/or local losses ($\Delta E = h_f$)

$$\frac{\alpha_1 \bar{v}_1^2}{2g} + \frac{p_1}{\rho g} + z_1 = \frac{\alpha_2 \bar{v}_2^2}{2g} + \frac{p_2}{\rho g} + z_2 + h_f \quad (2.18)$$

Critical flow

The *specific energy* (Bakhmeteff, 1912) is the energy per unit weight with respect to the channel bottom. The piezometric head in a point of the cross section is $(p/\rho g) + z$, which is equal to the water depth y in that particular cross section: $(p/\rho g) + z = y$. For open channel flow, the piezometric head in a vertical in a cross section is equal to the water depth. Therefore, the specific energy E_s is the sum of the water depth and the velocity head (assuming that the streamlines are straight and parallel):

$$E_s = y + \alpha \bar{v}^2 / 2g \tag{2.19}$$

$$E_s = y + \alpha Q^2 / 2gA^2 \tag{2.20}$$

Where:

y = water depth (m)

Q = discharge (m^3/s)

A = area of the cross section (m^2)

\bar{v} = mean velocity in a cross-section (m/s)

$V = \bar{v}$ = mean or average velocity (m/s)

E_s = specific energy with respect to the bottom (m)

For a given cross-section and a constant discharge Q , the specific energy is a function of the water-depth y only. Plotting this water-depth y against the specific energy E_s gives a specific energy curve for the discharge Q (see Figure 2.6).

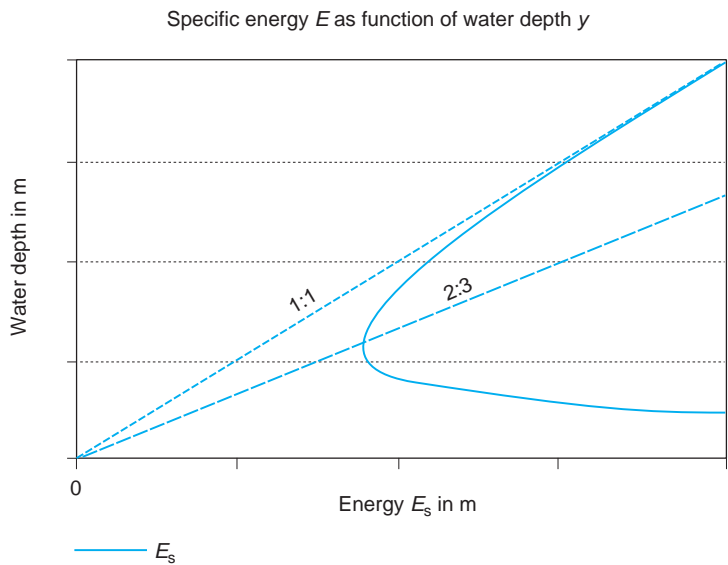


Figure 2.6. Specific energy as function of the water depth y .

From this figure with $E_s = y + Q^2/2gA^2$ follows that for a given discharge Q and a specific energy E_s , which should be larger than a certain

threshold, there are *two alternate water depths*. For the threshold value, the specific energy is the minimal energy needed to convey that discharge Q through that specific cross section. In the case of the minimum energy the two alternate depths coincide for the given discharge Q and the water depth becomes the ‘critical depth’ (y_c). The Froude number for that discharge and water depth becomes 1 ($Fr^2 = 1$). In other words, for this critical depth the specific energy has a minimum value for the given discharge Q and cross section A .

When the flow depth is greater than the critical depth, the flow is subcritical; if it is less the flow is supercritical (see Table 2.2). For any given discharge Q there are two possible flow regimes, but in reality only one will occur. These two flow regimes are either a slow and deep subcritical flow or a fast and shallow supercritical flow.

Table 2.2. Flow type as a function of the actual water depth.

Actual depth y in relation to y_c	Froude number	Flow type
$y > y_c$	$Fr^2 < 1$	Subcritical
$y = y_c$	$Fr^2 = 1$	Critical
$y < y_c$	$Fr^2 > 1$	Supercritical

For critical flow conditions:

- and for a given discharge Q the specific energy E_s has a minimum value;
- and for a given specific energy E_s the discharge Q has a maximum value;
- the velocity head is half the hydraulic depth D ;
- the Froude number Fr^2 is one (unity);
- and for a given discharge Q the specific force has a minimum value;
- the velocity of a disturbance in canals with a mild slope is equal to the celerity of small gravity waves.

2.5 VELOCITY DISTRIBUTION

In the next chapters it will be shown that the average velocity $v = Q/A$, and the deviation from this average velocity, are very important aspects in hydraulics and sediment transport. Water flowing in a cross section with a rigid or movable boundary (bottom and wall) will show a specific velocity distribution across that section. The velocity will be zero at the fixed boundary. Next, the velocity increases rapidly towards the middle and upper part of the channel. The velocity in a specific point is a function of the x , y and z coordinates (Figure 2.7).

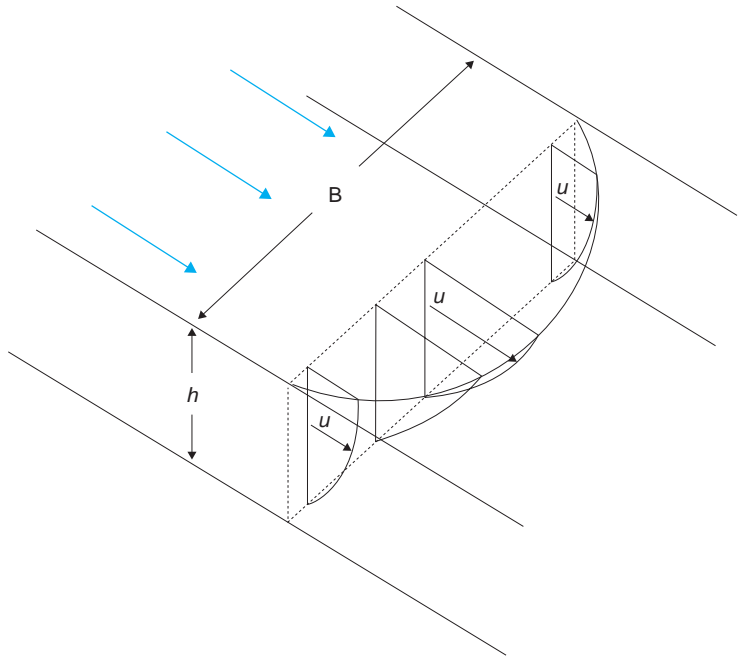


Figure 2.7. Distribution of the velocity in a rectangular channel.

The velocity profile in the vertical direction for a rectangular cross section can be approximated by the logarithmic equation as given by van Rijn (1984):

$$v_z = \frac{u_*}{\kappa} \ln \left(\frac{z}{z_0} \right) \quad (2.21)$$

Where:

u_* = shear velocity (m/s)

v_z = the velocity at a point z (m/s)

κ = constant of von Karman (from measurements $\kappa = 0.4$)

z_0 = level of the zero velocity (m)

z = the level of a point above a datum (m)

By definition the shear velocity $u_* = \sqrt{\tau/\rho}$ and it can be expressed as:

$$u_* = \sqrt{\frac{\tau}{\rho}} = \sqrt{gRS_0} \quad (2.22)$$

By using $\kappa = 0.4$ the relationship for v_z becomes:

$$v_z = 2.5u_* \ln \left(\frac{z}{z_0} \right) \quad (2.23)$$

The velocity v_z is equal to the average velocity \bar{v} for $z = 0.4y$.

$$\bar{v} = 2.5u_* \ln\left(\frac{0.4y}{z_0}\right) = 5.75u_* \log\left(\frac{0.4y}{z_0}\right) \tag{2.24}$$

Results from measurements show that the logarithmic velocity profile gives a good approximation for the full depth of the flow due to a simultaneous decrease both in shear stress and mixing length l with z . Values of z_0 were determined from experiments with smooth and rough boundaries.

For smooth boundaries, a viscous sub-layer exists in which viscous effects predominate. The approximate thickness of this layer is $\delta = 10 \nu/u_*$ and $z_0 = 0.01\delta = 0.1 \nu/u_*$. For rough boundaries with uniform roughness Nikuradse has determined $z_0 = 0.03 k_s$, in which k_s is the size of the sand particles used as roughness in the experiments. This k_s is also used as a standard roughness for other types of roughness (see Figure 2.8).

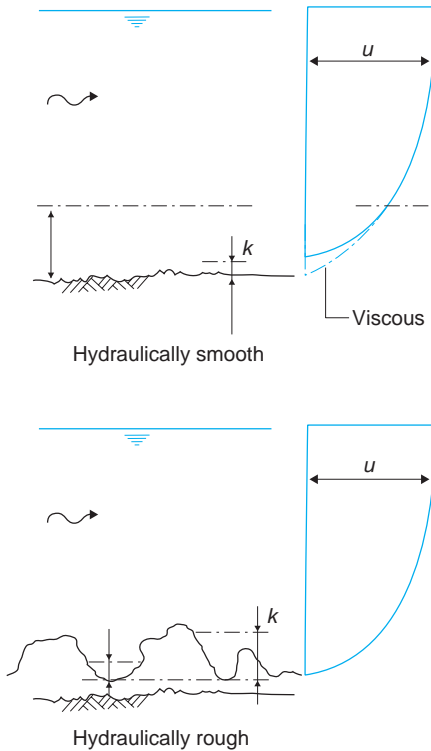


Figure 2.8. Hydraulically rough and hydraulically smooth boundary layers.

A boundary is:

- hydraulically rough for $k_s > 6 \delta$
- hydraulically smooth $k_s < 0.1 \delta$
- for intermediate values of k_s , the boundary is in a transition region.

White-Colebrook established an accurate good interpolation by taking $z_0 = 0.03 k_s + 0.01 \delta$. For this transition region the equation reads:

$$\bar{v} = 5.75 u_* \log \left(\frac{12y}{k_s + 0.03 \delta} \right) \quad (2.25)$$

The last equation can be transformed to the uniform flow equation of the de Chézy (see Section 2.6).

In the horizontal direction, the velocity distribution is influenced by the B/y ratio. For a non-wide canal ($B/y < 5$), the velocity distribution is three-dimensional. When the B/y ratio is larger than 5, the velocity distribution becomes almost two-dimensional with the exception of a small region near the vertical sidewalls.

Corrections in view of the average velocity

The velocity distribution in the vertical and width direction of a canal incorporates the fact that the velocity is not the same in all the points of the cross section. For that reason, the velocity in a point A (v_A) is not equal to the average velocity $\bar{v} = Q/A$, but it can be written as $v_A = \bar{v} \pm \Delta v$. The discharge Q is by definition equal to the average velocity \bar{v} times the total area A , but it is also the sum of the volumes of water passing the small areas ΔA with a velocity v_A .

$$Q = \sum v_A \Delta A = \sum (\bar{v} \pm \Delta v) \Delta A = \sum \bar{v} \Delta A \pm \sum \Delta v \Delta A$$

By definition: $Q = \sum (\bar{v} \Delta A)$ and hence: $\pm \sum (\Delta v \Delta A) = 0$

The total energy in a cross section comprises the potential energy, the pressure energy and the kinetic energy; the latter is expressed by the velocity head $v^2/2g$. The velocity head for the average velocity differs from the summation of the velocity head for each point and, therefore, it should be multiplied by the coefficient of Coriolis (α) to obtain the total head.

The mass of water flowing with a velocity v_a through a small area ΔA is $\rho v_a \Delta A$. The kinetic energy passing that area per unit of time is the product of the mass and the velocity squared: $\frac{1}{2} \rho v_a^3 \Delta A$ and the total kinetic energy for the whole cross section is: $\frac{1}{2} \sum \rho v_A^3 \Delta A$.

The total kinetic energy for the whole cross section can be expressed as $\alpha \rho A (\bar{v}^3 / 2g)$

Equating this quantity with $\frac{1}{2} \sum \rho v_A^3 \Delta A$ results in

$$\alpha = \frac{\sum (v_A^3 * \Delta A)}{(\bar{v}^3 * A)} = \frac{\sum (\bar{v} \pm \Delta v)^3 \Delta A}{(\bar{v}^3 * A)}$$

$$\alpha = \frac{\sum (\bar{v}^3 \Delta A \pm 3\bar{v}^2 \Delta v \Delta A + 3\bar{v} \Delta v^2 \Delta A \pm \Delta v^3 * \Delta A)}{\bar{v}^3 * A}$$

As shown before $\sum \Delta v * \Delta A = 0$; also Δv^2 is always larger than zero and $\Delta v^3 * \Delta A$ can be ignored as it is very small. Hence, the coefficient of Coriolis can be presented as:

$$\alpha = 1 \pm 3 * \frac{\sum \Delta v^2 * \Delta A}{\bar{v}^2 * A} \tag{2.26}$$

Another example of the effect of the velocity distribution on a hydraulic equation is the application of the second law of Newton in some hydraulic problems. The law states that the sum of all external forces is equivalent to the rate of change of momentum

$$\sum \vec{P} = \Delta m \vec{v} = (m\vec{v})_{out} - (m\vec{v})_{in} \tag{2.27}$$

The mass of water flowing with a velocity v_a through an area ΔA is $\rho v_a \Delta A$. The momentum passing that area per unit of time is the product of the mass and the velocity: $\rho v_a^2 \Delta A$. The momentum for the whole cross section with area A is: $\sum \rho v_a^2 \Delta A$. The total momentum for the whole cross section can also be expressed by the average velocity \bar{v} as: $\beta \rho \bar{v}^2 A$.

Equating this quantity with $\sum \rho v_a^2 \Delta A$ results in

$$\beta = \frac{\sum v_a^2 * \Delta A}{(\bar{v}^2 * A)}$$

$$\beta = \frac{\sum (\bar{v} \pm \Delta v)^2 \Delta A}{\bar{v}^2 * A} = \frac{\sum (\bar{v}^2 \pm 2\bar{v} * \Delta v + \Delta v^2) \Delta A}{\bar{v}^2 * A}$$

Where $\sum \Delta v * \Delta A = 0$

$$\beta = 1 + \frac{\sum \Delta v^2 \Delta A}{\bar{v}^2 A} \tag{2.28}$$

Where β = coefficient of Boussinesq

2.6 UNIFORM FLOW

Uniform flow in open channels is characterized by:

- a. the depth, cross section, velocity and discharge are constant in every section;
- b. the lines that represent the energy, water surface and channel bottom are parallel; the slopes are $S_o = S_f = S_w$.

It is assumed that uniform flow in open channels is steady and turbulent (meaning that $Re \gg 600$). Flow in open channels encounters friction

and for uniform flow ($v = Q/A = \text{constant}$) the component of gravity in the flow direction balances the friction forces. These two assumptions form the basis for the equations for uniform flow, including the de Chézy formula.

When water flows in a channel, a force is developed that acts on the bed in the flow direction and is called the tractive force. In uniform flow, the tractive force is equal to the component of the gravity force acting on the control body parallel to the bottom (Simons & Sentruk, 1992).

The tractive force follows from the product of the shear stress and the contact area. Assume that the average shear stress on the perimeter P is τ . Next, the balance between the component of the gravity force and the frictional resistance (tractive force) is used to derive that average shear stress (see Figure 2.9). The shear stress τ follows from the weight component ($= \rho g A L S_0$) and the frictional resistance ($= \tau P L$):

$$\tau = \rho g R S_0 \tag{2.29}$$

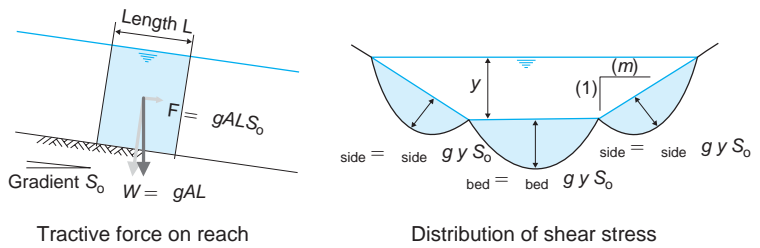


Figure 2.9. Tractive force and the distribution of the shear stress in a trapezoidal channel.

By definition the shear velocity $u_* = \sqrt{\tau/\rho}$ and can be expressed as:

$$u_* = \sqrt{\frac{\tau}{\rho}} = \sqrt{gRS_0} \tag{2.30}$$

For fully turbulent flow Prandtl showed that the shear stress τ is a function of v^2 and the relationship between v and τ can be written as $\tau = K v^2 = \rho g R S_0$. From this relation follows:

$$v^2 = \frac{\rho g}{K} R \cdot S_0 = C^2 R S_0 \tag{2.31}$$

This relation is normally presented as the de Chézy equation:

$$v = C \sqrt{R S_0} \tag{2.32}$$

Investigations in laboratories and measurements in the field have resulted in the following expression, proposed by White and Colebrook, for the coefficient C :

$$C = 18 \log \frac{12R}{k + \delta/3.5} \tag{2.33}$$

Where:

k = length characterizing the roughness = $1/2 a$ (Nikuradse)

δ = thickness of the laminar sub-layer = $11.6 \nu/v_*$

$$v_* = \sqrt{gRS_0}$$

$\nu = 10^{-6} \text{ m}^2/\text{s}$ (for $T = 20^\circ\text{C}$)

Values of the de Chézy coefficient as function of the hydraulic radius R , the wall roughness k and the thickness of the laminar sub-layer δ are presented in Figure 2.10.

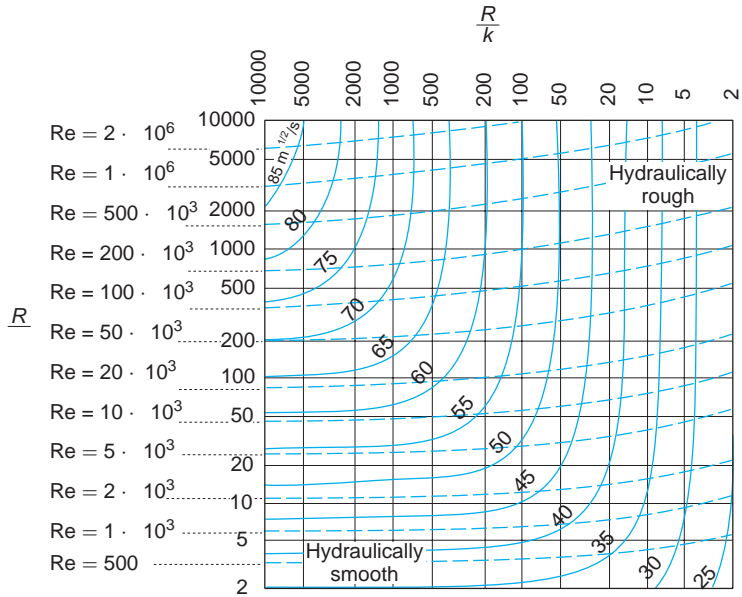


Figure 2.10. Values of the de Chézy coefficient C as function of the hydraulic radius R , the wall roughness k and the thickness of the laminar sub-layer δ .

Another, frequently used, equation for uniform flow is the Manning equation with n for the roughness:

$$v = \frac{1}{n} R^{2/3} S_0^{1/2} \tag{2.34}$$

In some countries, the Strickler equation is preferred; this equation uses k_s for the roughness.

$$v = k_s R^{2/3} S_0^{1/2} \tag{2.35}$$

The relationship between C of de Chézy and Manning's n can be found by taking the same average velocity v .

$$C = \frac{R^{1/6}}{n} \tag{2.36}$$

2.7 NON-UNIFORM STEADY FLOW

A gradually varied flow is a steady flow, whose depth varies gradually along the channel:

1. Hydraulic flow characteristics remain constant in time,
2. Streamlines are practically parallel; hydrostatic pressure prevails,
3. Bed friction is assumed to be equal to the friction in uniform flow (e.g. as used in the equations of Manning and de Chézy).

Figure 2.11 gives the energy considerations for unsteady flow in open channels, which also can be used for gradually varied flow (steady flow with $dv/dt = 0$).

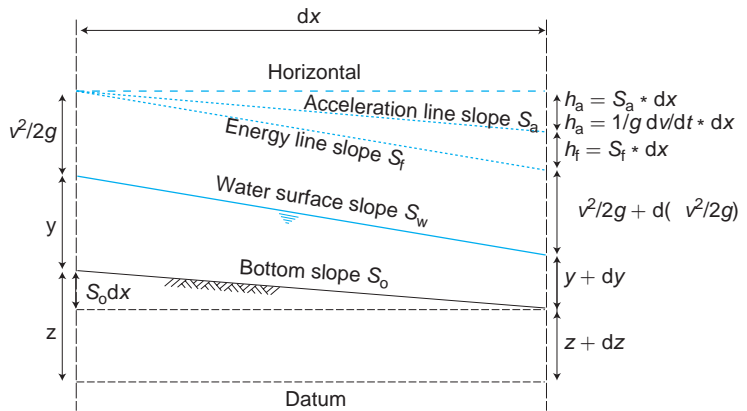


Figure 2.11. Energy considerations in a channel with unsteady flow.

A gradually varied flow (wide rectangular channels) is based upon:

$$\frac{dy}{dx} = \frac{S_o - S_f}{1 - Fr^2} \tag{2.37}$$

Where:

dy/dx = change of the water depth in the x-direction;

dy/dx = slope of the water surface relative to the channel bottom

S_o = bottom slope

S_f = slope of the energy line

Fr^2 = Froude number

Depending on whether dy/dx is negative or positive, the following water surface profiles can be distinguished:

$$\frac{dy}{dx} > 0 \implies \text{Backwater curve}$$

$$\frac{dy}{dx} = 0 \implies \text{Uniform flow}$$

$$\frac{dy}{dx} < 0 \implies \text{Drawdown curve}$$

The critical slope for a given discharge Q is by definition that bottom slope for which the normal water depth is equal to the critical depth; $S_o = S_c$ for $y_n = y_c$. An actual bottom slope can be compared with this critical slope. Table 2.3 gives a classification of the bottom slopes.

Table 2.3. Type of bottom slope.

Slope description	Bottom slope	Type of slope
Horizontal	$S_o = 0$	H
Mild	$0 < S_o < S_c$	M
Critical	$S_o = S_c$	C
Steep	$S_o > S_c$	S
Adverse or negative	$S_o < 0$	A or N

A particular discharge Q in a canal gives a normal and a critical water depth for a given bottom slope S_o . The actual water depth y in the canal can be related to these two water depths, namely the actual water depth can be either larger or smaller than the two water depths or is between the two water depths (see Table 2.4).

Table 2.4. Flow types based on the energy line, bottom slope and Froude number.

Actual water depth y in relation to y_n	Relation energy line and bottom slope	Flow type
$y > y_n$	$S_f < S_o$ or $S_o - S_f > 0$	Gradually varied
$y = y_n$	$S_f = S_o$ or $S_o - S_f = 0$	Uniform
$y < y_n$	$S_f > S_o$ or $S_o - S_f < 0$	Gradually varied
Actual water depth y in relation to y_c	Froude number	Flow type
$y > y_c$	$Fr < 1$ or $1 - Fr^2 > 0$	Subcritical
$y = y_c$	$Fr = 1$ or $1 - Fr^2 = 0$	Critical
$y < y_c$	$Fr > 1$ or $1 - Fr^2 < 0$	Supercritical

Therefore, the actual water depth can be classified in one of the following three water depth regions:

Region 1: $y > y_n$ and $y > y_c$

Region 2: y between y_n and y_c

Region 3: $y < y_n$ and $y < y_c$

Another classification of flow types is based on the relative bed slope and the actual water depth (see Table 2.5). Table 2.5 gives a summary of the most common water surface profiles in wide canals; a graphical presentation of these water surface profiles is given in Figure 2.12. Figure 2.13 gives an overview of the most common water surface profiles in wide canals. These canals are characterised by a large width B so that the hydraulic radius R is equal to y and the normal and the critical water depth are a function of the specific discharge $q = Q/B$ and the bottom roughness only.

Table 2.5. Summary of water surface profiles.

Bottom slope	Water surface profile			Depth range of y , y_c and y_n			Type of curve	Flow type
	1	2	3	Region 1	Region 2	Region 3		
Steep S $S_0 > S_c$ $y_n < y_c$	S1			$y > y_c > y_n$			Backwater	Subcritical
		S2			$y_c > y > y_n$		Drawdown	Supercritical
			S3			$y_c > y_n > y$	Backwater	Supercritical
Critical C $S_0 = S_c$ $y_n = y_c$	C1			$y > y_c = y_n$			Backwater	Subcritical
		C2			$y_c = y = y_n$		Uniform	Critical
			C3			$y < y_c = y_n$	Backwater	Supercritical
Mild M $0 < S_0 < S_c$ $y_n > y_c$	M1			$y > y_n > y_c$			Backwater	Subcritical
		M2			$y_n > y > y_c$		Drawdown	Subcritical
			M3			$y_n > y_c > y$	Backwater	Supercritical
Horizontal H $S_0 = 0$ $y_n = \text{infinite}$						n.a.		
		H2			$y_n > y > y_c$		Drawdown	Subcritical
			H3			$y_n > y_c > y$	Backwater	Supercritical
Adverse A $S_0 < 0$ $y_n = \text{none}$						n.a.		
		A2			$y > y_n$		Drawdown	Subcritical
			A3			$y_n > y$	Backwater	Supercritical

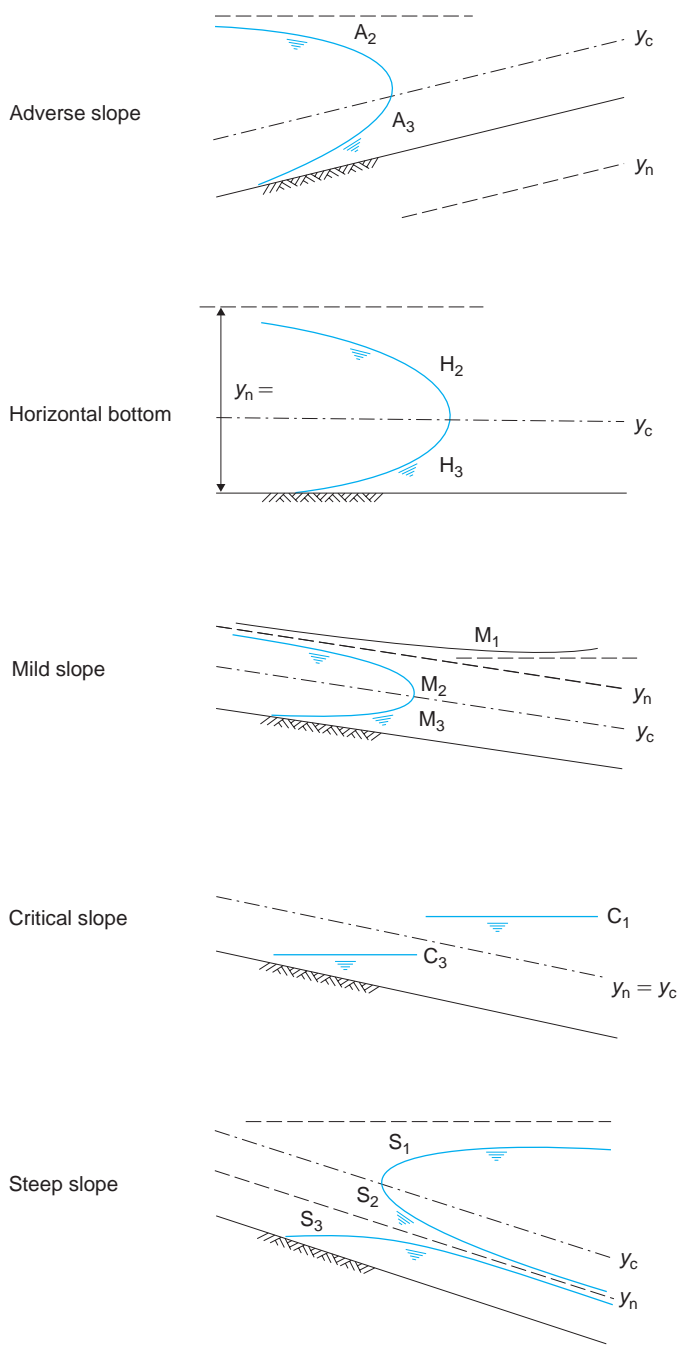


Figure 2.12. Summary of water surface profiles in wide canals ($R = y$ and $q = Q/B$).

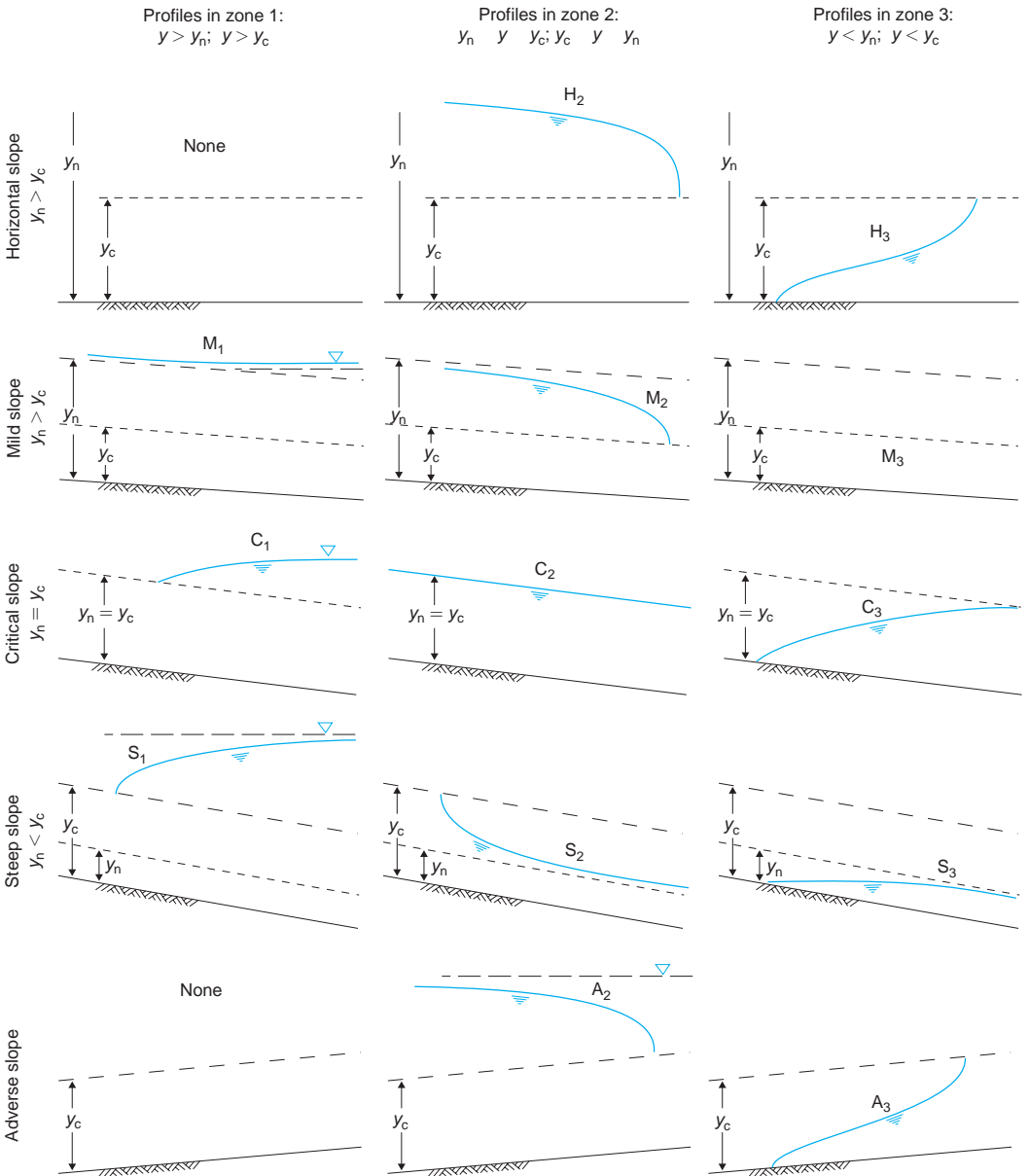


Figure 2.13. Overview of the most common water surface profiles in wide canals.

Gradually varied flow can be computed by three methods: direct integration; graphical integration and numerical integration. Some characteristics of these methods are presented in Table 2.6.

Table 2.6. Summary of the methods for computing gradually varied flow.

Method	Distance from depth	Depth from distance	Cross section	Remarks
Bresse	O	O	Prismatic; broad; rectangle	Use of tables recommended Use of Chézy formula <i>Recommendation for computation steps:</i> In upstream direction for subcritical flow In downstream direction for supercritical flow
Bakhmeteff	O		All shapes	Use of tables recommended Use of hydraulic exponents N and M
Graphical integration	O		Prismatic; non-prismatic	For $y \rightarrow y_n$ large errors may occur
Direct step	O		Prismatic	<i>Recommendation for computation steps:</i> In upstream direction for subcritical flow In downstream direction for supercritical flow
Standard step		O	All shapes	Iteration required Recommended for natural channels Eddy and other losses can be included Use of field data possible <i>Recommendation for computation steps:</i> In upstream direction for subcritical flow; In downstream direction for supercritical flow
Predictor corrector		O	All shapes	Iteration not required Straightforward water depth computation

2.8 SOME GENERAL ASPECTS OF UNSTEADY FLOW

Unsteady flow in open channels occurs when the flow parameters change with time at a fixed point, e.g. the water depth y or the discharge Q varies at a certain point of the canal system with time. Waves travelling in canals are examples of unsteadiness; they can be classified as:

- Translatory waves with a net transport of water in the direction of the wave; translatory waves are the most common type of waves in open channels.
- Oscillatory waves – a temporal variation in the water surface that is propagated through water, for instance wind waves, without a net transport of water. Oscillatory waves are normally ignored in the design and operation of irrigation networks.

A translatory wave is a gravity wave with a substantial displacement of water particles in the flow direction. The waves can be divided into gradually and rapidly varied unsteady flow. In gradually varied flow, the wave profile is gentle and the change in depth is gradual; examples are waves due to a slow gate operation in a canal. Rapidly varied unsteady flow examples are surges caused by the rapid opening or closing of regulating structures.

A special wave is the solitary wave that is characterised by a rising limb and a single peak, followed and preceded by steady flow. A downstream solitary wave moves down and an upstream wave moves up a channel slope.

A positive wave has an increase in water level and a negative wave has a decrease in water level from a steady flow. A short wave is characterized by a ratio of water depth and wave length smaller than 0.05 ($y/L < 0.05$).

The celerity of a wave is the speed of propagation of the disturbance relative to the water flow. In general, the celerity c for a wave with small amplitude and a two-dimensional flow follows from Airy's theory, which neglects the viscosity and surface tension: $c^2 = (gL/2\pi) \tanh(2\pi y/L)$.

For short waves and small \tanh the celerity become: $c^2 = gy$ (the Lagrange equation).

These lecture notes will discuss the sediment transport in irrigation canals in more detail. The criteria for the hydraulic design of a canal network will include the requirement that the water level is kept as much as possible at the required supply level and that the amount of water supplied is in line with the changing water requirements during the growing season. Therefore, it is logical to present some unsteady flow concepts here, especially in view of the impact of the schematisations of the sediment transport and water flow as proposed in the next chapters.

As mentioned before, the flow in irrigation networks is usually controlled for the optimal use of the available water, which will result in variations in time. A fast control may even lead to unwanted results, such as the development of hydraulic jumps. Although the design of many irrigation networks is based upon steady flow concepts, the hydraulic performance under operation usually requires a closer inspection based on unsteady flow computations.

Unsteady flows are characterized by either more or less significant variations in water depth and discharge, both in time and space. The related hydraulic problems are governed by two concepts, namely storage and conveyance. For an incompressible flow in canal networks the storage concept deals with the conservation of water volume. The conveyance concept deals with the balance of forces acting upon a water mass and their effect on the momentum balance. In this context, the amount of momentum loss due to channel friction relative to the increase of momentum due to the gravity forces is an essential aspect.

One of the important parameters influencing the capability of a canal network to adapt itself to changes is its storage capacity. If the storage capacity in a canal reach is relatively large compared to the difference in inflow and outflow, the time scale of adaptation is also large and the changes in the canal will show a very unsteady flow behaviour. If the storage capacity between the boundaries of the canal reach is small, the adaptation of the canal to the new boundary conditions may be fast and the flow may pass through a series of almost steady state. This adaptation of the

canal network also depends on the capability of the water flow to accelerate or decelerate. If the adaptation of the velocity of the flow particles occurs quickly, then the network will pass through a series of nearly steady states; otherwise, the flow in the network will clearly show an unsteady behaviour.

An example is the flow through a hydraulic structure in an irrigation canal. Usually this flow is assumed to be steady. The discharge through the structure at any moment depends on the water level boundary conditions. Although the water level may vary rapidly, the discharge generated will respond more or less instantaneously. The immediate response of the flow to the changing boundary conditions is due to lack of storage between the upstream and downstream sections and the relatively small water mass to be accelerated or decelerated. Generally a hydraulic structure is a steady flow element in a network and how the network as a whole will behave depends on the flow characteristics of the other elements in the network.

2.9 BASIC DIFFERENTIAL EQUATIONS FOR GRADUALLY VARIED UNSTEADY FLOW

Unsteady flow equations will describe the dependent variables, namely the velocity v and water depth y , as functions of the independent variables x (space coordinate) and t (time coordinate). The definition of the two dependent variables requires the formulation of two equations to solve them. In open channel flow, they are usually based upon the mass (volume) and momentum conservation. The conservation of mass assumes that the fluid is incompressible and that the density is constant. The conservation of mass leads to the continuity equation.

Gradually varied unsteady flow refers to an unsteady flow in which the curvature of the wave profile is mild; the change of depth with time is gradual; the vertical acceleration of the water particles is negligible in comparison with the total acceleration and the effect of the boundary friction can not be neglected. Figure 2.14 gives a schematized wave in the x , t and y direction as an example of unsteady flow.

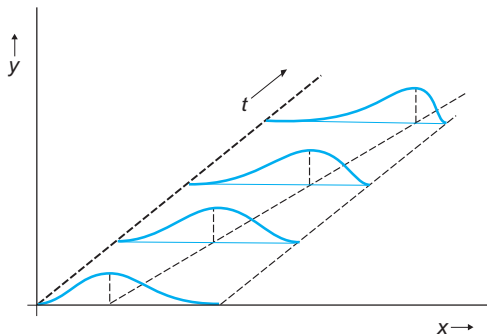


Figure 2.14. An unsteady flow presented in the x , t and y direction.

Only a few gradually varied, unsteady flow problems can be solved analytically; most problems require a numerical solution of the equations. The gradually varied unsteady flow can be described by the de St. Venant equations, which consist of the continuity and the dynamic equation. Unsteady flow in open channels is assumed to be a one-dimensional flow with straight and parallel flow lines. The dynamic equation includes the change of velocity v with time and consequently the acceleration, which produces the forces and causes the energy losses in the flow.

The dynamic equation

Unsteady flow analysis for open channels deals with the changes of discharge Q and water depth y with position and time. Here the depth y and velocity v are the dependent variables. Remember that in steady flow the gradient dE/dx represents the total energy line and is equal, but opposite in sign to the friction slope $S_f = v^2/C^2R$. When the increase in depth y and the downstream distance x are taken as positive, the equation for the total energy may be written as:

$$E = z + y + \frac{\alpha v^2}{2g}$$

$$\frac{dE}{dx} = \frac{dz}{dx} + \frac{dy}{dx} + \frac{2v}{2g} \frac{dv}{dx}$$

Remember that $v = f(x, t)$; hence the acceleration can be expressed by partial differentials as:

$$\frac{dv}{dx} = \frac{\partial v}{\partial x} + \frac{\partial v}{\partial t} \frac{\partial t}{\partial x}$$

$$\frac{\partial E}{\partial x} = \frac{\partial z}{\partial x} + \frac{\partial y}{\partial x} + \frac{v}{g} \left(\frac{\partial v}{\partial x} + \frac{\partial v}{\partial t} \frac{\partial t}{\partial x} \right)$$

$$v = \frac{\partial x}{\partial t} \text{ or } \frac{\partial t}{\partial x} = \frac{1}{v}$$

$$-S_f = -S_o + \frac{\partial y}{\partial x} + \frac{v}{g} \frac{\partial v}{\partial x} + \frac{1}{g} \frac{\partial v}{\partial t}$$

Thus:

$$S_f = S_o - \frac{\partial y}{\partial x} - \frac{v}{g} \frac{\partial v}{\partial x} - \frac{1}{g} \frac{\partial v}{\partial t} \quad (\text{de Saint Venant equation}) \quad (2.38)$$

$$S_f = S_o - \frac{\partial y}{\partial x} - \frac{v}{g} \frac{\partial v}{\partial x} - \frac{1}{g} \frac{\partial v}{\partial t} = \frac{v^2}{C^2R} \quad (2.39)$$

This is the de Saint Venant equation, where:

y = water depth (m)

t = time (s)

v = average velocity of the flow (m/s)

x = longitudinal distance (m)

S_o = channel slope (m/m)

S_f = friction slope = slope of the energy line (m/m)

By definition $Q = vA$ and $v = Q/A$

$$S_o - S_f - \frac{\partial y}{\partial x} - \frac{v}{gA} \frac{\partial Q}{\partial x} - \frac{1}{gA} \frac{\partial Q}{\partial t} = 0 \tag{2.40}$$

Dynamic equation for gradually varied unsteady flow

This general dynamic equation for gradually varied unsteady flow is only true when the pressure is hydrostatic, meaning that the vertical components of the acceleration are negligible and that the flow lines are straight and parallel.

The first two terms on the right hand side ($S_o - S_f = 0$) signifies steady uniform flow. The first four terms together [$S_o - S_f - \partial y/\partial x - v/gA(\partial Q/\partial x) = 0$] express a steady gradually varied flow.

The dynamic equation may also be written in another form:

$$\frac{\partial y}{\partial x} + \frac{v}{g} \frac{\partial v}{\partial x} + \frac{1}{g} \frac{\partial v}{\partial t} + S_f - S_o = 0 \tag{2.41}$$

$$g \frac{\partial y}{\partial x} + v \frac{\partial v}{\partial x} + \frac{\partial v}{\partial t} + g(S_f - S_o) = 0 \tag{2.42}$$

These equations clearly show the four variables in unsteady, open channel flow, namely x , t , v and y .

Continuity equation

The law of continuity for an unsteady, one-dimensional flow can be found by considering the conservation of mass of a small canal length (dx) between two cross-sections. The difference in outflow and inflow in the canal reach during a time step dt is equal to the change of storage over that distance dx . Moreover, assume that the surface width over the distance dx is constant (prismatic section) and that the water is incompressible. For the unsteady flow conditions the discharge Q changes with distance dx , namely dQ/dx and the water depth y changes with time: dy/dt . The change of discharge Q through space in a small time-step dt is $(dQ/dx) dx dt$. The corresponding change in storage in space is $B_s dy/dt dx dt = (dA/dt) dx dt$ (with $dA = B_s dy$). From continuity considerations (volumetric balance)

follows that a change of discharge Q in Δx -direction must be accompanied by a change in water depth y in time step Δt :

$$\left(\frac{dQ}{dx}\right) dx dt + B_s \frac{dy}{dt} dx dt = 0$$

$$\frac{\partial Q}{\partial x} + B_s \frac{\partial y}{\partial t} = 0 \quad \text{Continuity equation for unsteady flow} \quad (2.43)$$

From this equation follows that the sign of the change in discharge Q in the Δx -direction is opposite to the sign of the change in depth y during time step Δt .

Assuming that there is no lateral discharge (no inflow or outflow: $\Delta q = 0$) in Δx and with $Q = v A$

$$\frac{\partial Q}{\partial x} = \frac{\partial A \cdot v}{\partial x} = v \frac{\partial A}{\partial x} + A \frac{\partial v}{\partial x}$$

$$A \frac{\partial v}{\partial x} + v \frac{\partial A}{\partial x} + B_s \frac{\partial y}{\partial t} = 0 \quad \text{Continuity equation for a channel with a general shape} \quad (2.44)$$

The first term on the left-hand side represents the prism storage, the second term represents the wedge storage and $B \partial y / \partial t$ is the rate of rise of the water level with time t .

Prism storage + wedge storage + rate of rise of water level = 0

With the hydraulic depth $D = A/B_s$ and with $dA = B_s dy$, the continuity equation becomes:

$$D \frac{\partial v}{\partial x} + v \frac{\partial y}{\partial x} + \frac{\partial y}{\partial t} = 0 \quad \text{Continuity equation for a channel with a general shape} \quad (2.45)$$

For a rectangular channel with $q = Q/B$, $v = q/y$ and $A = By$ follows:

$$y \frac{\partial v}{\partial x} + v \frac{\partial y}{\partial x} + \frac{\partial y}{\partial t} = 0 \quad \text{Continuity equation for a rectangular channel} \quad (2.46)$$

Where:

y = water depth (m)

t = time (s)

v = average velocity of the flow (m/s)

x = longitudinal distance (m)

Summarising, the continuity and dynamic equations for unsteady flow in open channels read:

$$v \frac{\partial A}{\partial x} + A \frac{\partial v}{\partial x} + B_s \frac{\partial y}{\partial t} = 0 \quad \text{Continuity equation for unsteady flow} \quad (2.47)$$

$$\frac{\partial y}{\partial x} + \frac{v}{g} \frac{\partial v}{\partial x} + \frac{1}{g} \frac{\partial v}{\partial t} + S_f - S_o = 0 \quad \text{Dynamic equation for unsteady flow} \quad (2.48)$$

The continuity and dynamic equation in this form are also known as the de St. Venant equations.

From a combination of the dynamic equation and the continuity equation follows:

$$\frac{\partial Q}{\partial t} - \frac{2QB_s}{A} \frac{\partial y}{\partial t} + gA \left(1 - \frac{Q^2 B_s}{gA^3} \right) \frac{\partial y}{\partial x} - gAS_o + gAS_f = 0 \quad (2.49)$$

Combination of the dynamic and continuity equation for a canal with a general shape.

2.10 SOLUTION OF THE DE ST. VENANT EQUATIONS

The continuity and dynamic equation compose a set of gradually varied, unsteady flow equations, which together form a complete dynamic model of the flow. This complete model can provide accurate results for an unsteady flow, but at the same time, the model can be very demanding in view of the required computations. Moreover, the model is limited by the assumptions made in the deduction of the de St. Venant equations and the suppositions required for their application for specific problems, e.g. assumptions regarding channel irregularities. The set of the two simultaneous equations has to be solved for the two unknowns, v and y , given appropriate boundary conditions and initial conditions. Nowadays this set of equations can easily be solved with the aid of available computer technology.

At present three main numerical methods are available to solve the de St. Venant equations, namely:

- Finite differences (FD)
- Method of characteristics (MOC)
- Finite element method (FEM)

The solution of the de St. Venant equations is complicated, also for simple rectangular channels. General solutions are only possible by using one of the numerical methods. The method with finite differences is the most common one. The method of characteristics is adequate for waves due

Table 2.7. Summary of the methods to solve the de St. Venant equations.

de St. Venant Equations				
Numerical Methods				Approximate Methods
Direct	Method of characteristics			Finite element method
Implicit	Explicit	Characteristic nodes Implicit Explicit	Rectangular grid Implicit Explicit	Storage routing Muskingum Diffusion analogy Kinematic wave

to sudden gate operations. The finite element method can accommodate canals with irregular boundaries.

The solution method of the various methods can be explicit or implicit:

- Explicit: the discharge Q and water depth y at the next time-step are expressed in terms of the discharge Q and water depth y at the current time step; this method is straightforward, but it must be in line with the Courant stability criterion ($c(\Delta t/\Delta x) < 1$). This condition imposes a severe limitation on the time-distance grid.
- Implicit: the discharge Q and water depth y are related to subsequent and previous time steps, which is a more complex solution method, but a stable one.

2.11 RECTANGULAR CHANNELS AND THE METHOD OF CHARACTERISTICS

The set of continuity and momentum equations is very useful for the formulation of solutions on the basis of finite differences, but a transformation of the equations might help to understand the continuity and dynamic equations more easily. For the transformation the auxiliary variable $c = \sqrt{gD}$ will be used.

The transformation will use the de St. Venant equations and the differential of the area A to x :

$$\frac{\partial A}{\partial x} = \frac{\partial(\alpha B_s y)}{\partial x} = B_s \frac{\partial y}{\partial x} + \alpha y \frac{\partial B_s}{\partial x}$$

The term $\alpha y(\partial B_s/\partial x)$ accounts for non-prismatic channels and $\partial B_s/\partial x$ is the increase of the surface width in the flow direction. The coefficient α is the Coriolis coefficient. The value of α depends on the geometry of the

cross-section, but it is generally between 0.5 and 1.0. The value of α is about 0.5 for triangular and about 1.0 for rectangular cross-sections.

The continuity equation can be written as:

$$v B_s \frac{\partial y}{\partial x} + \alpha y v \frac{\partial B_s}{\partial x} + A \frac{\partial v}{\partial x} + B_s \frac{\partial y}{\partial t} = 0$$

$$v \frac{B_s}{A} \frac{\partial y}{\partial x} + \frac{\alpha y v}{A} \frac{\partial B_s}{\partial x} + \frac{\partial v}{\partial x} + \frac{B_s}{A} \frac{\partial y}{\partial t} = 0$$

By definition the hydraulic depth D is A/B_s

$$\frac{v}{D} \frac{\partial y}{\partial x} + \frac{\partial v}{\partial x} + \frac{1}{D} \frac{\partial y}{\partial t} + \frac{\alpha y v}{A} \frac{\partial B_s}{\partial x} = 0$$

$$v \frac{\partial y}{\partial x} + D \frac{\partial v}{\partial x} + \frac{\partial y}{\partial t} + \frac{\alpha y v D}{A} \frac{\partial B_s}{\partial x} = 0$$

Rearrange this equation and introduce the auxiliary variable $c = \sqrt{gD}$ (Lagrange), where c is the velocity of a long wave in water depth y . In other words c becomes a measure of y .

$$v \frac{\partial y}{\partial x} + \frac{c^2}{g} \frac{\partial v}{\partial x} + \frac{\partial y}{\partial t} + \frac{\alpha y v}{A} D \frac{\partial B_s}{\partial x} = 0$$

For a rectangular channel the surface width B_s and bottom width B are equal and therefore $dB_s/dx=0$ and the hydraulic depth becomes $D=A/B_s=y$. Substituting the Lagrange wave speed approximation, namely $gy=c^2$; $dy=2/gc dc$ and $dy/dx=2c/g dc/dx$, the dynamic equation $S_f = S_o - (\partial y/\partial x) - v/g(\partial v/\partial x) - 1/g(\partial v/\partial t)$ will change into:

$$2c \frac{\partial c}{\partial x} + v \frac{\partial v}{\partial x} + \frac{\partial v}{\partial t} = g(S_o - S_f) \tag{2.50}$$

Dynamic equation for a rectangular channel

Substituting the Lagrange wave speed approximation in the continuity equation for a rectangular channel, which is $y(\partial v/\partial x) + v(\partial y/\partial x) + (\partial y/\partial t) = 0$, results in:

$$2v \frac{\partial c}{\partial x} + c \frac{\partial v}{\partial x} + 2 \frac{\partial c}{\partial t} = 0 \tag{2.51}$$

Continuity equation for a rectangular channel

By writing first the sum and then the difference of the two above given equations, two new equations will be obtained. First, the addition will be presented.

1. The continuity equation divided by c/g and the dynamic equation multiplied by g , results in:

$$2v \frac{\partial c}{\partial x} + c \frac{\partial v}{\partial x} + 2 \frac{\partial c}{\partial t} + 2c \frac{\partial c}{\partial x} + v \frac{\partial v}{\partial x} + \frac{\partial v}{\partial t} + g(S_f - S_o) = 0$$

$$2(v + c) \frac{\partial c}{\partial x} + 2 \frac{\partial c}{\partial t} + (v + c) \frac{\partial v}{\partial x} + \frac{\partial v}{\partial t} + g(S_f - S_o) = 0$$

$$(v + c) \frac{\partial(v + 2c)}{\partial x} + \frac{\partial(v + 2c)}{\partial t} = g(S_o - S_f) \quad (2.52)$$

2. Similarly the continuity equation divided by c/g minus dynamic equation multiplied by g :

$$(v - c) \frac{\partial(v - 2c)}{\partial x} + \frac{\partial(v - 2c)}{\partial t} = g(S_o - S_f) \quad (2.53)$$

$g(S_o - S_f)$ is called the energy term.

Finally a combination of 2.47 and 2.48 results in a general equation for non-steady flow:

$$(v \pm c) \frac{\partial(v \pm 2c)}{\partial x} + \frac{\partial(v \pm 2c)}{\partial t} - g(S_o - S_f) = 0 \quad (2.54)$$

General equation of non-steady flow in a rectangular channel

Remember that the general mathematical expression for a change of a function f in the x - t -diagram when going from a given point 1 to a neighbouring point 2 can be given by the partial derivatives of the function in the t -direction and the x -direction.

$$df = \frac{\partial f}{\partial t} dt + \frac{\partial f}{\partial x} dx \quad \text{or} \quad \frac{df}{dt} = \frac{\partial f}{\partial x} \frac{dx}{dt} + \frac{\partial f}{\partial t}$$

In this equation f is a variable dependent on the two independent variables x and t , and the equations give the rate of change of f if x and t are simultaneously varied in a prescribed manner, given by dx/dt . Assume that the function f is, for example, the water depth y ($f = y(x, t)$).

$$\frac{dy}{dt} = \frac{\partial y}{\partial x} \frac{dx}{dt} + \frac{\partial y}{\partial t}$$

Here we have assumed that the function y is the water depth and we may think of the situation in the following way: to an observer walking with a speed dx/dt along a dike of an open canal, the depth y will appear to vary with time at the rate given by the equation for dy/dt . A similar result would of course be true for any other parameter such as v , q , or c .

The total differential du/dt for the function $u = v + 2c$ can be found in the same way as dy/dt and will give:

$$\frac{du}{dt} = \frac{\partial u}{\partial x} \frac{dx}{dt} + \frac{\partial u}{\partial t} \quad \text{with } v = f(x, t) \quad \text{and} \quad \frac{dx}{dt} = v + c$$

Assume that S_0 is constant and that S_0 and S_f are both relatively small. Then from this assumption follows that $g(S_0 - S_f)$ is also very small and a new set of equations for the unsteady flow can be written as:

$$(v \pm c) \frac{\partial(v \pm 2c)}{\partial x} + \frac{\partial(v \pm 2c)}{\partial t} = g(S_0 - S_f) \tag{2.55}$$

$$(v \pm c) \frac{\partial(v \pm 2c)}{\partial x} + \frac{\partial(v \pm 2c)}{\partial t} = 0 \tag{2.56}$$

Equation of non-steady flow in a rectangular channel

The first two terms at the left-hand side, namely $(v \pm c) \partial(v \pm 2c)/\partial x + \partial(v \pm 2c)/\partial t$, represents the rate of change of $(v \pm 2c)$ from the view point of two observers, one moving in the $x-t$ plane with velocity $(v + c)$ and the other moving with a velocity $(v - c)$.

The path of the two imaginary observers can be plotted on the $x-t$ plane and a complete solution will be obtained for any prescribed unsteady flow situation. Only in simple cases does the process lead to explicit solutions, but in more complex cases numerical methods may be used without any great difficulty (see Figure 2.15).

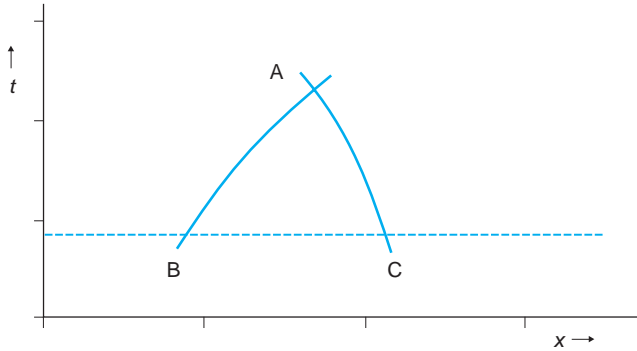


Figure 2.15. Method of characteristics in the x and t plane, with an explicit solution.

Along the line with the direction $dx/dt = v + c$, the expression $d(v + 2c)/dt = 0$ holds and along the line with the direction $dx/dt = v - c$ the expression $d(v - 2c)/dt = 0$ holds. The line with the direction $dx/dt = v + c$ is called the positive characteristic ($c+$) and the other is the negative characteristic ($c-$).

Integration of $d(v + 2c)/dt = 0$ gives that $v + 2c = \text{constant}$. The equation $d(v \pm c)/dt = 0$ means that $v \pm c$ can be treated as constant for Δt . If $dx/dt = (v \pm c)$ then $u = v \pm 2c + g(S_f - S_0)t$. The reciprocal value gives $dt/dx = 1/(v \pm c)$ which defines two lines in $x-t$ space.

Thus in this specific case that two observers move with two velocities, namely $(v \pm c)$, the two velocities $(v \pm 2c)$ appear to remain constant. The results are two families of curves in the $x-t$ plane, which have inverse slopes, namely $(v + c)$ and $(v - c)$. These lines are the characteristic lines.

Summary of the four characteristic equations of unsteady flow in a rectangular channel

The method of characteristics gives two lines:

- one line has a slope $1/(v + c)$
- the other line has a slope $1/(v - c)$

Along these two lines $\frac{du}{dt} = \frac{\partial u}{\partial x} \frac{dx}{dt} + \frac{\partial u}{\partial t} = 0$

$\frac{dt}{dx} = \frac{1}{v + c}$ defines a positive characteristic along which $v + 2c$ is constant

$\frac{dt}{dx} = \frac{1}{v - c}$ defines a negative characteristic along which $v - 2c$ is constant

In principle the terms $v \pm 2c$ and $g(S_f - S_0)$ are constant

$$\frac{dt}{dx} = \frac{1}{v \pm c} \quad (2.57)$$

$$\frac{d(v \pm 2c + g(S_f - S_0)t)}{dt} = 0 \quad (2.58)$$

The solution of the method of characteristics is based on the construction of a network of points in the $x-t$ plane where the dependent variables are computed. From a given set of two points on the network, a new point may be constructed by drawing a characteristic of one family from one point that intersects with the characteristics of the other family drawn from the other point. In general, these directions are not known initially as they depend on the solution of the dependent variables at the intersection point (see Figure 2.16). However, the solution of these variables can be found through the Riemann invariants. The almost exact direction of these characteristics can then be drawn based on the average characteristic direction at the connecting points.

The significance of the method of characteristics lies in the fact that the characteristics are to be seen as lines along which some information on the state of the fluid propagates. Along the characteristic lines, a special condition is valid, which implies that these lines are unique lines and that

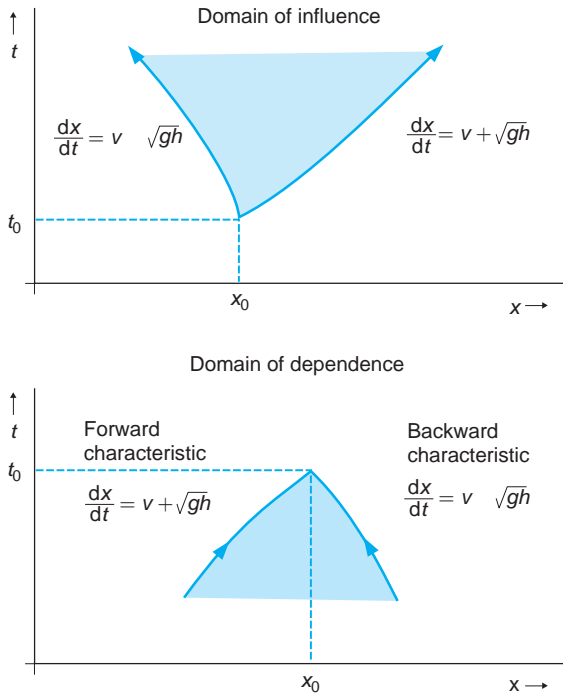


Figure 2.16. Characteristics in the x and t plane with an example of the domain of influence and of the domain of dependence.

information only travels along these characteristics. With the characteristics, it is possible to compute solutions for v and y from known conditions at an earlier point in time.

In the derivation of the method of characteristics, the auxiliary variable $c = \sqrt{gD}$ ($D = C^2/g$) has a special meaning as part of the direction of the characteristics. For example when $v=0$, the direction of both characteristics is the same in magnitude, but they have a different, opposite sign. This means that the effect of any disturbance at a certain point in a canal propagates in both directions (upstream and downstream) with the same speed c , which is a function of the square root of the water depth. The variable c here means the celerity with which disturbances propagate in stagnant water.

When $v > 0$, the characteristic directions no longer have the same magnitude and at a particular point information on the fluid state travels faster in the downstream than in the upstream direction. For increasing velocities this leads to the very specific case that no information is able to travel in the upstream direction. This happens when the celerity is equal to the velocity ($v = c$) or when the Froude number equals unity ($Fr = 1$).

For smaller velocities the flow is subcritical (the Froude number is less than unity) and the state of flow at any point in time is controlled by both the upstream and downstream conditions. In the case of supercritical flow, the state of fluid is only controlled by upstream conditions.

Wide rectangular channel

A very particular example of unsteady flow in a rectangular canal is a canal with a relatively large width. For a wide rectangular canal, the hydraulic radius is equal to the water depth ($R=y$) and the friction slope results from:

$$\frac{d(v \pm 2c)}{dx} = g(S_o - S_f)$$

$$S_f = \frac{v^2}{C^2 R} \cong \frac{v^2}{C^2 y} \text{ and } S_o = \frac{v_o^2}{C_o^2 R} = \frac{v_o^2}{C_o^2 y_o}$$

The water depth y_o ; the velocity v_o and the Froude number Fr_o are the values for normal (uniform) flow for the given discharge Q .

When we assume for this case that C is independent of the water depth (constant), then:

$$C \cong C_o \text{ and } Fr = \frac{v}{\sqrt{gy}}$$

$$S_o - S_f = S_o \left(1 - \frac{v^2}{C^2 y S_o} \right) = S_o \left(1 - \frac{v^2 y_o}{v_o^2 y} \right) = S_o \left(1 - \frac{Fr^2}{Fr_o^2} \right)$$

Remember: $v + 2c = c(v/c + 2) = c(Fr + 2)$, therefore:

$$\frac{d(v \pm 2c)}{dx} = g(S_o - S_f) \text{ becomes: } \frac{d(c(Fr \pm 2))}{dt} = g S_o \left(1 - \frac{Fr^2}{Fr_o^2} \right)$$

The Froude number, $Fr = 2$, has a special significance. If $g(S_o - S_f)$ is very small, then dc/dt and dFr/dt will have the same sign if $Fr < 2$. In most cases $Fr < 2$ will apply.

Additional information

For a canal with a general shape the hydraulic depth is $D = A/B_s$ and $c = \sqrt{gD}$

When introducing $w = \int_o^A cdA/A = \int_o^y \sqrt{gD} dy$, the following equation can be derived:

$$(v \pm c) \frac{\partial(v \pm w)}{\partial x} + \frac{\partial(v \pm w)}{\partial t} = g(S_o - S_f) \quad (2.59)$$

Channels with a general shape

This equation is similar to the equation for a rectangular canal and the velocity w corresponds to two times the celerity: $2c$.

Simple wave problem

An interesting example for the method of characteristics is the event of the simple wave, which is characterised by the straight, positive characteristics of one *family*. The simple wave and its region in the $x-t$ plane will help to understand the behaviour of complex waves and their region of interaction.

When the flow path in the $x-t$ plane is straight, meaning a line with a slope $dt/dx = 1/(v + c)$ that is constant, then the value of $(v + c)$ is constant for the positive characteristic. Moreover, for a horizontal bed without friction ($S_o = S_f \approx 0$), the value of $(v + 2c)$ becomes constant along this line and in this case both v and c are constant along the characteristic. This case is called a simple wave.

From the statements $v + c = \text{constant}$ and $v + 2c = \text{constant}$ follows that c is constant and v is constant. Furthermore, it can easily be shown that if one characteristic line is a straight line all other characteristics (of the same, positive or negative family) must also be straight lines (see Henderson, 1966).

Consider an initially steady and uniform flow (v and y constant, for example v_o and y_o , the latter gives $c = c_o$) that is then disturbed either in discharge or in water depth y , resulting in an unsteady flow, which will propagate into the initially steady region (e.g. after opening of a gate). The undisturbed flow is also uniform; this property helps to define the simple wave problem.

The acceleration terms in the dynamic equation are large compared with S_f and S_o . The total derivatives of $(v \pm 2c)$ in the equations are zero; this means that the quantities $(v \pm 2c)$ appear to remain constant to two observers moving with a velocity $(v \pm c)$.

$$(v \pm c) \frac{\partial(v \pm 2c)}{\partial x} + \frac{\partial(v \pm 2c)}{\partial t} = 0$$

The paths of these observers can be traced on the $x-t$ plane, which gives rise to two families of lines, the characteristics. Along each member of the first family the inverse slope of the line dx/dt is $(v + c)$ and its value $(v + 2c)$ is constant. Similarly along each member of the second group the inverse slope of the line dx/dt is $(v - c)$ and the quantity $(v - 2c)$ is constant.

Remember that in an unsteady flow problem there are four variables, namely x , t , v and y (or c). Consider a point along the t -axis with $x = 0$ and $t > T$. For the undisturbed zone we assume that the uniform velocity $v = v_o$ and $c = c_o$.

For any positive characteristic line $dx/dt = v + c = \text{constant}$. This means that for $t = 0$, along the first positive characteristic line $dx/dt = v_o + c_o = \text{constant}$. This gives $v + c = v_o + c_o$ and here either v or c can be expressed in the other parameters: $v = -c + v_o + c_o$ or

$c = -v + v_0 + c_0$. For any negative characteristic line $v - 2c = v_0 - 2c_0$ as it must cut $(dx/dt)_{t=0} = v_0 + c_0$; it follows that:

- $dx/dt = (3/2)v - (1/2)v_0 + c_0$; when c is eliminated in the inverse slope dx/dt
- $dx/dt = 3c + v_0 - 2c_0$; when v is eliminated in the inverse slope dx/dt

One equation can be used to compute c for any given v_0 and c_0 and for v_t at the origin (for $x, t = 0$). The other equation can be used to compute v for any given v_0 and c_0 and for c at the origin (for $x, t = 0$). From the four parameters v_0 and c_0 are known and one, either v or c , is given as a boundary condition; the given change in flow. Movement along the characteristics really represents the wave motion across the water surface; $(v + c)$ and $(v - c)$ are velocities of the waves relative to a stationary observer.

In a simple wave problem the term $(v - 2c)$ appears to be constant in the whole $t-x$ plane. The negative characteristics actually denote, therefore, waves of zero amplitude ($\Delta y = 0$). For negative waves (with y and c decreasing with time) dx/dt decreases and therefore the characteristic lines diverge; for positive waves the lines converge, which means that they eventually intersect giving at the point of intersection two depths i.e. a steep surge is formed with substantial energy losses. Therefore, the simple wave approach cannot be used beyond this point.

Final comment

The main advantage of the method of characteristics is the possibility to visualize the way in which flow disturbances or the effects of flow control travel through a canal network. The structure of the net of characteristics is also important in understanding the numerical procedures required for the practical solution of hydraulic phenomena. A good understanding of the physics of a hydraulic phenomenon will give guidance in the choice of the most appropriate numerical solution techniques and their numerical parameters. The characteristics will help to find the required initial ($t = 0$ and $x = 0$) and boundary ($t = T$ and $x = L$) conditions in the $x-t$ plane for any engineering problem simulation.

The concept of characteristics is very important for the understanding of unsteady hydraulic phenomena in canal networks; however, the method of characteristics gives an algorithm for the computation of unsteady flow only for simple cases. The inclusion of energy generating or dissipating terms, such as gravity and bottom friction terms, lateral inflow or outflow, and non-prismatic canal sections, is complicated for the method of characteristics, but is much easier in programmable solution algorithms that are based on the implicit finite difference schemes.

CHAPTER 3

Sediment Properties

3.1 INTRODUCTION

Sediments are fragmented material, primarily formed by the physical and chemical disintegration of rocks from the earth's crust; they can be divided into cohesive and non-cohesive sediments. For non-cohesive sediments there are no physical-chemical interactions between individual particles and the size and weight of an individual particle are important factors in their behaviour. In cohesive sediments the physical-chemical interactions between particles are important factors in the initiation of motion (erosion) and also in the transportation (flocculation); with cohesive sediments the size and weight of a particle have less significance. Most of the discussion on sediment transport in these lecture notes will deal with non-cohesive sediments.

Some of the major features of the individual particles and the sediments can be described by:

- Density and porosity
- Particle size and size distribution
- Shape
- Fall velocity
- Dimensionless parameters, such as the particle parameter, particle mobility parameter, excess shear stress parameter, dimensionless particle Reynolds number and transport rate parameter.

3.2 DENSITY AND POROSITY

The density of a sediment particle is the mass per unit of volume and it primarily depends on the mineral composition. Non-cohesive material originates generally from the disintegration or decomposition of quartz. The density (ρ_s) of quartz is approximately 2650 kg/m^3 and the density of clay minerals ranges from $2500\text{--}2700 \text{ kg/m}^3$.

The relative density is often expressed as Δ .

$$\Delta = \frac{(\rho_s - \rho_w)}{\rho_w} \quad (3.1)$$

The specific density s is expressed as:

$$s = \frac{\rho_s}{\rho_w} \quad (3.2)$$

$$\Delta = s - 1 = \text{relative density}$$

Where:

Δ = relative density; the relative density of quartz in water equals 1.65

s = specific density; the specific density s of quartz in water equals 2.65

ρ_s = density of the sediment particle (kg/m^3)

ρ_w = density of water (kg/m^3)

The dry bulk density of sediment is the mass per unit of volume on a dry weight basis and includes the pores between the particles. The bulk density is equal to:

$$\rho_{\text{dry}} = (1 - p)\rho_s \quad (3.3)$$

Where:

p = porosity (dimensionless)

p = the ratio of the volume pores and the total volume of a sediment sample

ρ_s = density of the sediment particles (kg/m^3)

ρ_{dry} = dry bulk density of the sediment (kg/m^3)

The porosity p often depends on the deposition and erosion processes. The bulk density of sand ($\rho_{s\text{-dry}}$) is approximately $1500\text{--}1550 \text{ kg/m}^3$. For silt the bulk density ranges between 1050 and 1320 kg/m^3 , while for clay these value may range between 500 and 1250 kg/m^3 .

Sometimes the specific weight is still used and is expressed as $\gamma = \rho_s g$ with γ in Newtons per unit of volume (N/m^3).

3.3 SIZE AND SIZE DISTRIBUTION

A first attempt to classify the individual, non-cohesive sediment particles, is based on their size; more specifically their diameter. Usually, sediments are referred to as gravel, sand, silt or clay, which refer to the size of the individual particles; listed here in decreasing magnitude. Many attempts have been made to describe the sediment by one distinct diameter and a range of sizes has been suggested, but none of them has proven to be

entirely suitable. Some of the main definitions for the diameter (Bogardi, 1974) include:

- Sieve diameter (d): diameter of the square mesh sieve, which will just let the particle pass. The sieve diameter is generally used for fractions greater than 0.1 mm.
- Settling or sedimentation diameter (d_s): diameter of a sphere with the same density and same fall velocity as the given particle in the same fluid and at the same temperature.
- Nominal diameter (d_n): diameter of a sphere or cube with the same volume as the particle.
- Tri-axial dimensions (a, b, c): the dimensions of a particle in the direction of three orthogonal axes. The largest dimension is called ' a ' and the smallest dimension is called ' c '.

The sizes can be determined by direct measurements, by sieving, by sedimentation or by microscope analysis. Table 3.1 shows a classification of sediments as recommended by the American Geophysical Union.

Table 3.1 The density of fresh water as a function of the temperature T .

T ($^{\circ}\text{C}$)	0	4	12	16	21	32
ρ_w (kg/m^3)	999.87	1000.0	999.5	999.0	998.0	995.0

Table 3.2 Classification of sediments according to their size.

Classification	$\text{mm} = 10^{-3} \text{ m}$	$\mu\text{m} = 10^{-6} \text{ m}$
Very coarse gravel	64–32	
Coarse gravel	32–16	
Medium gravel	16–8	
Fine gravel	8–4	
Very fine gravel	4–2	
Very coarse sand	2–1	2000–1000
Coarse sand	1.00–0.50	1000–500
Medium sand	0.50–0.25	500–250
Fine sand	0.25–0.125	250–125
Very fine sand	0.125–0.062	125–62
Coarse silt	0.062–0.031	62–31
Medium silt	0.031–0.016	31–16
Fine silt	0.016–0.008	16–8
Very fine silt	0.008–0.004	8–4
Coarse clay	0.004–0.002	4–2
Medium clay	0.002–0.001	2–1
Fine clay	0.001–0.0005	1–0.5
Very fine clay	0.0005–0.00024	0.5–0.24

Sediments normally have many particles with different sizes. The particle sizes result in a distribution, which is generally expressed as percent by mass (weight) versus particle size. The most common method to determine the distribution of particle sizes (size frequency) is a sieve analysis,

which can be used for particles larger than 74 μm. Next, the results are presented as a cumulative size-frequency curve. The fraction or the percentage of the sediment (by mass) that is smaller than a given size is plotted against the particle size (sometimes a fraction that is larger than a given size is plotted). The cumulative size distribution of various sediment sizes by mass can be approximated by a log-normal distribution, as shown in Figure 3.1. A log-normal distribution might result in a straight line when logarithmic probability paper is used.

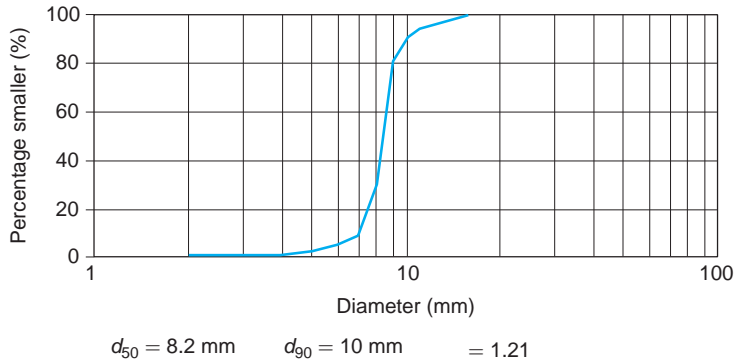


Figure 3.1. Example of particle size distributions.

From this cumulative size distribution the following sediment characteristics can be defined (van Rijn, 1993):

(a) Mean diameter (d_m or \bar{d}) is defined as:

$$d_m = \bar{d} = \frac{\sum P_i d_i}{\sum P_i} \tag{3.4}$$

Where:

P_i = fraction (percentage) with diameter d_i (%)

d_i = geometric mean of the size fraction limits = diameter for which i % of the sample is finer than d_i (mm)

(b) The median diameter (d_{50}) is assumed to give the best representation of the sediment mixture and is described by the diameter ‘ d ’ for which 50% of the sample is finer than ‘ d ’. Sometimes other values than d_{50} are used in the sediment transport predictors; examples are d_{16} , d_{35} , d_{65} , d_{84}

(c) The geometric mean diameter (d_g) is defined as:

$$d_g = \sqrt{d_{84} d_{16}} \tag{3.5}$$

Where:

d_{84} = diameter for which 84% of the sample is finer than d_{84}

d_{16} = diameter for which 16% of the sample is finer than d_{16}

(d) The standard deviation (σ_s) is described by:

$$\sigma_s = 0.5 \left(\frac{d_{84}}{d_{50}} + \frac{d_{50}}{d_{16}} \right) \quad (3.6)$$

Where:

d_{84} = diameter for which 84% of the sample is finer than d_{84}

d_{16} = diameter for which 16% of the sample is finer than d_{16}

d_{50} = diameter d for which 50% of the sample is finer than d_{50}

e) The geometric standard deviation (σ_g) is given by:

$$\sigma_g = \sqrt{\frac{d_{84}}{d_{16}}} \quad (3.7)$$

Where:

d_{84} = diameter for which 84% of the sample is finer than d_{84}

d_{16} = diameter for which 16% of the sample is finer than d_{16}

3.4 SHAPE

In addition to the diameter the shape of the sediment particle is also an important aspect. A flat particle will have a smaller fall velocity than a rounded particle and it will be more difficult to transport a flat particle as bed load. The shape of a particle can be characterized by sphericity, roundness or shape factor.

Sphericity is the ratio between the surface area of a sphere and the surface area of a particle at equal volume.

Roundness is the ratio of the average radius of the curvature of the edges and the radius of a circle inscribed in the maximum-projected area of the particle.

Sphericity and roundness are not used in sediment theories.

The shape factor is a useful definition that can be used to describe a particle. The shape factor (s.f.) is defined by:

$$\text{s.f.} = \frac{c}{\sqrt{ab}} \quad (3.8)$$

Here a , b and c are the dimensions of a particle in the direction of three axes. For spheres the shape factor is 1. For natural sand the shape factor (s.f.) is approximately 0.7 and for gravel it is approximately 0.9.

3.5 FALL VELOCITY

The velocity of sediment particles settling in a liquid is called the fall velocity w_s . This velocity is an important physical value to describe the

sedimentation and suspension behaviour of sediment particles. The basic fall velocity of sediment particles is derived from a single sphere with diameter d falling with a constant velocity in quiescent (quiet) water. At the beginning of the settling process, the fall velocity is small and the force of gravity is greater than the resistance. Hence, the sphere moves with acceleration, and the resistance increases with the velocity. In time the resistance equals the force of gravity and the sphere then falls with a constant velocity. The force of gravity acting on the sphere is in equilibrium with the resistance to the motion, which depends on the velocity and a drag coefficient.

From resistance force = gravity force:

$$C_d \frac{1}{2} \rho_w w_s^2 \frac{\pi}{4} d^2 = \frac{\pi}{6} d^3 g (\rho_s - \rho_w) \quad (3.9)$$

$$w_s = \sqrt{\frac{4}{3} \frac{g d \Delta}{C_d}} \quad (3.10)$$

The drag coefficient C_d is a function of the Reynolds number ($w_s d/\nu$). For low Reynolds numbers $C_d = 24/\text{Re}$.

For natural sand, a Reynolds number lower than 0.1 and $C_d = 24/\text{Re}$, Stokes law gives the fall velocity as:

$$w_s = \frac{(s-1)gd^2}{18\nu} \quad 1 \leq d \leq 100 \mu\text{m} \quad (3.11)$$

Where:

s = specific density of the sediment particle (dimensionless)

g = acceleration due to gravity (m/s^2)

d = diameter of the particle (m)

ν = kinematic viscosity (m^2/s)

w_s = fall velocity in clear water (m/s)

During the settling process, the motion of a particle also causes the surrounding fluid to move. If the Reynolds number is less than approximately 0.4, the effect of inertia forces induced in the fluid by the motion is much less than those due to the fluid viscosity. The settling of a single particle affects a large region of the surrounding fluid if the Reynolds number is low. When the inertia forces in the fluid are negligible then the drag coefficient is inversely proportional to the Reynolds number. The fall velocity is proportional to the square of the sphere diameter and the density, but it is inversely proportional to the viscosity of the fluid. Stokes law is valid for $\text{Re} < 0.4$ and in water at normal temperature the fall velocity is valid for particles smaller than $d = 0.076 \text{ mm}$.

For larger quartz particles Stokes law has to be adjusted and the fall velocity reads:

$$w_s = \frac{10\nu}{d} \left[\left(1 + \frac{0.01(s-1)gd^3}{\nu^2} \right)^{0.5} - 1 \right] \quad 100 \leq d \leq 1000 \mu\text{m} \quad (3.12)$$

$$w_s = 1.1\sqrt{(s-1)gd} \quad d \geq 1000 \mu\text{m} \quad (3.13)$$

Where:

w_s = fall velocity in clear water (m/s)

s = relative density of the sediment particles (dimensionless)

g = acceleration due to gravity (m/s^2)

d = diameter (m)

ν = kinematic viscosity (m^2/s)

Table 3.3 Fall velocity for sediment particles.

d (mm)	0.06	0.1	0.2	0.3	0.4	0.5	0.75	1.0	1.25	1.5	1.75	2.0	2.5
w_s (mm/s)	3.2	8.9	25	44	59	72	98	140	156	171	185	198	221

The presence of a large number of other particles during the settling process will decrease the fall velocity of a single particle. The fall velocity of a single particle influenced by the presence of other particles follows from:

$$w_{s,m} = (1 - c)^\gamma w_s \quad \text{with} \quad 2.3 \leq \gamma \leq 4.6 \quad \text{and} \quad 0 \leq c \leq 0.3 \quad (3.14)$$

Where:

$w_{s,m}$ = fall velocity influenced by other particles (m/s)

w_s = fall velocity in clear water (m/s)

c = volumetric sediment concentration (percent)

γ = coefficient, which is a function of the Reynolds number

The coefficient γ is slightly dependent on the particle shape, but this can be ignored. For fine sediments with a concentration of 1%, the reduction in fall velocity will be around 5%. The fall velocity of a particle in turbulent water is different from the velocity in quiescent water. A cluster of particles (cohesive sediments) will have a greater fall velocity.

Table 3.4 Coefficient γ as function of Reynolds number.

Reynolds number	<0.2	0.2–1	1–200	>200
γ	4.65	$4.35 \text{ Re}^{-0.03}$	$4.45 \text{ Re}^{-0.1}$	2.39

3.6 CHARACTERISTIC DIMENSIONLESS PARAMETERS

The equations of motion and continuity, both for water and sediment, roughly define the transport of water and sediment in irrigation canals. An analytical description of all the physical processes by the equations is not yet possible and therefore, the sediment transport theories still rely on data from field and experimental investigations and from dimensional analysis. Based on dimensional analysis several processes related to sediment transport can be expressed as a function of independent dimensionless parameters. The following parameters are widely used to describe the sediment transport in open channels (van Rijn, 1993).

Particle parameter (D_*) reflects the influence of gravity, density and viscosity on sediment transport and is given by:

$$D_* = \left[\frac{(s-1)g}{\nu^2} \right]^{1/3} d_{50} \quad (3.15)$$

Where:

- s = specific density of a sediment particle (dimensionless)
- g = acceleration due to gravity (m/s^2)
- d_{50} = median diameter (m)
- ν = kinematic viscosity (m^2/s)

Particle mobility parameter (θ) is the ratio of the drag force and the weight of the submerged particle and reads:

$$\theta_{\text{cr}} = \frac{u_{*\text{cr}}^2}{(s-1)g d_{50}} = \frac{\tau_{\text{cr}}}{(s-1)\rho g d_{50}} \quad (3.16)$$

Where:

- τ = shear stress (N/m^2)
- τ_{cr} = critical shear stress according to Shields (N/m^2)
- u_* = shear velocity (m/s)
- $u_* = \sqrt{\tau/\rho}$
- $u_{*\text{cr}}$ = critical shear velocity (m/s)
- $u_{*\text{crit}} = \sqrt{\tau_{\text{crit}}/\rho}$
- ρ = density (kg/m^3)
- Δ = relative density of the sediment (dimensionless)
- g = acceleration due to gravity (m/s^2)
- d_{50} = median diameter (m)

Excess bed shear stress parameter (T) is defined as:

$$T = \frac{\tau' - \tau_{cr}}{\tau_{cr}} \quad (3.17)$$

Where:

τ_{cr} = critical shear stress according to Shields (N/m²)

τ' = grain shear stress (N/m²), which is the skin resistance or the surface drag due to the grain roughness (see Chapter 5 for more details)

The particle Reynolds number parameter (Re_*) is represented by

$$Re_* = \frac{u_* d_{50}}{\nu} \quad (3.18)$$

Where:

u_* = shear velocity (m/s)

d_{50} = median diameter (m)

ν = kinematic viscosity (m²/s)

Transport rate parameter (ϕ) is represented by:

$$\phi = \frac{q_s}{(s - 1)^{0.5} g^{0.5} d_{50}^{1.5}} \quad (3.19)$$

Where:

q_s = volumetric sediment transport rate (m³/s per m width)

s = specific density of sediment (dimensionless)

g = acceleration due to gravity (m/s²)

d_{50} = median diameter (m)

The concentration (C) is the ratio between the sediment transport rate q_s and the discharge q per m width (both in volume). Here, q_s is the volume of sediment transported in 1 m³ of water-sediment mixture. The volumetric concentration reads as:

$$C = \frac{q_s}{q} \quad (3.20)$$

Where:

C = concentration of sediment in the water by volume (percentage or ppm)

q_s = volumetric sediment transport rate (m³/s per m width)

q = discharge (m³/s per m width)

The concentration C can be also expressed as a percentage by mass (C_g), which is the mass of sediment transported in a unit volume of a water-sediment mixture. The concentration C_g is expressed as the mass in kg per unit of volume in m³; the ratio of kg/m³ can also be expressed

as ppm (parts per million). For concentrations lower than 16,000 ppm, it can be assumed that 1 kg/m^3 is equivalent to 1000 ppm.

Both concentrations (by volume and by mass) are related by:

$$C_g = \Delta C \quad (3.21)$$

Where:

Δ = relative density (dimensionless);

$\Delta = 1.65$ for quartz particles in water

C = concentration of sediment by volume (percentage or ppm)

C_g = concentration of sediment by mass (percentage or ppm)

CHAPTER 4

Design Criteria for Irrigation Canals

4.1 INTRODUCTION

The objective of an irrigation canal is to meet the varying irrigation requirements during the irrigation season at the individual farms and therefore the canal design should preferably be based on the following criteria:

- *Capacity*: the capacity of an irrigation canal depends on the water delivery method. The delivery methods differ from each other through the scheduling of the water supply in time and place. The World Bank (1986) classifies the following delivery methods:
 - *on demand*: the water delivery reacts instantaneously to the water demand;
 - *continuous*: the irrigation canal supplies a continuous, either constant or varying, but continuous flow during the whole irrigation season;
 - *fixed rotation*: the water delivery is scheduled with a constant flow and a regular pattern of rotation;
 - *variable rotation*: the water delivery is programmed either for a fixed supply with variable periods (rotation) or for a variable supply and variable periods.
- *Command*: the requirement that most of the area must be irrigated (commanded) determines the water level in the canals. At any delivery point, the water level in the canal must be above the ground surface. Due to the presence of structures and the need to meet the varying irrigation requirements during the irrigation season the flow in an irrigation canal varies in time and space. The command level is also influenced by the method of flow control. For instance, the water level for downstream control and zero discharge in a canal is horizontal and above the level for full discharge (see Figure 4.1); the downstream control requires canal banks with a *level top* to facilitate the zero flow conditions (Ankum, 1995);
- *Sedimentation and/or erosion*: irrigation canals should be designed based on the criterion that no sedimentation and no erosion occur during a certain period. The design of a stable cross section will be the end result of this criterion;
- *Cost*: the final result of the design of earthen and lined canals will include the horizontal and vertical canal alignment and the cross

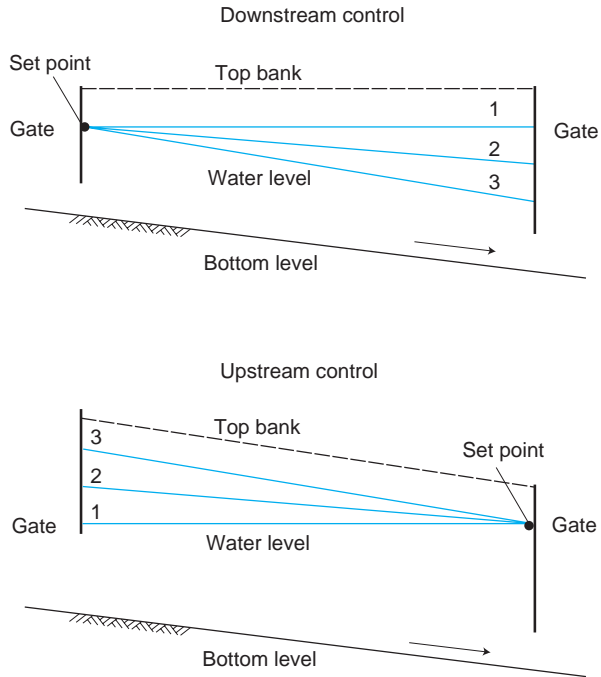


Figure 4.1. Example of a canal with downstream control and a canal with upstream control.

- 1 $Q = 0$
- 2 $0 < Q < Q_{max}$
- 3 $Q = Q_{max}$

sections of the canal. Moreover, the canal design should give the best performance at minimum cost, meaning that the final design should result in a balanced earthwork (including cut and fill) as far as possible.

4.2 THE ROLE OF SEDIMENT TRANSPORT IN THE DESIGN OF IRRIGATION CANALS

The design of irrigation canals for sediment-laden water should consider aspects related to the conveyance of irrigation water as well as the transport of sediments. The need to convey different quantities of water to meet the irrigation requirements at the required water level is the main criterion for canal design. Furthermore, the design must be compatible with a particular sediment load in order to avoid silting and/or scouring. The diverted discharge should meet the irrigation requirements and at the same time it should result in the least deposition and/or erosion in the canal network.

Vanoni (1975) stated that the canal design must be based on a comprehensive assessment of the canal operation to determine the future pattern

of the water demand. In that way the sediment transport characteristics along a canal network can be established in terms of place and time. Sediment may be deposited during one phase of operation and eroded during another phase, resulting in a balanced or stabilized condition.

According to FAO (1981), the objective of a canal design is to select the proper bottom slope and geometry of the cross section so that during a certain period the sediment flowing in is equal to the sediment flowing out of the canal. Changes that occur in the equilibrium conditions for sediment transport will result in periods of deposition and/or erosion.

Chang (1985) suggested that in view of these sediment problems, the bottom slope and the canal geometry must be interrelated in order to maintain the best possible sediment transport equilibrium. He stated that the sediment problem can be controlled by maintaining the continuity in sediment transport in the irrigation canals during the design stage.

Dahmen (1994) pointed out that an irrigation network should be designed and operated in such a way that:

- the required flow passes at the design water level;
- no erosion of the canal bottom and banks occurs;
- no deposition of sediment in the canal takes place.

The design of a canal that has to convey a certain sediment load requires a set of equations related to the water-sediment flow to provide the unknown variables of bottom slope and cross section (bottom width and water depth). The geometry of an irrigation canal that carries water and sediment will be the end result of a design process in which the flow of water and the transport of sediments interact.

In view of the design, irrigation canals can be divided into three categories (Ranga Raju, 1981) that can be described as follows:

- *canals with a rigid boundary*: the design is based on the determination of the velocity at which any sediment entering into the canal will not settle on the canal perimeter. High velocities are allowed, but they should not damage the lining or create large disturbances in the water surface. A numerical simulation of the most likely changes in the flow conditions during the irrigation season becomes an important tool to ensure that the sediment is not deposited, even when the velocity is low;
- *canals with an erodible boundary and carrying clean water*: the canal design is based on the determination of the maximum velocity for which the bed material in the cross section does not move. The minimum cross section with a maximum velocity that does not result in scouring of the bed should be the end result of the design;
- *canals with an erodible boundary and carrying water with sediment*: the design principle assumes that the canal should transport the water as well as the sediment. The cross section must ensure flow velocities as large as possible to convey the sediment and at the same time not too large to prevent scouring of the bed. It is evident that it is difficult

to meet both restrictions simultaneously and for the whole irrigation season. Therefore, the design must look for a stable canal over a longer period and this means that the total sediment inflow during a certain period must equal the total sediment outflow.

A major conclusion to be drawn from the previous section is the need for the design of stable irrigation canals during the full operating life of the irrigation network. Sediments may be deposited during one phase of the irrigation season and be eroded during another phase, but for the total operation period, there should be a balance between erosion and deposition in the canal.

Chow (1983), Raudkivi (1990), HR Wallingford (1992), Simons and Sentürk (1992), and others mention four methods for the design of stable canals:

- the regime method;
- the tractive force method;
- the permissible velocity method;
- the rational method.

4.2.1 *Regime method*

For the regime theory a set of simple, but empirical, equations are available. The equations are derived from observations of alluvial canal systems that are relatively stable or, in other words, are *in regime* (HR Wallingford, 1992). The regime method considers the three main features of a canal, namely the perimeter of the open canal, the amount of water and the sediment flowing in it, as a whole. It attempts to derive the most crucial characteristics of a stable (non-silting and non-scouring) canal primarily on the basis of field and laboratory studies that investigated the interaction of the above-mentioned factors (Naime, 1990). The regime theory originates from India and Pakistan and is completely empirical due to the fact that it is based on data observed in canals in regime. Most of the canal designs in these countries use this method, specifically the Lacey regime theory. The regime equations are based on past and present observations and experiences and they present a long-term average rather than an instantaneously variable state. Therefore, the regime method tries to express the natural tendency of canals that convey sediment within alluvial boundaries, in order to seek a dynamic stability.

Canals are described as in regime if they do not change over a period of one or more typical water years. Within this period, scour and deposition are allowed to occur as long as they do not interfere with canal operations. Since the observed canals withdraw varying amounts of water and sediment from different rivers and since sediment excluders may be in operation at some of the head works, the regime theory can only provide some approximate average design values. Nevertheless, the adequate

experience obtained from the design and operation of these canals give some proficient guidance for the design of stable channels with erodible banks and sediment transport. However, the applicability of this method can be challenged in the case of highly time-dependent operational regimes as practised in many irrigation systems at present (Bruk, 1986).

Some of the equations given by Lacey are (Ackers, 1992):

$$f = \sqrt{2520d} \quad (4.1)$$

$$P = 4.836Q^{0.5} \quad (4.2)$$

$$v = 0.6459(fR)^{0.5} \quad (4.3)$$

$$S_0 = 0.000315 \frac{f^{5/3}}{Q^{1/6}} \quad (4.4)$$

Where:

f = Lacey's silt factor for a sediment size d

d = sediment size (m)

P = wetted perimeter (m)

Q = discharge (m^3/s)

R = hydraulic radius (m)

v = mean velocity (m/s)

S_0 = bottom slope

According to Lacey (1958) these equations are applicable within the following range of flow and sediment characteristics:

- Discharge in the range of 0.15–150 m^3/s ;
- Bed material is non-cohesive;
- Bed form characterised by ripples;
- Bed material size in the range of 0.15–0.40 mm;
- Bed load is relatively small.

The following steps are recommended when using the Lacey equations for the design of earthen canals for a given diameter d and discharge Q ;

- Determine the factor f for the given diameter d ;
- Find the bottom slope S_0 and the perimeter P ;
- By trial and error determine the velocity v and area $A = Q/v$ and the hydraulic radius $R = A/P$;
- Determine the full cross section both by using the perimeter P and the hydraulic radius R and by assuming that the cross section is trapezoidal with a side slope of 1 V : 2 H.

Table 4.1 gives an example of the main dimensions of an earthen canal designed according to the Lacey method for a canal that conveys a discharge in the range from 1–8 m^3/s and that transports sediment with a diameter $d = 0.001$ and 0.0005 m, respectively. The f -values for these diameters are 1.58745 and 1.1225, respectively. The side slope m is 2.

Table 4.1 Example of the design of earthen canals for two sediment diameters according to the Lacey method.

Lacey regime theory in SI-units

Q m ³ /s	d in m	m	f	S_o	P	v	A	R	B -bottom	y	n Manning
1	0.001	2	1.58745	0.000680	4.836	0.515	1.940	0.401	2.316	0.563	0.028
2	0.001	2	1.58745	0.000606	6.839	0.579	3.457	0.505	3.863	0.666	0.027
3	0.001	2	1.58745	0.000567	8.376	0.619	4.846	0.579	5.065	0.740	0.027
4	0.001	2	1.58745	0.000540	9.672	0.649	6.159	0.637	6.091	0.801	0.026
5	0.001	2	1.58745	0.000520	10.814	0.674	7.418	0.686	7.004	0.852	0.026
6	0.001	2	1.58745	0.000505	11.846	0.695	8.635	0.729	7.835	0.897	0.026
7	0.001	2	1.58745	0.000492	12.795	0.713	9.819	0.767	8.604	0.937	0.026
8	0.001	2	1.58745	0.000481	13.678	0.729	10.975	0.802	9.324	0.974	0.026
1	0.0005	2	1.12250	0.000382	4.836	0.459	2.178	0.450	1.693	0.703	0.025
2	0.0005	2	1.12250	0.000340	6.839	0.515	3.880	0.567	3.275	0.797	0.025
3	0.0005	2	1.12250	0.000318	8.376	0.551	5.440	0.649	4.459	0.876	0.024
4	0.0005	2	1.12250	0.000303	9.672	0.579	6.914	0.715	5.463	0.941	0.024
5	0.0005	2	1.12250	0.000292	10.814	0.600	8.327	0.770	6.353	0.997	0.024
6	0.0005	2	1.12250	0.000283	11.846	0.619	9.693	0.818	7.163	1.047	0.024
7	0.0005	2	1.12250	0.000276	12.795	0.635	11.021	0.861	7.913	1.092	0.024
8	0.0005	2	1.12250	0.000270	13.678	0.649	12.319	0.901	8.614	1.132	0.024

As an extra illustration, the table also gives the bottom width B and the water depth y as well as the Manning’s roughness coefficient that has been calculated from the equation

$$v = \frac{1}{n} R^{2/3} S_o^{1/2}$$

For increasing discharge Q , the bed width B , the water depth y and the B/y -ratio will increase. The bottom slope S_o will decrease with an increase of the discharge Q . The regime theory results in relatively wide and shallow cross sections.

4.2.2 Tractive force method

The minimum velocity in an irrigation canal should not induce sedimentation and at the same time the velocity should limit unwanted aquatic weed growth and reduce health risks (for example, schistosomiasis). The minimum velocity is a function of the shape of the canal. For large canals, a velocity of 0.30 m/s is recommended (Dahmen, 1999). Smaller velocities result in uneconomic large cross sections. A velocity of 0.10 to 0.15 m/s is recommended for minor canals (for instance, tertiary and small secondary canals); smaller velocities result in uneconomic wide sections.

The maximum permissible velocity should not cause erosion of the bottom and side slopes and a critical shear stress criterion is applied, which is extremely dependent on the fact that:

- the resistance to erosion increases when smaller particles are washed out;
- an aged canal has more resistance to erosion than a newly constructed one;
- colloidal matter in the water will increase the cohesion of the particles that form the boundaries, resulting in a larger resistance;
- a higher ground water table than the canal water level will decrease the resistance; a lower ground water level will increase the resistance.

The tractive force depends on the shear stress at the bottom, which can be expressed as (Dahmen, 1994):

$$\tau = c\rho gyS_0 \quad (4.5)$$

Where:

τ = tractive force (N/m²)

c = correction factor; the correction factor c depends on the B/y ratio:

for $1 < B/y < 4$: $c = 0.77 e^{0.065(B/y)}$

for $B/y \geq 4$: $c = 1$

$\rho = \rho_w$ = density of water (1000 kg/m³)

S_0 = bed slope (m/m)

y = water depth (m)

g = acceleration due to gravity (m/s²)

The tractive force concept primarily originates from work carried out by the U.S. Bureau of Reclamation (USBR) under the direction of Lane (Raudkivi, 1990 and HR Wallingford, 1992). This method considers the balance of forces acting on sediment grains and is only used to evaluate the erosion limits. Since the method assumes no suspended and bed material transport, it is only relevant for canals with coarse bed material and zero or very small bed material input (HR Wallingford, 1992). Breusers (1993) also supported the statement that the tractive force method is only suitable when the water transports very little or no sediment.

The tractive force method was developed for the threshold condition of sediment transport, which occurs for the critical boundary shear stress along the canal's perimeter. Field studies on very coarse material showed that the 'critical shear stress', above which motion would start, is approximately $0.94 \cdot D_{75}$ (N/m²). For the canal design a boundary shear stress of 80% of the critical shear stress is recommended: $\tau_{\text{design}} = 0.75 \cdot D_{75}$ (D_{75} in mm). The allowable shear stress is a function of the mean diameter and the sediment concentration of the water; see Table 4.2.

Dahmen (1994) suggested as a *rule of thumb* for many irrigation engineers, that the maximum boundary shear stress in 'normal soil',

for a ‘normal canal’ and under ‘normal conditions’ can be between 3 and 5 N/m². When the shear stress is too high, the most sensitive factor to reduce this factor is a gentler bottom slope. Table 4.2 shows some recommended values for the critical shear stress (N/m²) along the boundary for fine, non-cohesive sediment.

Table 4.2 Recommended critical shear stress (N/m²) for fine, non-cohesive sediment (Dahmen, 1994).

Recommended critical boundary shear stress in N/m ²			
D ₅₀ (mm)	Clear water	Light load	Heavy load
0.1	1.20	2.40	3.60
0.2	1.25	2.49	3.74
0.5	1.44	2.64	3.98

For cohesive soils no definite criteria exist, but based on field data, the USBR gives the following values (see Table 4.3).

Table 4.3 Limiting boundary shear stress (N/m²) in cohesive material.

	Compaction			
	Loose	Fair	Well	Very well
Void ratio	2.0–1.2	1.2–0.6	0.6–0.3	0.3–0.2
Cohesive bed material	Limiting boundary shear stress (N/m ²)			
Sandy clays	1.91	7.52	15.7	30.2
Heavy clay soils	1.48	6.75	14.6	27.0
Clays	1.15	5.94	13.5	25.4
Lean clayey soils	0.96	4.60	10.2	16.9

Note: the void ratio is the ratio of the volume of voids and the volume of the solid particles.

The shear stress on the side slopes is only considered when the bed and sides are covered with coarse, non-cohesive material. For this situation the shear stress together with the angle of repose has to be taken into account. For fine, non-cohesive material and for cohesive material the component of the weight is small and can be ignored.

The values of the critical boundary shear stress are established for the design of straight canals and they should be reduced for sinuous canals; Table 4.4 presents some reduction values (in %) for non-straight canals.

Table 4.4 Reduction of the limiting boundary shear stresses in non-straight canals.

Slightly sinuous	10%
Moderately sinuous	25%
Very sinuous	40%

As discussed in this chapter, the design of irrigation canals needs at least four equations to establish the main dimensions of the canal. For earthen canals the side slope will be based on the (estimated) canal depth and soil properties and therefore, three equations are required to determine the remaining variables. Hence, the application of the tractive force method requires two other equations: for example one equation to compute the discharge (Manning, Strickler or de Chézy) and another for the relationship between the bottom width and the water depth (B/y).

The hydraulically optimal cross-section has a minimized perimeter P , which results in a maximum flow velocity at minimum cost. However, the optimum hydraulic section is hardly ever applied; this is because it will not be stable due to relatively deep excavations and also any change in discharge severely affects the water depth and the velocity. A deep section is nevertheless applied wherever possible, because the expropriation costs will be less, the velocity is higher in a deep than in a shallow canal and the sediment transport capacity is larger in deeper canals (the transport capacity is linear with the bottom width, but exponential with the water depth). To limit the excavation and expropriation cost, canal side slopes are designed to be as steep as possible. Soil material, canal depth and the danger of seepage determine the maximum slope of a stable side slope. The side slope has to be stable under *normal conditions*, also against erosion. For deep excavations, an extra berm can be included to improve the slope stability. Table 4.5 presents some values for side slopes in irrigation canals.

Table 4.5 Recommended side slope (m) in canals.

Material	Side slope 1 V : m H
Rock	0.0
Stiff clay	0.5
Cohesive medium soils	1.0–1.5
Sand	2.0
Fine, porous clay, soft peat	3.0

The top width of canal embankments depends on the soil type, the side slope and special requirements in view of maintenance and operation. Water levels may rise above the design water level due to deterioration of the canal embankment, a sudden closure of a gate or unwanted drainage inflow. A freeboard, being the distance between the design water level and the canal bank, is provided to safeguard the canal against *overflowing* during unexpected water level fluctuations and wave actions. USBR recommends a freeboard $F = C y$, where the coefficient C varies between 0.5 to 0.6 with a minimum freeboard of 0.15 or 0.20 m.

4.2.3 Permissible velocity method

Depending on the fact whether a canal will be erodible or non-erodible, the permissible velocity concept can be used as a design criterion for stable canals.

- The minimum permissible velocity is defined as that velocity that will not result in sedimentation or induce the growth of aquatic weeds. This velocity depends on the sediment transport capacity of the canal.
- The maximum permissible velocity is that velocity that will not cause erosion. This velocity is difficult to ascertain and is very variable; it can only be estimated with experience and sound judgment (Chow, 1983).

Table 4.6 presents some permissible velocities depending on the bed material (Simons and Sentürk, 1992) together with the maximum permissible velocities recommended by Fortier and Scobey. The USBR has derived from these velocities the corresponding tractive-force values (Chow, 1983).

Table 4.6 Maximum permissible velocity (v) and the corresponding tractive-force value (τ).

Material	Manning n	Clear water		Silt-loaded water	
		v (m/s)	τ (N/m ²)	v (m/s)	τ (N/m ²)
Fine sand, colloidal	0.02	0.46	1.30	0.76	3.61
Sandy loam, non-colloidal	0.02	0.53	1.78	0.76	3.61
Silt loam, non-colloidal	0.02	0.61	2.31	0.91	5.29
Alluvial silts, non-colloidal	0.02	0.61	2.31	1.07	7.22
Ordinary firm loam	0.02	0.76	3.61	1.07	7.22
Volcanic ash	0.02	0.76	3.61	1.07	7.22
Stiff clay, very colloidal	0.025	1.14	12.51	1.52	22.13
Alluvial silts, colloidal	0.025	1.14	12.51	1.52	22.13

4.2.4 Rational method

The design of irrigation canals typically tries to find the four unknown dimensions, which include the bottom slope S_0 , bottom width B , water depth y and side slope m . The side slope m should be based on the soil properties and the (estimated) canal depth y . Hence, three equations are required to determine the remaining variables. They might include an alluvial friction predictor (de Chézy, Manning, and Strickler), a sediment transport predictor and a minimum stream power or maximum sediment transport efficiency. Sometimes a regime relationship is used to provide a relationship for bottom width and water depth (HR Wallingford, 1992).

The rational method includes, amongst others, the method of White, Bettess and Paris (1982) and Chang (1985). The rational method is useful for the design of stable canals with very specific flow conditions.

For canals with large variations in discharge and sediment load the method is inadequate to describe accurately the sediment transport process and the conveyance of the sediment load through the whole canal network.

Transport of suspended load

To describe the conveyance of suspended sediment through the whole network it is practical to assume that the fine particles in suspension have an almost constant distribution over the full vertical. Normally the sediment particles in suspension fall in the range 'very fine' and their size is less than 50 to $70 \cdot 10^{-3}$ mm. De Vos (1925) stated that the relative transport capacity (T/Q) is proportional to the average energy dissipation per unit of water volume.

$$\frac{T}{Q} \propto \rho_w g v_{av} S_0 \quad (4.6)$$

Where:

T/Q = relative transport capacity

T = sediment transport load (m^3/s)

Q = discharge (m^3/s)

ρ_w = density of water (kg/m^3)

g = acceleration due to gravity (m/s^2)

v_{av} = average velocity (m/s)

S_0 = bottom slope (m/m)

From energy considerations follows that the sediment particles will be transported in any concentration by the flowing water when the fall velocity w is smaller than a certain threshold.

$$w \leq \left(\frac{\rho_w}{\rho_s - \rho_w} \right) v_{av} S_0 \quad (4.7)$$

Where:

w = fall velocity (m/s)

ρ_s = density of the sediment particles (kg/m^3)

ρ_w = density of water (kg/m^3)

S_0 = bottom slope (m/m)

To convey sediment in suspension the hydraulic characteristics of a canal network should be such that $\rho_w g v_{av} S_0$ or $v_{av} S_0$ either remains constant or does not decrease in a downstream direction. From $v_{av} = C (\gamma S_0)^{0.5}$ in which C is a general smoothness factor, follows that γS_0^3 or $\gamma^{1/3} S_0$ should be constant or non-decreasing in order to convey the suspended load in wide canals.

Transport of bed load

For canal networks that transport some material as bed load, it is possible to establish a comparable criterion as for the transport of suspended load.

Irrigation canals that carry substantial sediment loads can not be treated either by the rational method or in this way.

Bed load transport will mainly occur on or above the canal bottom; almost no transport will occur on the banks. The bed load might be some sediment with a diameter larger than $50 \text{ to } 70 \cdot 10^{-3} \text{ mm}$. The amount of bed load transport mainly depends on the shear velocity $v_* = (g y S_0)^{0.5}$. The continuous transport of bed load material can be described by one of the various sediment transport formulae, for example Engelund Hansen, Ackers-White, Brownlie, etc.

The relative transport capacity is:

$$\frac{T}{Q} \propto \frac{B * y^3 * S_0^3}{B * y * y^x * S_0^z} \tag{4.8}$$

$$\frac{T}{Q} \propto y^{2-x} S_0^{3-z} \tag{4.9}$$

Where:

T/Q = relative transport capacity

T = sediment transport load (m^3/s)

Q = discharge (m^3/s)

B = bottom width (m)

y = water depth (m)

S_0 = bottom slope (m/m)

x, z = exponents depending on the choice of the water flow equations, for instance Manning, Strickler, de Chézy or Lacey.

For example, the exponents for the regime theory are $x = 0.75$ and $z = 0.5$; for the Strickler equation they are $x = 3/2$ and $z = 0.5$.

To prevent sedimentation the relative transport capacity $T/Q = y^{2-x} S_0^{3-z}$ should either be constant or not decrease in the downstream direction of the irrigation network. For $x = 0.75$ and $z = 0.5$ the relationship T/Q is proportional with $y^{0.5} S_0$. Also with other flow equations (Manning, Strickler or de Chézy) and sediment transport predictors (for instance, Engelund-Hansen or Einstein-Brown) the relative sediment transport capacity proves to be almost proportional with $y^{0.5} S_0$.

To prevent erosion the boundary shear stress or the shear velocity should not increase, but should remain constant or decrease in a downstream direction.

The shear velocity follows from:

$$v_* = \sqrt{g y S_0} \tag{4.10}$$

In order to have no erosion in the canal network the shear stress should be constant or non-decreasing, meaning that $y S_0$ should be constant or non-decreasing.

It might be expected that when a flow only transports a small amount of bed load, the criterion for a continuous conveyance of bed load should be somewhere in between the two values. The criterion to convey any non-suspended (bed) material depends strongly on the water and sediment equations. Therefore, the criterion is that the relative transport capacity for bed load (T/Q) should be non-decreasing, or in the case of potential erosion, should remain constant; the numeric approximation for this bed load transport is that $y^{1/2} S_0$ is constant or non-decreasing.

Summarizing the rational method criteria

The design criterion for the conveyance of sediment through a canal system can be based on energy dissipation considerations; the relative sediment transport capacity follows from these considerations and is given by de Vos (1926) and Vlugter (1962).

Based on their works, Dahmen (1994) states that:

- for the conveyance of sediment in suspension, the hydraulic characteristics of the canal system should be such that:

$$\rho g v S_0 = \text{constant or non-decreasing in downstream direction} \quad (4.11)$$

- for the conveyance of non-suspended sediments, the hydraulic characteristics of the canal system should be such that:

$$y^{1/2} S_0 = \text{constant or non-decreasing in downstream direction} \quad (4.12)$$

4.3 FINAL COMMENTS

The preceding sections clearly show that the design of stable irrigation canals should be based on irrigation considerations, including engineering, agricultural, management and economic aspects. An optimal canal design is difficult to achieve and the final canal design will have to balance all these criteria to find the best solution for the explicit conditions of a specific irrigation system.

The existing design methods are based on the interrelation of equations for specific water flow and sediment transport conditions in an effort to design stable canals. However, the input variables will vary widely during the irrigation season and, moreover, during the lifetime of the irrigation network. Most of the time, non-equilibrium conditions prevail in the irrigation networks and therefore, the initial assumptions for a stable canal design are no longer valid. Also lined canals experience sedimentation problems due to variations in either flow conditions or incoming sediment load that produce non-equilibrium conditions for the transport of the sediment. Therefore, sediment problems in irrigation canals should be analysed in a more integrated context, including all the alternative operation scenarios for water flow and sediment transport in time and space.

The canal design methods as discussed above do not directly use available information on sediment characteristics, such as sediment size and concentration. Nowadays the design of irrigation canals is the product of complex and difficult to determine parameters such as water flow, required water levels, sediment load, structure control and operation and management strategies. No design packages are available that deal with all the parameter at the same time. When analyzing one parameter, others are either ignored or assumed to be constant. Therefore, it is obvious that a mathematical model for the specific conditions of irrigation canals will be an important tool for designers and managers of irrigation systems.

CHAPTER 5

Sediment Transport Concepts

5.1 INTRODUCTION

From a mathematical point of view, the interrelation between specific water flow and sediment transport conditions for a one-dimensional phenomenon without changes in the shape of the cross section can be described by the following equations (Cunge, 1980):

- *Continuity equation for water movement:*

$$\frac{\partial A}{\partial t} + \frac{\partial Q}{\partial x} = 0 \quad (5.1)$$

- *Dynamic equation for water movement:*

$$\frac{\partial h}{\partial x} + \frac{v^2}{C^2 R} + \frac{\partial z}{\partial x} + \frac{v}{g} \frac{\partial v}{\partial x} + \frac{1}{g} \frac{\partial v}{\partial t} = 0 \quad (5.2)$$

- *Friction factor predictor* which can be given as a function of:

$$C = f(d_{50}, v, h, S_0) \quad (5.3)$$

- *Continuity equation for sediment transport:*

$$(1 - p)B \frac{\partial z}{\partial t} + \frac{\partial Q_s}{\partial x} = 0 \quad (5.4)$$

- *Sediment transport equation* which can be given as a function of:

$$Q_s = f(d_{50}, v, h, S_0) \quad (5.5)$$

Where:

Q_s = sediment discharge (m^3/s)

B = bottom width (m)

d_{50} = mean diameter of sediment (m)

p = porosity (dimensionless)

z = bottom level above datum (m)

v = average velocity (m/s)

$h = y$ = water depth (m)

S_0 = bottom slope (m/m)

R = hydraulic radius (m)

These five equations form a non-linear partial differential system, which cannot be solved analytically, but instead by a numerical method (Cunge, 1980). These implicit equations are not independent; they depend on each other. For instance, the water flow influences the roughness coefficient and, vice versa, the sediment transport depends strongly on the water flow.

Many mathematical models are based on the finite difference method in which the equations are replaced by a set of discrete numerical equations, which can be solved by one of the following methods:

- *Uncoupled solution*: firstly, the equations related to the water movement are separated from the total set of equations. Next, these equations are solved and the results are used to solve the sediment transport equation and the continuity equation for sediment transport. The uncoupled solution can be used for long-term simulations that experience gradual changes (Chuang, 1989);
- *Coupled solution*: the equations for the water movement and sediment transport are solved simultaneously, which requires general boundary conditions for the water flow and the sediment transport. In this way, numerical oscillations or instabilities are reduced. This method is recommended for short-term simulations that experience rapid changes (Chuang, 1989).

Although one-dimensional flow is rarely found in nature, in this book the water flow in an irrigation canal will be considered to be one-dimensional. The main assumptions for a one-dimensional flow are that the main flow direction is along the canal axis (x-direction), that the velocity is averaged over the cross section and that the water level perpendicular to the flow direction is horizontal. Other assumptions are that the effect of the boundary friction and turbulence are accounted for by the resistance laws and that the curvature of the streamlines is small and has a negligible vertical acceleration. For these assumptions, the general equations for one-dimensional flow can be described by the de Saint-Venant equations, which read as (Cunge et al, 1980):

$$\frac{\partial A}{\partial t} + \frac{\partial Q}{\partial x} = 0 \quad (5.6)$$

and

$$\frac{\partial h}{\partial x} + \frac{v^2}{C^2 R} + \frac{\partial z}{\partial x} + \frac{v}{g} \frac{\partial v}{\partial x} + \frac{1}{g} \frac{\partial v}{\partial t} = 0 \quad (5.7)$$

The amount of water flowing into irrigation canals during the irrigation season and moreover during the lifetime of the irrigation network is not constant. Seasonal changes in crop water requirement, water supply and

variation in size and type of the cropping pattern occur frequently during the life of an irrigation canal. Hence, the canal must be designed and constructed with a certain degree of flexibility to deliver different amounts of water. Irrigation canals are designed for a specific design flow, but most of the time they will convey a variety of discharges and therefore it is often necessary to have a certain control to maintain the desired flow rates and required water levels.

From a computational point of view, the significance of the unsteadiness of the flow in irrigation canals must be considered from two aspects:

- Firstly, the computation of the flow at any point of the system requires a good knowledge of the response time in order to deliver the right amount of water to the right place and at the right time. The water delivery requires proper planning and operation and the flow has to be controlled. The delivery methods will result in unsteady flow conditions due to the initiation and termination of the water supply, changes in flow rate, stoppage of lateral flows, changes in gate settings, etc. Unsteady flow conditions exist most of the time and will seriously affect the water distribution. The response time of an irrigation system is a function of the distance between the origin of the disturbance and the point of interest, the celerity of the wave propagation and the operation time of the structures (see Figure 5.1). It is essential that the response time is known in view of the various changes in flow conditions (Schuurmans, 1991).
- Secondly, the flow computations for the determination of the temporal morphological changes in the canal can be based upon the assumption that the flow can be easily schematised as quasi-steady. Observations of the morphological changes in the canal bottom have shown them to be so slow that for the computation of the water movement the bottom can be considered to be fixed during a single time step (de Vries, 1965).

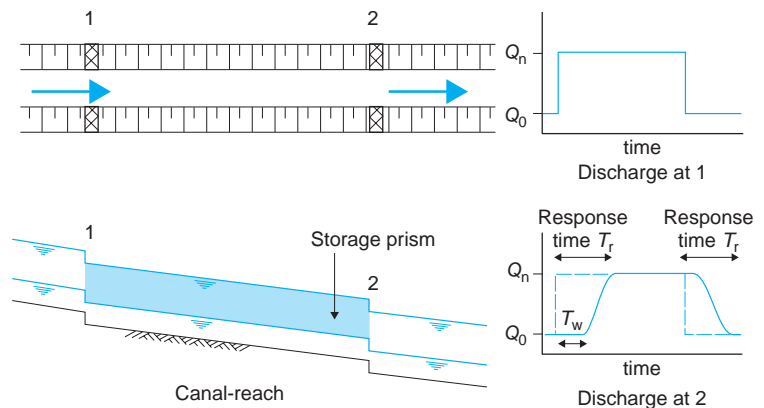


Figure 5.1. Hydro-dynamic performance of an irrigation canal with the intended and actual flow at the cross-sections 1 and 2.

For the assumption as to whether the unsteady flow in the irrigation canal may be treated as a quasi-steady flow, two facts are considered.

- In order to avoid a very wavy water surface in the canals, which will affect the canal operation, it is recommended to maintain low Froude numbers and to limit the number to a maximum of 0.30–0.40 (Ranga-Raju, 1981). For Froude numbers smaller than 0.4 the celerity of a disturbance along the water surface is not influenced by the mobility of the bed. For this condition the wave celerity is about 200 times faster than the celerity of the bed disturbances. The relative celerity of the disturbances along the water surface, being the ratio between the wave celerity and the flow velocity, is to a great extent larger than 1; while the relative celerity of the bed disturbances, being the ratio between the celerity of these disturbances and the flow velocity, is much smaller than 0.005. When the wave celerity along the water surface is much larger than the celerity of the bed disturbances it can be assumed that the disturbances of the bed will have a negligible influence on the water movement (de Vries, 1987).
- On the other hand, control structures in irrigation networks are operated in a very slow but sure way to avoid surges with steep wave fronts. This means that changes in discharge are very gradual over time and therefore the unsteady flow in an irrigation system can be approximated by a quasi-steady flow (Mahmood, 1975).

This text focuses on sediment transport processes in irrigation canals and not on water delivery; therefore, the flow will be schematised as a quasi-steady flow. Hence, the terms $\delta v/\delta t$ and $\delta A/\delta t$ in the continuity and

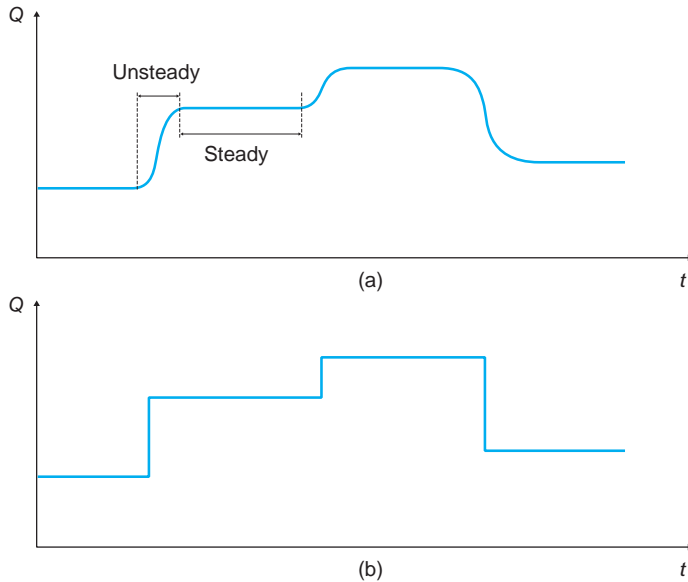


Figure 5.2. Hydrographs in an irrigation canal: (a) typical, (b) schematised.

dynamic equation can be ignored. Figure 5.2 shows two hydrographs in an irrigation canal: (a) a typical one; (b) a schematised one for a quasi-steady state.

Based on these considerations the flow equations can be simplified as:

- *Continuity equation:*

$$\frac{\partial Q}{\partial x} = 0 \quad (5.8)$$

Q is constant for steady flow.

- *Dynamic equation:*

$$\frac{dh}{dx} = \frac{S_o - S_f}{1 - Fr^2} \text{ with } Fr = \frac{v}{\sqrt{gh}} \text{ for gradually varied flow} \quad (5.9)$$

5.2 FRICTION FACTOR PREDICTORS

The hydraulic resistance of water flowing in open canals is also influenced by the development of bed forms such as ripples, mega-ripples and dunes. This resistance is measured in terms of a friction factor, for instance, the de Chézy coefficient. Other examples of friction factors are the Darcy-Weisbach and the Manning/Strickler coefficients.

The determination of the de Chézy coefficient of a movable bed is complex and requires knowledge of the implicit process of flow conditions and bed form development. The hydraulic resistance or roughness depends on the flow conditions, such as velocity, water depth and sediment transport rate, but these conditions also strongly affect the bed form development and hence the roughness. In fact, the dynamics of the bed form development and the variety of bed configurations that may simultaneously occur obstruct the development of an equation that accurately describes the roughness and the related friction factor.

Another important feature that determines the flow in canals is the correct estimation of the composite roughness. In many canals the flow very often encounters a roughness along the bottom that is different from the roughness of the sides. Also the development of bed forms on the bottom; different roughness along the bottom and the sides; and vegetation on the side banks are some of the characteristic conditions in irrigation canals that might influence the flow of water and sediment. Canals with different roughness along the perimeter need a composite roughness that should be based on the weighted roughness of the various components. In the past, several methods have been developed to compute the composite roughness from some basic assumptions concerning the flow in the canal.

5.2.1 Bed form development

The flow in most irrigation canals is sub-critical, meaning that the Froude number is smaller than 1. More especially the flow in irrigation canals is found in the lower flow region with Froude numbers smaller than 0.7 and even smaller than 0.4 (Ranga-Raju, 1981). Bed features for these low flow regimes can be described as a flat bed, as ripples or as dunes. The latter two forms are characterized by rough triangles in the longitudinal profile with a gentle sloping upstream face and a more inclined downstream face (see Figure 5.3).

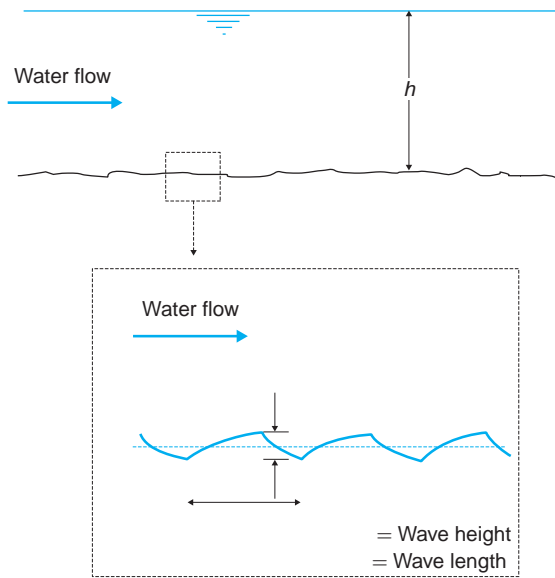


Figure 5.3. Schematic representation of bed forms for the low flow regime.

No sharp distinction exists between ripples and dunes, but they show some subtle differences. ASCE (1966b) described these bed forms as:

- *flat bed*: a flat bed is a surface without any bed form. There is no motion of the sediment on flat beds;
- *ripples*: ripples are a bed form to be found in canals with bed material smaller than 0.6 mm; the wave length is shorter than 30 cm and the wave height is a few centimetres. When the velocity is slightly greater than the threshold value several ripples will be formed in the bed. The ripple geometry is almost independent of the flow conditions;
- *dunes*: dunes are a bed form that occurs in flows with a larger velocity. Dunes develop for all sizes of bed sediment and their length and height are greater than those of ripples. Moreover, the sediment transport in

canals with dunes is larger than in canals with ripples. The geometry of the dunes strongly depends on the flow depth.

Several authors have analysed the bed forms as observed under flume and field conditions and tried to explain the type of bed forms for certain flow conditions. They presented graphical solutions for the prediction of bed forms by using dimensional and non-dimensional plots. Some of these authors are Liu (1957), Simons and Richardson (1966), Bogardi (1974) and van Rijn (1993). Each theory is based on a particular classification parameter as presented in Table 5.1.

Table 5.1. Classification parameter used in bed form theories.

Author	Classification parameter
Liu (1957)	u_* / w_s and $u_* d_{50} / \nu$
Simons & Richardson (1966)	τv and d_{50}
Bogardi (1974)	$g d_{50} / u_*^2$
van Rijn (1993)	T and D_*

In order to find an appropriate theory to describe and predict the type of bed forms in irrigation canals the theories developed by Liu (1957), Simons and Richardson (1966), Bogardi (1974) and van Rijn (1984c) have been compared on the basis of field and laboratory data. These theories explain the bed forms for one-directional flows and for homogeneous conditions, both in time and space (Jansen, 1994). Brownlie compiled an extensive set of data on sediment transport and bed forms from the laboratory and field data available at that time. For the development of the computer program SETRIC (see Chapter 6), a selection of data was made from the compilation that was published in 1981 and this data was used to compare the various theories on bed forms.

The selection of the data was based on the flow conditions and the sediment characteristics that are normally encountered in irrigation canals. The selection criteria included:

- the compiled data had to comprise all the quantities necessary to compute the four classification parameters as mentioned in Table 5.1;
- the sediment size d_{50} had to be smaller than 0.5 mm;
- the Froude number had to be smaller than 0.5;
- the shear stress on the bottom had to be smaller than 5 N/m²;
- the B/h ratio had to be larger than 10 in order to minimize the influence of the sides;
- the compiled data had to include a detailed description of the bed forms.

The theories were compared on a relative basis, which means that the number of relatively accurately predicted (*well-predicted*) bed forms according to each theory was related to the total number of observed bed forms. The predictability of each of the four theories was measured

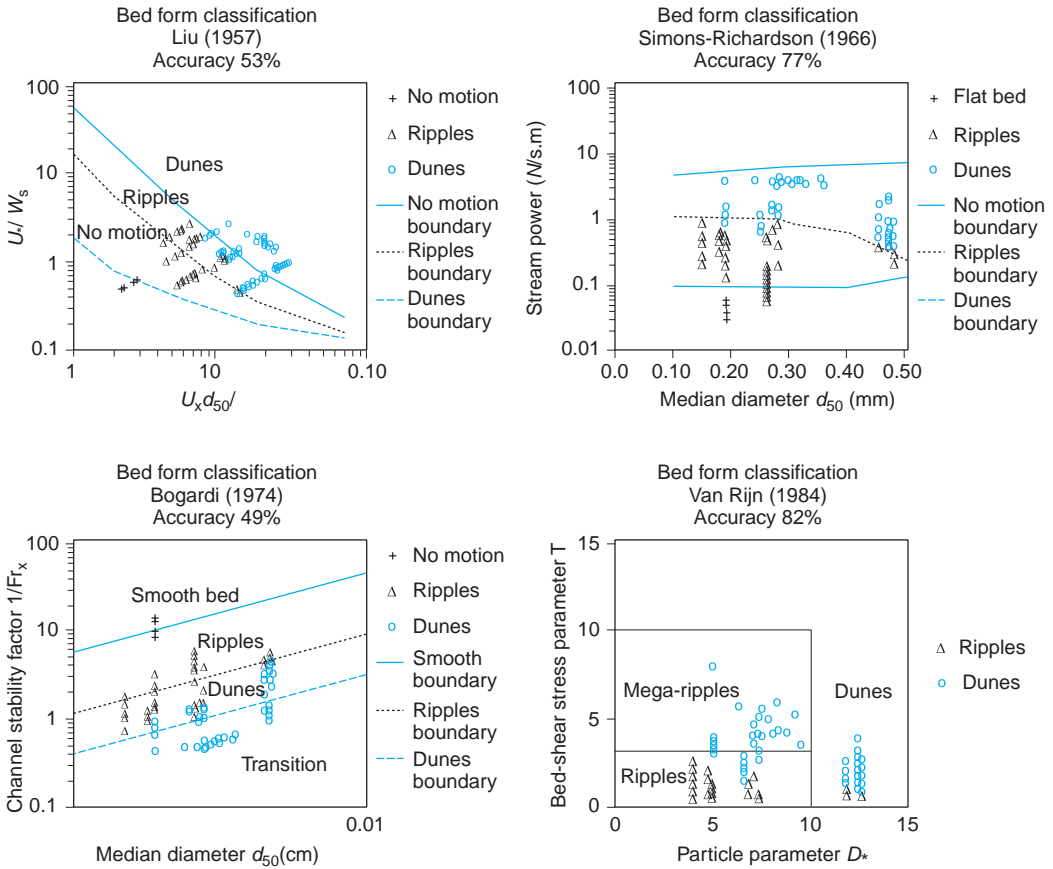


Figure 5.4. Comparison of theories for predicting bed forms for lower flow regimes.

in terms of accuracy (number of *well-predicted* values), which is represented by:

$$\text{Accuracy (\%)} = \frac{\text{number of well-predicted values}}{\text{total number of data}} \times 100 \quad (5.10)$$

The accuracy of each method to predict the bed forms has been used to draw some conclusions:

- the theories presented by van Rijn (1984c) and Simons and Richardson (1966) appear to be the best theories to predict the bed form in irrigation canals. The accuracy shows that approximately 82% and 77% respectively of the observed bed forms are predicted in a relatively accurate way (*well predicted*) by the two theories;

- all the bed forms described for the lower flow regime (ripples, mega-ripples and dunes) can be expected in irrigation canals.

According to van Rijn (1993), bed forms can be classified by the following parameters:

- particle parameter D_* , which reflects the influence of density and diameter of the particle, gravity and viscosity:

$$D_* = \left[\frac{(s-1)g}{\nu^2} \right]^{1/3} d_{50} \quad (5.11)$$

Characteristic values for the particle parameter D_* in irrigation canals are in the range of 1.5 to 7.3 (Table 5.2).

Table 5.2. D_* parameter for sediment sizes encountered in irrigation canals.

d_{50} (mm)	0.05	0.1	0.15	0.20	0.25	0.30	0.35	0.40	0.45	0.50
D_*	1.2	2.5	3.7	5.0	6.2	7.5	8.7	10.0	11.2	12.5

- Excess bed shear stress parameter T which is defined by:

$$T = \frac{\tau' - \tau_{cr}}{\tau_{cr}} \quad (5.12)$$

Where

$$\tau' = \rho g \left(\frac{v}{C'} \right)^2 \quad \text{and} \quad C' = 18 \log \left(\frac{12h}{4.5d_{90}} \right) \quad (5.13)$$

The ranges described by van Rijn (1993) are shown in Table 5.3.

Table 5.3. Classification of bed forms according to van Rijn (1984c).

		Particle parameter	
		$1 \leq D_* \leq 10$	$D_* > 10$
Lower transport regime	$0 \leq T \leq 3$	Mini-ripples	Dunes
	$3 \leq T \leq 10$	Mega-ripples	Dunes
	$10 \leq T \leq 15$	Dunes	Dunes

T = transport stage parameter = excess bed shear stress parameter.

Figure 5.5 shows the ranges established by van Rijn (1984c) to distinguish ripples, mega-ripples and dunes. The curves of the maximum values of the classification parameter T for small irrigation canals (hydraulic radius $R = 0.5$ m) are given for Froude numbers of 0.15, 0.25, 0.35 and 0.45. For larger irrigation canals ($R \approx 4$ m), the curves are for Froude numbers of 0.08, 0.12 and 0.16. Higher Froude numbers in large canals show that the actual shear stress on the bottom is larger than the approximate 4–5 N/m² allowed.

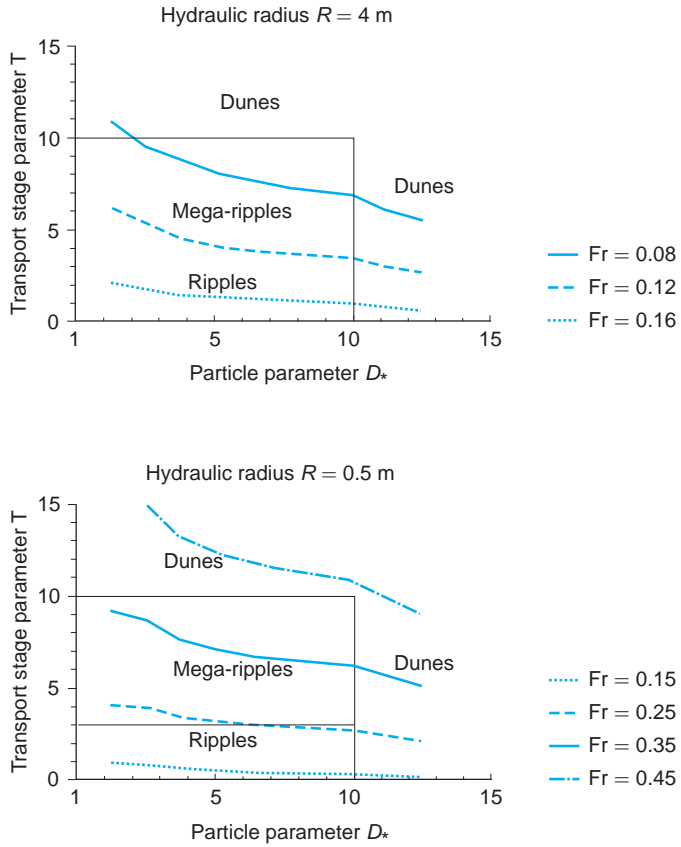


Figure 5.5. Classification of bed forms according to van Rijn (1984c) and expected bed forms in irrigation canals.

5.2.2 Effect of bed forms on the flow resistance

The hydraulic resistance to flowing water in open channels is affected by the development of bed forms such as ripples, mega-ripples and dunes. The hydraulic resistance due to the bed roughness is expressed by a friction factor. Most common friction factors are:

- the Darcy-Weisbach friction factor f :

$$f = \frac{8gRS_f}{v^2} \quad \text{from} \quad f = \frac{8g}{C^2} \tag{5.14}$$

the de Chézy coefficient:

$$C = \frac{v}{\sqrt{S_f R}} \tag{5.15}$$

- the Manning (n) or Strickler (k) roughness coefficient:

$$n = \frac{R^{2/3} S_f^{1/2}}{v} \quad \text{for Manning} \quad (5.16)$$

$$k = \frac{v}{R^{2/3} S_f^{1/2}} \quad \text{for Strickler with } n = 1/k \quad (5.17)$$

The Manning coefficient can be related to the de Chézy coefficient by:

$$C = \frac{R^{1/6}}{n} \quad (5.18)$$

In these notes, mainly the de Chézy coefficient will be used to describe the friction in irrigation canals. The use of the roughness coefficients according to the Darcy-Weisbach and Manning/Strickler coefficients follows from the equations above described.

Not only the wall (grain) roughness, but also the bed forms, are elements that resist the flow in open channels and the total resistance in channels with a movable bed consists of two components:

- the surface or skin resistance due to the grain roughness; the resistance has a grain-related shear stress τ' ;
- the form resistance due to hydrodynamic forces acting on the macro scale of the bed forms has a form-related shear stress τ'' .

Figure 5.6 presents the total shear stress due to skin and form resistance for different velocities. For low velocities, the bed shear stress is smaller than the threshold value and no motion of particles occurs: the bed remains flat and the total bed shear stress is represented by the grain related shear stress τ' . For increasing velocity, especially beyond the threshold, transport of sediment will start, the bed becomes unstable and some bed configuration takes place. For velocities that are slightly larger than the threshold value small disturbances in the form of ripples will develop. Higher velocities will produce dunes and at this stage, the total bed shear stress consists of the two above-mentioned components, namely the skin and the form resistance. The total shear stress is:

$$\tau = \tau' + \tau'' \quad (5.19)$$

The definition of the Darcy-Weisbach friction factor gives:

$$\tau = \rho g R S \quad (5.20)$$

$$\tau = \frac{f \rho v^2}{8} \quad (5.21)$$

$$f = \frac{8gRS}{v^2} \quad (5.22)$$

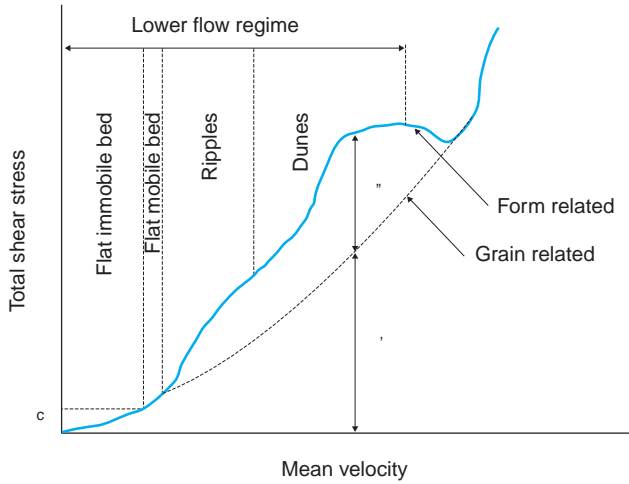


Figure 5.6. Total shear stress due to skin resistance and bed forms as a function of the mean velocity (Jansen, 1994).

In the same way, the total friction factor f can be considered to have two components:

$$f = f' + f'' \tag{5.23}$$

Using $f = 8g/C^2$ results in:

$$\frac{1}{C^2} = \frac{1}{(C')^2} + \frac{1}{(C'')^2} \tag{5.24}$$

When using the same reasoning Manning's n results in:

$$n = n' + n'' \tag{5.25}$$

5.2.3 Determination of the friction factor

A summary of the most widely used methods to predict the friction factor includes the methods:

- van Rijn (1984c);
- Brownlie (1983);
- White, Bettess and Paris (1979);
- Engelund (1966).

The methods of Engelund, White et al and Brownlie predict the friction factor as a function of the flow condition and sediment size. No explicit bed form characteristics are required. The van Rijn method is based on flow conditions and sediment size as well as on bed form and grain related parameters such as bed form length and height. More details

about the methods that can be used to predict the friction factor are given in appendix B.

The four methods to predict the flow resistance have been compared to find the most appropriate method for situations similar to those encountered in irrigation canals. The comparison has been based on field and flume data, and includes:

- RIJ (van Rijn, 1984c);
- BRO (Brownlie, 1983);
- WBP (White, Bettess and Paris, 1979);
- ENG (Engelund, 1966).

The accuracy of the prediction methods is evaluated by:

$$\frac{C_{\text{measured}}}{f} \leq C_{\text{predicted}} \leq C_{\text{measured}}^* f \quad (5.26)$$

$$\text{Accuracy} = \frac{\text{Number of well predicted values}}{\text{Total number of values}} \quad (5.27)$$

Where:

C_{measured} = measured de Chézy coefficients from the data set compiled by Brownlie (1981)

$C_{\text{predicted}}$ = predicted de Chézy coefficients as determined by one of the four methods

f = error factor.

The overall accuracy of each prediction method is used to draw some conclusions concerning the applicability of each method:

- the four methods use only the bottom friction for the prediction of the friction factor. The B/h ratio of all the data used is larger than 10 and the effect of the sidewall is considered to be negligible. However, for a non-wide canal the sidewalls will have a significant effect on the friction factor. Especially, the varying water depth above the sidewall and the roughness of the sidewall without any bed form will require a weighted friction factor;
- the van Rijn method (1984c) to predict the friction factor appears to give the best results when compared with the data from the Brownlie set. About 41%, 71%, 88%, 97% and 98% of *well-predicted* bed forms for an error factor (f) of 1.1, 1.2, 1.3, 1.4 and 1.5 respectively are obtained (Figure 5.7). The van Rijn method shows good results over the whole range of measured friction factors.

5.2.4 Composite roughness for non-wide irrigation canals

The most common cross section of an irrigation canal has a trapezoidal shape with a relatively small bottom width-water depth ratio. In this

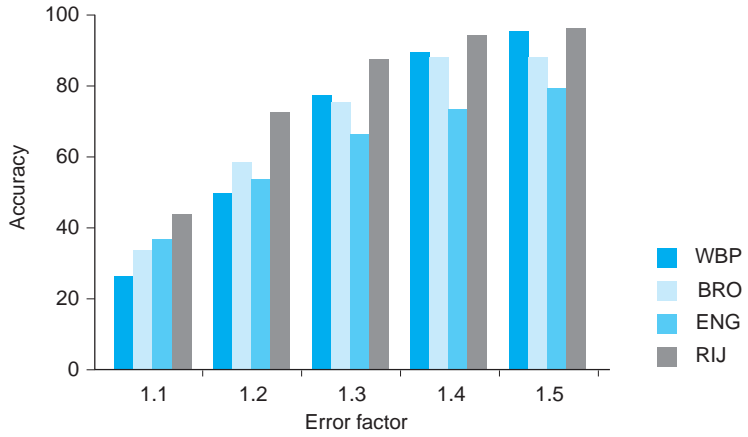


Figure 5.7. Accuracy of the methods to predict the friction factor for different error factors f .

type of cross section, the velocity distribution is strongly affected by the varying water depth perpendicular to the sidewall and by the boundary condition imposed to the velocity by the sidewall. An important interaction and transfer of momentum between the side parts and the central part of the canal will take place. The existing methods to estimate the composite roughness were developed for rivers in which the cross section is divided into a main canal and two flood plains. The assumptions made are not valid for non-wide, trapezoidal or rectangular canals. The main shortcomings are firstly, the lack of attention to the effect of the varying water depth on the friction and secondly, the hypothesis that the mean velocity and/or the hydraulic radius is the same in all the sub-sections.

Normally, the flow in irrigation canals is turbulent and it can be assumed that the lateral velocity distribution in a trapezoidal canal is more governed by the varying water depth above the sides than by the boundary condition imposed by the wall. Based on this hypothesis, the composite roughness can be derived by assuming that the cross section consists of an infinite number of stream tubes (slices). The water depth and the local friction of each stream tube govern the resistance in the stream tube. To evaluate the resistance it is assumed that there is no transfer of momentum between the stream tubes and that the local resistance can be expressed by the de Chézy coefficient (see Figure 5.8).

In irrigation canals the roughness of the bottom and the sides are often different. Several cases of composite roughness in an irrigation canal can be distinguished:

- *Rigid boundaries*: When the boundary is rigid and unchanging then the resistance only depends on the skin roughness. The composite roughness depends on the material of the wall and bottom. Roughness coefficients for the walls and bottom follows from recommended

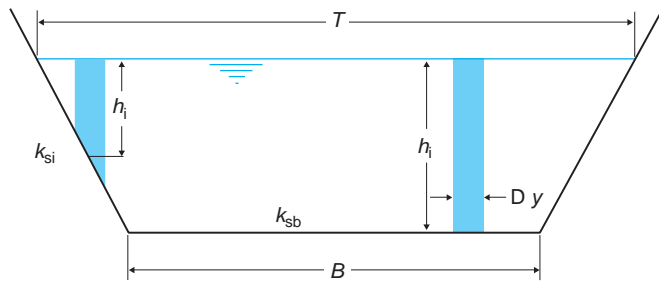


Figure 5.8. Composite roughness in a trapezoidal canal.

values for the type of material on the bottom and walls, respectively. Chow (1983) gives an extensive list of roughness coefficients.

- *Movable bed*: When the canal bed is movable then the roughness may change through the development of bed forms on the bottom, but not on the sides. The sediment particles on the sides are subject to the fluid force and to the gravity force. Therefore, the critical shear stress for the initiation of motion of these particles is much smaller due to the component of the gravity force along the slope. For slopes that are steeper than the angle of repose the critical shear stress for the initiation of motion is reduced to zero (Ikeda, 1982b). Recommended slopes for unlined irrigation canals are between 1 and 3. For most cases the slope angle is between 45° and 18.5° and exceeds the natural angle of repose of wet sand, which is between 15° and 25° (Kinori, 1970). Due to this fact, it is expected that sediment particles will be deposited on the bottom and not on the slopes.

The two most common cases for composite roughness of canals with a movable bed are:

- *Bed forms on the bottom and flat sidewalls*: the roughness of the bottom follows from the bed form characteristics and the roughness of the sidewall follows from the type of material.
- *Bed forms on the bottom and vegetation on the sidewalls*: vegetation on the sidewalls is a type of roughness (Chow, 1983) and this roughness is often given by a single value drawn from field measurements. However, the roughness of canals with vegetation is more complex and is a function of many variables related to the flow conditions and vegetation characteristics, which cannot be expressed by a single value. The flow resistance for a canal with vegetation is difficult to determine and requires ample research before the phenomena involved are completely understood (Kouwen, 1969 and 1992). So far, it is almost impossible to make a proper estimate of the resistance based on analytical or theoretical considerations only (Querner, 1993).

In the past several methods have been developed to describe the composite roughness in open channels. The methods are based on a number of

assumptions for the flow conditions in a cross section. One of the assumptions is that a trapezoidal cross section can be divided into a number of sub-sections (see Figure 5.8) and that the Manning coefficient can be used to express the resistance. Below the most accurate methods (methods 1, 2, 3a, 3b, and 4) will be discussed.

Method 1: Vanoni (1975), Chow (1983), and Raudkivi (1990) have stated that the composite roughness of a cross section can be found by considering the total cross section as an area composed by a number of sub-sections. The mean velocity and energy gradient of each sub-section is the same as the velocity and energy gradient of the entire cross section. The composite roughness for the whole cross section is then determined by:

$$A = \sum_{i=1}^N A_i \quad \therefore \left(\frac{v P^{2/3} n_e}{S^{1/2}} \right)^{3/2} = \sum_{i=1}^N \left(\frac{v P_i^{2/3} n_i}{S^{1/2}} \right)^{3/2} \quad (5.28)$$

$$n_e = \left(\sum_{i=1}^N \frac{P_i n_i^{3/2}}{P} \right)^{2/3} \quad (5.29)$$

Method 2: Chow (1983), Krishnamurthy and Christensen (1972), Motayed and Krishnamurthy (1980) assumed that the total hydraulic resistance in a cross section is equal to the summation of the flow-resisting forces in each sub-section and that the hydraulic radius of each sub-section is equal to the radius of the whole cross section.

$$\tau P = \sum_{i=1}^N \tau_i P_i \quad \text{with } \tau = \rho g R S \text{ and } S = \frac{v^2 n^2}{R^{4/3}} \quad (5.30)$$

Replacing and rearranging:

$$n_e = \left(\sum_{i=1}^N \frac{P_i n_i^2}{P} \right)^{1/2} \quad (5.31)$$

Method 3a: The same authors described another method, which assumed that the total discharge in the whole cross section is equal to the summation of the discharges in the specific subsections:

$$\frac{A R^{2/3} S^{1/2}}{n_e} = \sum_{i=1}^N \frac{A_i R_i^{2/3} S_i^{1/2}}{n_i} \quad (5.32)$$

$$n_e = \frac{PR^{5/3}}{\sum_{i=1}^N \frac{P_i R_i^{5/3}}{n_i}} \quad (5.33)$$

Method 3b: Asano et al (1985) modified the above method by replacing the hydraulic radius R by a composite hydraulic radius R_e , which is given by:

$$R_e = \left(\sum_{i=1}^N \frac{P_i R_i^{5/3}}{P} \right)^{3/5} \quad (5.34)$$

$$n_e = \frac{\sum_{i=1}^N P_i R_i^{5/3}}{\sum_{i=1}^N \frac{P_i R_i^{5/3}}{n_i}} \quad (5.35)$$

Method 4: Krishnamurthy and Christensen (1972) proposed that the summation of the discharges in the sub-sections with roughness coefficient k_{si} is equal to the sum of the discharges in the sub-sections with a composite roughness k_{se} . The flow in each section is assumed to be turbulent and the velocity distribution is logarithmic. This method is similar to the one described by Asano (1985) and differs only in the description of the mean velocity in the sub-sections. The composite roughness follows from:

$$q_i = v_i h_i \, dy \quad (5.36)$$

$$\left(\frac{v_i}{u_{*i}} \right) = 8.48 + 2.5 \ln \left(\frac{0.368 h_i}{k_{si}} \right) \quad (5.37)$$

Expressed in terms of the composite equivalent hydraulic roughness, k_{se} gives:

$$\left(\frac{v_i}{u_{*i}} \right) = 8.48 + 2.5 \ln \left(\frac{0.368 h_i}{k_{se}} \right) \quad (5.38)$$

The hydraulic roughness is related to Manning's roughness coefficient by (Henderson, 1966):

$$n = 0.034 k_s^{1/6} \quad (5.39)$$

Equating the discharges gives:

$$\ln n_e = \frac{\sum_{i=1}^N P_i R_i^{3/2} \ln n_i}{\sum_{i=1}^N P_i R_i^{3/2}} \tag{5.40}$$

Where:

- n_e = composite Manning's roughness coefficient for the whole cross section
- n_i = Manning's roughness coefficient in sub-section i
- u_{*i} = shear velocity in sub-section i
- v_i = mean velocity in sub-section i
- A = area of the entire cross section
- A_i = area of sub-section i
- S = energy gradient
- q_i = discharge in sub-section i
- τ_e = shear stress for the whole cross section
- τ_i = shear stress in sub-section i
- P = wetted perimeter of the whole cross section
- P_i = wetted perimeter of sub-section i
- R = hydraulic radius for the whole cross section
- R_i = hydraulic radius for the sub-section i
- R_e = composite hydraulic radius
- h_i = water depth of sub-section i
- k_{si} = composite hydraulic roughness in each sub-section i
- k_{se} = composite equivalent hydraulic roughness
- dy = width of sub-section i .

5.2.5 *A recommended method for the prediction of composite roughness in trapezoidal canals*

This section will propose a new method (Method 5) for the prediction of composite roughness in trapezoidal cross sections. The total discharge in an open channel with the same roughness along the bottom and sides of the wetted perimeter is computed by the de Chézy equation:

$$v = C\sqrt{RS_f} \quad \text{and} \quad Q = Av \tag{5.41}$$

$$C = 18 \log \left(\frac{12R}{k_s} \right) \tag{5.42}$$

In an open channel with composite roughness along the wetted perimeter, the de Chézy coefficient is described by:

$$C_e = 18 \log \left(\frac{12R}{k_{se}} \right) \quad (5.43)$$

Where:

C_e = effective de Chézy coefficient for the entire cross section

k_{se} = effective hydraulic roughness for the entire cross section

R = hydraulic radius.

It is more difficult to compute the discharge in a trapezoidal canal with different roughness along the bottom and the sides. The total discharge depends on an accurate estimate of the de Chézy coefficient and of the effective hydraulic roughness for the entire cross section (Equation 5.44). The de Chézy coefficient for the whole cross section is a function of the effective hydraulic roughness for the entire cross section (k_{se}). The latter depends on the composite hydraulic roughness of each stream tube i (k_{si} and k_{sb} in Figure 5.8).

The method used to estimate the effective hydraulic roughness and de Chézy coefficient in trapezoidal channels with composite roughness along the wetted perimeter assumes that the total discharge in the whole cross section is the summation of the discharge of each individual stream tube:

$$Q = Q_{lat} + Q_{cen} = 2 \int_0^{mh} C_i h_i \sqrt{h_i S_f} dy + \int_0^B C_i h_i \sqrt{h_i S_f} dy \quad (5.44)$$

With

$$C_i = 18 \log \left(\frac{12h_i}{k_{si}} \right) \quad (5.45)$$

Where:

Q = total discharge

Q_{lat} = discharge in the lateral part

Q_{cen} = discharge in the central part

h_i = water depth in each stream tube i

C_i = Chézy coefficient in each stream tube i

B = bottom width

m = side slope

k_{si} = hydraulic roughness in each stream tube i

S_f = energy slope

dy = stream tube width.

Rearranging the terms gives:

$$\ln k_{se} = \frac{0.8 m \ln k_{sl} + (B/h) \ln k_{sb}}{0.8 m + (B/h)} \tag{5.46}$$

Where:

m = side slope

h = water depth in m

B = bottom width in m

k_{se} = effective hydraulic roughness in each stream tube i

k_{sl} = hydraulic roughness along the sides

k_{sb} = hydraulic roughness along the bottom.

This equation clearly shows the influence of the side slope ‘ m ’ and the bottom width B (the central part) of a trapezoidal canal on the effective roughness of the whole cross section. For small B/h -ratios the effect of the lateral part on the flow becomes as important as the central part. The influence of the lateral part in canals with large B/h -ratios can be ignored and the effective roughness of the entire cross section is mainly controlled by the roughness of the bottom.

5.2.6 *Comparison of the composite roughness predictors in a trapezoidal canal*

In order to predict the composite roughness in a trapezoidal canal the previously described methods 1, 2, 3a, 3b and 4 and the recommended method 5 have been compared with the results of laboratory tests carried out at Wageningen University (WUR). The aim of the experiments was to investigate the composite roughness in non-wide canals with a strong influence of the sidewalls on the roughness and the velocity distribution.

The accuracy of the predictor methods has been established by the following criteria:

- the number of relatively accurately predicted values that are within an error band, which is given by:

$$\frac{\text{Measured value}}{K} \leq \text{Predicted value} \leq \text{Measured value} * K \tag{5.47}$$

The predictability of each of the predictor methods was measured in terms of accuracy (number of *well-predicted* values), which is represented by:

$$\text{Accuracy} = \frac{\text{number of well predicted values}}{\text{number of total values}} * 100 \tag{5.48}$$

Where:

K = error factor (the aim of this factor is the same as the one of the error factor f).

The computation results of the various methods and the values measured in the laboratory are compared in Figure 5.9, which shows the number of *well-predicted* values for several error factors K . Details of the comparison of each method for an error factor of 1.15 are shown in Figure 5.10.

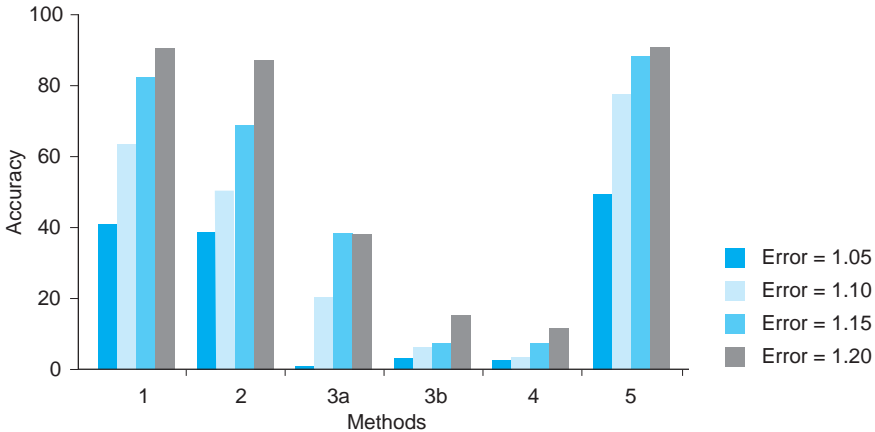


Figure 5.9. Comparison of predicted values for various error factors by using the WUR data.

The prediction methods 1, 2, 3a, 3b, 4 and 5 were also compared with a set of data from Krüger (1988). The criteria for the selection of data from the Krüger set were to obtain the results of tests in non-wide canals only and included the following:

- a trapezoidal cross section;
- a Froude number less than 0.5;
- a bottom width-water depth ratio smaller than 8.

The five prediction methods and the specific data from Krüger (1988) have been compared in a similar way to the comparison of the five methods with the WUR data. Figure 5.11 shows the accuracy of the methods when compared with the Krüger data for several different values of error factor (1.05, 1.10, 1.15 and 1.20). Details of the comparison for the methods and for an error factor of 1.15 are shown in Figure 5.12.

The comparison of the five methods to predict the composite roughness in a trapezoidal cross section with laboratory data from Wageningen and Krüger results in the following conclusions:

- comparison of the overall performance of the five methods with the two experimental data sets shows that the methods can be ranked in descending order, namely 5, 1, 2, 4, 3a and 3b;
- methods 1, 2, 3a, 3b and 4 were developed for river conditions, in which the channel consists of a main canal and two parallel flood plains. The

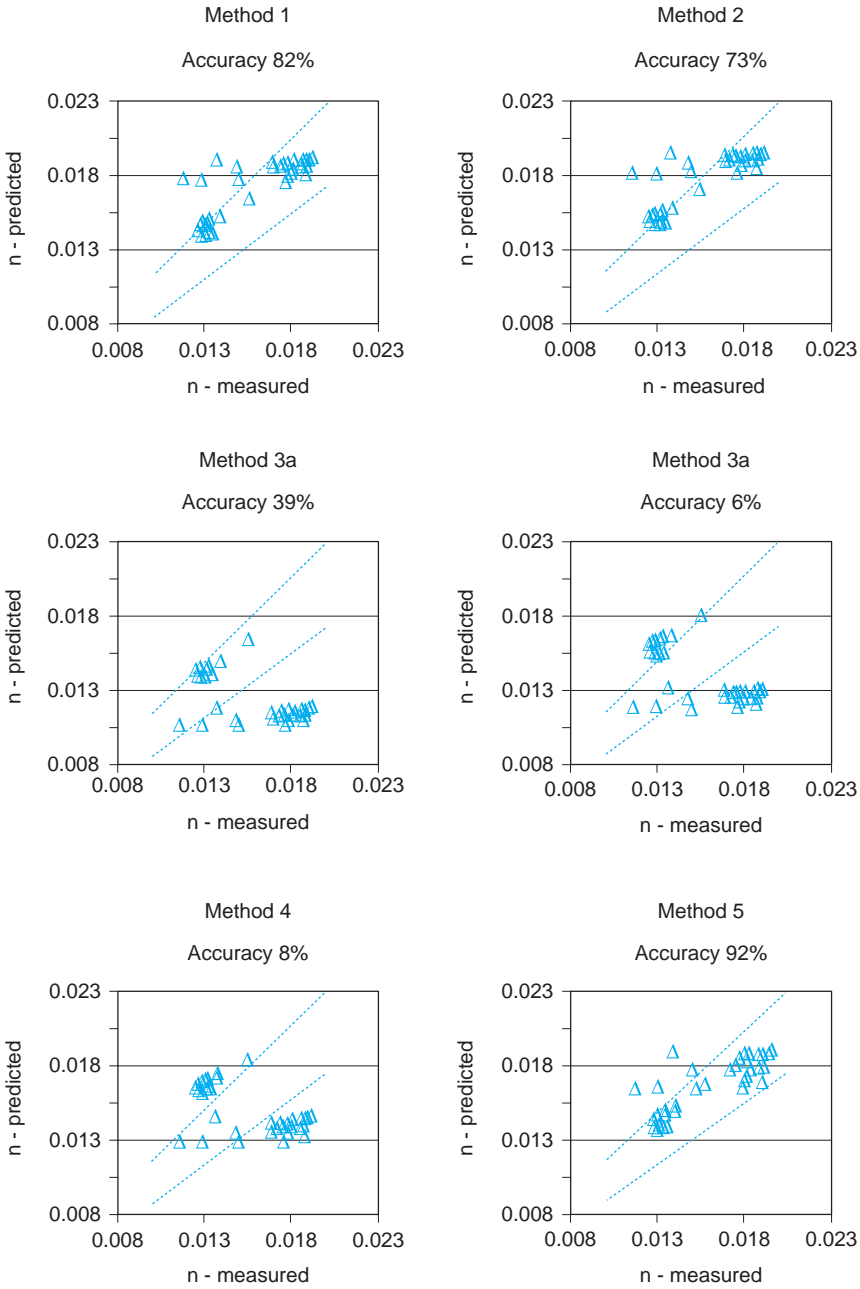


Figure 5.10. Comparison of the results of the five prediction methods for composite roughness with the measured WUR data at an error factor of 1.15.

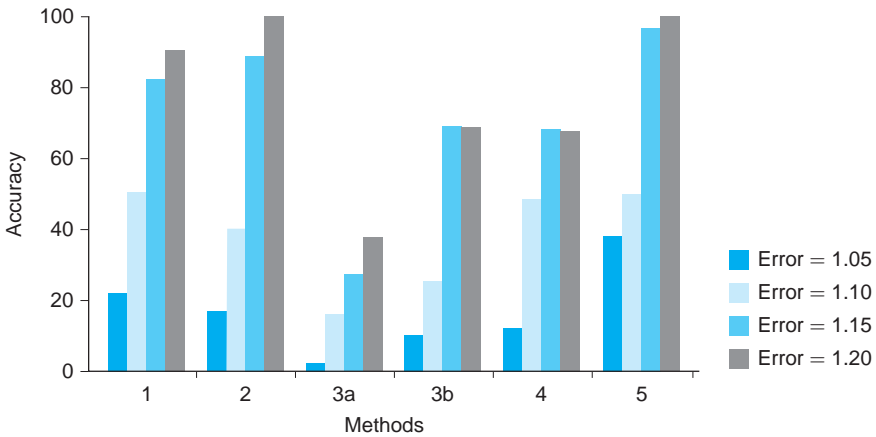


Figure 5.11. Comparison of predicted values for various error factors by using the Krüger data.

water depths in both main canal and flood plains do not vary in a lateral direction;

- method 5 takes into account the effect of the varying water depth on the roughness coefficient; it does not take into account any transfer of momentum;
- method 5 appears to give better results for error factors smaller than 1.2. This method predicts the two measured data sets with an accuracy larger than 90% for an error factor of 1.15. The minimum standard error of the predicted values was also observed for method 5;
- methods 1 and 2 behave similarly. The assumptions for both methods give similar results; they weigh the side parts in the same way as the central part without considering the differences in velocity and water depth.
- methods 3b and 4 are rather similar; they differ in the description of the mean velocity in the sub-sections.

5.2.7 Prediction of composite roughness in a rectangular canal

For canals with a rectangular cross section, the existing methods to find the composite roughness can not be directly used. Rectangular cross-sections do not have a clearly defined area that can be associated with each type of roughness along the wetted perimeter. Therefore, the estimate of the composite roughness follows the same principles as used for the sidewall correction method, which is a calculation procedure initially proposed by Einstein (1942) to determine the shear stress at the bottom as well as the shear velocity, friction factor, etc. The method does not include any correction for the effect of the sidewalls on the velocity distribution and sediment transport (ASCE, 1977).

A non-wide rectangular canal with bottom width B and water depth h can be replaced by another canal, namely a *wide canal* with a bottom width

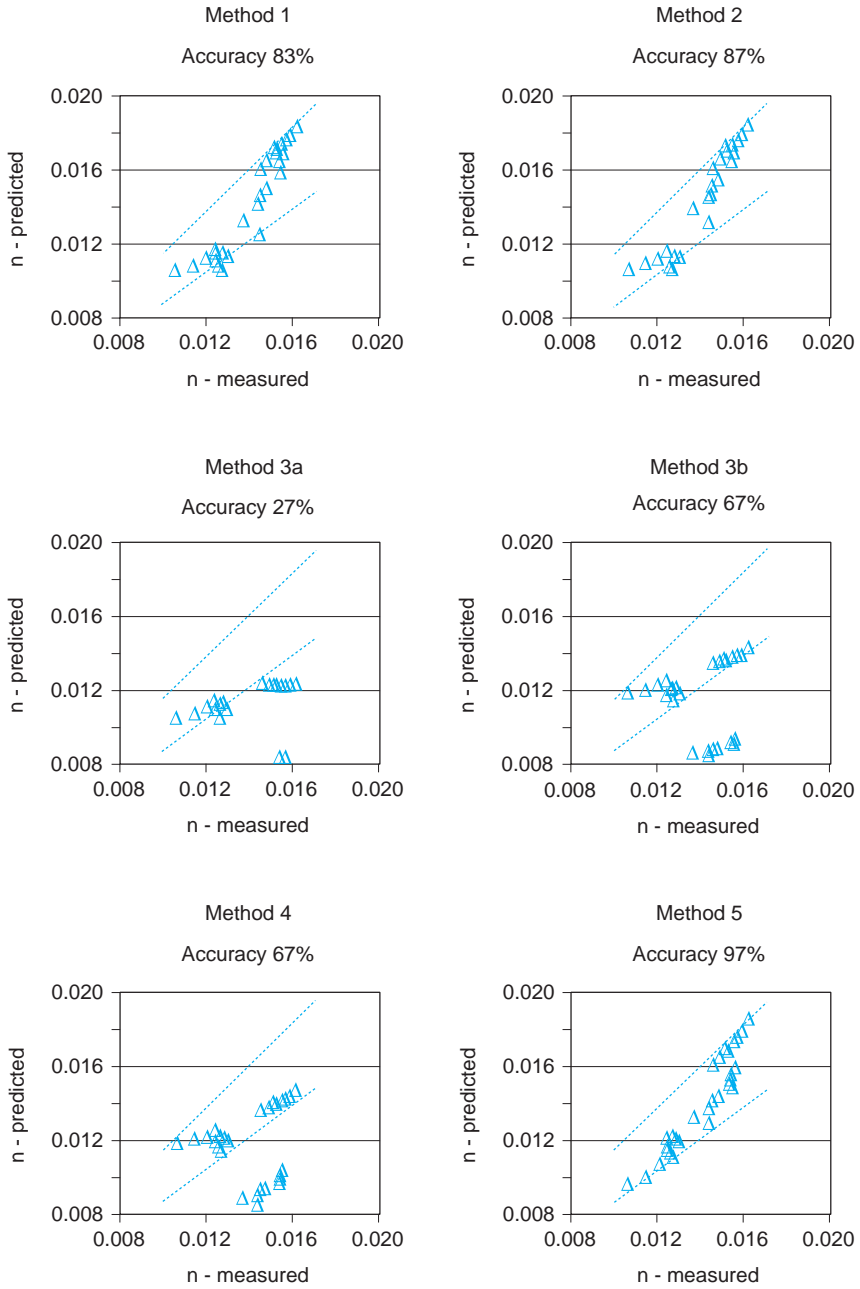


Figure 5.12. Comparison of the results of the five prediction methods for composite roughness with the measured Krüger data at an error factor of 1.15.

B_* ($B_* = B + 2h$) and a water depth R ($R = A/P$) as shown in Figure 5.13. The area $A = R * (B + 2h)$ and the total discharge of the *wide*, rectangular canal is expressed by:

$$Q = vA = 2C_L h R \sqrt{RS_f} + C_b BR \sqrt{RS_f} \quad (5.49)$$

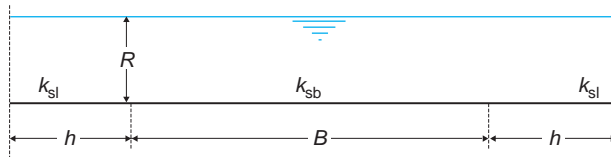
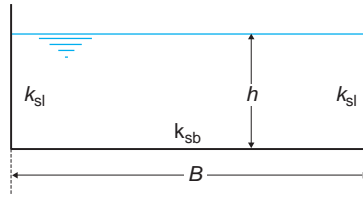


Figure 5.13. Non-wide rectangular canal schematised as a wide canal.

Replacing the de Chézy coefficients in the equation (5.49) by a function of the surface roughness and water depth gives:

$$Q = 2 \left(18 \log \frac{12R}{k_{sl}} \right) hR \sqrt{RS_f} + \left(18 \log \frac{12R}{k_{sb}} \right) BR \sqrt{RS_f} \quad (5.50)$$

Expressing the discharge in terms of the equivalent composite surface roughness gives:

$$Q = \left(18 \log \frac{12R}{k_{se}} \right) (B + 2h)R \sqrt{RS_f} \quad (5.51)$$

Equating both equations and rearranging the terms gives:

$$\log k_{se} = \frac{2 \log k_{sl} + (B/h) \log k_{sb}}{2 + (B/h)} \quad (5.52)$$

Where:

h = water depth in m

B = bottom width in m

k_{se} = effective hydraulic roughness in each stream tube i

k_{sl} = hydraulic roughness along the sides

k_{sb} = hydraulic roughness along the bottom.

Expressed in terms of the Manning’s coefficient results in:

$$n_e = \frac{2 + \frac{B}{h}}{\frac{2}{n_1} + \frac{B}{h} \frac{1}{n_b}} \tag{5.53}$$

The method to estimate the composite roughness in rectangular canals has been tested with a selected set of laboratory data from Krüger (1988). The selection criteria for the data were similar to those used for the trapezoidal canals and the comparison of the prediction method for the composite roughness in rectangular canals with the selected data is similar to the one given earlier in Section 5.2.6. Manning’s coefficient is used to evaluate the roughness coefficient and the results of that comparison are given in the next figure. The method predicts about 92% of the measured values of the composite roughness in rectangular canals with an error smaller than 7.5%.

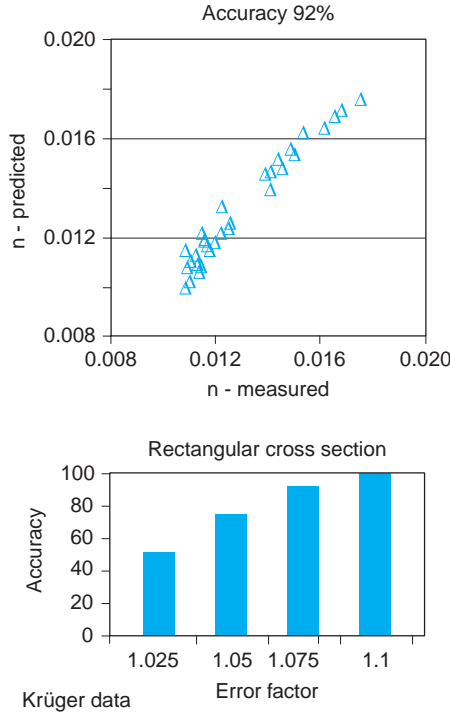


Figure 5.14. Accuracy for several error factors and the predictability at an error factor of 1.075 of the prediction method for composite roughness in rectangular canals.

5.3 GOVERNING EQUATIONS FOR SEDIMENT TRANSPORT

Sediment can be transported in equilibrium or non-equilibrium conditions. Equilibrium conditions mean that for specific hydraulic conditions the

flow conveys a certain amount of sediment without deposition or erosion. Sediment transport predictors are supposed to describe the transport for equilibrium conditions. The sediment transport under non-equilibrium conditions describes how the flow conveys a certain amount of sediment, as well as the erosion and deposition that take place at the same time.

The aim of sediment research is to predict the sediment transport capacity in relation to known sediment input values. Three modes of motion can be distinguished in the sediment transport induced by flowing water: *rolling and sliding, saltation and suspension*. The modes of motion are related to the flow conditions and the bed material, specially the hydrodynamic forces, which are expressed in terms of mean velocity or bottom shear stress acting on a bed of sediments. Firstly, the hydrodynamic forces have to reach a critical or threshold value for the initiation of motion, before a small increase of the forces will put the grain or aggregate into motion by irregular jumps or by rolling of the particles. Secondly, when the hydrodynamic forces reach a threshold value for the initiation of suspension then the sediment particles start to diffuse into the water flow.

Based on the three modes of motion two different types of sediment transport can be defined:

- bed load;
- suspended load.

Bed load is that part of the sediment transport that is in contact with the bed during the transport and it includes the *rolling and sliding and the saltation* modes.

Suspended load is that part of the sediment transport that moves with the water flow without contact with the bottom. It includes the suspension mode and the wash load, which consists of cohesive and very fine sediments (smaller than 0.05 mm) and which tends to be suspended by Brownian motion (Raudkivi, 1990).

Due to the fact that the sediments entering irrigation canals are from external sources (for instance, rivers), the particle size of the sediment is usually different from the parent bed material. The particle size of the sediment depends on the operation of the sediment trap or intake structure at the head of the canal network. Normally the sediments entering into the irrigation canals are in the range of fine sand, silt and clay (Worapansopak, 1992). Bigger particles have preferably been excluded from entering the canal system by a careful skimming of the water at the intake or have been allowed to settle in a sediment trap in the first reach of the canal system (Dahmen, 1994). In view of these provisions at the head of an irrigation network the sediment sizes are assumed to be in the range of $0.05 \text{ mm} < d_{50} < 0.5 \text{ mm}$. It is also assumed that only non-cohesive material will be present in the irrigation system, despite some degree of cohesion that is present for the smaller particle sizes.

Yalin (1977) expressed that process by:

$$\tau < \tau_{cr} \quad \text{no motion} \quad (5.54)$$

$$\tau_{cr} \leq \tau \leq \tau'_{cr} \quad \text{bed load transport} \quad (5.55)$$

$$\tau \geq \tau'_{cr} \quad \text{bed and suspended load transport} \quad (5.56)$$

Where:

τ = bottom shear stress

τ_{cr} = critical shear stress for initiation of motion

τ'_{cr} = critical shear stress for initiation of suspension.

In reality, there is not *one* critical value at which the motion and suspension suddenly begins, but it fluctuates around an average value. The movement of the particles is highly unsteady and depends on the turbulence of the flow. It is not possible to give a single value that presents zero movement and for that reason it is easier to define the condition for initiation of motion as the one below a certain value for which the sediment transport rate has no practical meaning (Paintal, 1971).

Initiation of motion: Several authors have developed theories to explain the initiation of motion. Most of them are based either on a critical depth-averaged velocity or on a critical bed shear stress. The theories based on critical velocity require water depths that completely satisfy the flow condition at which the initiation of motion occurs, whereas the theories based on critical shear stress describe the flow condition for the initiation of motion by using a single critical value for the shear stress. ASCE (1966a) recommends that data on critical shear stress should be used wherever possible. Among the theories based on critical shear stress, the Shields' diagram is the most widely accepted criterion to describe the conditions for initiation of motion of uniform and non-cohesive sediment on a horizontal bed.

The Shields' diagram (see Figure 5.15) offers the relation between the critical mobility Shields' parameter (θ_{cr}) and the dimensionless particle Reynold's number (Re_*). The particle Reynold's number represents the hydraulic condition on the bed and is based on the grain size and the shear velocity. The initiation of motion will occur when the mobility Shields' parameter (θ) is greater than the critical mobility Shields' parameter (θ_{cr}).

These parameters are expressed by:

$$\theta_{cr} = \frac{u_{*,cr}^2}{(s-1)g d_{50}} = \frac{\tau_{cr}}{(s-1)\rho g d_{50}} \quad (5.57)$$

$$Re_* = \frac{u_{*,cr} d_{50}}{\nu} \quad (5.58)$$

$$\theta = \frac{u_*^2}{(s-1)g d_{50}} = \frac{\tau}{(s-1)\rho g d_{50}} \quad \text{with } u_* = \sqrt{ghS_0} \quad (5.59)$$

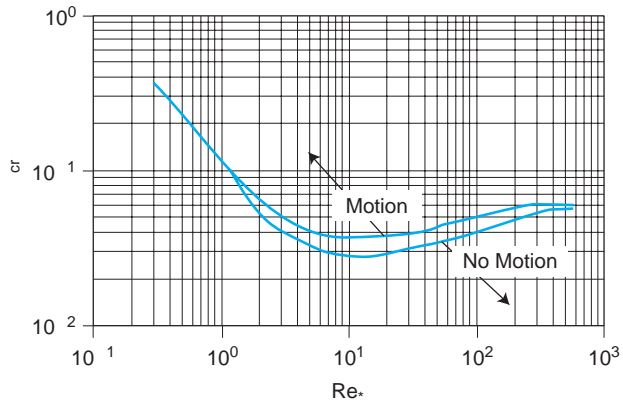


Figure 5.15. Shields' diagram for initiation of motion (after van Rijn, 1993).

The use of the Shields' diagram is not very practical, since the u_* value appears in both parameters and in both axes of the diagram, and can only be solved by trial and error. This imperfection of the Shields' diagram is eliminated by introducing the particle parameter D_* which is represented by (Yalin, 1977):

$$D_* = \frac{Re_*^2}{\theta} = \left[\frac{(s-1)g}{\nu^2} \right]^{1/3} d_{50} \quad (5.60)$$

In this way the critical mobility parameter θ_{cr} will be expressed as a function of D_* and van Rijn (1993) presents the relationship between θ_{cr} and D_* as:

$$\theta_{cr} = 0.24 D_*^{-1} \quad \text{for } 1 < D_* \leq 4 \quad (5.61)$$

$$\theta_{cr} = 0.14 D_*^{-0.64} \quad \text{for } 4 < D_* \leq 10 \quad (5.62)$$

$$\theta_{cr} = 0.04 D_*^{-0.1} \quad \text{for } 10 \leq D_* \leq 20 \quad (5.63)$$

$$\theta_{cr} = 0.013 D_*^{0.29} \quad \text{for } 20 \leq D_* \leq 150 \quad (5.64)$$

$$\theta_{cr} = 0.055 \quad \text{for } D_* > 20 \quad (5.65)$$

Initiation of suspension: van Rijn (1984b) describes the initiation of suspension by:

$$\theta_{cr} = \frac{16}{D_*^2} \frac{w_s^2}{(s-1)gd_{50}} \quad \text{for } 1 < D_* \leq 10 \quad (5.66)$$

$$\theta_{cr} = 16 \frac{w_s^2}{(s-1)gd_{50}} \quad \text{for } D_* > 10 \quad (5.67)$$

Where:

- θ = mobility Shields' parameter (dimensionless)
- θ_{cr} = critical mobility Shields' parameter (dimensionless)
- Re_* = particle Reynolds number (dimensionless)
- s = relative density (ρ_s/ρ)
- u_* = local shear velocity (m/s)
- w_s = fall velocity (m/s)
- D_* = particle parameter (dimensionless)
- d_{50} = median diameter (m)
- g = acceleration due to gravity (m/s^2).

Irrigation canals are man-made canals and their design takes into account aspects related to the irrigation criteria and sediment transport. On the one hand, the canals should meet the irrigation requirements and on the other hand, no deposition of the sediment entering into the system or scouring of the parent material should occur. Suggested values for non-scouring bottom shear stress are available in the literature. Kinori (1970) and Chow (1983) give minimum values for the non-scouring shear stress for water containing fine sediments in the range between 1.5 N/m^2 (fine sand, sandy loam) and 15 N/m^2 (hard clay and gravel). Dahmen (1994) suggests a maximum value for the design of irrigation canals of $3\text{--}4 \text{ N/m}^2$. Even though the design values for the shear stress can be reduced due to changes in the operation strategies during the irrigation season, the value of the remaining shear stress is still high enough to initiate motion and further suspension of the previously deposited sediment. However, it is no longer so high as to produce scouring of the parent material of the canal.

Figure 5.16 shows the Shields' curve for initiation of motion and the criteria used by van Rijn (1993) to initiate suspension. This figure presents a range of shear stresses between 1 N/m^2 and 4 N/m^2 , which is a range of

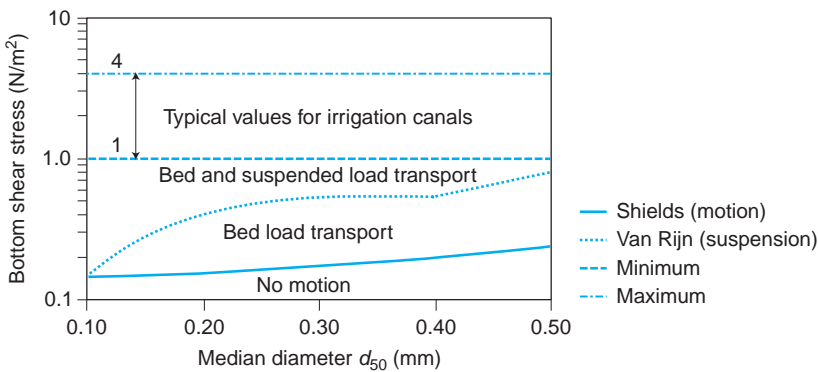


Figure 5.16. Initiation of motion, initiation of suspension and values of shear stress commonly used in irrigation canals as function of D_* .

shear stress commonly used for the design of irrigation canals. In addition it clearly shows that typical flow conditions in irrigation canals are large enough to produce suspension of sediment particles. The sediment in irrigation canals is transported in two modes: suspended load and bed load.

The flow conditions prevailing in irrigation canals clearly show that the sediment is transported both as bed load and as suspended load. Therefore, any predictor to estimate the sediment transport in irrigation canals should consider this fact and the predictor should be able to compute either implicitly the total transport (bed load + suspended load) or the bed load and suspended load separately. Only for very fine sediment ($d_{50} < 0.1$ mm) can a suspended sediment transport predictor be used to estimate the sediment transport capacity of irrigation canals.

5.3.1 *Sediment transport capacity*

There is no universally accepted predictor to estimate the total sediment transport capacity of irrigation canals. Many methods have been proposed to predict the transport rate under a large range of flow conditions and sediment characteristics. The total sediment transport can be found either in an indirect way by summation of the bed load and the suspended load or by a direct determination of the total sediment transport. The first group of indirect summation includes the theories of Einstein (1950), Bagnold (1966), Toffaletti (1969), and van Rijn (1984a and 1984b). The theories of Colby (1964), Bishop et al. (1965), Engelund and Hansen (1967), Ackers and White (1973), Yang (1973) and Brownlie (1981) directly determine the total sediment transport. However, the predictability of all of them is still rather poor and van Rijn (1984a) stated that it is almost impossible to predict the sediment transport rate with an accuracy of less than 100%. A brief description of some of the most widely known sediment transport predictors is presented in Appendix A.

The sediment transport predictors are established for very diverse and miscellaneous conditions and the use of the equations should be restricted to the conditions for which they were tested. However, a comparison of the various methods for similar flow conditions and sediment characteristics, both in irrigation canals and from field and laboratory data, will result in a very useful tool to evaluate the suitability of each method under these specific conditions.

5.3.2 *Comparison of sediment transport capacity*

A way to evaluate the predictor methods for sediment transport is to compare the results to measured sediment transport rates. Once the hydraulic and sediment characteristics (e.g. mean velocity, flow depth, sediment

size, etc) are known, each of the selected methods can predict the sediment transport. Next, the predicted rates will be compared with the measured values of the sediment transport. Therefore, five of the most widely used methods to compute sediment transport will be briefly described. They are:

- Ackers and White;
- Brownlie;
- Engelund and Hansen;
- van Rijn;
- Yang.

The Ackers and White (A-W), Brownlie (BRO), Engelund-Hansen (E-H), van Rijn (RIJ) and Yang (YAN) methods to predict sediment transport have been evaluated and compared to field and laboratory data, in which the flow conditions and sediment characteristics are similar to those prevailing in irrigation canals. From the evaluation some conclusions can be drawn:

- a prediction of the sediment transport in irrigation canals within an error factor smaller than 2 is often impossible. Even in the case of the most reliable method, only 61% of the measured values are predicted with an error factor of 2. For error factors smaller than 2, the predictability of the methods is considerably less. Figure 5.17 shows the results of the comparison for an error factor of 1.1, 1.50, 1.75, 2, 2.5, and 3.00;
- the Brownlie predictor has a tendency to underpredict the sediment transport, while the Engelund-Hansen predictor overpredicts in most cases;
- these theories have a general tendency to overpredict the sediment transport for low concentrations. In terms of *goodness to fit* to the

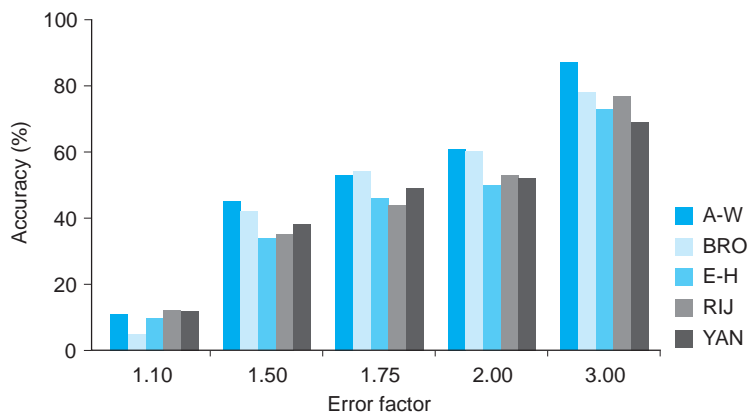


Figure 5.17. Range of accuracy of the sediment transport predictors for different error factors.

measured low concentrations, most methods do not perform well. Ackers and White, and Brownlie are the best methods to predict the sediment transport for concentrations smaller than 500 ppm;

- based on the overall performance of each method according to all the evaluation criteria, the Ackers and White, and Brownlie methods appear to be the best methods to predict sediment transport in irrigation canals.

5.3.3 Sediment transport computation in non-wide canals

The use of a sediment transport relationship that implies the velocity as variable has often been applied without considering the variation in channel geometry, distribution of the flow velocity and/or sediment transport in the cross section (Simons and Senturk, 1992). Sediment transport predictors have been developed for wide canals and they consider a channel with an infinite width without taking into account the effect of the side walls on the water flow and sediment transport. The effect of the side walls on the velocity distribution in the lateral direction is ignored and consequently the velocity and the sediment transport are considered to be constant in any point of the cross section. Under these assumptions a uniformly distributed shear stress on the bottom and an identical velocity and sediment transport in any point over the width of the canal are assumed. In this way, these variables can be easily expressed per unit width. For other, non-wide channels, the shape will have an important impact on the water flow and sediment transport. The existence of sidewalls and the varying water depth on the sides will cause a non-uniform distribution over the width for both the shear stress and the velocity and, as a consequence for the sediment transport.

Generally, the most common shape of an irrigation canal is a trapezoidal cross section. Most of these canals can not be considered as a wide canal; recommended values for the ratio of bottom width and water depth (B/h) are smaller than 8 (Dahmen, 1994). For this cross section, the imposed boundary condition for the velocity and the varying water depth on the sides will affect the shear stress and the velocity and sediment distribution in the y -direction (lateral direction). In other words, the variables related to the water flow and the sediment transport, vary in the y -direction. These impacts will be larger for smaller values of the B/h ratio.

The cross section integrated approach is based on the assumption of a quasi two-dimensional model and the cross section is composed by a series of parallel stream tubes (Figure 5.18). Within each stream tube, the velocity distribution is considered to be uniform and therefore can be described in a one-dimensional way. The sediment transport in each stream tube is considered as a function of the flow in that stream tube only without taking into account the diffusion in the y -direction.

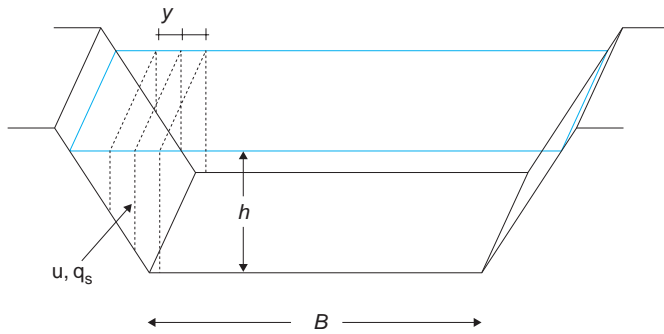


Figure 5.18. Schematization of stream tubes in a trapezoidal cross section.

The total sediment transport in a trapezoidal cross section can be calculated by:

$$Q_s = \sum (q_s)_i dy \tag{5.68}$$

Where:

Q_s = total sediment discharge

q_s = sediment discharge of the stream tube i per unit width

dy = width of the stream tube.

This cross section integrated approach will be named Procedure 3.

In most empirical equations for one-dimensional, uniform flow in non-wide channels, the hydraulic radius is universally used as the single quantity to describe the geometry of the cross section and the mean velocity. The mean velocity over the whole cross section (Figure 5.19) will replace the non-uniform distribution of the velocity (u_i). However, the sediment transport per unit width given by $q_s = MV^N$ is not the average of the sediment transport of each local velocity in the cross section $q_s = Mu_i^N$. The difference between the two transport values is due to the non-linear relationship between the sediment transport and the velocity, so that a correction factor α for the sediment transport must be introduced in order to equal both values for the sediment transport capacity.

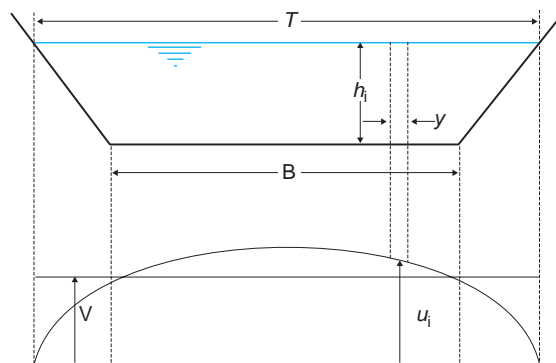


Figure 5.19. Velocity distribution in a non-wide canal.

The total sediment transport for the total cross section is estimated by:

$$Q_s = \alpha B q_s \quad \text{with } q_s = f(V) \tag{5.69}$$

Where:

α = correction factor for calculating the total sediment transport in a non-wide canal

B = bottom width (m)

V = mean velocity (m/s)

Q_s = sediment transport capacity for the whole cross section (m³/s)

q_s = sediment transport capacity per unit width (m³/s.m)

Referring to the Figure 5.20, the sediment transport passing through the whole cross section can also be computed by:

$$Q_s = \int_T M u^N dy \tag{5.70}$$

Equating the equations gives:

$$\alpha = \frac{\int_T M u^N dy}{B M V^N} \tag{5.71}$$

By assuming constant coefficients M and N for the entire cross section then the equation becomes:

$$\alpha = \frac{\sum \left(\frac{u}{V}\right)^N \Delta y}{B} \tag{5.72}$$

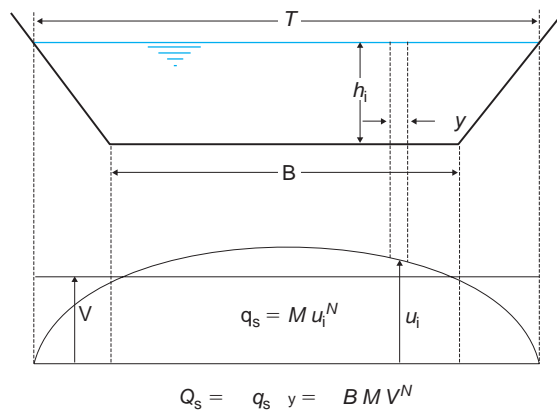


Figure 5.20. Velocity distribution in a non-wide trapezoidal canal.

The correction factor α for the computation of the total sediment transport is a function of the velocity distribution in the cross section and the exponent N in the relationship of the velocity and the sediment transport predictor.

The sediment transport predictors can be schematized by using a simple relation between q_s and V in the following way:

$$q_s = MV^N \quad (5.73)$$

Where:

q_s = sediment transport per unit width ($\text{m}^3/\text{s.m}$)

V = mean velocity (m/s)

M, N = exponents depending on water flow and sediment characteristics.

Derivation of the exponent N can be done by:

$$\begin{aligned} \frac{dq_s}{dV} &= MN V^{N-1} \\ N &= \frac{dq_s}{dV} \frac{1}{MV^{N-1}} = \frac{V}{q_s} \frac{dq_s}{dV} \end{aligned} \quad (5.74)$$

and therefore,

$$N = \frac{V}{q_s} \frac{dq_s}{dV} \quad (5.75)$$

The sediment transport predictors of Ackers-White, Brownlie and Engelund-Hansen are used to derive the values of the exponent N .

- The Ackers-White sediment transport predictor gives:

$$N = 1 + \frac{mF_{gr}}{F_{gr} - A} \quad (5.76)$$

- The Brownlie sediment transport predictor gives:

$$N = 1 + \frac{1.978 F_g}{F_g - F_{gr}} \quad (5.77)$$

- The Engelund-Hansen sediment transport predictor gives:

$$N = 5 \quad (5.78)$$

Figure 5.21 shows the relationship between the correction factor α and the exponent N for non-wide channels.

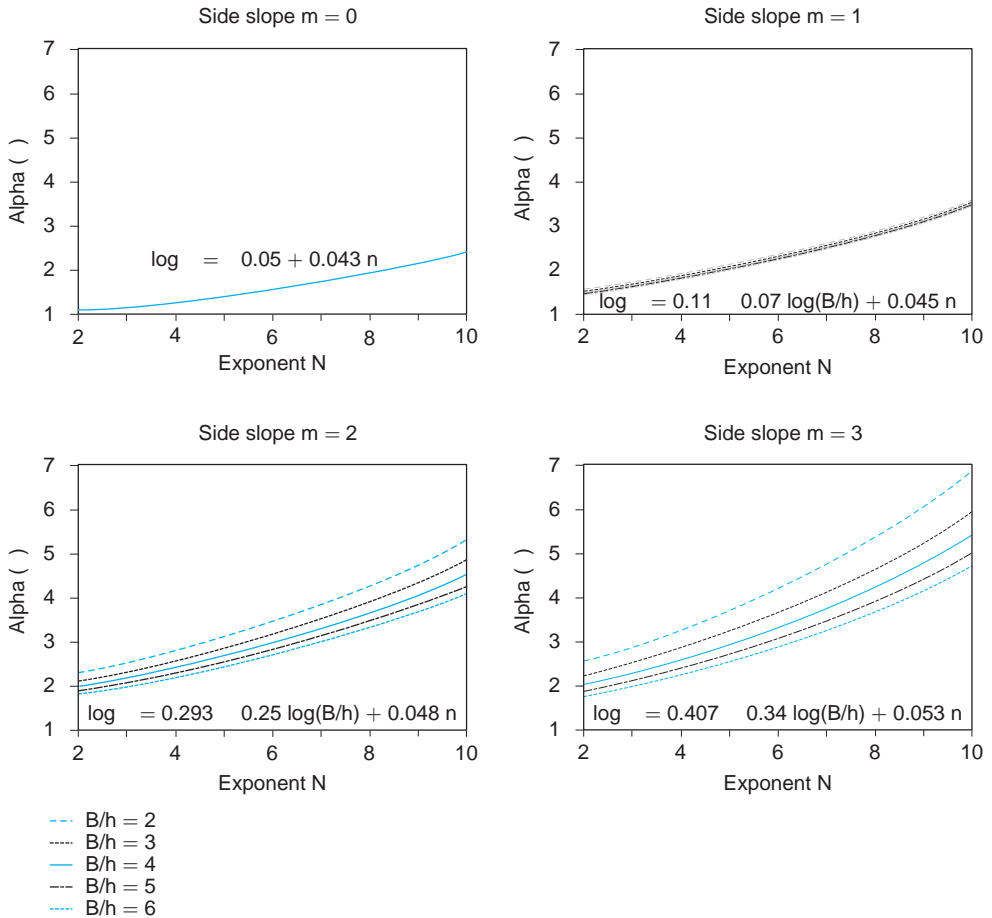


Figure 5.21. Relationship between the correction factor α and the exponent N .

5.3.4 Comparison of the procedures for computing the total sediment transport

Several procedures have been developed to compute the total sediment discharge in open channels and they will be named here procedures 1, 2 and 3.

Procedure 1: the sediment discharge per unit width (q_s) is calculated by using the hydraulic radius as a characteristic variable for the water flow. The average width of the canal represents the width of the canal and the total sediment transport is determined by the multiplication of these variables:

$$Q_s = q_s * B_{av.} \quad \text{with } q_s = f(R) \tag{5.79}$$

Procedure 2: the sediment transport per unit width (q_s) is calculated by using the water depth as characteristic variable for the water flow. Next, the total sediment transport Q_s is calculated by multiplying the sediment transport per unit width (q_s) and the bottom width (B):

$$Q_s = q_s * B \quad \text{with } q_s = f(h) \quad (5.80)$$

Procedure 3: the total sediment transport is determined by using the procedure described in the previous section, which is based on the computation of the sediment transport in the stream tubes (the cross section integrated approach):

$$Q_s = \int_{i=1}^n q_{s(i)} dy \quad (5.81)$$

In order to compare the three procedures in terms of the ability to compute the total sediment transport in non-wide canals, these procedures have been applied to a selected set of laboratory data. A correct method to compute the sediment transport should take into account the effect of the cross section on the velocity distribution and the non-linear relationship between the velocity and the sediment transport. In the comparison, the Ackers and White, the Brownlie and Engelund and Hansen methods have been applied to compute the sediment transport.

The sediment transport as calculated by the procedures 1, 2 and 3 has been compared with the measured sediment transport. The predictability of each procedure is measured in terms of accuracy, the *well-predicted* values of the sediment transport with a certain accuracy and is expressed as:

$$\frac{\text{Measured value}}{f} \leq \text{Predicted value} \leq \text{Measured value} * f \quad (5.82)$$

$$\text{Accuracy} = \frac{\text{number of well-predicted values}}{\text{total values}} \quad (5.83)$$

Where f = error factor.

Figure 5.22 shows the results of the accuracy for all three procedures, for the sediment transport predictors and for different levels of error factor (f), when compared with the selected data. The comparison shows that the prediction of the procedure 3 is closer to the measured values than the

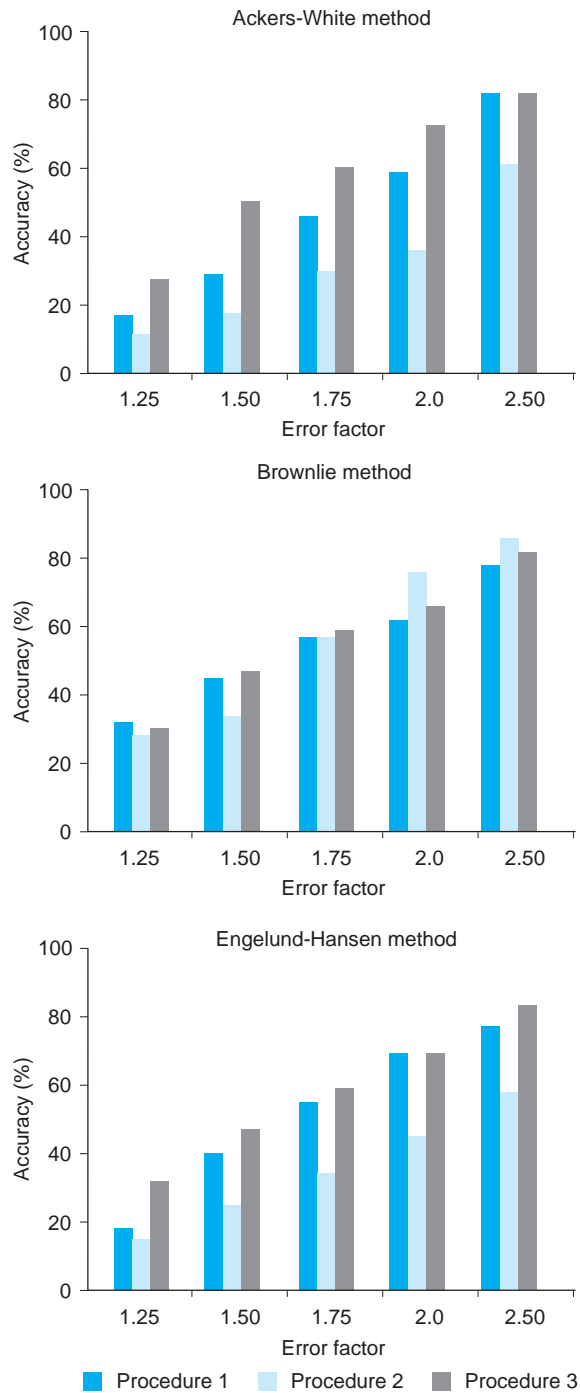


Figure 5.22. Comparison of procedures to compute sediment transport in non-wide canals.

predicted values of the other two procedures for all the sediment transport theories.

5.3.5 *Sediment transport in non-equilibrium conditions*

Sediment transport in a long, steady and uniform flow has a unique equilibrium transport rate, but the transport rate under variable conditions differs from this steady uniform and equilibrium case. Non-equilibrium conditions are very significant for suspended load because the travel length of a suspended particle is in general much longer than the step length of a bed load motion (Nagakawa, 1989). While it is possible to relate the bed load transport to the local and instantaneous characteristics of water flow and bottom composition, no distinct relation can be established for the suspended load transport since this part of the transport mode is substantially influenced by upstream conditions (Armanini and Di Silvio, 1988).

Mathematical models for the simulation of non-equilibrium, suspended sediment transport in open canals might be based on the solution of:

- 1) the 1-D, 2-D or 3-D convection-diffusion equations;
- 2) depth integrated models.

1-D, 2-D or 3-D Convection-diffusion equations: they are based on the solution of the diffusion-convection equation that for two-dimensional problems can be written as:

$$\frac{\partial c}{\partial t} + u \frac{\partial c}{\partial x} + w \frac{\partial c}{\partial z} = w_s \frac{\partial c}{\partial z} + \frac{\partial}{\partial z} \left(\varepsilon_x \frac{\partial c}{\partial x} \right) + \frac{\partial}{\partial z} \left(\varepsilon_z \frac{\partial c}{\partial z} \right) \quad (5.84)$$

Where:

c = sediment concentration

w_s = fall velocity (m/s)

t = time coordinate (s)

x, z = length coordinates (m)

u, w = velocity components in x and z direction (m/s)

$\varepsilon_x, \varepsilon_z$ = sediment-mixing coefficient in x and z direction (m^2/s).

The equation can be solved when the mean velocity components, the fall velocity and the mixing coefficients ε_x and ε_z are known.

Depth integrated models: the models are based on a depth-integrated approach; the model describes how the mean concentration adapts in time and space towards the local mean equilibrium concentration. The resulting model for the suspended sediment transport can be used together with the depth-averaged hydrodynamic equations.

Galappatti (1983) developed a depth-integrated model for suspended sediment transport in unsteady and non-uniform flow based on the 2-D convection-diffusion equation. In his model the vertical dimensions are

eliminated by means of an asymptotic solution in which the concentration $c(x, z, \text{ and } t)$ is expressed in terms of the depth-averaged concentration $c(x, t)$. The latter concentration is represented by a series of previously determined profile functions.

Wang and Ribberink (1986) have studied the validity of the Galappatti model and they concluded that the use of the model is not suitable for large deviations of the concentration profile from the equilibrium profile. They recommended some specific requirements to be applied in the Galappatti model for the computation of suspended sediment transport. These requirements are:

- the Galappatti model is only valid for fine sediment. The factor w_s/u_* should be much smaller than unity; recommended values of w_s/u_* are between 0.3 and 0.4;
- the time scale of the flow variations should be much larger than h/u_* ;
- the length scale of the flow variations should be larger than Vh/u_* .

Where:

u_* = local shear velocity (m/s)

w_s = fall velocity (m/s)

h = water depth (m)

V = mean velocity (m/s).

The main concepts, on which the depth-integrated model of Galappatti is based, include:

- the horizontal diffusive transport (ε_x) and the vertical component of the velocity (w) are ignored. Hence, the 2-D convection-diffusion equation reduces to:

$$\frac{\partial c}{\partial t} + u \frac{\partial c}{\partial x} = w_s \frac{\partial c}{\partial z} + \frac{\partial}{\partial z} \left(\varepsilon_z \frac{\partial c}{\partial z} \right) \quad (5.85)$$

- the concentration $c_{x,z,t}$ (Figure 5.23) is expressed in a depth-averaged concentration $c_{x,t}$ (Figure 5.24).

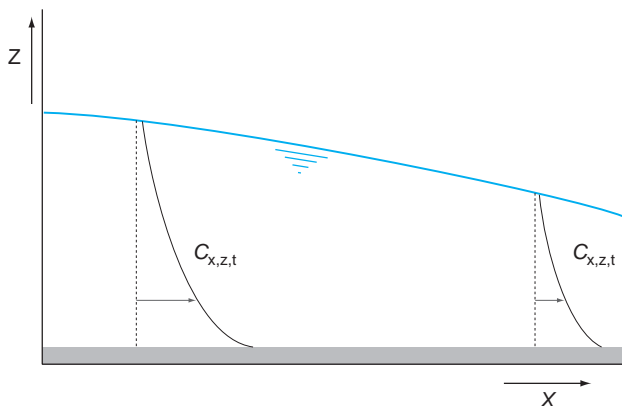


Figure 5.23. Schematization of the 2-D suspended sediment transport model.

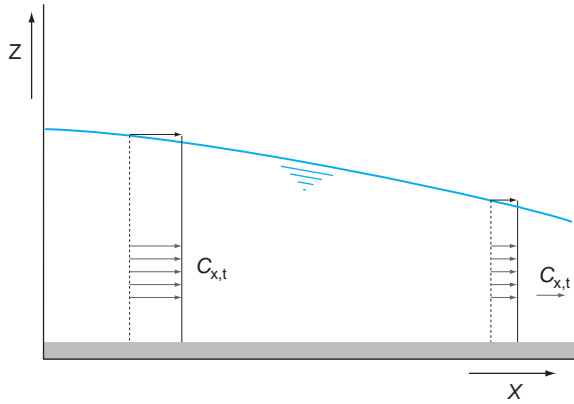


Figure 5.24. Schematization of a depth-integrated model.

In a uniform flow carrying sediments in non-equilibrium conditions, the variation in concentration can be written according to the Galappatti's depth-integrated model as:

$$c_e = c + T_A \frac{\partial c}{\partial t} + L_A \frac{\partial c}{\partial x} \quad (5.86)$$

With

$$T_A = \frac{w_s}{u_*} \frac{h}{w_s} \exp(f) \quad (5.87)$$

$$\frac{T_A u_*}{h} = \exp(f) \quad (5.88)$$

$$L_A = \frac{w_s}{u_*} \frac{Vh}{w_s} \exp(f) \quad (5.89)$$

$$\frac{L_A}{h} = \frac{w_s}{u_*} \frac{V}{w_s} \exp(f) \quad (5.90)$$

$$f = \sum_{i=1}^4 \left(a_i + b_i \frac{u_*}{V} \right) \left(\frac{w_s}{u_*} \right)^{i-1} \quad (5.91)$$

Where:

c_e = concentration of suspended load in equilibrium condition

c = concentration of suspended load at distance x

T_A = adaptation time (s)

L_A = adaptation length (m)

w_s = fall velocity (m/s)

u_* = shear velocity (m/s)
 V = mean velocity (m/s)
 h = water depth (m)
 a_i, b_i = constants.

The adaptation length (L_A) and adaptation time (T_A) are constant for uniform flow. They are defined as the interval (both in length and in time) required for the mean actual concentration to approach the mean equilibrium concentration. The adaptation length represents the length scale and the adaptation time represents the time scale (Ribberink, 1986).

Values of a_i and b_i for $z_a/h = 0.01$ are given in Table 5.4 (Galappatti, 1983). For values of z_a/h less than 0.01, the same values of a_i and b_i will be used, because for smaller values the influence of z_a/h on the adaptation time and length is insignificant (Kerssens, 1979).

Table 5.4. Values of a_i and b_i for $z_a/h = 0.01$ (after Galappatti, 1983).

	a_1	b_1	a_2	b_2	a_3	b_3	a_4	b_4
T_A	1.978	0.000	-6.321	0.000	3.256	0.000	0.193	0.000
L_A	1.978	0.543	-6.326	-3.331	3.272	0.400	0.181	1.790

For a steady sediment flow:

$$c_e - c = L_A \frac{\partial c}{\partial x} \quad (5.92)$$

After integration the equation results in:

$$c = c_e - (c_e - c_0) \exp\left(\frac{x}{L_A}\right) \quad (5.93)$$

Where:

c_e = concentration of suspended load in equilibrium condition

c_0 = concentration of suspended load at distance $x = 0$

c = concentration of suspended load at distance x

L_A = adaptation length (m)

x = length coordinate (m).

In the introductory sections of this chapter it was shown that the rates of suspended load and bed load transport of particles larger than 0.3 mm are comparable and the more reliable sediment transport predictors in irrigation canals computes the total load (suspended and bed load). For that reason, it will be essential to consider the sediment transport in non-equilibrium conditions as a whole. Although the bed load reacts instantaneously from a non-equilibrium condition to an equilibrium condition, it is assumed that the characteristic adaptation length for the bed load is the same adaptation length as for suspended load. Therefore, the total

sediment transport under non-equilibrium conditions can be described by using the total sediment concentration (bed and suspended load) instead of a suspended sediment concentration.

This leads to:

$$C = C_e - (C_e - C_0) \exp \frac{x}{L_A} \quad (5.94)$$

Where:

- C = total sediment concentration at distance x
- C_e = total sediment concentration in equilibrium condition
- C_0 = total sediment concentration at distance $x = 0$
- L_A = adaptation length (m)
- x = length coordinate (m).

5.4 MORPHOLOGICAL CHANGES OF THE BOTTOM LEVEL

The one-dimensional computation assumes fixed sidewalls and the occurrence of deposited or entrained sediments on the bottom of the irrigation canals. The interrelation between the water movement and the morphological changes on the bottom can be summarized by the following equations:

$$\frac{dh}{dx} = \frac{S_o - S_f}{1 - Fr^2} \quad (5.95)$$

$$\frac{\partial Q_s}{\partial x} + B(1 - p) \frac{\partial z}{\partial t} = 0 \quad (5.96)$$

These equations will be solved in sequence. First, the gradually varied flow equation is solved to determine the flow profile for given boundary conditions for water level and discharge. Details of that procedure were discussed in Chapter 2. Next, the output values of the hydraulic equation are used to solve the equation of the mass balance for the total sediment transport. The first term (dQ_s/dx) represents either the total entrainment or deposition rate between two sections (points) along the x -axis of the canal. It will depend on a balance between the canal transport capacity and the existing sediment load along the x -axis. The second term represents the net flux of sediment across a horizontal plane near the bed that will lead to a change of the bottom level (see Figure 5.25).

Several finite difference methods based on explicit and implicit schemes have been used to solve the equation of the mass balance for the total sediment transport. Cunge (1980), de Vries (1987) and Vreugdenhil (1982 and 1989) describe the Lax, modified Lax, Lax-Wendroff and the 4-points implicit scheme as methods to solve the morphological

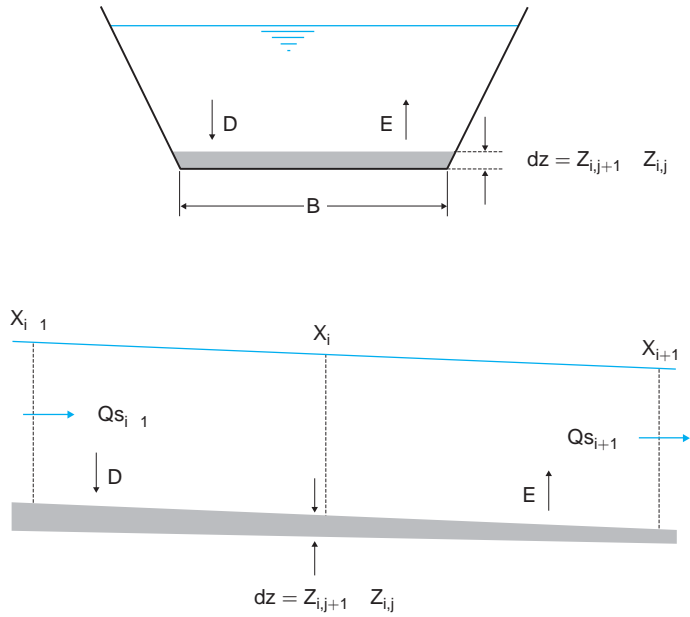


Figure 5.25. Schematization of computations of changes in the bottom level.

equation. The modified Lax scheme can be used quite successfully, though it is not claimed to be the best method (Abbot & Cunge, 1982).

The modified Lax method can be expressed as:

$$z_{i,j+1} = z_{i,j} - \frac{1}{B(1-p)} \left[\frac{Q_{s_{i+1,j}} - Q_{s_{i-1,j}}}{2\Delta x} - \frac{1}{2\Delta t} [(\alpha_{i+1,j} + \alpha_{i,j}) \times (z_{i+1,j} - z_{i,j}) - (\alpha_{i,j} + \alpha_{i-1,j})(z_{i,j} - z_{i-1,j})] \right] \quad (5.97)$$

The numerical scheme cannot be applied to the downstream and upstream boundaries. An adapted scheme for the downstream boundary is described by:

$$z_{i,j+1} = z_{i,j} - \frac{1}{B(1-p)} \left[\frac{Q_{s_{i+1,j}} - Q_{s_{i-1,j}}}{2\Delta x} + \frac{1}{2\Delta t} [(\alpha_{i,j} + \alpha_{i-1,j}) \times (z_{i,j} - z_{i-1,j})] \right] \quad (5.98)$$

And for the upstream boundary by:

$$z_{i,j+1} = z_{i,j} - \frac{1}{B(1-p)} \left[\frac{Q_{s_{i+1,j}} - Q_{s_{i-1,j}}}{2\Delta x} - \frac{1}{2\Delta t} [(\alpha_{i+1,j} + \alpha_{i,j}) \times (z_{i+1,j} - z_{i,j})] \right] \quad (5.99)$$

In which the subscripts i and j mean:

$$i \equiv i \Delta x$$

$$j \equiv j \Delta t$$

And where:

$$Q_s = \text{sediment discharge (m}^3/\text{s)}$$

$$p = \text{porosity (dimensionless)}$$

$$B = \text{bottom width (m)}$$

$$\Delta x = \text{distance (m)}$$

$$z = \text{bottom level (m)}$$

$$\Delta t = \text{time step (m)}$$

$$\alpha = \text{parameter used for stability and accuracy of the numerical scheme.}$$

The stability of the scheme is given by (Vreugdenhil, 1989):

$$\sigma^2 \leq \alpha \leq 1 \quad (5.100)$$

Accuracy of this scheme is increased if (Vreugdenhil, 1989):

$$\alpha \approx \sigma^2 + 0.01 \quad (5.101)$$

$$\sigma = NV \frac{Q_s/Q}{1 - Fr^2} \frac{\Delta t}{\Delta x} \quad (5.102)$$

Where:

$$\sigma = \text{the Courant number}$$

$$N = \text{exponent of the velocity in the sediment transport equations}$$

$$Q = \text{discharge (m}^3/\text{s)}$$

$$Q_s = \text{sediment discharge (m}^3/\text{s)}$$

$$V = \text{mean velocity (m/s)}$$

$$\Delta t = \text{time interval (s)}$$

$$\Delta x = \text{distance (m)}$$

$$Fr = \text{Froude number.}$$

Figure 5.25 shows a schematization of the deposition or entrainment computation at the bottom of the canal and Figure 5.26 shows the calculation of changes in the bottom level according to the modified Lax method.

Figures 5.27 to 5.29 show some schematizations for different flow conditions in a canal and they illustrate the procedure to compute the sediment mass balance after one time step. Let us take a uniform flow as an example. When the sediment transport capacity Q_{se} is smaller than the actual sediment transport Q_s ($\Delta Q_s/\Delta x < 0$), deposition is expected up to the point where Q_s reaches the equilibrium sediment transport. An adaptation length will occur for the adjustment of the actual sediment transport to the equilibrium sediment transport capacity. From this point onwards, the sediment transport will remain constant. For Q_{se} larger than

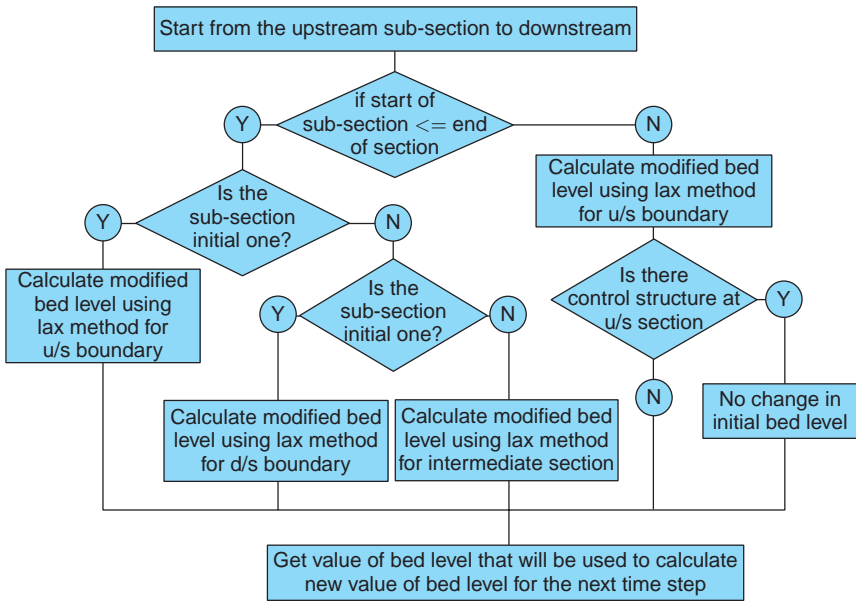


Figure 5.26. Calculation of the change in the bottom level using the modified Lax method.

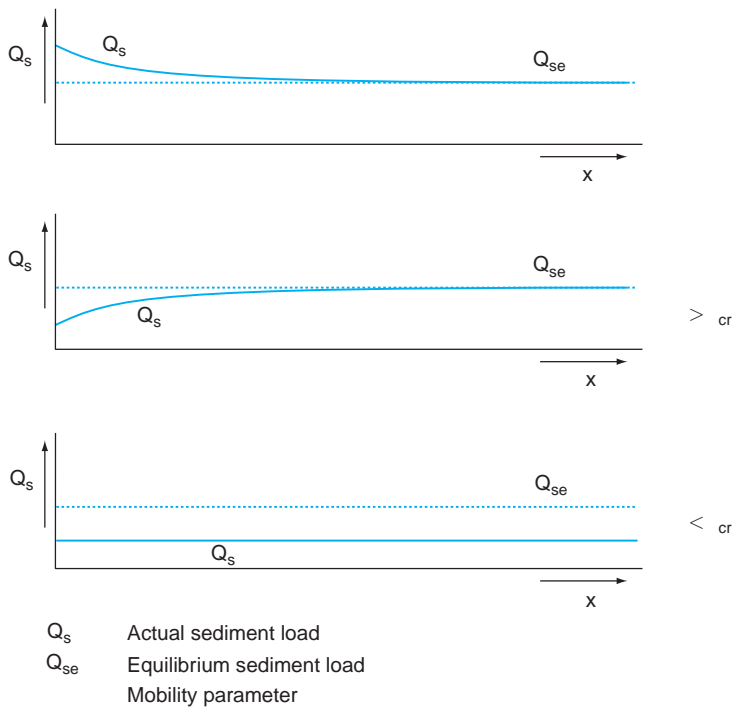


Figure 5.27. Sediment transport for uniform flow.

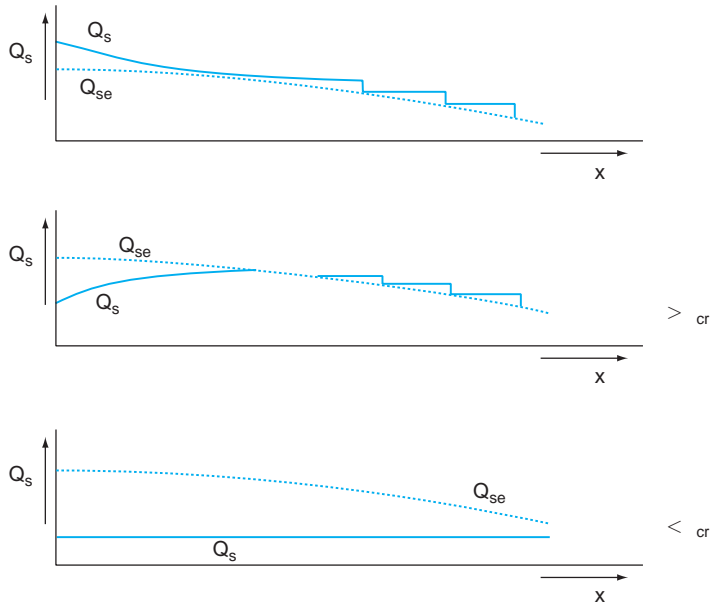


Figure 5.28. Sediment transport for gradually varied flow (backwater effect).

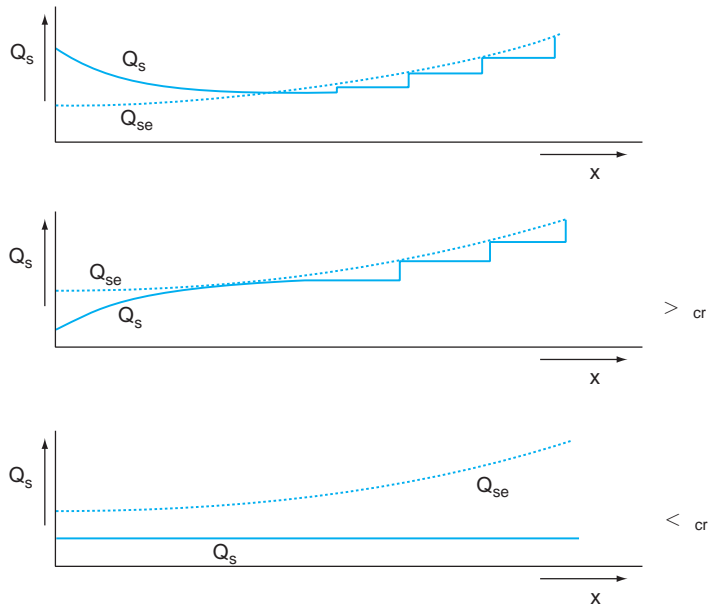


Figure 5.29. Sediment transport for gradually varied flow (drawdown effect).

Q_s two possibilities can occur depending on whether there is any sediment motion on the bottom or not. Motion of sediment is evaluated in terms of the mobility parameter θ and the critical mobility parameter θ_{cr} . In the first case ($\theta > \theta_{cr}$) entrainment of particles and increasing sediment transport occurs until adaptation to the sediment transport capacity of the canal has occurred. In the second case, without motion of sediment along the bottom ($\theta < \theta_{cr}$), the actual sediment load is conveyed without changes.

For gradually varied flows, a distinction between backwater and draw-down effects has to be made. Figure 5.27 shows the effect of a backwater profile on the sediment transport in a canal. For Q_s larger than the Q_{se} ($\Delta Q_s/\Delta x < 0$) deposition will occur to reach adaptation to the equilibrium sediment transport capacity of the canal ($Q_{se} = Q_s$). From that point onward a continuous deposition in a downstream direction may be expected. For Q_s lower than the Q_{se} ($\Delta Q_s/\Delta x > 0$), the actual sediment transport can either remain constant along the canal ($\theta < \theta_{cr}$) or increase up to Q_{se} equal to Q_s ($\theta > \theta_{cr}$). A continuous deposition in downstream direction is expected. The effect for a drawdown profile is shown in Figure 5.28. For Q_s larger than Q_{se} deposition will occur up to the equilibrium condition ($Q_{se} = Q_s$). From that point onwards a continuous entrainment is expected. When Q_{se} is larger than Q_s either the latter remains constant ($\theta < \theta_{cr}$) or increases to reach Q_s ($\theta > \theta_{cr}$) and a continuous entrainment in the downstream direction will occur.

5.5 CONCLUSIONS

Applications of the existing sediment transport concepts under flow conditions and sediment characteristics encountered in irrigation canals were analysed in the previous sections. Those applications were intended to evaluate the suitability of those concepts in particular conditions. In that way any increase in unavoidable uncertainties and inaccuracies during the computations of the sediment transport in irrigation canals can be kept to a minimum.

From the applications of the sediment transport concepts for the conditions prevailing in irrigation canals some conclusions can be drawn.

General

- there are several theories to estimate friction factors and sediment transport rates (equilibrium and non-equilibrium conditions). These theories rely on field and laboratory observations, but they are not able to explain with a very high degree of accuracy the friction factors and sediment transport rates in irrigation canals;

Bed forms

- for the lower flow regime in irrigation canals all types of bed forms (ripples, mega-ripples and dunes) can be expected;
- the van Rijn method describes the bed forms more accurately than other methods; more than 75% of the observed bed form types were *well-predicted* by the van Rijn method.

Friction factor predictors

- the van Rijn method for predicting the friction factor gives good results when compared with measured values of the friction factor. This method was able to predict more than 90% of the measured values within an error band of 30%;
- existing friction factor predictors only consider the bottom friction. For non-wide canals the sidewalls have an important impact on the friction factor. Therefore, a weighted value of the friction factor is required; the proposed method for predicting the effective roughness in a trapezoidal canal with different roughness along the wetted perimeter appears to give better results than the existing methods. More than 90% of the measured values were *well predicted* by this method. Also the minimum value of the standard error and the narrowest range of variation of the predicted values were observed for the proposed method;
- the existing methods for predicting the effective roughness in a rectangular canal with different roughness along the wetted perimeter cannot be explicitly applied; the proposed method to estimate the effective roughness in a rectangular canal with composite roughness along the wetted perimeter predicted more than 95% of the measured values within a error band of 15%.

Sediment transport predictors

- based on the characteristic flow conditions and the sediment sizes usually encountered in irrigation canals, the sediment could be transported as bed load and as suspended load. Therefore the sediment transport predictors should be able to compute both types of sediment transport;
- existing predictors of the sediment transport capacity of wide canals do not take into account the geometry and its effect on the velocity distribution over the cross section; the existing predictors do not reliably describe the sediment transport capacity in canals. For the best prediction methods, only 60% of the measured values were *well-predicted* within an error band of 100%;
- the Ackers and White and the Brownlie method provide more accurate estimates of the sediment transport capacity under the prevailing flow conditions and sediment characteristics in irrigation canals.

CHAPTER 6

SETRIC, a Mathematical Model for Sediment Transport in Irrigation Canals

6.1 INTRODUCTION

Clogging of the structures that supply water to secondary and tertiary units, and sedimentation of the canal network are some of the main problems in the operation and maintenance of irrigation systems. High annual investments are required for rehabilitation and maintenance to keep the systems suitable for their purpose. To reduce these expenses and to preserve and sometimes improve the performance of the irrigation networks, the sediment transport should be properly estimated in terms of time and space. An accurate prediction of the sediment deposition along the entire canal network during the irrigation season will contribute to an improved operation of the canals in such a way that the irrigation needs are fully met and at the same time a minimum deposition might be expected.

Although it is difficult to predict the quantity of sediment that will be deposited in irrigation canals (Brabben, 1990), numerical modelling of sediment transport offers the possibility to predict and evaluate the sediment transport under very general flow conditions (Lyn, 1987). A mathematical model, which includes the latest sediment transport concepts for the specific conditions of irrigation canals, will be an important and helpful tool for the designers and managers of these systems. This chapter will describe the computer model SETRIC, which has been in development at UNESCO-IHE since 1994 and which includes some of the specific characteristics of sediment transport in irrigation canals, as discussed in the previous chapter.

6.2 WATER FLOW EQUATIONS

Water flow in irrigation canals will be schematised as quasi-steady flow in which the governing equations are represented as:

- Continuity equation:

$$-\frac{\partial Q}{\partial x} = 0 \quad \therefore Q = \text{constant} \quad (6.1)$$

- Continuity equation at confluences and/or bifurcations:

$$- Q \pm q_l = 0 \quad (6.2)$$

- Dynamic equation:

$$- \frac{dh}{dx} = \frac{S_o - S_f}{1 - Fr^2} \quad (6.3)$$

Several methods are available to solve the dynamic equation of gradually varied flow for prismatic canals. Henderson (1966), Chow (1983), Depeweg (1993) and Rhodes (1995) present a comprehensive description of the available methods, including graphical-integration, direct integration, direct step, standard step, the Newton-Raphson solution and the predictor-corrector method. A summary of those methods is given in Chapter 2.

6.3 SEDIMENT TRANSPORT EQUATIONS

The numerical solution of the one-dimensional sediment equations that include the friction factor predictor, continuity equation for sediment and the sediment transport predictor (see Chapter 5) requires boundary conditions for water flow and sediment transport. These conditions are:

- description of the geometrical variables of the canal during a time step: width, slope and level of the bottom;
- description of the flow conditions along the entire canal during a time step: discharge, velocity, roughness, water depth and slope of the energy line;
- the characteristics of the incoming sediment, namely the sediment load and sediment size at the upstream boundary;
- the sediment transport rate along the entire canal;
- the changes in bottom level and/or bottom width;
- specific confluences and bifurcations can be incorporated by applying continuity for water flow and sediment load.

In order to compute the sediment transport along the entire canal, it is necessary to consider how the sediment load that is entering the canal adapts to the sediment transport capacity of the reaches; this is given in terms of the sediment concentration C , which follows from Galappatti's depth-integrated model:

$$C = C_e - (C_e - C_0)e^{-\frac{x}{L_A}} \quad \text{with } L_A = f\left(\frac{u_*}{v}, \frac{w_s}{u_*}, y\right) \quad (6.4)$$

Where:

- C = actual concentration
- C_e = equilibrium concentration
- C_0 = initial concentration
- x = distance along the canal
- L_A = adaptation length

In order to determine the actual sediment concentration in the x -direction of the canal, the values of the variables C_0 , L_A , Δx and C_e have to be known. The first one, the initial concentration C_0 , does not depend on the local flow condition, but instead depends on the source of water and sediment and on whether a sediment-trap is located at the head of the irrigation network. At boundaries between canal reaches, the sediment load passing through the downstream boundary of the upstream reach will become C_0 for the next canal reach.

In a gradually varied flow the values of C_e , y , v , u_* and f are functions of x . These variables may be known in advance at any point along the canal network if the flow equations are solved first (using the uncoupled technique). That means that in any point of the canal, $i = 0, 1, 2, \dots, n$ are given C_e , y , v , u_* and the dimensionless parameters u_*/v and w_s/u_* . These variables are determined according to the following procedure:

- the Δx -value is fixed according to the required degree of accuracy for the numerical solutions and the need for representing the adaptation of the actual non-equilibrium condition to the sediment transport capacity (the equilibrium condition) of the canal. The Δx -value should be much smaller than the adaptation length (L_A) of the actual sediment transport to the sediment transport capacity of the canal;
- computation of the L_A -value. For the local flow conditions the values of w_s/u_* , u_*/v and the water depth are known in advance. The maximum values of the parameter w_s/u_* should satisfy the requirements for the validity of the depth-integrated model (Ribberink, 1986);
- once the motion of sediment has been initiated, the values of the de Chézy coefficient can be estimated depending on the type of roughness along the wetted perimeter of the canal by:

$$C = 18 \log \frac{12R}{k_s} \quad \text{for single roughness} \quad (6.5)$$

$$C'_e = 18 \log \frac{12R}{k_{se}} \quad \text{for composite roughness} \quad (6.6)$$

- the value of the depth-averaged equilibrium concentration C_e will be determined by one of the sediment transport predictors, such as Ackers-White, Brownlie or Engelund-Hansen. The predictors compute the sediment transport per unit width (q_s), which is determined by the local flow conditions and the sediment properties. The total sediment transport across the whole canal section Q_{se} is calculated by:

$$Q_{se} = \alpha B q_s \quad (6.7)$$

- Next, the equilibrium concentration C_e is calculated by:

$$C_e = \left(\frac{\rho_s}{\rho} \frac{Q_s}{Q} \right) * 1,000,000 \quad (\text{in ppm}) \quad (6.8)$$

- Some internal conditions along the canal can be taken into account for the computation of the sediment transport distribution either at boundaries between canal reaches or at boundaries at branches (bifurcations or confluences). Application of the continuity for the water flow and for the sediment transport rate is helpful when changes either in bottom width or bottom level, or at bifurcations or confluences have to be incorporated in the model. The distribution of water and sediment at bifurcations will depend on the local flow pattern at the branches.

6.4 GENERAL DESCRIPTION OF THE MATHEMATICAL MODEL

The computer program SETRIC simulates the water flow, sediment transport and changes of bottom level in an open network with a main canal and several laterals with or without tertiary outlets. Various flow conditions along the canal network and during the irrigation season can be simulated. Figure 6.1 shows the flow diagram for calculating the change of the bottom level in a canal reach during one time step. Flow diagrams of the computer program SETRIC for the water flow and sediment transport calculations in a canal reach are shown in Figures 6.2 and 6.3.

The background for the hydraulic and sediment transport computations was described in the previous chapter.

The general framework of the computer program consists of:

Hydraulic aspects

- The water flow can be modelled as a sub-critical, quasi-steady, uniform or gradually varied flow (backwater as well as drawdown curves). The water profiles for the subcritical, gradually varied flow include: H2, M1, M2, C1, S1 and A2;
- The water flow is in open channels with a rectangular or trapezoidal cross section; only friction losses are considered: no local losses due to changes in the bottom level, cross section or discharge will be taken into account. The canal sections are characterized by the following geometrical dimensions, namely:
 - length (l) presents the length of a canal section (m);
 - bottom width (B);
 - side slope (1 vertical : m horizontal);
 - the roughness is defined by the equivalent roughness coefficient (k_s); the total friction factor follows from the composite roughness for the entire cross section;
 - coordinates to give the relative location of a canal section; the most upstream boundary is defined as $x = 0$ m;
 - bottom slope (S_0 in m/m);
 - bottom elevation above a reference level (datum) at the beginning of each canal section (z_b).

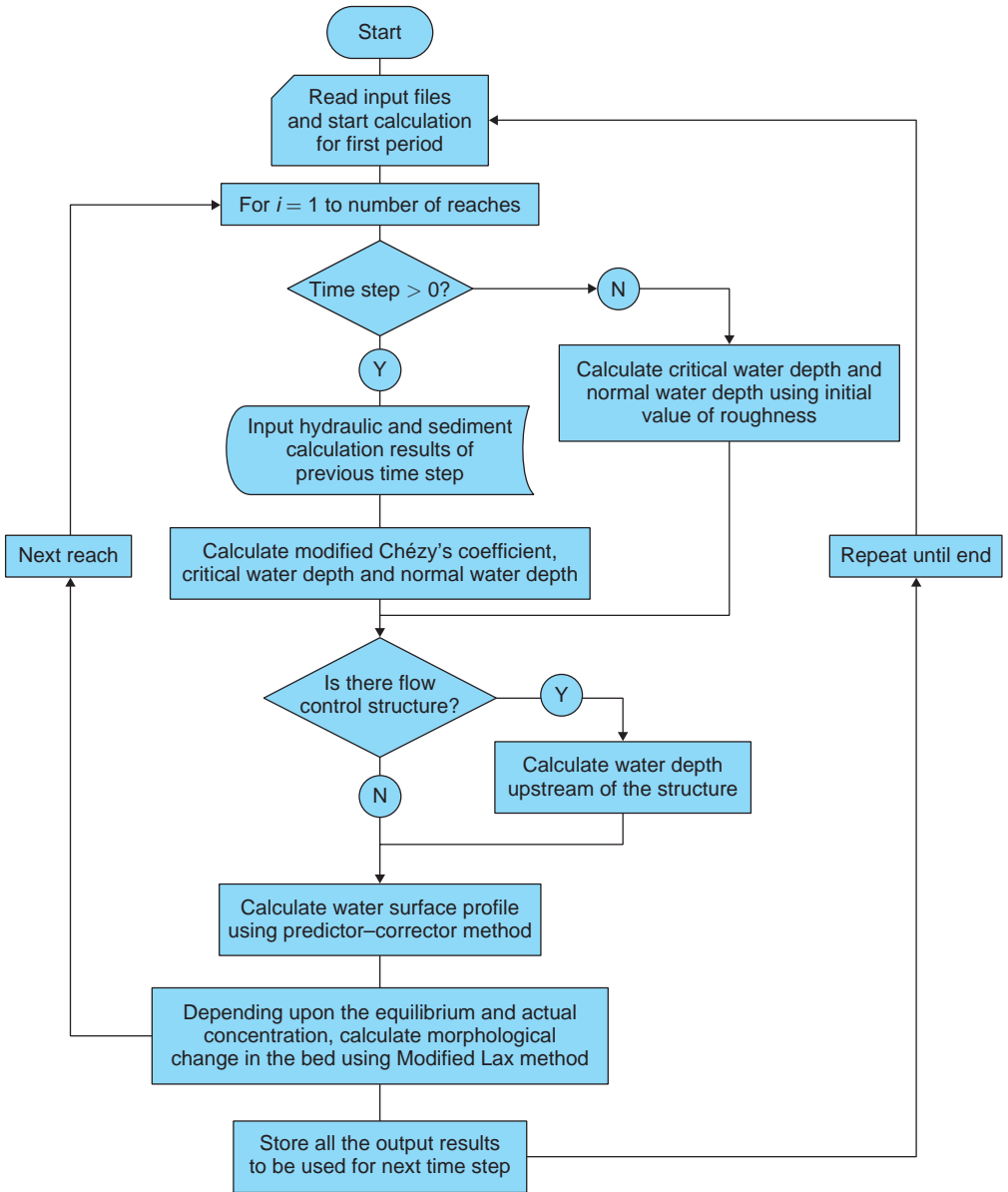


Figure 6.1. Flow diagram of SETRIC for calculating the water flow, sediment transport and changes in bottom level in main and/or lateral canals (after Paudel, 2002).

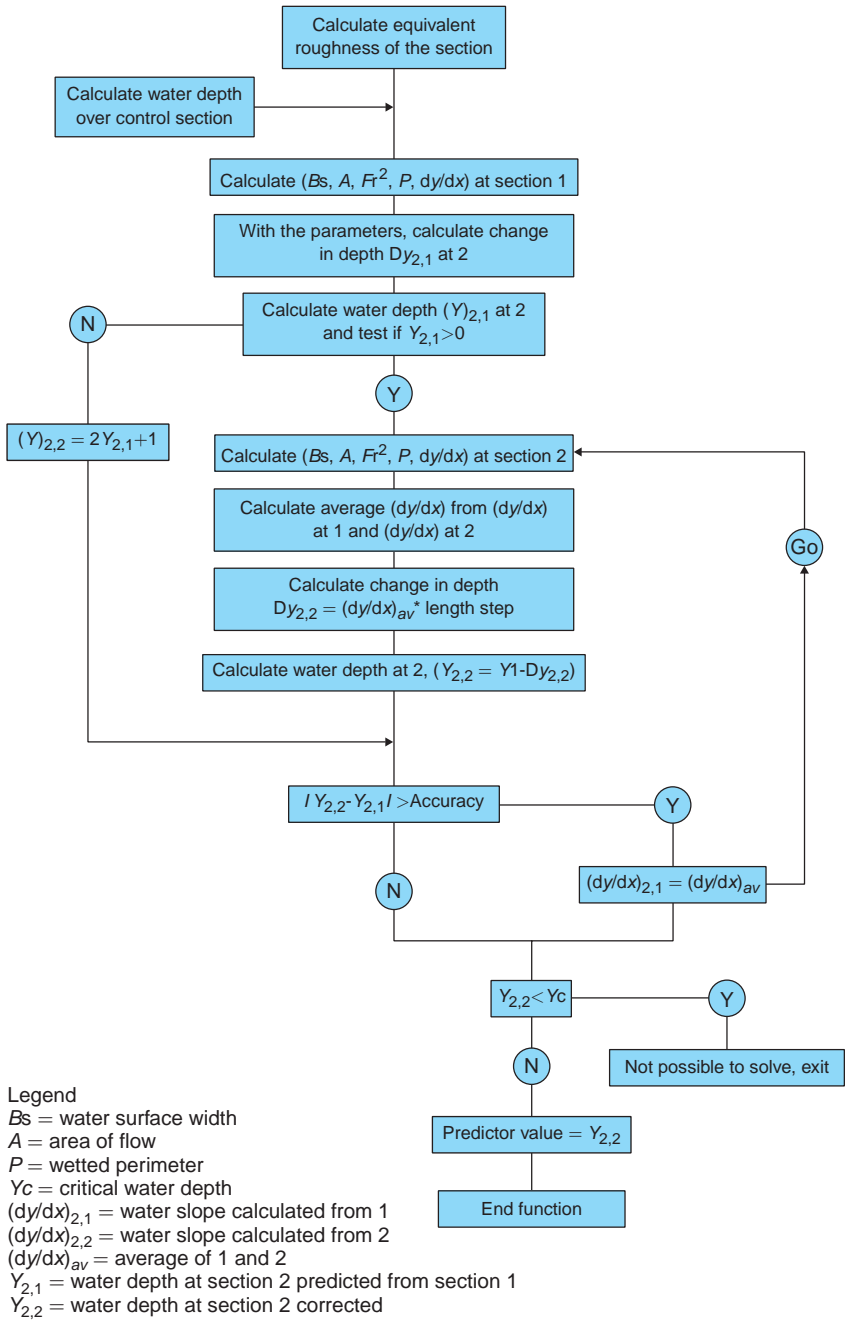


Figure 6.2. Flow diagram of SETRIC for calculating the water flow in main and lateral canals during a time step (after Paudel, 2002).

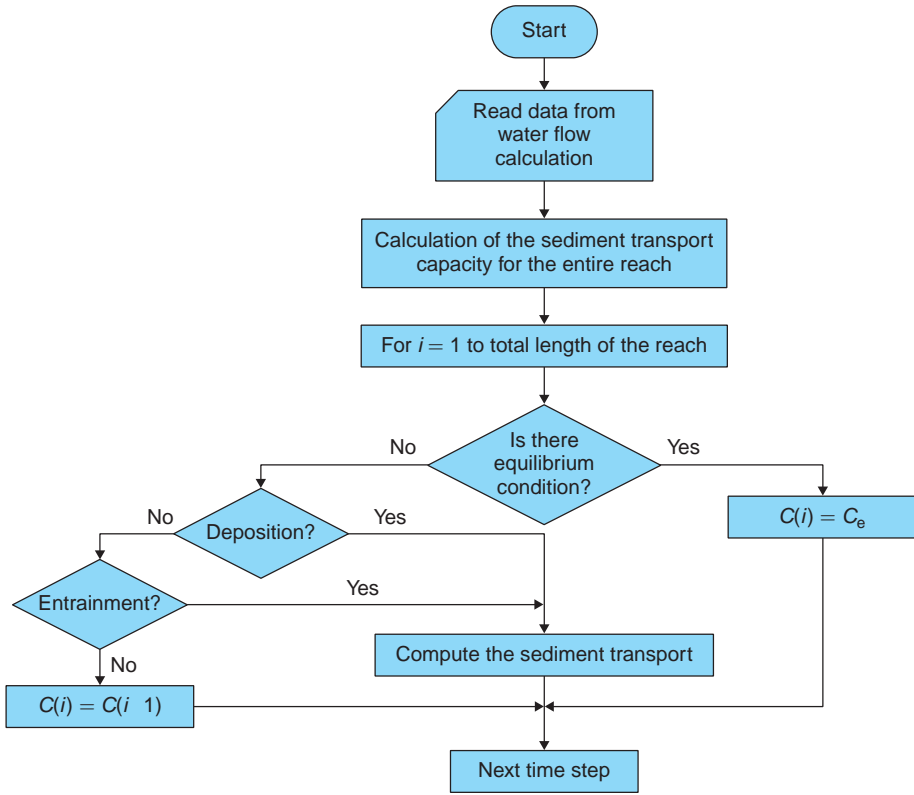


Figure 6.3. Flow diagram of SETRIC for calculating the sediment transport in the main canal and lateral canals during a time step.

Sediment aspects

- The sediment is characterized by:
 - sediment concentration (ppm) at the furthest upstream boundary of the main canal;
 - sediment size by the mean diameter d_{50} .
- Variations of the roughness conditions over time are incorporated in the model; sedimentation during the irrigation season will induce the development of bed forms, which depend on the flow conditions (different flow conditions will produce different types of bed form). The friction factor is computed for every time step and for each flow condition in each cross section of the schematisation.

Irrigation aspects

- The model of the irrigation network can be most simply composed of a main canal and secondary canals with tertiary outlets. Each canal is divided into several reaches or sections;

- the model can include changes in the bottom level at the upstream boundary of a canal section;
- control sections can be set at the downstream end of the main canal or secondary canals; the type of structure located at the downstream end of a section sets the water level;
- the network might include lateral inflow or outflow; these lateral flows should be located at the end of a canal section;
- the flow control structures that can be incorporated, include:
 - *overflow type*: crest width, crest level;
 - *undershot type*: width and height of the rectangular opening;
 - *submerged culverts and inverted siphons*: number and diameter of pipes;
 - *flumes*: constants of the upstream head-discharge relationship;
 - *drops*: incorporated as a different bottom level at the boundary between two reaches;
- the variation in crop water requirement during the irrigation season can be incorporated and mainly depends on the climate, cropping pattern, stage of the crops, leaching requirement and water losses. The growing season is divided into four stages depending on the crop development and climate (FAO, 1984). The water supply in the model can be attuned to the varying water requirement and follows the changes in area and time;
- maintenance activities in view of weed growth on the banks can also be included and the growth is referred to by an obstruction degree. The effect of maintenance on the roughness can be expressed by:
 - ideally maintained: negligible obstruction degree over time;
 - well maintained: a maximum obstruction degree of 10% is assumed;
 - poorly maintained: more than 75% obstruction degree is assumed.

6.5 INPUT AND OUTPUT DATA

Input data

For the computation of the water flow and sediment transport, the program requires several input data, which include:

- *Simulation period*: characteristics of the period to be simulated include:
 - number of periods in which the irrigation season is divided;
 - type of maintenance to be expected during each period of the irrigation season;
 - number of days for each period and the number of irrigation hours per day.
- *Canal dimensions*: the geometrical dimensions of main and secondary canals contain:
 - for each canal: number of sections, type of roughness data;

- for each section: location from upstream boundary, length, slope, width and elevation of the bottom; roughness coefficient, side slope.
- *Main and lateral discharges*: the schedule of irrigation flows (inflow (+) and outflow (–)) during each period of the irrigation season; the discharge entering the main canal for each period together with the lateral flows at the furthest upstream boundary of each lateral and for each period.
- *Sediment data*: mean sediment concentration and mean diameter of the sediment particles entering the main canal; SETRIC computes the sediment concentration flowing to the laterals.
- *Control sections*: the control section at the downstream end of the main canal and at each lateral has to be specified and they include the water level and the location of each control section. Control structures at the boundaries between canal-reaches are specified by the type of structure and its main hydraulic characteristics. SETRIC computes the upstream water level that will act as a control level for the next canal-reach.

Output data

The computer program is able to present the results of the water flow and suspended sediment transport calculations in tables or graphs depending on the selected option. Moreover, the results can be presented on the monitor or on paper. The program can show the following tables:

- General information:
 - results related to the water flow: normal and critical depth, discharge;
 - results related to the sediment transport: fall velocity, length step, minimum and maximum shear stress, shear velocity.
- Concentrations: table with the water depth, equilibrium concentration and actual concentration for the entire canal.
- Bottom level: the initial bottom level and the change in bottom level at the end of the period are presented.

6.6 CONCLUSIONS

The mathematical model SETRIC for predicting the water flow and the sediment transport together with the variation in bottom level of the canal is based on an uncoupled solution of the water flow and sediment transport equations. The model can be used for simulating the sediment deposition in an irrigation network under changing flow conditions and sediment characteristics during the whole irrigation season and over one or more years. The model can be used for evaluating the effects of the interrelation between irrigation practice (operation and maintenance) and

sediment deposition. The direct effect of irrigation practices on the sediment deposition may include changes in discharge, changes in sediment load, flow control structures, controlled deposition, operation and maintenance activities, diverted sediment load to the farmlands, etc. Sediment deposition in the canal reaches may affect the following hydraulic aspects, such as water level variation (overtopping of canals), water distribution at outlets and flow control structures.

The Sediment Transport Model SETRIC and its Applications

7.1 INTRODUCTION

The amount of water and sediment that enters into an irrigation canal will vary during the growing season and, moreover, throughout the entire life of an irrigation system. Variations in crop water requirement, water supply, size of the irrigation area, planned cropping pattern and sediment concentration frequently occur during the lifetime of irrigation systems. The design of canals and flow control structures incorporates a certain degree of flexibility in the delivery of different irrigation flows at fixed or variable supply levels. This design approach also assumes that the conveyance of the incoming sediment is, for the given design conditions, in a state of equilibrium. Once the flow conditions diverge from the design values, the flow velocity and thus the capacity to transport the sediment load will vary in time and space along the irrigation network. Then, the initial assumptions related to the conveyance of the sediment load in equilibrium conditions are no longer valid for these changed flow conditions. Due to these changes, the sediment transport in the irrigation canal will essentially be under non-equilibrium conditions. Therefore, the transport will strongly depend on the variation of the initial flow and the changes in the incoming sediment load during the irrigation season and the lifetime of the canal. For that reason sediment transport should be viewed in a more general context, which should take into account the time and place of the varying operation requirements of the irrigation system.

The sediment transport model SETRIC offers the possibility of predicting the sediment deposition and erosion in time and space, and for particular flow conditions and incoming sediment loads. This chapter will present some examples of sediment transport modelling in irrigation canals with the aim of showing the possible applications of the developed model and of improving the understanding of sediment transport processes for situations commonly encountered in irrigation systems.

Sediment that enters a canal network can either be transported without any deposition along the canal or the sediment concentration can adapt

itself from a non-equilibrium condition to the transport capacity of the canal. The adjustment towards the sediment transport capacity is assumed to follow Galappatti's depth-integrated model. A mass sediment balance in each canal reach will result in either net deposition or net entrainment. When the incoming sediment load is larger than the transport capacity of the reach, deposition will occur. When the incoming sediment load is less than the transport capacity two possibilities can be identified. In the first case entrainment of previously deposited sediment occurs until the sediment transport is fully adapted to the transport capacity. In the second case, no entrainment takes place and the sediment load is conveyed without any change.

The sediment deposition over a certain irrigation period will be simulated for an irrigation canal, for which the geometrical and hydraulic design data and the incoming sediment characteristics will be described in details.

The SETRIC model will be used to evaluate the effects of the following strategies on the sediment behaviour:

1. Changes in the discharges;
2. Changes in the incoming sediment load;
3. Controlled sediment deposition;
4. Flow control structures;
5. Operation activities.

The five cases of simulation will take place in a single, straight irrigation canal composed of a few reaches. Some other assumptions include the hydraulic conditions and sediment characteristics during the simulation period:

- the sediment size and sediment concentration are kept constant during the whole simulation period;
- erosion of the original bottom is not possible; only previously deposited sediment can be entrained during the simulation period;
- the side slopes are stable;
- the initial roughness of the canal will be characterized by one single roughness along the wetted perimeter;
- variations of the roughness conditions might occur over time due to changes in flow conditions, the occurrence of bed forms and the obstruction by aquatic weed (if applicable);
- the water level at the downstream end of the main canal is kept constant;
- the water level at the downstream end of a canal reach is managed either by a control structure or by the water level of the downstream reach;
- the sediment transport capacity and the actual sediment load are the equilibrium concentration and actual sediment concentration respectively; these concentrations are expressed in ppm by weight (parts per million).

The geometrical, hydraulic and sediment characteristics of the irrigation canal are:

length (L)	= 10,000 m
bottom width (B)	= 10 m
side slope (m)	= 2
equivalent roughness (k_s)	= 0.01 m
bottom slope (S_o)	= 0.00008 (0.08 m/km)
bottom level (begin)	= +40.00 m
bottom level (end)	= +39.20 m
design discharge (Q)	= 25.75 m ³ /s
sediment size (d_{50})	= 0.15 mm
equilibrium sediment concentration at the inlet	= 253 ppm
simulation period	= 90 days
flow control structure	= undershot type
water level at the end of the canal	= +41.65 m
flow condition	= nearly uniform flow
water depth	= 2.45 m

7.2 CASE 1 – CHANGES IN THE DISCHARGES

A key problem in the operation of irrigation canals is to find the correct flow conditions for which the water requirements are met for minimum sediment deposition in those canals.

A reduction in the irrigation supply, caused either by a drop in crop water requirements or in water availability or by a variation in cropping pattern and the need to deliver water at a certain supply level to the command area, is the most important cause of sediment deposition in the canals. The effect of a reduction in water supply for a constant water level at the downstream canal end on the sediment transport and hence, on the deposition, will be presented in Case 1 (see figure 7.1).

The reduction of the discharge is specified in terms of a relative discharge (Rd), which reads:

$$Rd = \frac{\text{actual discharge}}{\text{design discharge } (Q = 25.75 \text{ m}^3/\text{s})} \quad (7.1)$$

The canal has been designed in such a way that no deposition and erosion will take place for the design flow. The design discharge, which has a relative discharge Rd equal to 1, transports the sediment in equilibrium conditions; the sediment transport capacity of the canal is equal to, or larger than, the incoming sediment load and remains constant during the whole simulation period. Once the discharge decreases from the design discharge to a smaller one, a gradually varied flow will develop due to the fact that the water level (set point) at the downstream end remains

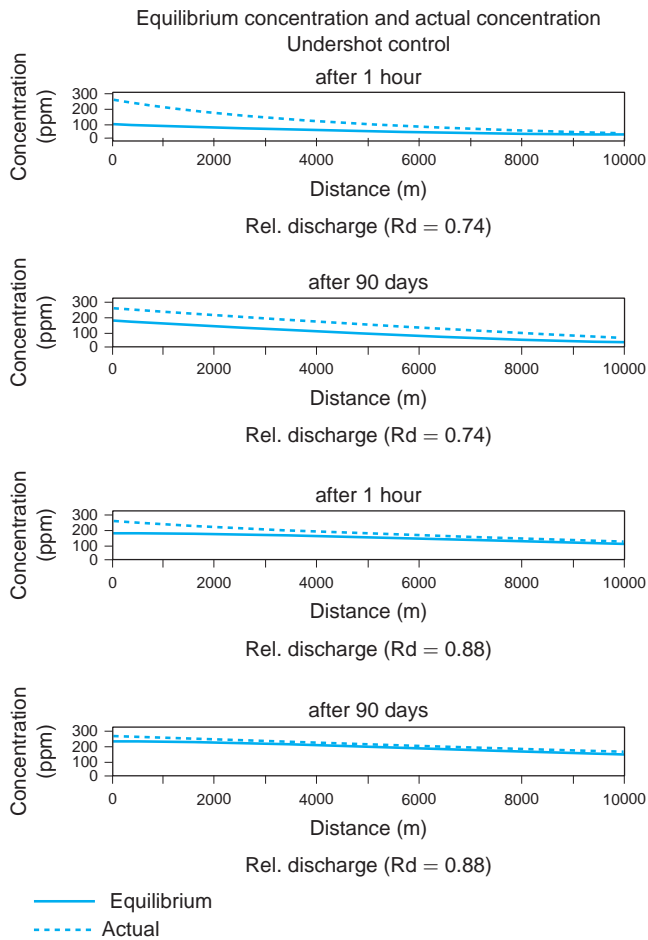


Figure 7.1. Equilibrium and actual concentration at the beginning and at the end of the simulation for a relative discharge of 0.74 and 0.88.

constant. The sediment transport capacity at the head will decrease due to the reduction in discharge; in addition, this transport capacity shows a continuous decrease in the downstream direction. Due to this decrease in the transport rate, deposition will occur along the canal due to the backwater curve caused by the downstream structure (actual water depth > normal water depth).

Figure 7.1 shows the equilibrium and actual concentration for a relative discharge of $R_d = 0.74$ and $R_d = 0.88$, respectively. At the end of the simulation period of 90 days, the equilibrium concentration for $R_d = 0.74$ is much smaller than for $R_d = 0.88$, which means that the deposition for $R_d = 0.71$ is much larger than for $R_d = 0.88$. The difference between the actual and equilibrium concentration is larger for a smaller R_d than for a large R_d .

In this case, the sediment concentration (ppm) entering the canal remains constant over the simulation period, which means that the volume of sediment entering the system will decrease with the discharge. However, smaller discharges result in smaller velocities and the sediment deposition in the canal is considerably larger for these discharges. Due to the fact that the total incoming sediment load during the simulation period is different for each relative discharge R_d , a relative deposition has been introduced to describe the sediment deposition in a comparable way. This relative deposition is the ratio of the sediment deposited in the entire canal and the total sediment load entered at the head of the canal, both during the simulation period:

$$\text{Relative deposition (\%)} = \frac{\text{total deposition}}{\text{total incoming sediment load}} * 100 \quad (7.2)$$

Figure 7.2 shows the amount of total deposited sediment in m^3 and the relative deposition (%) for a range of relative discharges ($R_d = 0.71-1$) after the simulation period of 90 days.

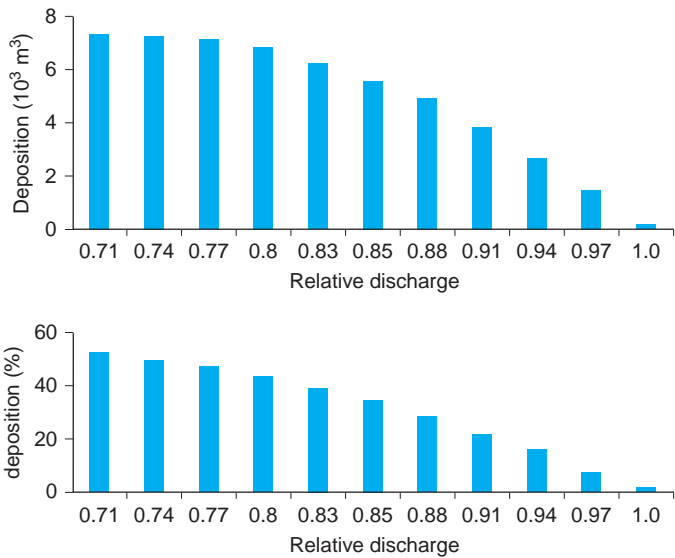


Figure 7.2. Sediment deposition and relative sediment deposition along the irrigation canal at the end of the simulation period as a function of the relative discharge.

Undershot control

7.3 CASE 2 – CHANGES IN THE INCOMING SEDIMENT LOAD

The sediment load entering an irrigation network depends on the specific conditions of the river and it is evident that the sediment concentration

will vary during an irrigation season and even more during the life of an irrigation system. The changes in incoming sediment load will include the variation in concentration as well as in the median sediment size. For Case 2, the changes will be related to the concentration (236 ppm) and to the sediment size (0.15 mm) as assumed for the equilibrium conditions.

To estimate the deposition, the sediment concentration and the median size will be changed during an irrigation period of 90 days. Variations in the sediment characteristics are expressed in terms of the ratio between the actual sediment load and the sediment transport capacity of the canal (equilibrium condition) and the ratio between the actual median size and the design value of the median diameter of the sediment (0.15 mm):

$$\text{Relative sediment load} = \frac{\text{actual sediment load}}{\text{equilibrium sediment load (236 ppm)}} \quad (7.3)$$

$$\text{Relative median sediment size} = \frac{\text{actual median sediment}}{\text{equilibrium median sediment size}(d_{50} = 0.15 \text{ mm})} \quad (7.4)$$

In view of the fact that the total incoming sediment during the simulation period is different for each relative sediment load, a relative deposition value has been used to describe the deposition in the entire irrigation canal. The relative deposition is expressed in terms of the ratio of the total sediment deposited and the total sediment load entering the canal both during the simulation period. It is expressed as:

$$\text{Relative deposition(\%)} = \frac{\text{total deposition}}{\text{total incoming sediment load}} * 100(\%) \quad (7.5)$$

The deposition in an irrigation canal depends very much on the characteristics of the incoming sediment. A relatively small deviation from the design equilibrium concentration results in a larger sediment load per unit length and a considerable deposition in the entire canal (Figure 7.3). The changes in the relative sediment size have an even larger impact on the deposition as shown in Figure 7.4.

7.4 CASE 3 – CONTROLLED SEDIMENT DEPOSITION

Uncontrolled sediment deposition in the canals may result in clogging (obstruction) of tertiary turnouts, reduction of the conveyance capacity, large variation in water levels, unpredictability of the relationship between water depth and discharge for structures, and high costs for canal desilting. Once the sediment enters a canal network it can be conveyed by the canals to the farm plots or it can be removed from the water, for example, either

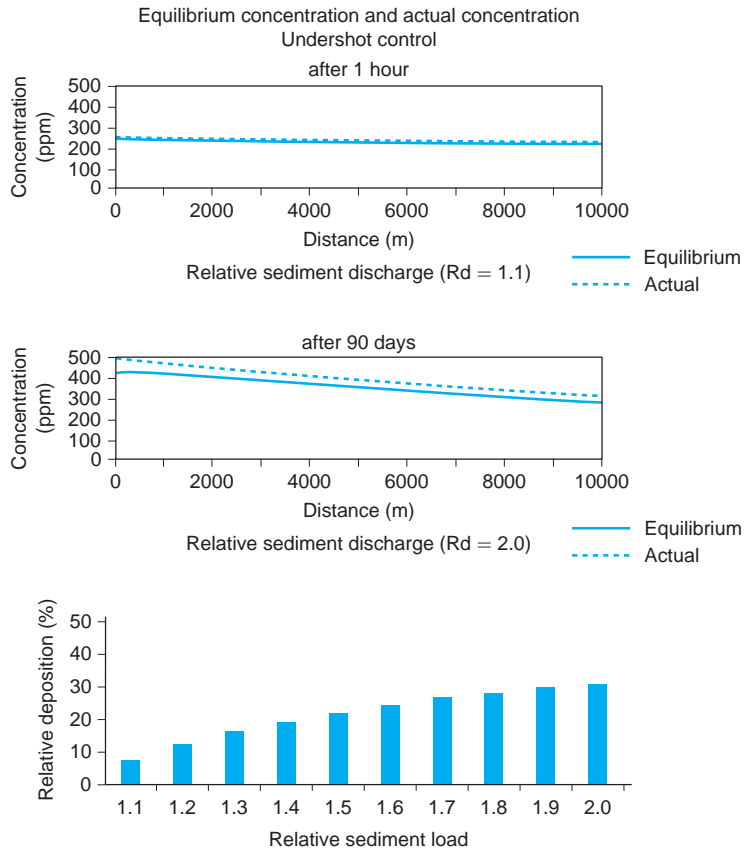


Figure 7.3. Total sediment deposition and relative sediment deposition after 90 days as a function of the variation in the relative sediment load.

by deposition along the entire canal or by deposition in a sediment-trap within some of the canal reaches where it can be periodically removed at minimum cost. Controlled deposition can be obtained by the design of a sediment trap in the network by deepening or widening one or more canal reaches. This solution can be an attractive alternative for controlling the deposition, but making a careful selection for the location of the sediment trap during the design phase is a very important requirement in view of the future operation costs.

Two scenarios will be presented to show how the deposition can be controlled and how a major part of the sediment load can be deposited in some modified canal reaches. When the actual sediment load is larger than the equilibrium load during the irrigation season, a change in the cross section might reduce the transport capacity in such a way that part of the sediment will be deposited. In the scenarios that have been presented the canal receives a sediment load of 300 ppm at the entrance and is unable to

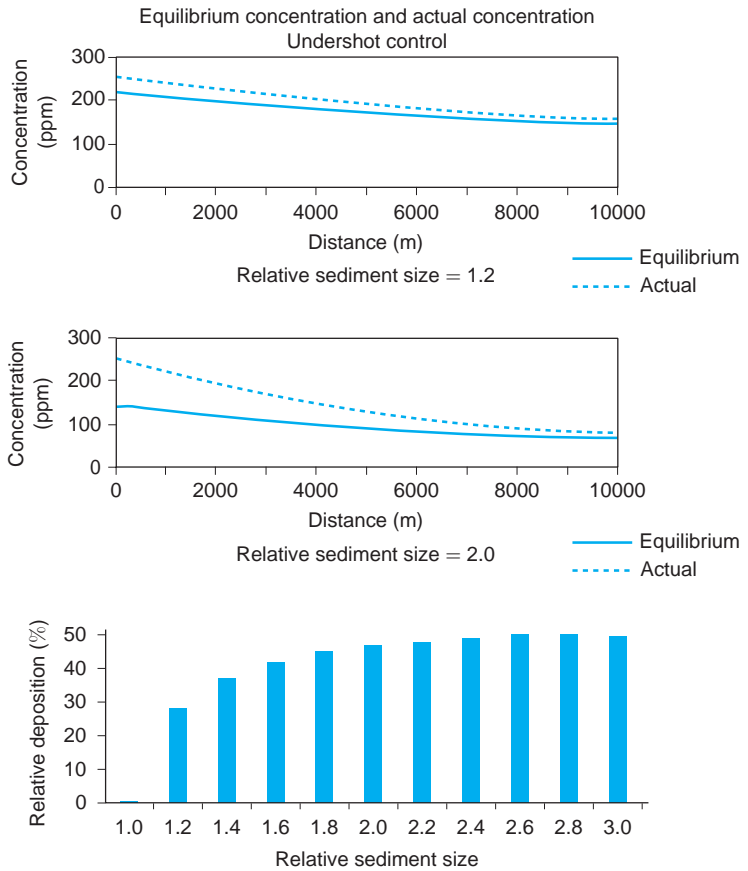


Figure 7.4. Total sediment deposition and relative sediment deposition after 90 days as a function of the variation in relative median sediment size.

transport the sediments to the fields for the duration of the entire irrigation season. Therefore, when no special measures are taken to control the deposition, it will occur along the entire length of the network.

The aim of the scenarios is to control the deposition in the head reach by reducing the transport capacity in that reach only. The head of the irrigation canal will be converted into a settling basin that can be described as:

1. *Scenario 1*: widening of the bottom width from 10 m to 14 m for the first 1000 m;
2. *Scenario 2*: deepening of the design canal bottom by 0.50 m for the first 1000 m.

No other alternatives will be evaluated for additional optimization of costs and/or sediment deposition. The previously mentioned geometrical and hydraulics canal data will be kept constant for both scenarios.

The simulation results of the two scenarios will be compared with the simulation result of the irrigation canal without any provision to trap the sediment in the first 1000 m. A relative deposition will be used for comparison of the simulation cases. The relative deposition is expressed as:

$$\text{Relative deposition} = \frac{\text{volume of deposited sediment in the first 1000 m}}{\text{total volume of entering sediment}} \quad (7.6)$$

Results of the simulations are compared in figure 7.5. Scenario 2 (deepening) holds more sediment than Scenario 1 (widening) for the same flow and sediment transport conditions. Scenario 2 has even accumulated four times more sediment than the canal without any sediment control. The controlled deposition by the two scenarios is very effective for the whole simulation period.

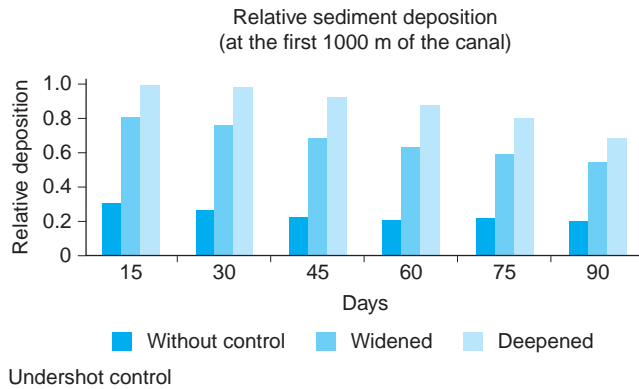


Figure 7.5. Relative sediment deposition of the two scenarios for controlling the sediment deposition.

The simulation results of the deposition due to the deepening of the canal are shown in figure 7.6. The figure gives the actual and equilibrium concentration at the beginning of the simulation period and after 90 days. The sediment trap gives very small equilibrium concentrations and a high deposition during the simulation period. At the end of the 90 days the equilibrium concentration rises to the actual concentration and the point at which the sediment trap is cleaned becomes critical.

The simulation results of the deposition due to the widening of the first canal reach are shown in figure 7.7. The behaviour of the actual and equilibrium concentration is rather similar to the one previously described. The widening shows much less deposition than the deepening of the canal.

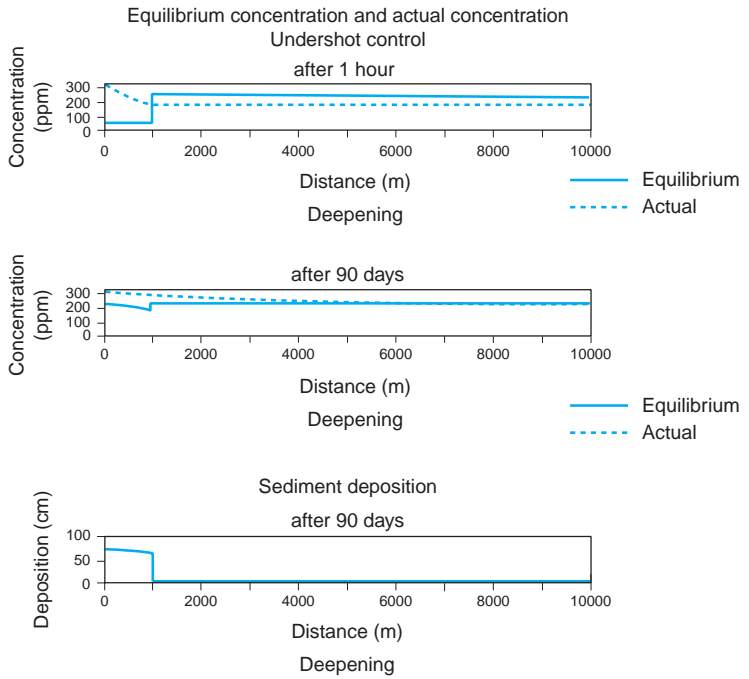


Figure 7.6. Sediment transport and sediment deposition in an irrigation canal with controlled deepening (a deepening of 0.50 m of the bottom over the first 1000 m of the canal).

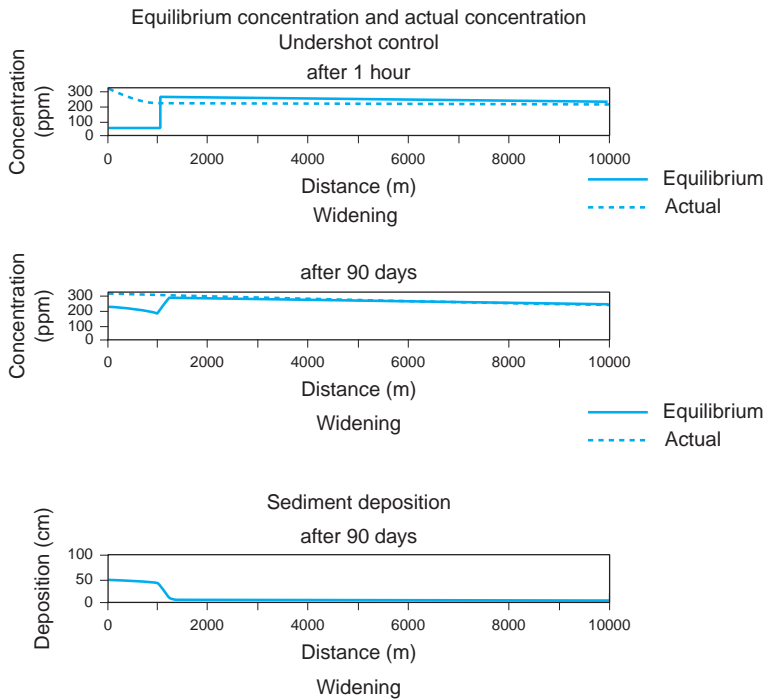


Figure 7.7. Sediment transport and sediment deposition in an irrigation canal with controlled deepening (by widening the bottom width over the first 1000 m of the canal).

7.5 CASE 4 – FLOW CONTROL STRUCTURES

One of the main design criteria for irrigation canals is the command level, which states that the canals should be able to deliver irrigation water at the right elevation to the command area. In view of this criterion flow control structures are needed to keep the water level at the command or target level for any discharge during the irrigation season. Two cases with a different type of control structure will be considered; namely:

- a structure with undershot flow (Case 4.1);
- a structure with overflow (Case 4.2).

Here the ability of structures to convey sediments will be evaluated; other (operational) aspects that might influence the selection of a structure will not be considered. Bed load and suspended load are conveyed by all structures with undershot flow; structures with overflow are also able to convey the suspended load, but any bed load will be trapped. To compare both control structures, they are placed at the downstream end of the canal and will maintain the water level at +41.65 m above reference level.

To compare the two structures the total deposition in the two cases is used on a relative basis:

$$\text{Relative sediment deposition} = \frac{\text{total sediment deposition in Case 4.2}}{\text{total sediment deposition in Case 4.1}} \quad (7.7)$$

The distribution of the deposition along the canal is evaluated by a relative change in bottom level, which is expressed as:

$$\text{Relative change in bottom level} = \frac{\text{variation of bottom level in Case 4.2}}{\text{variation of bottom level in Case 4.1}} \quad (7.8)$$

Figure 7.8 shows the simulation results after 90 days, namely the volume of sediment deposited before each structure and the relative deposition according to equation 7.7. The relative deposition shows that the deposition in Case 4.2 (overflow) is always larger than in Case 4.1 (undershot). The bed load passing the undershot structure is larger than the capacity of the overflow structure. In this Case 4 the three sediment predictors have also been compared. The Engelund-Hansen gives the largest sedimentation and the Ackers-White method gives the smallest

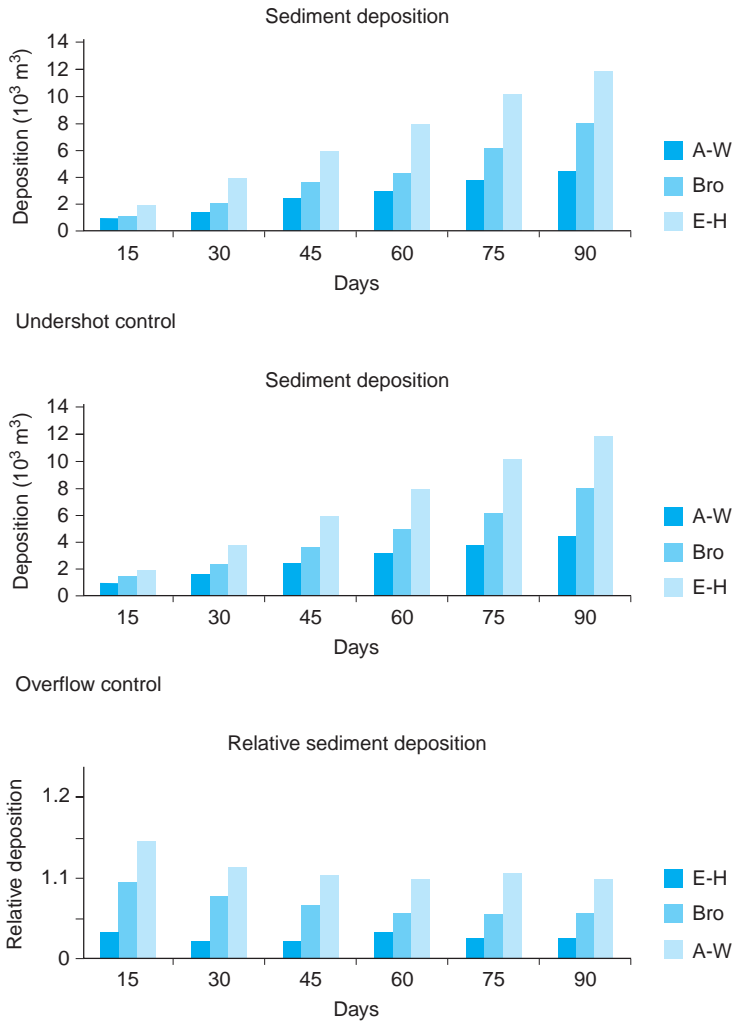


Figure 7.8. Total sediment deposition and relative sediment deposition for the two types of flow control structures.

sedimentation; these observations are in line with the discussions in Chapter 5.

Figure 7.9 shows the variation in bottom level for both structures along the entire canal. The graph presents an important difference in the distribution of the deposition before the two structures. The overflow structure shows a clear increase in sedimentation for the last 400 m upstream of the structure. The deposition in the reach from 0 m–9000 m is comparable for both structures. The relative change in bottom level in both cases is shown in figure 7.9.

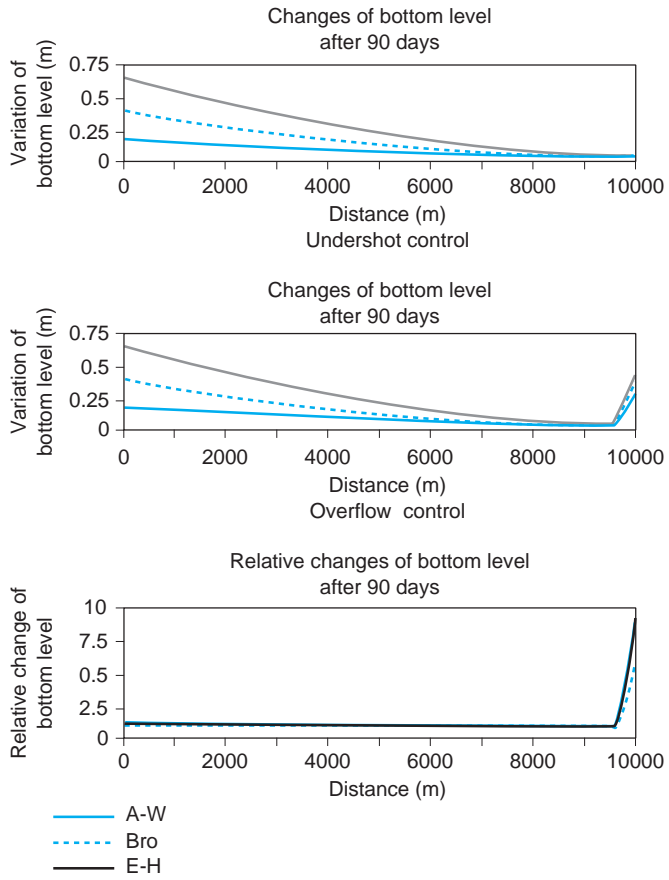


Figure 7.9. Comparison of changes in bottom level for the two types of flow control structures.

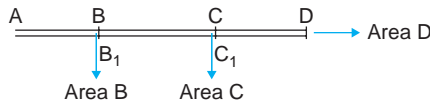
7.6 CASE 5 – OPERATION ACTIVITIES

Sustainable management of an irrigation system comprises all the necessary operation and maintenance activities to deliver water to the users at the right time, at the correct level and with the proper discharge. Each irrigation scheme is operated in a different way. The operation depends on various factors, such as the water availability, management of the water supply, scheduling of water delivery, control of water levels and discharges, water measurement, qualification of the operation personal, institutional limitations, field water requirements, water rights, evaluation and monitoring and maintenance activities. This large range of miscellaneous options and constraints makes it difficult to develop a general selection procedure for the most effective operation (Walker, 1993). Formulation of an operation plan for a certain system requires the evaluation

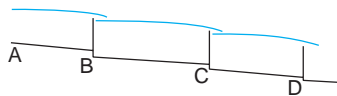
of several scenarios in view of the reliability of the water delivery. One of the aspects related to the reliability is the risk of sediment deposition in the system. The simulation of several operation scenarios will support the evaluation of various effects of the operation on the deposition in a canal network. In order to assess these effects a canal network will be schematized and the main data include the irrigation requirements, the geometrical and hydraulic data and incoming sediment characteristics. The network consists of a 16 km long main canal that delivers water to two laterals and to a reach downstream of the main canal. The main canal has three reaches, namely AB, BC and CD. The lateral B_1 delivers water to the area B that is 5 km from the head of the main canal. The second lateral C_1 conveys water to the area C and is about 11 km downstream of the intake. The reach CD conveys water to the canal downstream of D, which will irrigate the area D. Long crested weirs at the division points B, C and D control the water flow. One drop of 0.66 m is integrated in the structure at node B and another drop of 0.60 m is located at node C. Table 7.1 shows the geometrical and hydraulic characteristics of the reaches AB, BC and CD. Figure 7.10 shows the schematization of the network and the longitudinal profile of the main canal.

Table 7.1 Geometrical characteristics of a main irrigation canal.

Reach (-)	Length L (m)	Width B (m)	Roughness k_s (m)	Side slope m (-)	Bottom slope S_0 (10^{-3})
A-B	5000	10	0.03	2	0.08
B-C	6000	10	0.03	2	0.08
C-D	5000	8	0.03	2	0.10



(a) Schematization of an irrigation system



(b) Longitudinal profile of a main canal

Figure 7.10. Schematization of an irrigation system and longitudinal profile of the main canal.

The irrigation season is characterized by three periods in which the water requirement for each area is given in Table 7.2.

For the simulation of the effects of the operation plan on the deposition in the main canal, four scenarios are analyzed. All of them comply with the water requirements and the water supply for the irrigated areas. The Ackers-White sediment transport predictor is used to compute the

Table 7.2 Water needs during the irrigation season of the irrigated area.

Irrigated area		Period					
Area	ha	1		2		3	
		Duration in days	Needs in l/s.ha	Duration in days	Needs in l/s.ha	Duration in days	Needs in l/s.ha
B	5000	28	0.8	28	1	28	0.8
C	5000	28	0.8	28	1	28	0.8
D	15000	28	0.8	28	1	28	0.8

sediment transport capacity. In this hypothetical case the distribution efficiency of the main canal is assumed to be 100%. The incoming sediment load at the head A during the whole irrigation season is characterized by:

- median diameter $d_{50} = 0.15$ mm
- sediment concentration = 300 ppm

The four scenarios are:

- *Scenario 1 (continuous flow)*: a continuous flow to all canals during the whole season;
- *Scenario 2 (rotational flow by hour)*: the rotational flow during a day towards the lateral B₁ and C₁; each lateral receives water for 12 hours every 24 hours;
- *Scenario 3 (rotational flow by day)*: a rotational flow on a daily basis for the lateral B₁ and C₁; each lateral receives water for every other day;
- *Scenario 4 (rotational flow by week)*: a rotational flow on a weekly basis for the lateral B₁ and C₁; each lateral receives water for every other week.

The deposition during the season is determined for the entire canal ABCD for each scenario. The equilibrium sediment concentration for Scenario 1 (continuous flow) is always smaller than the incoming, the actual sediment load, in terms of time as well as space (see figure 7.11). Only at the downstream end of the canal reaches is the equilibrium concentration (sediment transport capacity) larger than the actual concentration; this is due to the local hydraulic aspects of the overflow structures (see the previous case). The mean velocities at these structures are increased due to the contraction at, and the drop downstream of, the structures. Although the transport capacity increases to some extent during the second period, a decreasing sediment transport capacity can still be observed in the downstream direction and along the entire main canal. As the actual load is larger than the transport capacity of the canal, sediment deposition occurs during all the periods and in the entire canal. Details of the sediment concentration at the end of each irrigation period (periods 1, 2

and 3) are shown for a continuous flow in figure 7.11. The figure at the bottom of Figure 7.11 shows the variation in bottom level at the end of Period 3. At the head of the canal the deposition is about 0.30 m, which decreases in the downstream direction; at the downstream end, in the reach CD, the deposition is about 0.10–0.15 m. The overflow structure clearly increases the sediment deposition.

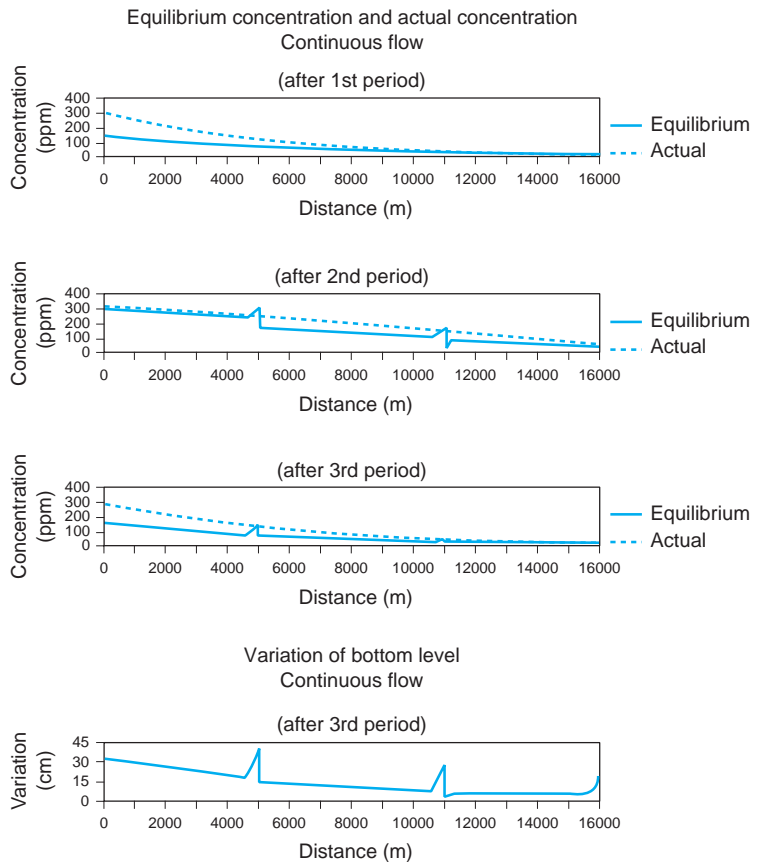


Figure 7.11. Equilibrium and actual concentration at the end of the irrigation periods 1, 2 and 3 and variation of the bottom level at the end of the simulation (continuous flow).

Figures 7.12 and 7.13 shows the sediment transport on the last day at the end of the three simulation periods, when the water has been diverted to the lateral B₁ and lateral C₁ respectively on a rotational 12-hourly basis. The transport capacity changes over time. The first change is due to the varying flow condition in the reach BC that follows from the rotational flow to either B or C. The second change is due to the varying irrigation requirements during the three irrigation periods that result in changing discharges. These changes in canal flow produce alternatively deposition and entrainment.

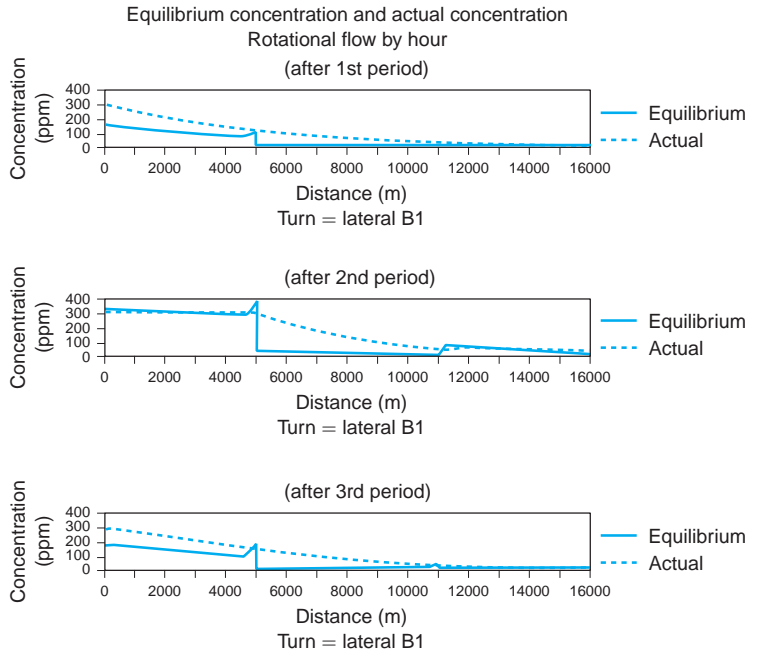


Figure 7.12. Equilibrium and actual concentration at the end of the irrigation periods 1, 2 and 3 during the first turn of irrigation (rotational flow by hour).

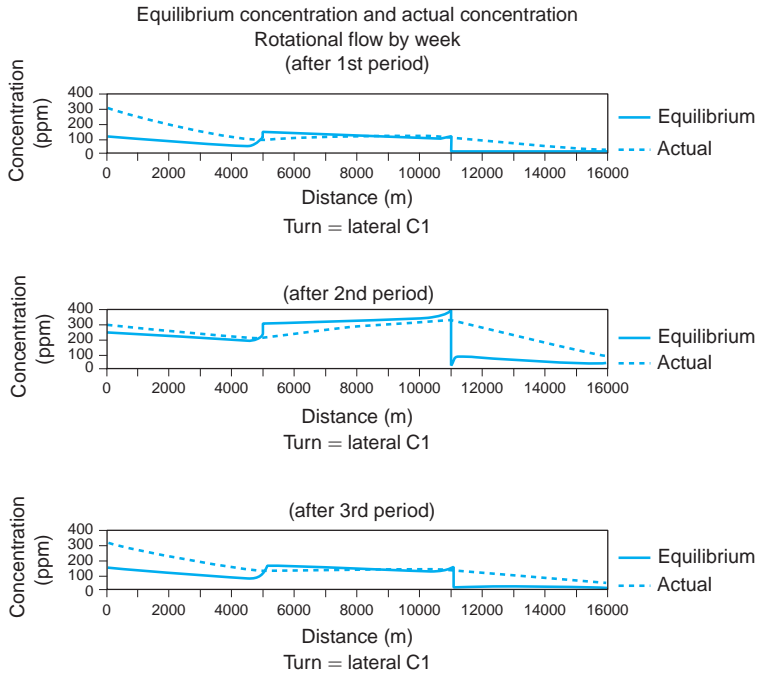


Figure 7.13. Variation of the equilibrium and actual concentration at the end of each irrigation period during the second turn of irrigation (rotational flow by hour).

In the reach AB the incoming concentration is always larger than the equilibrium concentration during Period 1 and deposition will occur. During the second period the discharge and the equilibrium concentration increase and the sediment load in reach AB is conveyed in a nearly equilibrium condition and with a minimum of deposition to the second reach BC.

The flow in reach BC is characterized by a gradually varied flow (back-water curve) with a very low velocity decreasing in downstream direction. In the first half of the day (fig. 7.12) the lateral B₁ is open and the lateral C₁ is closed. Deposition is observed in the reach BC during that part of the day. The increase of the discharge during the second period is not large enough to convey the sediment load entering reach BC. The concentration entering the next reach CD is small due to the large deposition in the previous reach and the sediment load is transported to the end of the canal with only very small deposition in reach CD. In the second half of the day (fig. 7.13), the lateral B₁ is closed and the lateral C₁ is open. The reach AB behaves rather similarly to the previous turn, but with a lower equilibrium concentration due to the fact that the water level over the weir crest is slightly higher than in the previous turn. The sediment transport capacity in reach BC is larger than the actual sediment load. In the second irrigation period the increase of the discharge in the reach BC produces a gradually varied flow (drawdown curve). Therefore an increasing transport capacity in the downstream direction and the entrainment of the previous deposited sediment are observed. The sediment load entering the next reach (reach CD) is larger due to the entrained sediment in the previous reach. For this flow condition, sediment deposition is observed throughout the whole season in the reach CD.

The variation of the bottom level at the end of the simulation period for this operation scenario (2) is shown in figure 7.14. The figure clearly shows that the main depositions occur in the reach AB and CD, while the deposition in reach BC is limited due to the rotational flow.

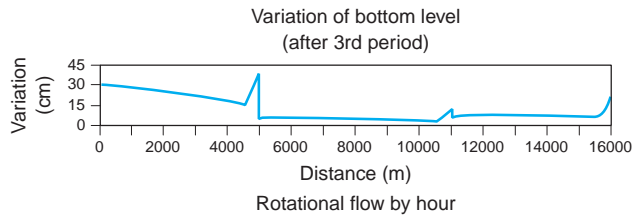


Figure 7.14. Variation of the bottom level during the simulation period (rotational flow by hour).

In scenarios 3 and 4 (rotational flow either by day or by week) the sediment transport behaves completely similarly to Scenario 2, but with other time intervals for the deposition and entrainment due to the different irrigation intervals for the three scenarios. Figures 7.15 and 7.16 shows the variation in the equilibrium and actual concentration at the end of the three periods (periods 1, 2 and 3) during the second turn of irrigation,

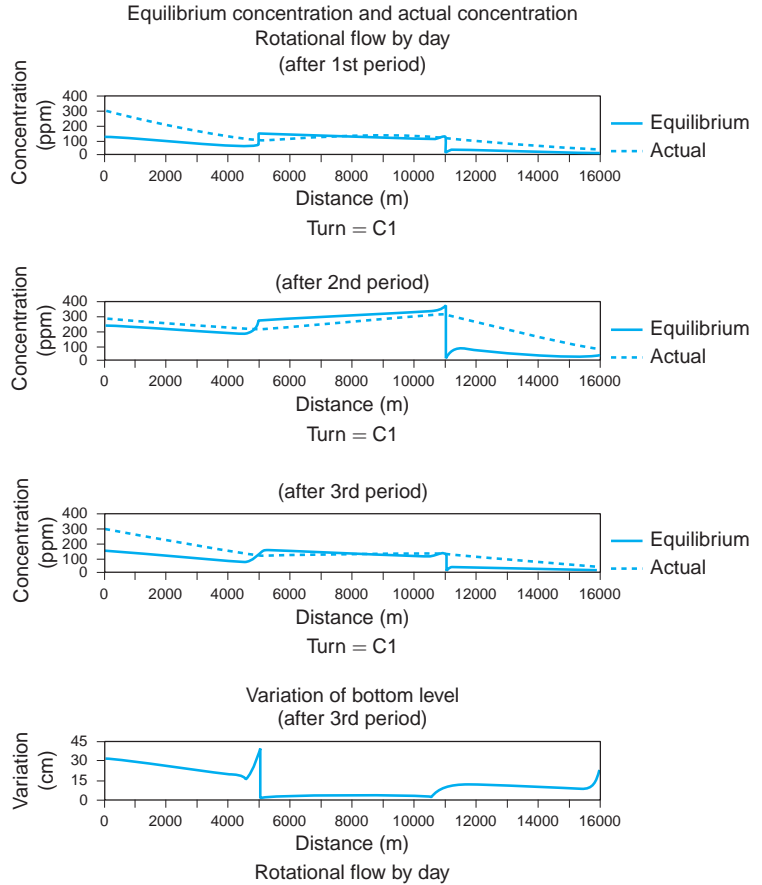


Figure 7.15. Equilibrium and actual concentration at the end of the irrigation periods 1, 2 and 3 and variation of the bottom level at the end of the simulation period (rotational flow by day).

namely after the rotational flow to branch C_1 . As explained in the previous scenario (2) the transport capacity during the second period reaches values larger than the incoming sediment load, and deposition and erosion of the previously deposited sediment is observed. The total sediment deposition for the three scenarios is almost the same and the observed differences mainly occur in the location of the deposition in each of the reaches.

In order to compare the deposition for each scenario, a relative sediment deposition is used that is related to the deposition observed for continuous flow (Scenario 1) and is expressed as:

$$\text{Relative deposition} = \frac{\text{computed sediment deposition by scenario 1}}{\text{computed sediment deposition by scenarios 2, 3, or 4}} \quad (7.9)$$

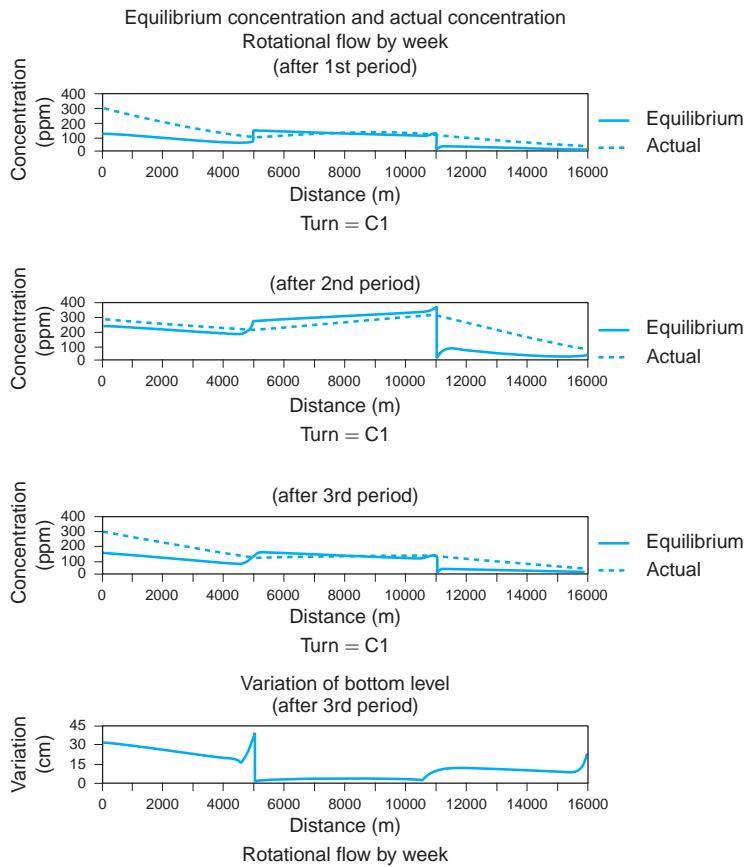


Figure 7.16. Equilibrium and actual concentration at the end of the irrigation periods 1, 2 and 3 and variation of the bottom level at the end of the simulation (rotational flow by week).

Figure 7.17 gives the relative deposition for each scenario and the following conclusions:

- the largest deposition in the entire canal (all reaches together) is observed for Scenario 1. The deposition for this scenario is about 20% larger than for the other scenarios; the relative deposition is about 1.2. The sediment depositions in scenarios 2, 3 and 4 are almost the same;
- in the reach AB the deposition in all the scenarios is about the same; the differences are less than 5% . These small differences can be explained by the different time intervals that a specific head occurs on the weir during each of the four scenarios;
- the deposition in reach BC for Scenario 1 is 2–3.5 times the deposition for Scenario 2, 3 and 4. In the latter scenarios, the equilibrium concentration increases during the time that lateral C₁ is open and lateral B₁ is closed and during the second period. This increase is beyond the incoming sediment load and produces entrainment of the previously deposited sediment;

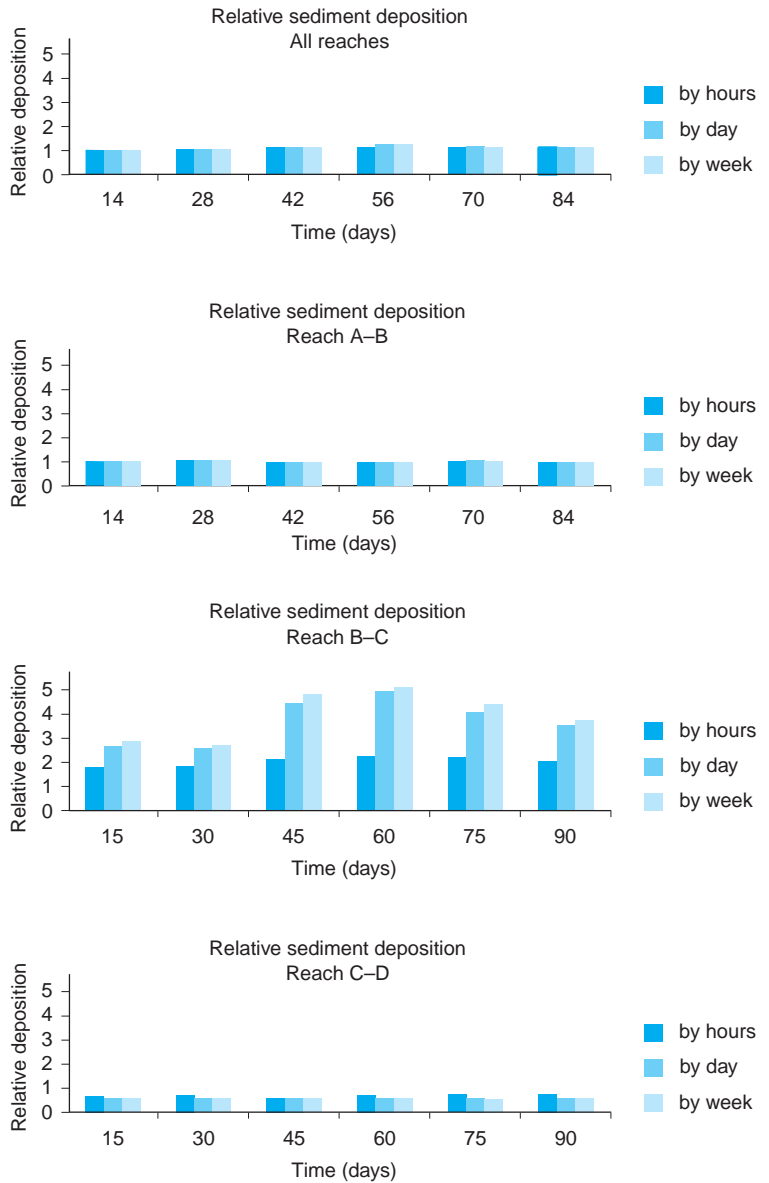


Figure 7.17. Relative sediment deposition in the reaches and the irrigation canal when compared with the sediment deposition observed in Scenario 1 (continuous flow).

- in reach CD the deposition of Scenario 1 is approximately half the deposition of scenarios 2, 3 and 4. In the scenarios 2, 3 and 4 the sediment load leaving reach BC is very small due to the relative large deposition in that reach and therefore the sediment load entering reach CD can be transported with a minimum of deposition;

- the total deposition in and its distribution over the canals are important aspects in the selection of the optimal operation strategy for the water delivery by an irrigation network.

7.7 CONCLUSIONS

Reflecting on the previously presented simulation results for the different scenarios, it can be concluded that the SETRIC model is a useful tool for a qualitatively assessment of the sediment deposition within irrigation canals under diverse flow conditions and sediment characteristics. Nonetheless, the mathematical model still has to be calibrated and validated before the model can be fully used as a simulation tool. The performance of the model has to be confirmed by field measurements that should prove whether the physical processes are well represented by the model or whether there are some deficiencies as a result of the assumptions used to describe those processes. Monitoring of the sediment deposition in an irrigation network is needed to evaluate the model and to investigate the response of the bottom level in time and space to determine water flows and sediment characteristics. Influences such as the type and operation of flow control structures, geometrical characteristics of the canals, water flow and the incoming sediment characteristics on the deposition, which the mathematical model predicts, will contribute to an enhanced understanding of the sediment transport processes under the flow conditions prevailing in irrigation canals.

References

- Ackers P. & W. R. White, 1973. Sediment transport: new approach and analysis. *Journal of Hydraulic Division, ASCE*. Vol. 99, No. 11. New York, USA.
- Ackers P., 1994. Sediment transport in open channels: Ackers and White update. *Proc. Instn. Civ. Engrs. Wat., Marit. & Energy*. Technical note No. 619. United Kingdom.
- Ankum P., 1995. *Lectures notes on flow control in irrigation and drainage*. IHE. Delft, the Netherlands.
- Armanini A. & G. Di Silvio, 1988. A one dimensional model for the transport of a sediment mixture in non-equilibrium condition. *Journal of Hydraulic Research, IAHR*. Vol. 26, No. 3. the Netherlands.
- Asano T. et al., 1985. Characteristics of variation of Manning's roughness coefficient in a compound cross section. *21st IAHR congress*. Melbourne, Australia.
- ASCE, 1963. Friction factor in open channels. *Journal of Hydraulic Division, ASCE*. Vol. 89, No. 2. New York, USA.
- ASCE, 1966a. Initiation of Motion. Task committee on preparation of sedimentation manual. *Journal of Hydraulic Division, ASCE*. New York, USA.
- ASCE, 1993. Unsteady-flow modelling of irrigation canals. *Task Committee on Irrigation Canal Hydraulic Modelling*. ASCE. New York, USA.
- Bagnold R., 1966. An approach to the sediment transport problem from general physics. *Geological Survey Prof. Paper 422.I*. Washington, USA.
- Bakker B. et al., 1989. Regime theories updated or outdated. *Delft Hydraulics*. Publication no. 416. Delft, the Netherlands.
- Bakry M. et al., 1992. Field Measured Hydraulic Resistance Characteristic in Vegetation Infested Canal. *Journal of Hydraulic Division, ASCE*. New York, USA.
- Bettess R., W. R. White & C. E. Reeve, 1988. Width of regime channels. *International conference on river regime. Hydraulic research*. Wallingford, United Kingdom.
- Bishop A. et al., 1965. Total bed material transport. *Journal of Hydraulic Division, ASCE*. Vol. 91, No. 2. New York, USA.

- Biswas A., 1995. Water for the developing world in the 21 century: issues and implications. *ICID journal*. New Delhi, India.
- Blench T., 1970. Regime theory design of canals with sand beds. *Journal of Irrigation and Drainage Division, ASCE*. Vol. 96, No. 2. New York, USA.
- Bogardi J., 1974. *Sediment transport in alluvial streams*. Akademiai Kiado. Budapest, Hungary.
- Brabben T., 1990. Workshop on Sediment Measurement and Control, and Design of Irrigation Canals. *Hydraulic Research*. Wallingford, United Kingdom.
- Breuser H. N., 1993. *Lecture notes on sediment transport*. IHE. Delft, the Netherlands.
- Brownlie W., 1981. Prediction of flow depth and sediment discharge in open channels. California Institute Technology. W. M. Keck Lab. Rep. No. KH-R-54. California, USA.
- Brownlie W., 1983. Flow depth sand bed channel. *Journal of Hydraulic Division, ASCE*. Vol. 109, No. 7. New York, USA.
- Bruk S., 1986. Sediment Transport and Control in Irrigation System. *International Conference on water Resources Needs and Planning in Drought Prone Area*. Khartoum, Sudan.
- Carruthers I. et al., 1997. Irrigation and food security in the 21st century. *Irrigation and drainage systems*. Vol. 11. Kluwer Academic Publishers. Dordrecht, the Netherlands.
- Celik I. & W. Rodi, 1985. Mathematical Modelling of Suspended Sediment Transport. *21st IAHR Congress*. Melbourne Australia.
- Celik I. & W. Rodi, 1988. Modelling Suspended Sediment Transport in non Equilibrium Situation. *Journal of Hydraulic Division, ASCE*. Vol. 14. New York, USA.
- Chang Howard, 1985. Design of stable alluvial canals in a system. *Journal of Hydraulic Division, ASCE*. New York, USA.
- Chitale S. V., 1994. Lacey divergence equation for alluvial canal design. *Journal of Hydraulic Division, ASCE*. Vol. 120, No.1. New York, USA.
- Chow Ven Te, 1983. *Open channel hydraulics*. Mc Graw Hill International Book Company. Tokio, Japan.
- Chuang Yang et al., 1989. Semi-coupled Simulation of Unsteady Non uniform Sediment Transport in Alluvial Canal. *23rd IAHR congress*. Ottawa, Canada.
- Clemmens A. J., F. M. Holly & W. Schuurmans, 1993. Description and evaluation of Dufrow. *Journal of Hydraulic Division, ASCE*. Vol. 119, No. 4. New York, USA.
- Cunge J. A., F. M. Holly & A. Verwey, 1980. *Practical Aspects of Computational River Hydraulics*. Pitman Advanced Publishing Program. London, United Kingdom.
- Dahmen E. R., 1994. *Lecture notes on canal design*. IHE. Delft, the Netherlands.

- Dahmen E. R., October 1999, *Irrigation and Drainage Systems Part 1*, Lecture Notes of Hydraulic Engineering, IHE-Delft, the Netherlands.
- Davies T. R. H., 1982. Lower flow regime bed forms: rational classification. *Journal of Hydraulic Division, ASCE*. Vol. 108, pp. 343–360. New York, USA.
- Depeweg H., 1993. *Lecture notes on applied hydraulics: gradually varied flow*. IHE. Delft, the Netherlands.
- Depeweg H. & V. Néstor Méndez, 2002. Sediment Transport Applications in Irrigation Canals. *Irrigation and Drainage*. Vol. 51: 167–179. John Wiley & Sons Ltd.
- Depeweg, H. & K. P. Paudel, 2003. Sediment Transport Problems in Nepal Evaluated by the Setric Model. *Irrigation and Drainage*. Vol. 52: 247–260. John Wiley & Sons Ltd.
- Depeweg, H. & E. Rocabado Urquieta, 2004. GIS Tools and the Design of Irrigation Canals. *Irrigation and Drainage*. Vol. 53: 301–314. John Wiley & Sons Ltd.
- DHI (Danish Hydraulics Institute), 1993. *Mike 11: technical reference guide*. Danish Hydraulics Institute. Copenhagen, Denmark.
- DHL (Delft Hydraulics Laboratory) & Ministry of Transport, Public Works and Water Management, 1994. *SOBEK: technical reference guide*. Delft Hydraulics. Delft, the Netherlands.
- Engelund F., 1966. Hydraulic resistance of alluvial stream. *Journal of Hydraulic Division, ASCE*. Vol. 92, No. 2. New York, USA.
- Engelund F. & E. Hansen, 1967. *A monograph on sediment transport in alluvial streams*. Teknisk Forlag, Copenhagen, Denmark.
- Galappatti R., 1983. A Depth Integrated Model for Suspended Transport. *Report no 83-7*. Delft University of Technology. Delft, the Netherlands.
- Henderson F. M., 1966. *Open Channel Flow*. Mac Millan Publishing Co. Inc. New York, USA.
- Hofwegen P. J. M. van, 1992. *Lecture notes on principles of irrigation management*. IHE. Delft, the Netherlands.
- Hofwegen P. J. M. van, 1993. *Lecture notes on irrigation and drainage system*. IHE. Delft, the Netherlands.
- HR Wallingford, 1992. *DORC: user manual*. HR Wallingford. Wallingford, United Kingdom.
- Huang J. & Liu Hexian, 1993. A Research on the Operation schemes for an Irrigation Project with Plenty of Sediment Inputs. *25th IAHR congress*. Tokyo, Japan.
- Huang J. et al., 1993. A Study on the Sediment Transport in an Irrigation Scheme. *15th ICID congress*. The Hague, the Netherlands.
- IHE, 1998. *Duflow-manual*. IHE-Delft. Delft, the Netherlands.
- Ikeda S., 1982a. Lateral bed load transport on side slopes. *Journal of Hydraulic Division Vol. 108, No. HY11, ASCE*. New York, USA.

- Ikeda S., 1982b. Incipient motion of sand particles on side slopes. *Journal of Hydraulic Division* Vol. 108, No. HY1, ASCE. New York, USA.
- Jansen P., 1994. *Principles of river engineering*. Delftse Uitgevers Maatschappij. Delft, the Netherlands.
- Kouwen N., 1969. Flow retardance in vegetated channels. *Journal of Irrigation and Drainage Division, ASCE*. Vol. 95, No.2. New York, USA.
- Kouwen N., 1992. Modern approach to design of grassed channels. *Journal of Hydraulic Division, ASCE*. Vol. 118, No. 5. New York, USA.
- Krishnamurthy M. & B. Christensen, 1972. Equivalent roughness for shallow channels. *Journal of Hydraulic Division, ASCE*. Vol. 118, No. 5. New York, USA.
- Krüger F., 1988. Flow laws in open channels. Doctoral thesis at the Dresden University of Technology. Dresden, Germany.
- Lawrence E. F. & Miguel Marino, 1987. Canal design: optimal cross section. *Journal of Hydraulic Division, ASCE*. Vol. 113, No. 3. New York, USA.
- Lawrence P., 1990. Canal Design, Friction and Transport Predictor. *Workshop on Sediment Measurement and Control, and Design of Irrigation Canals. Hydraulic Research*. Wallingford, United Kingdom.
- Lawrence P., 1993. Deposition of Fine Sediments in Irrigation Canals. *15th ICID congress*. The Hague, the Netherlands.
- Leliavsky S., 1983. *Irrigation Engineering: canals and barrages*, Chapman and Hall, London
- Lyn D. A., 1987. Unsteady Sediment Transport Modelling. *Journal of Hydraulic Division, ASCE*. Vol. 113. New York, USA.
- Magazine M. K. et al., 1988. Effect of bed and side roughness on dispersion in open channel. *Journal of Hydraulic Division, ASCE*. Vol. 114, No. 7. New York, USA.
- Mahmood K., 1973a. Sediment Equilibrium Consideration in the Design of Irrigation Canal Network. *Proc. IAHR. International Symposium on River Mechanics*. Bangkok, Thailand.
- Mahmood K., 1973b. Sediment routing in irrigation canal systems. *ASCE, National Water Resources Engineering Meeting*. Washington D.C, USA.
- Meadowcroft I., 1988. The applicability of sediment transport and alluvial friction prediction in irrigation canals. *Report technical note OD-TN 34. HR Wallingford*. Wallingford, United Kingdom.
- Mendez N., 1995. Suspended sediment transport in irrigation canals. *MSc thesis. IHE*. Delft, the Netherlands.
- Motayed A. & M. Krishnamurthy, 1980. Composite roughness of natural channels. *Journal of Hydraulic Division, ASCE*. Vol. 106, No. HY6. New York, USA.
- Naimed Ullah M., 1990. Regime and Sediment Transport Concepts Compared as Design Approaches. *Workshop on Sediment Measurement and Control, and Design of Irrigation Canals. Hydraulic Research*. Wallingford, United Kingdom.

- Nakato T., 1990. Test of Selected Sediment Transport Formula. *Journal of Hydraulic Engineering, ASCE*. New York, USA.
- Ogink H. J. M., 1985. The effective viscosity coefficient in 2-D depth-averaged flow models. *Proc. 21st IAHR congress*. Melbourne, Australia.
- Orellana V. O. M. & J. F. Via Giglio, 2004. Computer Aided Design of Canals. *MSc thesis. IHE*. Delft, the Netherlands.
- Paintal A. S., 1971. Concept of critical shear stress in loose boundary open channel. IAHR. No. 9. Delft, the Netherlands.
- Paudel K. P., 2002. Evaluation of the sediment transport model SETRIC for irrigation canal. *MSc thesis. IHE*. Delft, the Netherlands.
- Paudel K. P. & H. Depeweg, 2005. Effects of Canal Operation on Sediment Transport. Sunsari Morang Irrigation Scheme, Nepal. *Proceedings ICID Congress*, Beijing China.
- Petryk S. & G. Bosmajian III, 1975. Analysis of flow through vegetation. *Journal of Hydraulic Division, ASCE*. Vol. 120, No. 5. New York, USA.
- Querner E., 1993. Aquatic weed control within an integrated water management framework. Doctoral thesis, *Agricultural University of Wageningen*. Wageningen, the Netherlands.
- Ranga Raju K. G., 1981. *Flow through open channels*. Tata McGraw-Hill. New Delhi, India.
- Raudkivi A. J., 1990. *Loose Boundary Hydraulics*. 3rd Edition. Pergamon Press. Great Britain.
- Raudkivi A. J. & H. Witte, 1990. Development of bed features. *Journal of Hydraulic Division, ASCE*. Vol. 116, No. 9. New York, USA.
- Ribberink J. S., 1986. Introduction to a depth integrated model for suspended sediment transport (Galappatti, 1983). *Report No. 6-86. Delft University of Technology*. Delft, the Netherlands.
- Rocabado U. E., 2002. GIS and Computer Applications in Irrigation Canal Design. *MSc thesis. IHE*. Delft, the Netherlands.
- Sakhuja V. S., 1987. A compilation of methods for predicting friction and sediment transport in alluvial channels. *Report OD/Tn 2, Hydraulic Research*. Wallingford, United Kingdom.
- Sanmuganathan K., 1990. Sediment research at hydraulic research; the quantitative approach to design and performance prediction. *Workshop on sediment measurement and control, and the design of irrigation canal*. Edited by Tom Brabben. Wallingford, United Kingdom.
- Schultz B., 1997. Drainage for the 21st century: Policy issues and strategies for emerging problems. *7th ICID International drainage workshop: Drainage for the 21st century*. Proceedings. Vol. 1. Penang, Malaysia.
- Sherpa K., 2005. Use of the Sediment Transport Model Setric in an Irrigation Canal. *MSc Thesis*. UNESCO-IHE, the Netherlands.
- Simons D. B. & E. V. Richardsons, 1961. Forms of bed roughness in alluvial channels. *Journal of Hydraulic Division, ASCE*. No. 3. New York, USA.

- Simons D. B. & E. V. Richardsons, 1966. Resistance to flow in alluvial channels. *Geological Survey Prof. Paper 422-I*. Washington, USA.
- Simons D. & Fuat Senturk, 1992. *Sediment Transport Technology*. Water Resources Publications. Colorado, USA.
- Sloff C. J., 1993. Analysis of Basic Equations for Sediment-Laden Flows. *Delft University of Technology*. Delft, the Netherlands.
- Timilsina P., 2005. One-Dimensional Convection Diffusion Model for Non-Equilibrium Sediment Transport in Irrigation Canals. *MSc Thesis*. UNESCO-IHE, the Netherlands.
- Vanoni V., 1974. Factors determining bed forms in alluvial streams. *Journal of Hydraulic Division, ASCE*. Vol. 100, No. 3. New York, USA.
- Vanoni V. (Ed.), 1975. Sedimentation Engineering. *Manuals and reports on engineering practice No. 54*. ASCE. New York, USA.
- Vanoni V., 1984. Fifty years of sedimentation. *Journal of Hydraulic Division, ASCE*. New York, USA.
- Van Rijn L. C., 1982. Equivalent roughness of alluvial bed. *Journal of Hydraulic Division, ASCE*. New York, USA.
- Van Rijn L. C., 1984a. Sediment Transport Part I: Bed load Transport. *Journal of Hydraulic Division, ASCE*. Vol. 110, No. 10. New York, USA.
- Van Rijn L. C., 1984b. Sediment Transport Part II: Suspended Load Transport. *Journal of Hydraulic Division, ASCE*. Vol. 110, No. 11. New York, USA.
- Van Rijn L. C., 1984c. Sediment transport part III: Bed form and alluvial roughness. *Journal of Hydraulic Division, ASCE*. Vol. 110, No. 12. New York, USA.
- Van Rijn L. C., 1993. *Lecture notes on principles of sediments transport in rivers, estuaries, coastal seas and oceans*. IHE. Delft, the Netherlands.
- Vlugter H., 1962. Sediment transportation by running water and design of stable alluvial channels. *De Ingenieur*. The Hague, the Netherlands.
- Vreugdenhil C., 1989. *Computational Hydraulics*. Springer-Verlag. Berlin, Germany.
- Vries M. de, 1975. A morphological time scale for rivers. *IAHR*. Sao Paulo, Brazil.
- Vries M. de, 1982. A Sensitivity Analysis Applied to Morphological Computations. *Report No. 85-2*. Delft University of Technology. Delft, the Netherlands.
- Vries M. de, 1987. *Lecture notes on Morphological Computations*. Delft University of Technology. Delft, the Netherlands.
- Wang Shang-yi, 1984. The principle and application of sediment effective power. *Journal of Hydraulic Division, ASCE*. New York, USA.
- Wang S. (editor), 1989. Sediment transport modelling. *Proceeding of the international symposium, ASCE*. New York, USA.
- Wang Z. B. & J. S. Ribberink, 1986. The validity of a depth integrated model for suspended sediment transport. *Journal of Hydraulic Research, IAHR*. Vol. 24, No. 1. Delft, the Netherlands.

- White W. R. et al., 1979. A new general method for predicting the frictional characteristics of alluvial streams. Hydraulic Research Limited, Wallingford, United Kingdom.
- White W. R., 1989. Regime principle applied to the design of mobile bed physical models. *23rd IAHR congress*. Ottawa, Canada.
- White R., R. Bettes & E. Paris, 1982. Analytical approach to river regime. *Journal of Hydraulic Division, ASCE*. Vol. 108, No. 10. New York, USA.
- Woo H. et al., 1988a. Performance test of some selected transport formulae. *Journal of Hydraulic Division, ASCE*. New York, USA.
- Worapansopak J., 1992. Control of Sediment in Irrigation Schemes. *M.Sc. thesis. IHE*. Delft, the Netherlands.
- World Bank, 1995. The World Bank and Irrigation. *World Bank Operation Evaluation Department. The World Bank*. Washington DC, USA.
- Wormleaton, P. R. et al., 1982. Discharge assessment in compound channel flow. *Journal of Hydraulic Division, ASCE*. Vol. 108, pp 975–994. New York, USA.
- Yalin M. S., 1977. *Mechanics of Sediment Transport*. Pergamon Press. Oxford, Great Britain.
- Yalin M. S., 1985. On the determination of ripple geometry. *Journal of Hydraulic Division, ASCE*. New York, USA.
- Yang C. T., 1973. Incipient motion and sediment transport. *Journal of Hydraulic Division, ASCE*. Vol. 99. No. 110. New York, USA.
- Yang C. T., 1979. Unit stream power equation for total load. *Journal of Hydrology Division, ASCE*. Vol. 99. No. 110. New York, USA.
- Yang C. T. & A. Molinas, 1982. Sediment transport and Unit stream power. *Journal of Hydraulic Division 40*. Amsterdam, the Netherlands.
- Yang J. C., J. Y. Wang & C. L. Wang, 1989. Semi-coupled simulation of unsteady non-uniform sediment transport in alluvial channel. *23rd IAHR congress*. Ottawa, Canada.

Symbols

SI-UNITS

Basic units

Quantity	Unit	SI symbol
Length	meter	m
Mass	kilogram	kg
Time	second	s
Plane angle	radian	rad

Derived units

Quantity	Unit	SI symbol
Acceleration	meter per second squared	m/s^2
Area	square meter	m^2
Density	kilogram per cubic meter	kg/m^3
Discharge	cubic meter per second	m^3/s
Energy	Joule	$\text{J} = \text{N} \cdot \text{m}$
Force	Newton	$\text{N} = \text{kg} \cdot \text{m/s}^2$
Pressure	Pascal	$\text{Pa} = \text{N/m}^2$
Power	Watt	$\text{W} = \text{Nm/s}$
Velocity	meter per second	m/s
Viscosity, dynamic	Pascal-second	$\text{Pa} \cdot \text{s}$
Viscosity, kinematic	square meter per second	m^2/s
Volume	cubic meter	m^3

SYMBOLS

Symbol	Quantity	Unit	Dimension
A	Area, cross section area	(m ²)	L ²
a	Height of half roughness $k/2$	(m)	L
B	Channel bottom width	(m)	L
B_0	Channel width; bed width	(m)	L
B_s	Water surface width	(m)	L
B_s	Sediment transport width	(m)	L
B_s	Water surface width	(m)	L
C	de Chézy resistance coefficient	(m ^{1/2} /s)	L ^{1/2} T ⁻¹
C'	de Chézy coefficient due to skin resistance	(m ^{1/2} /s)	L ^{1/2} T ⁻¹
C''	de Chézy coefficient due to form resistance	(m ^{1/2} /s)	L ^{1/2} T ⁻¹
c	Sediment concentration	(%, ppm by mass)	—
C	Sediment concentration	(%, ppm by mass)	—
c_0	Concentration at length $x = 0$	(%, ppm by mass)	—
C_0	Total sediment concentration at $x = 0$	(%, ppm by mass)	—
c_a	Reference concentration at level 'a' from the bottom	(%, ppm by mass)	—
c_b	Bed load concentration	(%, ppm by mass)	—
C_c	Contraction coefficient	(—)	—
C_d	Discharge coefficient	(—)	—
C_D	Drag coefficient	(—)	—
c_e	Equilibrium concentration	(%, ppm by mass)	—
C_e	Total equilibrium sediment concentration	(%, ppm by mass)	—
C_e	Effective Chézy coefficient	(m ^{1/2} /s)	L ^{1/2} T ⁻¹
C'_e	Modified effective Chézy coefficient	(m ^{1/2} /s)	L ^{1/2} T ⁻¹
C_f	Friction coefficient, $(u_* / v)^2$	(—)	—
c_t or C_t	Total sediment concentration	(%, ppm by mass)	—
C_v	Velocity coefficient	(—)	—
d	Particle diameter	(m)	L
D	Diameter	(m)	L
d^*	Dimensionless particle diameter	(—)	—
D_*	Dimensionless particle parameter	(—)	—
d_{50}	Median particle diameter	(m)	L
d_i	Diameter of i -percent finer than d_i	(m)	L
d_i	Representative particle diameter	(m)	L
d_r	Discrepancy ratio	(—)	—
e	Exponential number; $e = 2.71828$	(—)	—
E	Total energy in relation to a horizontal datum	(J/N)	—
E_s	Specific energy in relation to lowest point of a cross-section	(Nm/N)	L
f	Darcy-Weisbach resistance coefficient	(—)	—
f	Friction factor	(—)	—
f	Lacey's silt factor	(—)	—
F	Shape factor	(—)	—
$f(\dots)$	Function of	(—)	—
F_g	Grain Froude number	(—)	—
F_g	Weed factor	(—)	—
F_{gr}	Critical grain Froude number	(—)	—
F_{gr}	Dimensionless mobility parameter	(—)	—
Fr	Froude number	(—)	—

(Continued)

Symbol	Quantity	Unit	Dimension
g	Acceleration due to gravity	(m/s ²)	LT ⁻²
G_{gr}	Dimensionless mobility parameter	(-)	-
h	Water depth	(m)	L
K	Error factor	(-)	-
k	Roughness height	(m)	L
k_s	Roughness height of Nikuradse	(m)	L
k'_s	Grain roughness height	(m)	L
k''_s	Bed form roughness height	(m)	L
k_{se}	Effective equivalent roughness	(m)	L
k_s	Strickler coefficient	(m ^{1/3} /s)	L ^{1/3} T ⁻¹
$k_{m,d}$	Modified k_m for a canal depth d (Strickler)	(m ^{1/3} /s)	L ^{1/3} T ⁻¹
$k_{m,1m}$	Reference k_m for a canal depth of 1.0 m (Strickler)	(m ^{1/3} /s)	L ^{1/3} T ⁻¹
l, L	Length	(m)	L
L_A	Adaptation length	(m)	L
m	Side slope (1: m)	(-)	-
M	Momentum function	(-)	-
n	Manning resistance coefficient	(s/m ^{1/6})	L ^{1/6}
n_e	Equivalent Manning coefficient	(s/m ^{1/6})	L ^{1/6}
P	Wetted perimeter	(m)	L
p	Porosity	(-)	-
P	Power	(W)	-
Q	Discharge; water discharge, flow discharge	(m ³ /s)	L ³ T ⁻¹
q	Discharge per unit width of flow	(m ³ /s/m)	L ² T ⁻¹
q_*	Dimensionless unit discharge	(-)	-
q_b	Bed load transport rate per unit width	(m ³ /s/m)	L ² T ⁻¹
q_e	Equilibrium sediment discharge	(m ³ /s/m)	L ² T ⁻¹
q_s	Volumetric rate of sediment transport per unit width of flow	(m ³ /s/m)	L ² T ⁻¹
q_s	Sediment discharge per unit width	(m ³ /s/m)	L ² T ⁻¹
Q_s	Total sediment discharge	(m ³ /s)	L ³ T ⁻¹
Q_{so}	Sediment discharge at upstream point	(m ³ /s)	L ³ T ⁻¹
q_{st}	Flow discharge in a stream tube	(m ³ /s)	L ³ T ⁻¹
q_{sus}	Suspended load transport per unit width	(m ³ /s/m)	L ² T ⁻¹
r	Radius	(m)	L
R	Hydraulic radius	(m)	L
Re	Reynolds number	(-)	-
Re _*	Particle Reynolds number	(-)	-
R_g	Grain Reynolds number	(-)	-
R_v	Velocity ratio	(-)	-
S	Slope	(-)	-
s	Relative density	(-)	-
s.f.	Shape factor	(-)	-
S_f	Friction slope	(-)	-
S_o	Bed slope	(-)	-
t	Time coordinate	(s)	T
T	Excess bed shear stress parameter	(-)	-
T_A	Adaptation time	(s)	T
T/Q	Relative transport capacity	(-)	-
u_*	Shear velocity	(m/s)	LT ⁻¹
$u_{*,cr}$	Critical shear velocity	(m/s)	LT ⁻¹
u, v, w	Component of velocity in the X, Y and Z direction	(m/s)	LT ⁻¹

(Continued)

Symbol	Quantity	Unit	Dimension
v	Local velocity in x direction	(m/s)	LT^{-1}
V	Volume	(m^3)	L^3
\bar{V}	Mean velocity of flow	(m/s)	LT^{-1}
v_*	Shear velocity	(m/s)	LT^{-1}
v_{*C}	Critical value of v_* associated with incipient motion of bed particles	(m/s)	LT^{-1}
V_{cr}	Critical mean velocity	(m/s)	LT^{-1}
v_y	Local velocity in y direction	(m/s)	LT^{-1}
v_{av}	Average velocity of the water	(m/s)	LT^{-1}
w	Local velocity in z direction;	(m/s)	LT^{-1}
w_s	Fall velocity of a sediment particle	(m/s)	LT^{-1}
x, y, z	Cartesian coordinates	(m)	L
y	Flow depth; vertical scale; water depth	(m)	L
y_c	Critical depth	(m)	L
y_n	Normal depth	(m)	L
z	Bed elevation above datum	(m)	L
Z	Suspension number	(-)	-
∞	Infinite	(-)	-

GREEK SYMBOLS

Symbol	Quantity	Unit	Dimension
α	Correction factor	(-)	-
α	Angle	radian	-
β	Momentum correction factor (Boussinesq)	(-)	-
γ	Specific weight	(N/m^3)	FL^{-3}
γ_d	Form factor	(-)	-
γ_r	Ripple presence	(-)	-
δ_b	Saltation height	(m)	L
δ	Boundary layer thickness	(m)	L
Δ	Increment	(-)	-
Δ	Relative density: $\Delta = (\rho_s - \rho)/\rho$	(-)	-
Δ	Bed form height	(m)	L
λ	Bed form length	(m)	L
ε	Mixing coefficient	(m^2/s)	L^2T^{-1}
η	Eddy viscosity	(kgs/m^2)	FTL^{-2}
σ_s	Geometric standard deviation	(-)	-
ρ	Density	(kg/m^3)	FT^2L^{-4}
ρ_s	Density of the sediment particles	(kg/m^3)	FT^2L^{-4}
ρ_w	Density of water	(kg/m^3)	FT^2L^{-4}
θ	Shields parameter	(-)	-
θ	Dimensionless mobility parameter	(-)	-
θ_{cr}	Dimensionless critical mobility parameter	(-)	-

(Continued)

Symbol	Quantity	Unit	Dimension
κ	von Karman's constant; 0.4	(-)	-
ϕ	Dimensionless bed load sediment transport rate	(-)	-
ϕ	Functional relationship among non-dimensional parameters	(-)	-
ψ	Stratification correction	(-)	-
ν	Kinematic viscosity $\nu = \mu/\rho$	(m ² /s)	L ² T ⁻¹
ν_t	Effective viscosity	(m ² /s)	L ² T ⁻¹
μ	Absolute viscosity or dynamic viscosity	(Pa · s)	
π	Ratio of circular circumference and diameter; $\pi = 3.14159$	(-)	-
τ	Shear stress	(N/m ² or Pa)	FL ⁻²
τ	Tractive force	(N/m ² or Pa)	FL ⁻²
τ_{bx}	Bottom shear stress	(N/m ²)	FL ⁻²
τ_{cr}	Critical shear stress	(N/m ²)	FL ⁻²
τ'_{cr}	Critical shear stress for initiation of suspension	(N/m ²)	FL ⁻²
τ'	Grain shear stress	(N/m ²)	FL ⁻²
τ_{xy}	Effective shear stress	(N/m ²)	FL ⁻²
σ	Standard deviation	(-)	-
Σ	Summation symbol	(-)	-

APPENDIX A

Methods to Estimate the Total Sediment Transport Capacity in Irrigation Canals

A.1 INTRODUCTION

The design and operation of irrigation canals are based on the principle that no deposition or erosion occurs during certain periods. Good designs of an irrigation network as well as a well-operated irrigation system require an accurate prediction of the sediment transport of irrigation canals.

There is no universally accepted equation to determine the total transport capacity of sediment in irrigation canals. Many methods predict the sediment transport under a large range of flow conditions and sediment characteristics. The available prediction methods include the methods of Lane-Kalinski (1941), Einstein (1950), Colby (1964), Bishop et al. (1965), Bagnold (1966), Engelund-Hansen (1967), Chang et al. (1967), Toffaletti (1969), Ackers-White (1973), Yang (1979), Brownlie (1981), van Rijn (1984), etc. However, the predictability of all of them is still poor. Van Rijn (1984) stated that it is impossible to predict sediment transport with an accuracy of less than 100%. Therefore, it is quite difficult to make firm recommendations about which method to use in practice. Nevertheless, a comparison of sediment transport methods under the typical flow conditions and sediment characteristics of irrigation canals could become a powerful tool to reduce inevitable errors and inaccuracy. It is not possible to check all the existing methods to predict sediment transport. In these notes five of the most widely used methods to compute sediment transport will be presented. These methods are:

- Ackers-White;
- Brownlie;
- Engelund-Hansen;
- Van Rijn;
- Yang.

A.2 ACKERS AND WHITE METHOD

The method as developed by Ackers and White (1973) is based on flume experiments with sediment with a uniform or nearly uniform size distribution, with fully established flow conditions including bed forms, for water depths smaller than 0.4 m and for flows in the lower flow regime with $Fr < 0.8$. The method uses three dimensionless parameters, namely the grain size sediment parameter D_* , the mobility parameter F_{gr} and the transport parameter G_{gr} to describe the sediment transport.

- The grain size sediment parameter D_* reflects the influence of gravity, density and viscosity:

$$D_* = \left[\frac{(s-1)g}{\nu^2} \right]^{1/3} d_{35} \quad (\text{A.1})$$

- The mobility parameter F_{gr} is the ratio of the shear force on a unit area of the bed to the immersed weight of a layer of grains. The equation for the transitional range ($1 < D_* < 60$) is:

$$F_{gr} = \frac{u_*^n}{\sqrt{g} d_{35}(s-1)} \left[\frac{V}{\sqrt{32} \log \left(\frac{10h}{d_{35}} \right)} \right]^{1-n} \quad (\text{A.2})$$

Where:

$$n = 1.00 - 0.56 \log D_* \quad (\text{A.3})$$

- The transport parameter G_{gr} is based on the stream power concept and the equation reads:

$$G_{gr} = c \left(\frac{F_{gr}}{A} - 1 \right)^m \quad (\text{A.4})$$

With

$$A = \frac{0.23}{\sqrt{D_*}} + 0.14 \quad (\text{A.5})$$

$$m = \frac{9.66}{D_*} + 1.334 \quad (\text{A.6})$$

$$\log c = 2.86 \log D_* - (\log D_*)^2 - 3.53 \quad (\text{A.7})$$

The Ackers and White function for the total sediment transport reads as:

$$q_s = G_{gr} \nu d_{35} \left(\frac{V}{u_*} \right)^n \quad (\text{A.8})$$

Where:

D_* = grain parameter (dimensionless)

d_{35} = representative particle diameter (m)

- h = water depth (m)
- ν = kinematic viscosity (m^2/s)
- F_{gr} = mobility parameter (dimensionless)
- A = value of F_{gr} at the nominal, initial movement
- G_{gr} = transport parameter (dimensionless)
- c = coefficient in the transport parameter G_{gr}
- m = exponent in the transport parameter G_{gr}
- n = exponent in the mobility parameter F_{gr}
- u_* = shear velocity (m/s)
- V = mean velocity (m/s)
- q_s = total sediment transport per unit width (m^2/s)

A.3 BROWNLIE METHOD

The Brownlie method (1981) to compute the sediment transport is based on a dimensional analysis and calibration of a wide range of field and laboratory data, where uniform conditions prevailed. The transport (in ppm by weight) is calculated by:

$$q_s = 727.6 c_f (F_g - F_{\text{grcr}})^{1.978} S^{0.6601} \left(\frac{R}{d_{50}} \right)^{-0.3301} \quad (\text{A.9})$$

- grain Froude number:

$$F_g = \frac{V}{[(s - 1)g d_{50}]^{0.5}} \quad (\text{A.10})$$

- critical grain Froude number:

$$F_{\text{grcr}} = 4.596 \tau_{*o}^{0.5293} S^{-0.1405} \sigma_s^{-0.1606} \quad (\text{A.11})$$

- critical shear stress

$$\tau_{*o} = 0.22Y + 0.06(10)^{-7.7Y} \quad (\text{A.12})$$

The value of Y follows from:

$$Y = (\sqrt{s - 1} R_g)^{-0.6} \quad (\text{A.13})$$

- grain Reynolds number:

$$R_g = \frac{(g d_{50}^3)^{0.5}}{31620 \nu} \quad (\text{A.14})$$

Where:

- c_f = coefficient for the transport rate;
- for laboratory conditions: $c_f = 1$
- for field conditions: $c_f = 1.268$

F_g = grain Froude number (dimensionless)

- F_{gr} = critical grain Froude number (dimensionless)
 τ_{*0} = critical shear stress
 σ_s = geometric standard deviation
 S = bottom slope (dimensionless)
 d_{50} = median diameter (mm)
 R_g = grain Reynolds number (dimensionless)
 R = hydraulic radius (m)
 ν = kinematic viscosity (m^2/s)

A.4 ENGELUND AND HANSEN METHOD

The method of Engelund and Hansen (1967) is based on energy considerations and a relationship between the transport and mobility parameters. The total sediment transport is calculated by:

- Transport parameter ϕ

$$\phi = \frac{q_s}{\sqrt{(s-1)g d_{50}^3}} \quad (\text{A.15})$$

- Mobility parameter θ

$$\theta = \frac{u_*^2}{(s-1)g d_{50}} \quad (\text{A.16})$$

The relationship between the parameters is expressed by:

$$\phi = \frac{0.1\theta^{2.5} C^2}{2g} \quad (\text{A.17})$$

The total sediment transport is expressed by:

$$q_s = \frac{0.05 V^5}{(s-1)^2 g^{0.5} d_{50} C^3} \quad (\text{A.18})$$

Where:

- q_s = total sediment transport ($\text{m}^3/\text{s.m}$)
 θ = mobility parameter
 ϕ = transport parameter
 V = mean velocity (m/s)
 C = de Chézy coefficient ($\text{m}^{1/2}/\text{s}$)
 u_* = shear velocity (m/s)
 d_{50} = mean diameter (m)

The Engelund and Hansen function for the total sediment transport has been evaluated with laboratory data that were characterized by graded sediment ($\sigma_s < 1.6$) with median diameters d_{50} of 0.19 mm, 0.27 mm,

0.45 mm and 0.93 mm. The method is not recommended for the cases, in which the median size of the sediment is smaller than 0.15 mm and the geometric standard deviation is greater than 2.

A.5 VAN RIJN METHOD

The van Rijn method (1984a and 1984b) computes the total sediment transport. The total transport is the summation of the bed and suspended load transport ($q_s = q_b + q_{sus}$). The bed load transport q_b is given by the product of the saltation height, the particle velocity and bed load concentration. The method assumes that the gravity forces dominate the motion of the bed particles. The method of van Rijn has been evaluated with data from tests that had the following characteristics:

- mean velocity = 0.31–1.29 m/s
- flow depth = 0.1–1.0 m
- median diameter = 0.32–1.5 mm

The bed load transport follows from:

$$q_b = u_b \delta_b c_b \tag{A.19}$$

- Particle velocity u_b

$$u_b = 1.5T^{0.6}[(s - 1)g d_{50}]^{0.5} \tag{A.20}$$

- Saltation height δ_b :

$$\delta_b = 0.3 D_*^{0.7} T^{0.5} d_{50} \tag{A.21}$$

- Bed load concentration c_b :

$$c_b = 0.18 c_o \frac{T}{D_*} \tag{A.22}$$

With:

$$T = \frac{(u'_*)^2 - (u_{*,cr})^2}{(u_{*,cr})^2} \tag{A.23}$$

$$u'_* = \frac{g^{0.5} V}{C'} \tag{A.24}$$

$$D_* = \left[\frac{(s - 1)g}{\nu^2} \right]^{1/3} d_{50} \tag{A.25}$$

Replacing equations A.20 to A.25 in equation A.19 gives:

$$q_b = 0.053(s - 1)^{0.5} g^{0.5} d_{50}^{1.5} D_*^{-0.3} T^{2.1} \tag{A.26}$$

Where:

q_b = bed load transport (m^2/s)

u_b = particle velocity (m/s)

c_b = bed load concentration

c_0 = maximum volumetric concentration = 0.65

T = bed shear parameter

D_* = particle parameter

u'_* = bed shear velocity related to grains (m/s)

C' = de Chézy coefficient related to grains ($m^{1/2}/s$)

$C = 18 \log(12 h/3d_{90})$

δ_b = saltation height (m)

d_{50} = median diameter (m)

The suspended load transport follows from:

$$q_{\text{sus}} = F V h c_a \quad (\text{A.27})$$

The suspended sediment transport q_{sus} , is the depth integrated product of the local concentration and the flow velocity. The method of van Rijn (1984b) is based on the computation of the reference concentration from the bed load transport.

The field and laboratory data came from tests with the following characteristics:

- mean velocity = 0.4–2.4 m/s
- flow depth = 0.1–17 m
- median diameter = 0.1–0.4 mm

With:

- shape factor F :

$$F = \frac{(a/h)^{Z'} - (a/h)^{1.2}}{(1 - a/h)^{Z'}(1.2 - Z')} \quad (\text{A.28})$$

- suspension parameter Z

$$Z = \frac{w_s}{\beta \kappa u_*} \quad (\text{A.29})$$

$$\beta = 1 + 2 \left(\frac{w_s}{u_*} \right)^2 \quad (\text{A.30})$$

- modified suspension parameter Z'

$$Z' = Z + \psi \quad (\text{A.31})$$

$$\psi = 2.5 \left(\frac{w_s}{u_*} \right)^{0.8} \left(\frac{c_a}{c_0} \right)^{0.4} \quad (\text{A.32})$$

- reference concentration c_a

$$c_a = \frac{0.015 d_{50} T^{1.5}}{a D_*^{0.3}} \quad (\text{A.33})$$

- reference level a

$$a = 0.5 \Delta \quad \text{or} \quad a = k_s \quad \text{with} \quad a_{\min} = 0.01 h \quad (\text{A.34})$$

- representative particle size of suspended sediment d_s

$$d_s = [1 + 0.011(\sigma_s - 1)(T - 25)]d_{50} \quad (\text{A.35})$$

Where:

F = shape factor

V = mean velocity (m/s)

u_* = shear velocity (m/s)

c_a = reference concentration

h = water depth (m)

D_* = particle parameter

a = reference level (m)

Z = suspension number

Z' = modified suspension number

β = ratio of sediment and fluid mixing coefficient

ψ = stratification correction

κ = constant of von Karman

σ_s = geometric standard deviation

d_{50} = median diameter (mm)

d_s = representative particle size of suspended sediment (m)

w_s = fall velocity of representative particle size (m/s)

T = transport stage parameter

Δ = bed form height (m)

k_s = equivalent roughness height (m)

$u_{*,cr}$ = critical bed shear velocity (m/s)

A.6 YANG METHOD

The method proposed by Yang (1973) is based on the hypothesis that the sediment transport in a flow should be related to the rate of energy dissipation. The rate of energy dissipation is defined as the unit stream power and can be expressed by the velocity times slope ($V * S$). The theoretical basis for Yang's unit stream power is provided by the turbulence theory. By integrating the rate of turbulence energy production over the depth, the suspended sediment transport can be expressed as function of the unit stream power.

The total sediment transport can be expressed in ppm by mass as a function of the unit stream power by:

$$\log c_t = I + J \log \left(\frac{VS - V_{cr}S}{w_s} \right) \quad (\text{A.36})$$

Yangs coefficients are:

$$I = 5.435 - 0.286 \log \left(\frac{w_s d_{50}}{\nu} \right) - 0.457 \log \left(\frac{u_*}{w_s} \right) \quad (\text{A.37})$$

$$J = 1.799 - 0.409 \log \left(\frac{w_s d_{50}}{\nu} \right) - 0.314 \log \left(\frac{u_*}{w_s} \right) \quad (\text{A.38})$$

- critical velocity for initiation of motion V_{cr} :

$$V_{cr} = 2.05 w_s \quad (\text{A.39})$$

The total load transport is calculated by:

$$q_s = 0.001 c_t V h \quad (\text{A.40})$$

Where:

q_s = total load transport (kg/s.m)

c_t = total sediment transport expressed in ppm by mass

V = mean velocity (m/s)

V_{cr} = velocity for initiation of motion (m/s)

h = water depth (m)

S = bottom slope

I, J = coefficients in Yang's function for the total sediment transport

w_s = fall velocity (m/s)

d_{50} = median diameter (m)

u_* = shear velocity (m/s)

ν = kinematic viscosity (m^2/s)

Equations A.36 and A.40 have been verified with laboratory and field data from tests within the following ranges:

- sediment size = 0.15–1.71 mm
- mean velocity = 0.23–1.97 m/s
- water depth = 0.01–15.2 m
- concentration = 10–585,000 ppm
- bottom slope = $0.043 * 10^{-3}$ – $27.9 * 10^{-3}$

APPENDIX B

Methods to Predict the Friction Factor

The selection of methods to predict the friction factor in irrigation canals include:

- van Rijn (1984c);
- Brownlie (1983);
- White, Bettess & Paris (1979);
- Engelund (1966).

The methods to estimate the friction factor in irrigation canals will make use of the de Chézy coefficient. The Darcy-Weisbach friction factor f as well as the coefficients of Manning (n) and Strickler (k_s) can be applied when the following relationships are used:

$$C = \sqrt{\frac{8g}{f}} \quad \text{or} \quad C = \frac{R^{1/6}}{n} \quad (\text{B.1})$$

Where:

C = de Chézy coefficient ($\text{m}^{1/2}/\text{s}$)

f = Darcy-Weisbach's friction factor

n = Manning's coefficient ($\text{m}^{1/3}/\text{s}$)

k_s = Strickler coefficient ($\text{s}/\text{m}^{1/3}$)

R = hydraulic radius (m)

g = gravity acceleration (m/s^2)

B.1 VAN RIJN

The de Chézy coefficient depends on the type of flow regime. Based on the bed-roughness condition the flow regime in open canals can be divided in: smooth, rough and a transition regime. Roughness conditions on the bottom are simulated by using an equivalent height of the sand roughness k_s , which is equal to the roughness of sand that gives a resistance similar to the resistance of the bed form. The dimensionless value of u_*k_s/ν is used as the classification parameter to distinguish the type of flow regime. Van Rijn (1993) described the type of flow regimes as presented in table B.1.

Table B.1. Hydraulic regime types.

Type of regime	Classification parameter u_*k_s/ν
Smooth	$u_*k_s/\nu < 5$
Transition	$5 < u_*k_s/\nu < 70$
Rough	$u_*k_s/\nu > 70$

Depending on the bed condition the flow regimes in irrigation canals can be determined as: *Plane bed*: for plane beds (no motion) the equivalent height k_s is related to the largest particles of the bed material. Van Rijn (1982) described the equivalent roughness height as $k_s = 3 d_{90}$.

Assuming a uniform sediment size distribution in irrigation canals ($d_{90} \approx 1.5 d_{50}$), the equivalent roughness height of the sediment for plane beds can be represented by:

$$k_s = 4.5 d_{50} \tag{B.2}$$

Where:

d_{50} = median diameter of the sediment (m)

k_s = equivalent height roughness (m).

The parameter u_*k_s/ν for a plane bed (bed without motion) follows from:

$$k_s = 4.5 d_{50};$$

u_* = critical Shield shear velocity ($u_{*,cr}$)

Values of this parameter for various sediment diameters and for a plane bed are shown in table B.2. The flow regimes that belong to the condition of a plane bed are the regimes smooth and transition.

Table B.2. u_*k_s/ν parameter for plane bed (no motion).

d_{50} (mm)	0.05	0.10	0.15	0.20	0.25	0.30	0.35	0.40	0.45	0.50
$u_{*,cr}k_s/\nu$	2.8	5.1	8.2	11.5	14.9	18.5	21.3	25.8	30.6	35.7

Bed forms: for higher velocities, the occurrence of bed forms changes the bed roughness. The effective roughness or the total equivalent height follows from van Rijn (1984c):

$$k_s = k'_s + k''_s \tag{B.3}$$

Where:

k_s = total equivalent height (m)

k'_s = equivalent height related to the grain (m)

k''_s = equivalent height related to the bed form (m)

Values for k'_s and k''_s follow from the equations given by van Rijn (1982):

$$k'_s = 3 d_{90} \text{ to } 4.5 d_{50} \tag{B.4}$$

$$k_s'' = 20\gamma_r \Delta_r \left(\frac{\Delta_r}{\lambda_r} \right) \quad (\text{Ripples}) \quad (\text{B.5})$$

$$k_s'' = 1.1\gamma_d \Delta_d (1 - e^{-25 \frac{\Delta_d}{\lambda_d}}) \quad (\text{Dunes}) \quad (\text{B.6})$$

Where:

- γ_r = ripple presence ($\gamma_r = 1$ for ripples alone)
- γ_d = form factor ($\gamma_d = 0.7$ for field conditions)
- Δ_r = ripple height ($\Delta_r = 50$ to $200 d_{50}$)
- Δ_d = dune height
- λ_r = ripple length ($\lambda_r = 500$ to $1000 d_{50}$)
- λ_d = dune length

The resistance due to the grain roughness is small compared to the one caused by the geometry of the bed form. Many attempts have been made to describe the geometry of ripples and dunes. Yalin (1985) described the geometry of ripples generated by a subcritical flow in channels with cohesionless and uniform bed material. The ripple length λ_r is in the interval:

$$600 D \leq \lambda_r \leq 2000 D \quad (\text{B.7})$$

The “largest population” of the ripple lengths can be found within the range:

$$900 d_{50} \leq \lambda_r \leq 2000 d_{50} \quad (\text{B.8})$$

A value that represents the ripple length well can be given by:

$$\lambda_r \cong 1000 d_{50} \quad (\text{B.9})$$

The ripple height can be described by Yalin (1985):

$$\Delta_r \text{ is } 50 \text{ to } 200 d_{50} \quad (\text{B.10})$$

Where:

- D = representative grain size ($D = d_{50}$)
- λ_r = ripple length (m)
- Δ_r = ripple height (m)

For practical purposes it can be assumed that for $\Delta_r = 100 d_{50}$ and $\lambda_r = 1000 d_{50}$:

$$\frac{\Delta_r}{\lambda_r} \approx 0.1 \quad \text{for} \quad 1 \leq D_* \leq 10 \quad \text{and} \quad T \leq 3 \quad (\text{B.11})$$

Another bed form in the lower regime ($Fr < 0.8$) is the dunes. The shape of the dunes is similar to the shape of ripples, but their length and height

are greater than those of ripples are. Relationships for dune length and dune height have been based on flume and field data and are given by van Rijn (1994):

$$\frac{\Delta_d}{h} = 0.11 \left(\frac{d_{50}}{h} \right)^{0.3} (1 - e^{-0.5T})(25 - T) \tag{B.12}$$

$$\lambda_d = 7.3 h \tag{B.13}$$

Where:

- T = excess bed-shear stress parameter
- λ_d = dune length (m)
- Δ_d = dune height (m)
- d_{50} = median diameter (m)
- h = water depth (m)

The greatest influence of k'_s (equivalent height related to the grain) on the total value of the equivalent roughness height k_s will occur for those bed forms that have the smallest equivalent height related to the bed form. The smallest height occurs for ripples and the influence of the height k'_s on the total equivalent roughness height k_s for the specific conditions of irrigation canals is approximately 1.5–2%.

$$\frac{k'_s}{k'_s + k''_s} = \frac{4.5 d_{50}}{4.5 d_{50} + 20\gamma_s \Delta_r \left(\frac{\Delta_r}{\lambda_r} \right)} \approx 2\% \text{ ripples occurrence} \tag{B.14}$$

For other bed forms the influence of the grains on the total roughness will be smaller than for ripples (smaller than 2%). For that reason and because the grain roughness is constant during changes of the bed form size, the grain roughness can be neglected. Hence, the equivalent height related to the bed form is recommended and for ripples the total equivalent roughness can be computed as:

$$k_s = k''_s = 20 * 1 * 0.1 * 100 * d_{50} = 200 d_{50} \tag{B.15}$$

Minimum values of the parameter $u_* k_s / \nu$ for ripples in irrigation canals follow from:

- $k_s = 200 d_{50}$;
- u_* = critical Shield shear velocity $u_{*,cr}$.

For those canals the values of the parameter $u_* k_s / \nu$ are shown in table B.3.

Table B.3. $u_* k_s / \nu$ parameter for ripples.

D_{50} (mm)	0.05	0.10	0.15	0.20	0.25	0.30	0.35	0.40	0.45	0.50
$u_{*,cr} k_s / \nu$	499	899	1450	2037	2650	3286	3782	4590	5445	6344

Once the sediment on the bottom of an irrigation canal comes into motion the flow will be considered as hydraulically rough. Figure B.1 shows the types of flow regime in irrigation canals.

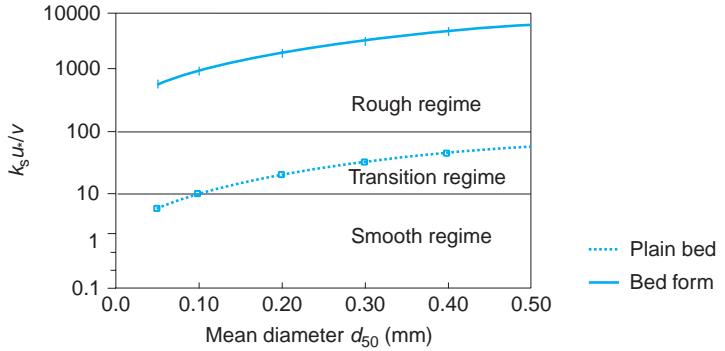


Figure B.1. Hydraulic regimes in irrigation canals.

For regimes with smooth and transitional flows, the de Chézy coefficient is a function of the flow condition only and follows from the equations given by van Rijn (1993):

$$C = 18 \log \left(\frac{12 h}{3.3 \frac{\nu}{u_*}} \right) \quad \text{Smooth flow regime} \quad (\text{B.16})$$

$$C = 18 \log \left(\frac{12 h}{k_s + 3.3 \frac{\nu}{u_*}} \right) \quad \text{Transition flow regime} \quad (\text{B.17})$$

$$C = 18 \log \left(\frac{12 h}{k_s} \right) \quad \text{Rough flow regime} \quad (\text{B.18})$$

Where:

C = de Chézy coefficient ($\text{m}^{1/2}/\text{s}$)

h = water depth (m)

η = kinematic viscosity (m^2/s)

u_* = shear velocity (m/s)

k_s = total equivalent roughness (m)

A good approximation of the de Chézy coefficient for canals with ripples is obtained by replacing the total equivalent height by the height related to the bed form k_s'' (equation B.15) and can be represented by:

$$C = 18 \log \frac{h}{200 d_{50}} \quad (\text{B.19})$$

The de Chézy coefficient obtained from equation B.16 to B.19 considers only the bed forms on the bottom without taking into account the friction factor of the side banks. Therefore, it is necessary to find a weighted value of the de Chézy coefficient for the friction of both bed and side banks.

B.2 BROWNLIE

Brownlie (1983) proposed a method to predict the flow depth (and therefore the friction factor) when the discharge and the slope are known. No explicit calculation of the de Chézy coefficient is proposed, but once the resistance to flow is determined (equations B.20 and B.21) then the de Chézy coefficient will be calculated by equation B.22. The Brownlie method is based on a dimensional analysis, basic principles of hydraulics and verification with a large amount of field and flume data. Step by step, the de Chézy coefficient in the lower flow regime can be predicted by using the following relationships:

$$q_* = \frac{Q}{B g^{0.5} d_{50}^{1.5}} = \frac{q}{g^{0.5} d_{50}^{1.5}} \quad (\text{B.20})$$

$$h = 0.372 d_{50} q_*^{0.6539} S_0^{-0.2542} \sigma_s^{0.1050} \quad (\text{B.21})$$

and

$$q = C h \sqrt{h S_0} \therefore C = \frac{q}{h^{1.5} S_0^{0.5}} \quad (\text{B.22})$$

Where:

Q = discharge (m^3/s)

q = unit discharge (m^2/s)

B = bottom width (m)

h = water depth (m)

S_0 = bottom slope

d_{50} = median diameter (m)

σ_s = gradation of sediment ($\sigma_s = 1/2 (d_{84}/d_{50} + d_{50}/d_{16})$)

q_* = dimensionless unit discharge

B.3 WHITE, PARIS AND BETTESS

White et al (1979) describe the flow resistance by the following dimensionless numbers:

- Particle size D_*

$$D_* = \left[\frac{(s-1)g}{\nu^2} \right]^{1/3} d_{35} \quad (\text{B.23})$$

- Particle mobility F_{fg}

$$F_{fg} = \frac{u_*}{\sqrt{g d_{35}(s-1)}} \quad (\text{B.24})$$

- Mobility parameter related to the effective shear stress

$$F_{gr} = (F_{fg} - A) \left[1.0 - 0.76 \left(1 - \frac{1}{\exp(\log D_*)^{1.7}} \right) \right] + A \quad (\text{B.25})$$

- Mean velocity:

$$V = \sqrt{32} \log \left(\frac{h}{d_{35}} \right) \left[\frac{F_{gr} \sqrt{g d_{35}(s-1)}}{u_*^n} \right]^{\frac{1}{1-n}} \quad (\text{B.26})$$

With:

$$n = 1 - 0.56 \log D_* \quad (\text{B.27})$$

$$A = \frac{0.23}{\sqrt{D_*}} + 0.14 \quad (\text{B.28})$$

- The de Chézy coefficient follows from:

$$C = \frac{g^{0.5} V}{u_*} \quad (\text{B.29})$$

Where:

D_* = particle size

F_{fg} = particle mobility

F_{gr} = particle mobility related to the effective shear stress

d_{35} = particle size (m)

A = initial motion parameter

n = exponent in the mobility parameter related to the effective shear stress

h = water depth (m)

g = gravity (m/s^2)

u_* = shear velocity (m/s)

V = mean velocity (m/s)

s = relative density

C = de Chézy coefficient ($\text{m}^{1/2}/\text{s}$)

ν = kinematic viscosity (m^2/s)

B.4 ENGELUND

Engelund (1966) defined the shear stress due to skin and form resistance by:

$$\tau = \tau' + \tau'' \quad (\text{B.30})$$

With:

$$\tau = \rho g h S \quad \text{and} \quad \tau' = \rho g h' S \quad \text{and} \quad \tau'' = \rho g h'' S \quad (\text{B.31})$$

$$u_* = (g h S)^{0.5} \quad \text{and} \quad u'_* = (g h' S)^{0.5} \quad (\text{B.32})$$

With

$$h = h' + h'' \quad (\text{B.33})$$

Hence:

$$\left(\frac{u'_*}{u_*}\right)^2 = \frac{h'}{h} \quad (\text{B.34})$$

Expressing the shear velocity in terms of the mobility parameter θ the equation becomes:

$$\frac{\theta'}{\theta} = \frac{h'}{h} \quad (\text{B.35})$$

It was found for the lower regime that:

$$\theta' = 0.06 - 0.4 \theta^2 \quad (\text{B.36})$$

The mean velocity is calculated by:

$$\frac{V}{u'_*} = 6 + 2.5 \ln \left(\frac{h'}{2 d_{50}} \right) \quad (\text{B.37})$$

Combination of the equations will result in the de Chézy coefficient:

$$C = g^{0.5} \left(\frac{h'}{h} \right)^{0.5} \left[6 + 2.5 \ln \left(\frac{h'}{2.5 d_{50}} \right) \right] \quad (\text{B.38})$$

Where:

- $h = h' + h'' =$ water depth (m)
- $\tau = \tau' + \tau'' =$ effective shear stress (N/m²)
- $u_* =$ shear velocity (m/s)
- $\theta =$ dimensionless mobility parameter
- $\rho =$ density (kg/m³)
- $V =$ mean velocity (m/s)
- $C =$ de Chézy coefficient (m^{1/2}/s)
- $S =$ bottom slope

APPENDIX C

Hydraulic Design of Irrigation Canals

C.1 INTRODUCTION

In many cases, profitable and sustainable agricultural production needs an irrigation network that brings water from the source to the fields at the right place, at the right time, in the right quantity and at the right level (FAO, 1992). An irrigation network can be divided into main, secondary, sub lateral and tertiary canals. The design capacity of all the canals and appurtenant structures should be sufficient to handle the maximum envisaged flow in a convenient and reliable way. The design of the physical part of the irrigation network should enable the operation of the canal network according to the following criteria (Dahmen, 1999):

- The required flows are passed at design water levels.
- No erosion of canal bottoms and banks occurs.
- Any sediment that enters the system will be carried along the network and will discharge through outlets either to the fields, or to the natural drainage, or will settle in special designed silt traps.

The demand for irrigation water is not constant during the irrigation season, but is affected by the water requirements of the crops growing on the fields. Despite the fact that the water requirements vary during the irrigation season, the design discharge is defined as the maximum flow that can be handled in a proper way. The design discharge of a canal reach is the sum of the simultaneous, maximum flows through the outlets in this reach and the outflow into the next downstream reach plus seepage and other losses, including those due to the operation of the network. The simultaneous, maximum flow through the outlets will cover the maximum crop water requirement at field level, taking into account the number of farms irrigated at the same time and the application and distribution losses at farm and tertiary unit level. The water losses in a canal reach due to the operation are commonly included in the conveyance efficiency. When seepage losses in the canal reach are important they are

separately taken into account. Water losses as a result of breakage will normally not be considered.

As stated before, the canal design should result in the right canal dimensions to convey the flows at the required water levels and with the allowable velocities. Moreover, the conveyance of the water and sediments should take place without erosion or sedimentation in the network. Based on the fact that the earthworks for an irrigation network form a considerable part of the total project costs, an optimal canal design should result in minimal earthwork, an acceptable balance between cut and fill and a minimum of borrow pits and spoil banks. If a substantial imbalance exists, the canal design has to be changed and the bottom slope, water levels and canal dimensions have to be adjusted within acceptable ranges to achieve a well-balanced earthwork.

A correct canal design should be based on the design flows of each canal reach and the final design includes:

- The layout of the canal, consisting of the horizontal and vertical alignment.
- The cross sections, including the bottom width, side slopes, water depth, freeboard and width of the embankments and the right of way.

This appendix will discuss a canal design that is based on the uniform flow equation, boundary shear stress and sediment transport relationship. The sediment transport relationship will use the principle of minimum stream power, which states that the sediment transport capacity of a canal network should be constant or non-decreasing in the downstream direction.

This approach is simple and straightforward, but there are a few limitations, namely:

- The approach does not take into account the effect of sediment size and concentration; the stream power is related to velocity and bottom slope, but basically the slope depends on the sediment size; in this method the bottom slope is adjusted to get a low boundary shear stress and the stream power can be increased without considering the sediment characteristics;
- It does not include the effects of bed forms on the roughness; it does not account for the effect of the side slope on the effective roughness.

C.2 ALIGNMENT OF AN IRRIGATION CANAL

The layout of a canal mainly depends on the topography but is also influenced by specific geological, agricultural, engineering, and economic considerations. The alignment is largely effected by the existing topography and dominant soil conditions; areas with very steep cross-slopes or permeable soils or areas subject to landslides or that have a

natural tendency for sliding should be avoided. The alignment is more economic when the water levels are kept as low as possible in irrigation canals, preferably below the ground surface. The actual water levels should never be allowed to exceed the design levels and therefore surplus water must be evacuated to drains or natural watercourses. A correct canal alignment also depends on the bottom slope and one of the main design principles is that the average slope of a main canal is more gentle than the average slope of a secondary or branch canal (Serge Leliavsky, 1983).

The final design of the horizontal and vertical alignment should be the most economic solution in view of construction and maintenance costs and this design is not always the shortest distance between two points. The layout of an irrigation network depends on the location of the existing natural, main drains; they form the physical boundary conditions for the layout (in view of costs of land shaping). The horizontal alignment follows as much as possible the topography of the terrain and is preferably located on ridges, the main canal is situated along the watershed formed by the main ridge and the branch canals follow the less significant ridges. Curves in unlined canals should be as large as possible as they disturb the water flow and have a tendency to induce siltation on the inside and scour on the outside of the curve. The minimum radius for earthen irrigation canals depends on the size and capacity of the canal, the type of soil and the flow velocity. The recommended value for these curves is at least 8 times the design width at the water surface.

The vertical canal alignment is a compromise between the following design requirements:

- *Water levels* should be high enough to irrigate the highest areas for which irrigation is envisaged.
- *Maintenance costs* should be as low as possible; they are lower when the water level is below the ground surface. These lower water levels might hamper the illegal diversion of water by gravity.
- *Balance between cut and fill* is an economic criterion in view of the construction costs; but when this criterion results in canals in high fill it has to be mentioned that these canals are more difficult to construct and in general will lose more water by seepage.

C.3 WATER LEVELS

The water level or command is the location of the water surface in relation to a datum (reference level). The water level in a canal reach should be high enough to supply water to the highest farm plots for which irrigation is envisaged. In a gravity irrigation system water flows from the secondary canal through a turnout to a tertiary canal, and next through the farm canal system to the farm plot. The water level at the turnout, taking into

account the distance to and the ground level of the critical point, should be sufficient high to convey the water to the farm plot. The design water levels of a canal follow from the *water level diagram*. This diagram presents the longitudinal profile of the ground surface and indicates all the points where water is supplied to a lower level canal or to a tertiary unit. The water level in the main canal depends on the water levels in the branch canals at the regulators or division structures and the head loss at these structures. The water level at the head of a dividing canal is lower than the water level of the parent canal due to the necessary head losses in the regulator. The final design presents the water surface preferably by a continuous straight line, located at the same levels as or above the required levels at the regulating structures. For the main as well as for the branch canals the difference between water surface and ground level should preferably not be more than 0.30 m.

C.4 EARTHWORK

The design provides the right canal dimensions to convey the discharges at the required level to meet the crop water requirements and at the same time to avoid erosion of and sedimentation on the bottom and sides of a canal. However, an important aspect in the canal design is the feasibility of the earthwork, which has a great impact on the total construction costs. An optimal canal layout will result in an proper balance between cut and fill. A most favourable canal layout has a balanced earthwork, resulting in a minimum of borrow pits and spoil banks. Moreover, a well balanced cut and fill will minimise the seepage losses, especially when the bottom level is higher than the ground surface. The bottom, but preferably the whole canal, should be in cut after stripping the top soil. Reduced seepage will reduce the danger of landslides and water logging along the canal.

When water levels have been defined to supply water to the highest points, then the bottom slopes have to be established to prevent erosion and sedimentation in the canals. A preliminary longitudinal profile, based on the required water levels and appropriate bottom slopes in view of erosion and sedimentation, will give a clear visualisation of the bottom and the water levels in each reach in order to define the earthwork. When imbalances between cut and fill exist, the level and slope may be adjusted within acceptable ranges. If the imbalance persists it will be necessary to modify the irrigation area with its tertiary blocks and to re-define the layout until a balance is reached between cut and fill. This will result in a repetitive process until an optimal layout has been established. This process can be done by the nowadays available computational techniques as many times as required.

C.5 DESIGN OF IRRIGATION CANALS

The final design of the geometry of an irrigation canal should present the bottom width B , the water depth y , the side slope m and the freeboard F as function of the discharge Q , the bottom slope S and the roughness coefficient n . From these data follows the cross-sectional area A , the hydraulic radius R and the velocity v ; the latter should be within a certain range in view of erosion and sedimentation. From the known discharge Q , the appropriate side slope m and a criterion for the optimal b/y ratio, the other canal dimensions can be derived.

The discharge Q that a cross-section with a certain area A can convey increases for a larger hydraulic radius or for a smaller wetted perimeter. A section with a certain area A and the smallest wetted perimeter will convey the largest discharge and is called the best hydraulic section. However, this does not mean that these cross-sections are always optimal. In case the water level is below the ground surface a narrow canal will give minimum excavation, for canals with the water surface above the ground level a wide canal will result in less excavation.

The flow in a canal is time and space related. The flow is steady if the water depth, discharge and cross section do not change with respect to time. When these parameters do not change with respect to space, then the flow is uniform. The most often used equations for uniform flow are the de Chézy, Strickler and Manning formulae.

These formulae are:

$$Q = A * C * R^{0.5} * S^{0.5} \qquad \text{de Chézy} \qquad \text{(C.1)}$$

$$Q = A * k_s * R^{\frac{2}{3}} * S^{0.5} \qquad \text{Strickler} \qquad \text{(C.2)}$$

$$Q = A * \frac{1}{n} * R^{\frac{2}{3}} * S^{0.5} \qquad \text{Manning} \qquad \text{(C.3)}$$

Where:

Q = flow rate (m³/s)

A = wetted area (m²)

S = bottom slope (1)

R = hydraulic radius (m)

C = de Chézy flow resistance coefficient

k_s = Strickler smoothness factor

n = Manning roughness factor

The exponent '2/3' in the Strickler and in the Manning formula is not a constant, but it varies with the channel shape and roughness. Therefore some approximations use a modified k_s as function of the water depth y .

Based on field investigations and studies the modified k_s value can be expressed as:

$$k_{s,y} = k_{s,1m} * y^{1/3} \quad \text{for } y < 1.0 \text{ m} \quad (C.4)$$

$$k_{s,y} = k_{s,1m} * y^{1/6} \quad \text{for } y > 1.0 \text{ m} \quad (C.5)$$

Where:

$k_{s,y}$ = modified k_s for a canal depth y ;

$k_{s,1m}$ = reference k_s for a canal depth of 1.0 m, based on a well maintained, large canal section.

The k_s , the smoothness factor, should be carefully estimated and is based on:

- Canal geometry, expressed by the side slope m and a b/y ratio;
- Roughness (irregularities) of the bottom and side walls; including flow obstruction due to weeds (height and density of vegetation, including flattening of it at high flows);
- Sediment transport, namely the suspended and bed load.

For any canal the roughness changes during the year and will be a minimum shortly after maintenance and a maximum when no maintenance is done. Recommended k_s values for a 1 m deep earthen canal are 12, 24, 36 and 42.5 for none, poor, fair and good maintenance conditions, respectively. The Table C.1 gives these k_s values as function of the maintenance conditions.

Table C.1 Smoothness factors as function of maintenance conditions (for earthen canals).

Maintenance	None	Poor	Fair	Good
$k_{s,1.0m}$	12	24	36	42.5

The recommended k_s values for a 1 m deep canal and the modified k_s value as function of the water depth (see equation C.4 and C.5) result in the graph as presented in Figure C.1.

For one value of k_s , one bottom slope S and one side slope m still an infinite range of bed width/depth ratios (b/y) can be selected. Minimizing the wetted perimeter P gives the ‘best’ hydraulic cross sections and the b/y ratio is:

$$\frac{b}{y} = 2 * \left(\sqrt{1 + m^2} - m \right) \quad (C.6)$$

Where:

y = water depth (m)

b = bottom width (m)

m = cotangent of side slope (1)

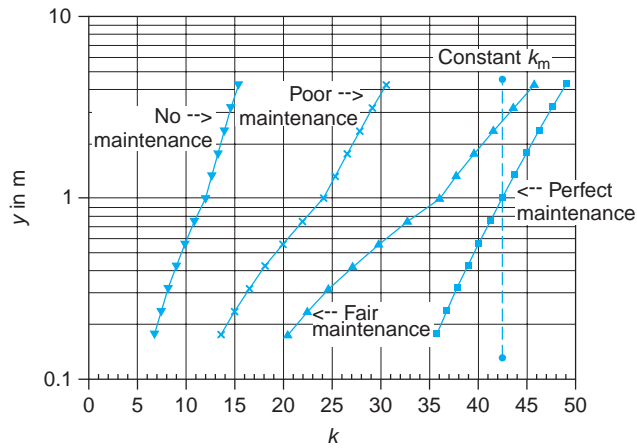


Figure C.1. Recommended k_s values for unlined irrigation canals as function of the water depth y for various maintenance conditions.

The ‘best’ hydraulic section with the smallest perimeter P results in a maximum flow at minimum cost. However, the best hydraulic section is rarely applied, because it will not be stable due to the relatively deep excavations and a change in discharge heavily affects the water depth and the velocity. A deep section is nevertheless applied wherever possible, because the expropriation costs will be less, the velocity is larger in a deep canal than in a shallow canal and the sediment transport capacity is larger in deeper canals (the transport capacity is linear with the bottom width, but exponential with the water depth). To limit the excavation and expropriation costs, the side slopes of a canal are designed as steep as possible. Soil material, canal depth and the danger of seepage determine the maximum slope of a side slope that is stable under ‘normal conditions’, also against erosion. For deep excavations an extra berm can be included to improve the stability of the slope. Table C.2 gives some recommended values for the side slope.

Table C.2 Side slopes in canals.

Material	m
Rock	0.0
Stiff clay	0.5
Cohesive medium soils	1.0 – 1.5
Sand	2.0
Fine, porous clay, soft peat	3.0

The top width of canal embankments depends on the soil type, the side slope and special requirements in view of maintenance and operation. Water levels may rise above the design water level due to deterioration of the canal embankment, a sudden closure of a gate or unwanted drainage

inflows. A freeboard, being the distance between the design water level and the canal bank, is provided to safeguard the canal against overtopping these unexpected water level fluctuations and wave actions. USBR recommends a freeboard $F = C * y$, where the coefficient C varies between 0.5 to 0.6 with a minimum of the 0.15 or 0.20 m.

The bed-width/depth ratio of a small earthen irrigation canal is often close to unity; but the ratio gradually increases for larger canals. Echeverry (1915) relates this ratio to the area of the cross section, which results in:

$$\frac{b}{y_{\text{recom}}} = 1.76 * Q^{0.35} \quad \text{for } Q > 0.20 \text{ m}^3/\text{s} \quad (\text{C.7})$$

$$\frac{b}{y_{\text{recom}}} = 1.0 \quad \text{for } Q \leq 0.20 \text{ m}^3/\text{s} \quad (\text{C.8})$$

Depending on the size of the canal, the bottom width is often rounded to a multiple of a metre or half metre. The design of a canal cross-section for a given discharge, a roughness k and a bed slope S requires iterative computations.

Re-writing the Strickler equation gives:

$$Q = A * k_s * R^{2/3} * S^{1/2}$$

$$A = (b + my)y = (b/y + m)y^2$$

$$P = \left[\frac{b}{y} + 2\sqrt{1 + m^2} \right] y \quad \text{for } n = b/y \quad (\text{C.9})$$

$$Q = k_s * S_0^{1/2} * \frac{(n + m)^{5/3}}{(m + 2\sqrt{(1 + m^2)})^{2/3}} \frac{y^{10/3}}{y^{2/3}} \quad (\text{C.10})$$

$$y^{8/3} = \frac{Q}{k_s * f * S^{1/2}} \quad (\text{C.11})$$

$$f = \frac{(n + m)^{5/3}}{(n + 2\sqrt{(1 + m^2)})^{2/3}} \quad (\text{C.12})$$

$$\frac{b}{y_{\text{recom}}} = 1.76 * Q^{0.35} \quad \text{for } 0.2 < Q < 10 \text{ m}^3/\text{s}$$

$$\frac{b}{y} = 1 \quad \text{for } Q < 0.2 \text{ m}^3/\text{s}$$

$$k_s = k_{s,1m} * y^a \quad a = 1/3 \quad \text{for } y < 1.0 \text{ m}$$

$$a = 1/6 \quad \text{for } y > 1.0 \text{ m} \quad (\text{C.13})$$

The design steps include:

- Assume a value for an initial Strickler k_s according to the maintenance condition and find a first approximation of y and b ;
- Next re-compute the design values to obtain the proper values of b and k_s ;
- Next fine-tune the design in view of a small adjustment of the design width b_{des} , i.e. a value that can be constructed (e.g. width on a half or whole meter). This fine-tuning has a minor impact on the final results, unless a completely different value from the originally suggested b is used.

When using the de Chézy equation in stead of the Strickler equation, the approach is the same as before.

The discharge for uniform flow is:

$$Q = A * C * R^{0.5} * S_0^{0.5} \quad \text{de Chézy} \quad (C.14)$$

$$C = 18 \log \frac{12 R}{k + \delta/3.5} \quad \text{White-Colebrook} \quad (C.15)$$

$$\delta = 11.6 \frac{\nu}{v_*} \quad (C.16)$$

$$v_* = \sqrt{g * R * S} \quad (C.17)$$

Where:

C = de Chézy's coefficient (m^2s^{-1})

k = length characterizing the roughness = $1/2 a$ (Nikuradse)

δ = thickness of the laminar sub-layer

v_* = shear velocity

Re-writing the Chézy equation gives:

$$Q = A * C * R^{0.5} * S_0^{0.5}$$

$$A = (b + my)y = (b/y + m)y^2$$

$$P = \left[\frac{b}{y} + 2\sqrt{1 + m^2} \right] y$$

$$Q = C S_0^{0.5} \frac{(b/y + m)^{3/2} y^3}{(b/y + 2\sqrt{(1 + m^2)y})^{1/2}}$$

$$\text{for } n = b/y : Q = C S_0^{0.5} \frac{(n + m)^{3/2} y^3}{(n + 2\sqrt{(1 + m^2)y})^{1/2}} \quad (C.18)$$

$$y^{5/2} = \frac{Q(n + 2\sqrt{(1 + m^2)})^{1/2}}{C S_0^{0.5} (n + m)^{3/2}} = \frac{Q}{C * S_0^{0.5} * f} \quad (C.19)$$

$$f = \frac{(n + m)^{3/2}}{(n + 2\sqrt{(1 + m^2)})^{1/2}} \quad (\text{C.20})$$

$$\frac{b}{y_{\text{recom}}} = 1.76 * Q^{0.35} \quad \text{for } 0.2 < Q < 10 \text{ m}^3/\text{s}$$

$$b/y = 1 \quad \text{for } Q < 0.2 \text{ m}^3/\text{s}$$

The design steps include:

- Assume a value for the wall roughness (Nikuradse value) and find a first approximation of C, y and b ;
- Next re-compute the design values to obtain the proper values of b and C ;
- Next fine-tune the design in view of a small adjustment of the design width b_{des} , i.e. a value that can be constructed (e.g. width on a half or whole meter). This fine-tuning has a minor impact on the final results, unless a completely different value from the originally suggested b is used.

The values found in the previous design steps have to be checked in view of the erosion and sedimentation considerations, that will be discussed in the next sections.

C.6 BOUNDARY SHEAR STRESSES

The minimum velocity in a canal is that velocity that will not induce siltation and that will reduce weed growth and health risks. A velocity of 0.30 m/s is a minimum velocity in large canals; smaller velocities result in uneconomically large sections. The maximum permissible velocity should not cause erosion of the bottom and side slopes. The maximum velocity follows from the critical shear stress, which preferably should be less than 3–5 N/m² at the bottom. This shear stress is strongly influenced by the fact that:

- The resistance to erosion increases when smaller particles are washed out.
- An aged canal has more resistance to erosion than a newly constructed one.
- Colloidal matter in the water will result in cohesion of the particles that form the boundaries, resulting in an increased resistance.
- A higher ground water table than the canal water level will decrease the resistance.

According to investigations the maximum tractive force are at:

- the bottom for $b/y > 4$ to 5: $\tau = \rho * g * y * S$;
- the banks for $b/y > 2$ to 3: $\tau = 0.75 * \rho * g * y * S$

The shear stress of the banks will not be considered unless the bed and sides are covered by coarse, non-cohesive material; in that case the angle of repose should be included.

The boundary shear stress at the bottom is:

$$\tau_{\max} = c * \rho * g * y * S \text{ (N/m}^2\text{)} \tag{C.21}$$

Where:

c = correction factor for various b/y ratios

ρ = density of water (kg/m^3)

g = acceleration due to gravity (9.81 m/s^2)

y = water depth (m)

S = bottom slope (m/m)

The correction factor c is a function of the b/y ratio:

$$c = 0.77 * e^{(b/y)*0.065} \quad \text{for } 1 < b/y < 4 \tag{C.22}$$

$$c = 1 \quad \text{for } b/y \geq 4 \tag{C.23}$$

Field studies on very coarse material have shown that the ‘critical shear stress’, above which motion of particles will start, is approximately $0.94 * D_{75}$ (N/m^2), where D is in mm. For the design a boundary shear stress of $0.80 * D_{75}$ or $0.75 * D_{75}$ is recommended.

The maximum boundary shear stress *in normal soils in normal canals and under normal conditions* can be between 3 and 5 N/m^2 . The USBR recommendations for fine material are given in Table C.3. In case that the shear stress is too high the most sensitive factor to reduce the stress is a gentler bottom slope.

Table C.3 Recommended critical boundary shear stress (N/m^2).

D_{50} (mm)	Clear water	Light load	Heavy load
0.1	1.20	2.40	3.60
0.2	1.25	2.49	3.74
0.5	1.44	2.64	3.98
1.0	1.92	2.87	4.31
2.0	2.88	3.83	5.27
5.0	6.71	7.90	8.87

The design values of critical boundary shear stress are established for straight canals, and should be reduced for sinuous canals. See Table C.4 for the reduction in percentage.

Table C.4 Reduction of the boundary shear stresses in non-straight canals.

Slightly sinuous	10%
Moderate sinuous	25%
Very sinuous	40%

C.7 SEDIMENT TRANSPORT CRITERIA

The velocity in a canal should be large enough to prevent siltation of suspended sediment. The conveyance of suspended sediment through the whole system assumes a concentration of very fine particles in suspension, which is almost evenly distributed over the vertical of the turbulent water. De Vos (1925) has stated that the relative transport capacity (T/Q) is proportional to the average energy dissipation per unit of water volume.

$$\frac{T}{Q} \propto \rho_w * g * v_{av} * S \quad (C.24)$$

Where:

T/Q = relative transport capacity

ρ_w = density of water (kg/m^3)

g = acceleration due to gravity (m/s^2)

v_{av} = average velocity (m/s)

S = bottom slope (m/m)

From energy considerations follows that sediment particles will be transported by the water in case:

$$w \leq \frac{\rho_w * v_{av} * S}{\rho_s - \rho_w} \quad \text{or} \quad w \leq \frac{v_{av} * S}{\Delta} \quad (C.25)$$

Where:

w = fall velocity (m/s)

ρ_s = density of the sediment particles (i.e. $2600 \text{ kg}/\text{m}^3$)

ρ_w = density of the water (kg/m^3)

Δ = relative density

To convey sediment in suspension the hydraulic characteristics of the canal system should remain constant or should not decrease in downstream direction. This means that $\rho_w * g * v_{av} * S$ (W/m^3) should be constant or non-decreasing in downstream direction.

In a wide canal the average velocity can be expressed by $v_{av} = C * (y * S)^{0.5}$, in which C is a general smoothness factor. From this velocity follows the criterion for the continued conveyance of suspended material, namely $y * S^{1/3}$ should be constant or non-decreasing in downstream direction.

C.8 TRANSPORT OF THE BED MATERIAL

In general the bed load particles in canals have a diameter of $D > 50 * 10^{-3} - 70 * 10^{-3}$ (mm) and their transport on or above the bottom is determined by the shear velocity (v_*) with

$$v_* = (g * y * S)^{0.5}$$

The criterion for continued conveyance of the bed load depends on the water and sediment transport formulas, for example Einstein-Brown, Engelund Hansen, Ackers-White, Brownlie, etc.

The relative transport capacity is:

$$\frac{T}{Q} \propto \frac{b * y^3 * S^3}{b * y * y^x * S^z} \quad (C.26)$$

Where x and z are exponents depending on the choice of the water transport relationship.

The criterion for the continued movement of suspended load for a wide canal gives that $y S^{1/3}$ should be constant or non-decreasing. To prevent erosion the boundary shear stress should be constant. From this follows that $y * S$ should be constant (or non-decreasing). Therefore it would be expected that for sediment laden water that only transports bed load, the criterion for continued conveyance of the sediments should be some where in between these two criteria. The criterion to convey non-suspended (bed) material depends strongly on the water and sediment equations. The best criterion is that the relative transport capacity for bed load should be non-decreasing or in the case of possible erosion, should remain constant. The numeric approximation for this transport is that $y^{1/2} * S$ is constant or non-decreasing.

To prevent erosion the boundary shear stress should be constant, which gives that $y * S$ should be constant (or non-decreasing). Therefore it would be expected that for sediment laden water that transports only bed load, the criterion for continued conveyance of the sediments is some where in between these two values. The criterion to convey any non-suspended material depends strongly on the water and sediment equations; the best criterion would be that the relative transport capacity for bed load should be non-decreasing, or in the case of possible erosion, should remain constant. The best numeric approximation for the conveyance of non-suspended material is that $y^{1/2} * S$ is constant or non-decreasing.

C.9 FINAL REMARKS

The design of a canal section starts from a given discharge Q and looks for the following unknown canal characteristics:

- the bottom width b ;
- the side slope m ;
- the roughness (smoothness) of the canal, k_s or C ;
- the water depth y ;
- the range for the bottom slope S_0 ;
 - a. the minimum recommended slope;
 - b. the maximum allowable slope.

The steps for the design of a canal as discussed in the previous section include:

- the equation for uniform flow;
- a side slope m that depends on geological criteria;
- a value of k_s that is a function of the maintenance condition and the water depth y ;
- the recommended value for the b/y -ratio;
- the sediment aspects:
 - a. the criterion in view of the erosion (tractive force);
 - b. the criterion to prevent sedimentation by controlling the relative transport capacity.

This iterative design process can be easily used for the development of a spreadsheet or a Visual Basic programme that uses all the presented criteria and equations, including the criteria for bed erosion and sediment transport. UNESCO-IHE has developed programs like Candes and Sysdes for the design of a single canal reach or a canal network with several sections, respectively.

After finalizing the design of the canal, next the model SETRIC can be applied to evaluate the design and to analyze the alternatives. The model can also be used as a decision support tool in the operation and maintenance of the irrigation network and to determine the efficiency of sediment removal facilities in the system. In addition to that the model will be helpful for the training of engineers to enhance their understanding of sediment transport in irrigation canals.

C.10 COMPUTER AIDED DESIGN OF CANALS

At present various stand-alone programs are available for the design of irrigation canals that allow the designer to evaluate a specific part of the design. In the past years UNESCO-IHE has looked for an integrated tool that combines some of the solitary programs and that results in a faster analysis of alternatives, saving time and helping to find the most feasible design. The time saved in the analysis of different canal alignments could be used for an in-depth analysis of the final selected alternative.

The newly developed tool has three modules, the first one looks for the canal alignment within the area with the least cost by using all the information produced by GIS programs (maps, tables, etc.). The second module performs the hydraulic design, including the introduction of the energy and sediment transport concepts, which avoids sedimentation and erosion in the canal network. Another feature of the tool is the possibility to export the design results of the canal design to DUFLOW (unsteady flow

program) and SETRIC (sediment transport program) for further analysis of the operation and maintenance. The third module connects the results of the previous two modules to calculate the volumes of earthwork (mass diagram). As mentioned before, these volumes have a large impact on the costs and therefore it is important to optimise the design at this stage.

Tests with the new tool and comparison of the model results with the results obtained from other studies have clearly shown the applicability of GIS technology and CAD principles in engineering design. Moreover, the files with the results of the model can be easily exported to the models DUFLOW and SETRIC; this transfer of the data results in a more powerful application of the design tool. In this way the tool gives the chance to test the influence of various operation scenarios on the proposed hydraulic design. SETRIC can investigate whether the design shows the expected behaviour of the sediment in the canal network; whether all the sediment that enters the system will be transported through the whole canal system. Moreover, it will be possible to investigate and to optimise the operation and maintenance by the simulation of different predefined management scenarios.

APPENDIX D

Description of the Main Aspects of the Regime Theory

For the regime theory a set of simple, but empirical equations are available. The equations are derived from observations of alluvial canals that are relatively stable or in regime (HR Wallingford, 1992). The regime method considers the three canal characteristics, namely the perimeter of the canal, the amount of water and the amount of sediment flowing in the canal as a whole and attempts to derive the features of a stable (non silting/ non scouring) canal primarily on the basis of empirical studies of the interaction of the above-mentioned factors (Naimed, 1990). The regime theory is completely empirical and is based on measurements and observations of canals and rivers in regime. The theory originates from India and Pakistan, where most of the canal designs follow this theory, especially the Lacey regime theory. The main equations for the design of stable canals are based on field observations and experiences that are still collected and evaluated. The equations of the regime theory present a long-term average profile rather than a instantaneously variable state. Therefore, they specify the natural tendency of channels that convey sediment within alluvial boundaries to obtain a dynamic stability.

The expression canals in regime means that the canals do not change over a period of one or several typical water years. Within this period, scour and deposition will occur in the canal, but they do not interfere with canal operation. The regime theory can only provide some approximate design values as the equations are based on observations of many canals in regime. These canals have received different amounts of water and sediment from a variety of rivers that have different sediment loads and characteristics. Moreover, some of the canals in regime may have sediment excluders or ejectors at the head works that have influenced the erosion and deposition. Nevertheless, the experience obtained from the design and operation of these canals give some guidance for the design of stable channels with erodible banks and sediment transport. However, the regime theory should be applied in a very careful way, especially when the design involves a canal network with highly time-dependent operational regimes as practised in many irrigation systems at present (Bruk, 1986).

Main equations of the regime theory as given by Lacey (Henderson, 1966)

SI-units	Foot-second units	
$f = \sqrt{2520d}$	$f = 8\sqrt{d}$	D.1
$P = 4.836\sqrt{Q}$	$P = 2.67\sqrt{Q}$	D.2
$v = 0.6459\sqrt{fR}$	$v = 1.17\sqrt{fR}$	D.3
$S_o = 0.000315 \frac{f^{5/3}}{Q^{1/6}}$	$S_o = \frac{f^{5/3}}{1750Q^{1/6}}$	D.4
f = silt factor for a sediment size d	f = silt factor for a sediment size d	
d = sediment size (m)	d = sediment size (inch)	
Q = discharge (m ³ /s)	Q = discharge (cusec)	
P = wetted perimeter (m)	P = wetted perimeter (foot)	
v = mean velocity (m/s)	v = mean velocity (foot/s)	
R = hydraulic radius (m)	R = hydraulic radius (foot)	
S_o = bottom slope	S_o = bottom slope	

According to Lacey (1958) these equations are applicable within the following range of parameters:

- Bed material size 0.15–0.40 mm
- Discharge 0.15–150 m³/s (5–5000 cfs)
- Bed load small
- Bed material non-cohesive
- Bed form ripples

The Lacey equations for the design of canals for given d and Q follow the next steps:

1. $f = (2520 \times d)^{0.5}$ (equation D.1);
2. Determine $P = 4.836 (Q)^{1/2}$ (equation D.2);
3. From $v = 0.6459 (fR)^{1/2}$ (equation D.3), $R = A/P$ and $A = Q/v$ follows the area of the cross section $A = 1.3383 \times ((P/f)^{0.5} \times Q)^{2/3}$
4. Next, find the bottom slope $S = 0.000315 f^{5/3}/Q^{1/6}$ (equation D.4);
5. From the given P and A the channel section is found as a trapezoidal channel with assumed side slope (m) of $1V : 2H$.
6. $y = P + (P^2 + 4A (m - 2(1 + m^2)^{0.5}))^{0.5}/(2(m - 2(1 + m^2)))$
 $B = P - 2y * (1 + m^2)^{0.5}$
 $R = A/P$

Table D.1 gives some examples of the design of earthen canals for two sediment diameters ($d = 0.0004$ m and $d = 0.00015$ m) and two side slopes ($m = 2$ and $m = 1.5$) and several discharges Q according to the Lacey method. The results are also presented in the Figure D.1 and D.2.

Table D.1. Example of the design of earthen canals for two sediment diameters and two side slopes according to the Lacey method.

SI-units											
Lacey regime theory											
Q	d in m	m	f	S_0	P	v	A	R	B_0	y	k_s
2.5	0.00040	2	1.00399	0.000272	7.646	0.515	4.850	0.634	3.662	0.891	42.3
3	0.00040	2	1.00399	0.000264	8.376	0.531	5.646	0.674	4.224	0.928	42.5
4	0.00040	2	1.00399	0.000252	9.672	0.557	7.176	0.742	5.223	0.995	42.9
6	0.00040	2	1.00399	0.000235	11.846	0.596	10.060	0.849	6.912	1.103	43.4
8	0.00040	2	1.00399	0.000224	13.678	0.626	12.785	0.935	8.351	1.191	43.7
10	0.00040	2	1.00399	0.000216	15.293	0.649	15.398	1.007	9.631	1.266	44.0
12	0.00040	2	1.00399	0.000210	16.752	0.669	17.925	1.070	10.797	1.332	44.2
15	0.00040	2	1.00399	0.000202	18.730	0.695	21.588	1.153	12.388	1.418	44.5
2.5	0.00015	2	0.61482	0.000120	7.646	0.438	5.712	0.747	2.006	1.261	48.5
3	0.00015	2	0.61482	0.000117	8.376	0.451	6.649	0.794	2.700	1.269	48.7
4	0.00015	2	0.61482	0.000111	9.672	0.473	8.450	0.874	3.782	1.317	49.1
6	0.00015	2	0.61482	0.000104	11.846	0.506	11.847	1.000	5.486	1.422	49.7
8	0.00015	2	0.61482	0.000099	13.678	0.531	15.056	1.101	6.897	1.516	50.1
10	0.00015	2	0.61482	0.000095	15.293	0.551	18.133	1.186	8.141	1.599	50.4
12	0.00015	2	0.61482	0.000093	16.752	0.568	21.108	1.260	9.270	1.673	50.7
15	0.00015	2	0.61482	0.000089	18.730	0.590	25.422	1.357	10.807	1.772	51.0
2.5	0.00040	1.5	1.00399	0.000272	7.646	0.515	4.850	0.634	4.693	0.819	42.3
3	0.00040	1.5	1.00399	0.000264	8.376	0.531	5.646	0.674	5.276	0.860	42.5
4	0.00040	1.5	1.00399	0.000252	9.672	0.557	7.176	0.742	6.318	0.930	42.9
6	0.00040	1.5	1.00399	0.000235	11.846	0.596	10.060	0.849	8.087	1.042	43.4
8	0.00040	1.5	1.00399	0.000224	13.678	0.626	12.785	0.935	9.597	1.132	43.7
10	0.00040	1.5	1.00399	0.000216	15.293	0.649	15.398	1.007	10.938	1.208	44.0
12	0.00040	1.5	1.00399	0.000210	16.752	0.669	17.925	1.070	12.159	1.274	44.2
15	0.00040	1.5	1.00399	0.000202	18.730	0.695	21.588	1.153	13.823	1.361	44.5
2.5	0.00015	1.5	0.61482	0.000120	7.646	0.438	5.712	0.747	3.856	1.051	48.5
3	0.00015	1.5	0.61482	0.000117	8.376	0.451	6.649	0.794	4.427	1.095	48.7
4	0.00015	1.5	0.61482	0.000111	9.672	0.473	8.450	0.874	5.441	1.173	49.1
6	0.00015	1.5	0.61482	0.000104	11.846	0.506	11.847	1.000	7.155	1.301	49.7
8	0.00015	1.5	0.61482	0.000099	13.678	0.531	15.056	1.101	8.615	1.404	50.1
10	0.00015	1.5	0.61482	0.000095	15.293	0.551	18.133	1.186	9.912	1.492	50.4
12	0.00015	1.5	0.61482	0.000093	16.752	0.568	21.108	1.260	11.093	1.570	50.7
15	0.00015	1.5	0.61482	0.000089	18.730	0.590	25.422	1.357	12.704	1.671	51.0

Example

- Given is a canal with a discharge $Q = 10 \text{ m}^3/\text{s}$ and sediment with size $d = 0.001 \text{ m}$
- Hence, $f = 1.58745$ and $P = 15.293 \text{ m}$
- The bottom slope $S_0 = 0.4636 \text{ m/km}$
- After trial and error follows $v = 0.76 \text{ m/s}$, $A = 13.22 \text{ m}^2$ and $R = 0.86 \text{ m}$
- For a side slope $m = 2$ and for the above given data follows:
 $B_0 = 10.65 \text{ m}$ and $y = 1.04 \text{ m}$.
- Using Manning gives $n = 0.026$ and according to Strickler $k_s = 38.7$

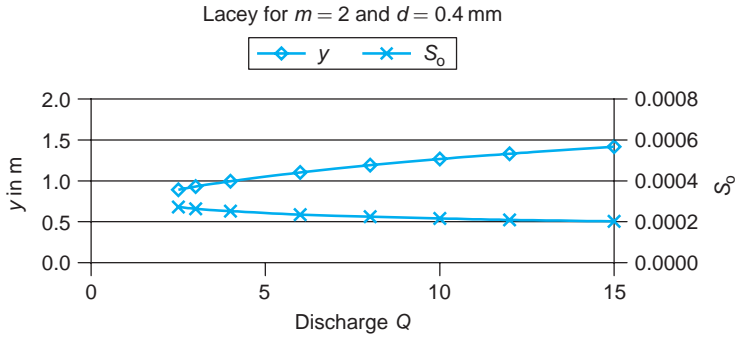


Figure D.1. Example of the design of an earthen canal according to the Lacey method for $m = 2$ and $d = 0.4$ mm.

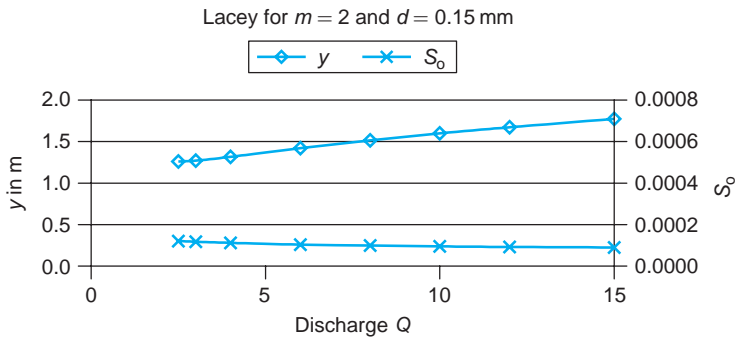


Figure D.2. Example of the design of an earthen canal according to the Lacey method for $m = 2$ and $d = 0.15$ mm.

D.1 SOME REGIME CONSIDERATIONS

D.1.1 *Sediments*

In general, irrigation canals have a less steep bottom slope, smaller cross sections and discharge than the rivers, which supply the irrigation water to the canal network. This means that the canals have a smaller sediment transport capacity than the parent river. Therefore, an important aspect in the design and operation of these canals is to consider sediment exclusion at the head works or sedimentation in silting ponds. The location and crest level of canal regulators at the head works should limit the sediment entry into the canal network.

D.1.2 *Maturing of canals*

The maturing of canals is an important aspect in view of the operation and maintenance of canals. The canal design according to the regime theory will be based upon the material transported by the river and not on the local soils that form the bed. The local soils might be different from the sediment transported by the river and only after a few years of operation, the bed material will be adjusted to the sediment entering the canal. The

canal will then show a quasi-equilibrium condition. The maturing of the canal includes the following negative aspects:

- Development of aquatic weeds on the side-slopes;
- Adjustments of the canal to the newly developed longitudinal slope;
- Changes and improvements of off-takes, irrigation turnouts and bifurcation structures to adjust their levels to the changes in the canal after maturing.

Stable alluvial canals are characterized by regular side slopes, which are developed by the deposition of fine silt and clay particles. The side slopes are generally much less permeable than the bed and may reduce the seepage losses through the sides. They also have a higher erosion resistance and limit any tendency to widen the canal.

D.1.3 Slope adjustments

The bottom slope of a canal after maturing will differ from the design and the difference can be significant for long canals. Slope adjustments are feasible by the construction of drop structures at regular intervals. During the maturing process the crest levels of the drop structures have to be raised or lowered to accommodate the slopes. The drops often form a part of bifurcation structures.

D.1.4 Diversion of the sediment

The distribution or division of the sediment over the canal branches is an important aspect in the design and operation of alluvial canals. The distribution of the flow velocity and of the sediment concentration over the flow depth is different and therefore, it is realistic to assume that the division of water and sediment at bifurcations is not proportional. Some canals will receive a larger or smaller concentration of sediment than the concentration conveyed by the parent canal. Remodelling of the bifurcation structures might be necessary to adjust the distribution of the sediment to the branches.

The aim of any irrigation network is to convey the water as well as the sediment through the farm turnouts to the fields. The sediment transport depends on the design and location of the turnout structures in relation to the canal bed. The discharge capacity of a turnout depends on the command area downstream of that turnout. When the command area increases with the development of new irrigation canals, the discharge has to be increased. Turnouts on irrigation canals are relatively inexpensive (adjustable pipe turn outs) and when the canals mature and the system attains equilibrium, the pipe turnouts can be replaced by (semi-permanent) modules. The crest level of the turnouts will then be based on sediment transport considerations as well as on the discharge variation in the canals. In smaller canals, the turnouts are important to the geometry of the canals.

It has been found from intensive observations that the average bed level of distributaries adjusts to the mean crest level of these turnouts. In unstable distributaries, which may be silted up, the lowering of the turnouts is one of the recommended solutions.

D.1.5 Maintenance aspects

All irrigation canals require maintenance; earthen canal banks are constantly eroded by wind and rainfall and have to be maintained. Their stability is based upon the stability of the canal bed and the cross sections. The canal width is generally maintained by providing bank protection by permeable spurs normal to the banks. Normally, bed levels are excavated during closures if the canals silt up.

The crest of drop structures might be raised if the bed shows scouring. Maintenance of the bed elevation and canal width is expensive. Experiences show that on larger canals, bank protection is rarely practised and bed clearance is never carried out. In the smaller distributaries both the maintenance of the width and the bed elevation are often done. The berms along these canals may become a problem as they may become beyond their design width and may have to be trimmed. The canal bed level may also have to be re-excavated to near design levels. In general, the frequency of these operations, where needed, is about once in the five years. The medium size canals are more stable. In these canals like in the large canals no bank protections are practised, but the bed level may be cleared once in the ten years.

The variation in discharge in the canals is an important factor in the stability of alluvial canals. Low discharges flowing in canals with high capacities often adopt a winding thalweg that may later erode the banks by concentrating flows against the banks. For this reason the minimum discharge in mature canals is limited to 55% of the design capacity. Similarly, the raising and lowering of the canal discharge is also controlled to prevent the failure of banks due to seepage forces.

D.1.6 Flow capacity

In recent years, the design capacities in almost all canals have been increased to meet the growing demand for irrigation water. In some areas, this might be done by modifying the cross-sections of the existing canal and in other places by changing the structures, raising the banks and forcing the larger water supply to flow in the canal. Often this has resulted in a change of the canal regime established in the past and in unsymmetrical cross sections.

D.1.7 Design considerations

To design a straight, earthen canal that has to convey a certain amount of water and sediment three equations are needed to find the bottom width,

water depth and bottom slope of the canal. However, normally there are only two equations available, namely a flow equation (Manning, Strickler or de Chézy) and a sediment transport equation. An equation to describe the shape of a stable channel is not yet available. If the tractive force along the canal perimeter is large enough to maintain sediment transport, one can rely on a kind of regime-like relationship to describe the stability of the canal.

APPENDIX E

Glossary Related to Sediment Transport

Abrasion	Frictional erosion by material transported by wind and water.
Absolute pressure	The pressure above absolute zero.
Absorbed water	Water held mechanically in a soil and possessing the same physical properties as ordinary water at the same temperature and pressure.
Accretion	Accumulation of sediment deposited by natural flow processes; increase of channel bed elevation resulting from the accumulation of sediment deposits.
Accuracy	The degree of conformity of a measured or calculated value to its definition or with respect to a standard reference.
Adequacy	The ratio of the amount delivered to the amount required.
Adjustable flow	Irrigation flow regulated at a specific discharge (flow rate).
Aggradation	Build-up or rising of channel bed due to sediment deposition.
Alignment	The course along which the centre line of a canal or drain is located.
Alluvial soil	A soil formed from deposits by rivers and streams (alluvium).
Alternate depth	In open channel flow, for a given flow rate and channel geometry, the relationship between the specific energy and flow depth indicates that, for a given specific energy, there is no real solution (i.e. no possible flow), one solution (i.e. critical flow) or two solutions for the flow depth. In the latter case, the two flow depths are called alternate depths. One corresponds to a subcritical flow, the second to a supercritical flow.
Altitude	Vertical height of a ground or water surface above a reference level (datum).
Amplitude	Half of the peak-to-trough range (or height).
Analytical model	System of mathematical equations that are the algebraic solutions of the fundamental equations.
Angle of repose	The maximum slope (measured from the horizon) at which soils and loose materials on the banks of canals, rivers or embankments stay stable.
Armouring	Progressive coarsening of the bed material resulting from the erosion of fine particles. The remaining coarse material layer forms armour, protecting further bed erosion.
Automatic control	Adjustment of the controlling element accomplished by an arrangement of equipment without attendance by an operator or continuous control of equipment without intervention of an operator to predetermined conditions.
Automatic system	System that starts and stops without human intervention in response to control, such as a switch, or a valve.

Backwater	Flow profile controlled by downstream flow conditions in a subcritical flow: e.g. a structure, change of cross-section; is commonly used for both supercritical and subcritical flow. Term backwater calculation or profile refers to the calculation of the flow profile.
Backwater calculation	Calculation of the free-surface profile in open channels.
Backwater curve	Longitudinal profile of the water surface in an open channel where the flow depth has been increased by e.g. an obstruction, increase in channel roughness, decrease in channel width or bottom slope. The water surface slope is less than the bottom slope; the curve is upstream of the obstacle that raises the water level and is concave upwards. Occasionally the term is used for other non-uniform profiles, upstream or downstream.
Bagnold	Ralph Alger Bagnold (1896–1990) – British geologist and expert on the physics of sediment transport by wind and water.
Bakhmeteff	Boris Alexandrovitch Bakhmeteff (1880–1951) – Russian expert on hydraulics, who developed the concept of specific energy and an energy diagram for open channel flows (1912).
Bank protection	The process by which the bank is protected from erosion by lining or by retarding the velocity along the bank; device to reduce scour by flowing water e.g. mattresses, groynes, revetments.
Bank, left/right-	Bank to the left/right of an observer looking downstream.
Barré de Saint-Venant	Adhémar Jean Claude Barré de Saint-Venant (1797–1886), French engineer, who developed the equation of motion of a fluid particle in terms of the shear and normal forces exerted on it.
Bazin	Henri Emile Bazin: French scientist (1829–1917) and engineer, worked as an assistant of Henri P.G. Darcy.
Bed erosion	Deepening of a channel by the gradual wearing away of bed material, mainly due to the forces of flowing water.
Bed forms	Channel bed irregularity that is related to the flow conditions; features on a channel bed resulting from the movement of sediment over it. Characteristic bed forms include ripples, dunes and anti-dunes.
Bed load	Sediment transport mode in which individual particles either roll, slide or hop along the bed as a shallow, mobile layer a few particle diameters deep; mass (or volume) of coarse sediment (silt, sand, gravel) in almost continuous contact with the bed and transported in unit time.
Bed material	Material with particle sizes that are found in significant quantities in that part of the bed affected by transport.
Bed material load	Part of the total sediment transport, which consists of the bed material and whose rate of movement is governed by the transporting capacity of the channel.
Bed or bottom slope	Difference in bed elevation per unit horizontal distance in the flow direction.
Bed profile	Shape of the bed in a vertical plane; longitudinally or transversely, which should be stated.
Bed shear stress	The way in which currents transfer energy to the channel bed.
Berm	Horizontal edge on the side of an embankment or channel section, to intercept earth rolling down the slope, or to add strength to the construction.

Bernoulli	Daniel Bernoulli (1700–1782); Swiss mathematician, physicist and botanist who developed the Bernoulli equation: ‘Hydrodynamica, de viribus et motibus fluidorum’ textbook (1st publication in 1738, Strasbourg).
Bifurcation	Location where a river or channel separates in two or more reaches, sections or branches (opposite of a confluence).
Boundary conditions	Physical conditions (hydraulic and/or others) used as boundary input to physical or numerical models.
Boundary layer	The flow region next to a solid boundary where the flow field is affected by the presence of the boundary and where friction plays an essential part. A range of velocities characterizes a flow across the boundary layer region; from zero at the boundary to the free-stream velocity at the outer edge of the boundary layer.
Boussinesq	Joseph Valentin Boussinesq (1842–1929) – French expert on hydro-dynamics ‘Essai sur la théorie des eaux courantes’ an outstanding contribution in hydraulics literature (1877).
Boussinesq coefficient	Momentum correction coefficient.
Bresse	Jacques Antoine Charles Bresse (1822–1883) – French applied mathematician and hydraulic expert, who made contributions to gradually varied flows in open channel hydraulics (Bresse 1860).
Bulk density	The mass of soil per unit of undisturbed bulk volume.
Canal	A man-made or natural channel used to convey and in some cases also to store water.
Capacity	The ability to receive or to hold power; the ability of a stream to transport water or sediment; the volume of artificial or natural reservoirs, basins.
Cartesian coordinate	One of three coordinates that locate a point in space and measure its distance from one of three intersecting coordinate planes measured parallel to one of the three straight-line axes that are the intersections of the other two planes. It is named after the mathematician René Descartes.
Caving	The collapse of a bank caused by undermining due to the wearing away of the bank by the action of flowing water.
Channel	Stream or waterway; ‘channel’ generally means the deep part of a river or other waterway.
Channel, open-	Longitudinal boundary consisting of the bed and banks or sides forming a passage for water with a free surface.
Channel, stable-	Channel in which the bed and sides remain stable over a significant period of time in the control reach and in which scour and deposition during floods is minimal.
Channel, unstable-	Channel in which there is frequently and significantly change in the bed and sides of a control reach.
Chézy coefficient	de Chézy coefficient is a resistance coefficient for open channel flows. Although it was thought to be a constant, the coefficient is a function of the relative roughness and Reynolds number.
Chézy, de	Antoine de Chézy (1717–1798).
Cohesion	The mutual attraction of soil particles due to strongly attractive forces. Cohesion is high in clay but significantly little in silt or sand.

Cohesionless	Referring to soil that consists primarily of silt or larger grain sizes and in which strength is directly related to confining stresses.
Cohesionless soil	Soil that has a little tendency to stick together whether wet or dry, such as sands and gravel.
Cohesive sediment	Sediment material of very small sizes (less than 50 μm) for which cohesive bonds between particles are significant and affect the material properties. The sediment contains significant proportion of clays, the electro-magnetic properties of which cause the sediment to bind together.
Cohesive soil	Very fine-grained unconsolidated earth materials for which strength depends upon moisture content.
Compound cross section	A cross section of a channel in which the width suddenly increases above a certain level.
Confidence interval	An interval around the computed value within which a given percentage of values of a repeatedly sampled variate is expected to be found.
Conjugate depth	Another name for sequent depth in open channel flow.
Continuity	The fundamental law of hydrodynamics, which states that for incompressible flows independent of time, the sum of the differential changes in flow velocities in all directions must be zero.
Control	Physical properties of a channel, which determine the relationship between stage and discharge at a location in that channel.
Control section	A section in an open channel where critical flow conditions take place resulting in a distinct relationship between water level and discharge; the concept of 'control' and 'control section' are used with the same meaning.
Coriolis	Gustave Coriolis (1792–1843) – French mathematician, who first described the Coriolis force (effect of motion on a rotating body).
Coriolis coefficient	Kinetic energy correction coefficient.
Critical depth	Depth in a canal of specified dimensions at which the mean specific energy is a minimum for a given discharge; the flow is critical.
Critical flow	Flow for which the specific energy is minimum for a given discharge; Froude number will be equal to unity and surface disturbances will not travel upstream.
Critical flow condition	The flow condition in open channel flows such that the specific energy is a minimum. Critical flow conditions occur for $Fr = 1$.
Critical slope	Slope of a channel in which uniform flow depth occurs at critical depth.
Critical tractive force	The threshold value of the tractive force of a water flow when bed material starts to move.
Cross-section	Section of a stream normal to the flow direction bounded by the wetted perimeter and the free surface.
Darcy-Weisbach friction factor	Dimensionless parameter characterizing the friction loss in a flow.
Datum	Any permanent line, plane or surface used as a reference datum to which elevations are referred.
Degradation	Lowering of channel bed elevation resulting from the erosion of sediments; downward and lateral erosion.

Density	Mass (in kg) per unit of volume of a substance.
Depth, hydraulic or mean-	Depth obtained by dividing the cross-sectional area by the free surface or top width.
Design discharge	A specific value of the flow rate, which after the frequency and the duration of exceedance have been considered, is selected for designing the dimensions of a structure or a system or a part thereof.
Design flow	Flow on which the cross sectional area of a canal or drain is determined.
Design flow depth	Depth of water in a channel when design flow moves through the cross-sectional area.
Desilting basin	Canal section with very low velocity, forming deposition of the sediment carried by the water.
Diffusion	The process whereby particles intermingle as the result of spontaneous movement and move from a region of higher concentration to one of lower concentration. Turbulent diffusion describes the spreading of particles caused by turbulent agitation.
Diffusion coefficient	Quantity of a substance that passes through each unit of cross-section per unit of time.
Dimensional analysis	Technique to reduce the complexity of a problem, by expressing the relevant parameters in terms of numerical magnitude and associated units, and grouping them into dimensionless numbers.
Discharge	Volume of water per unit time flowing along a pipe or channel, or the output rate of plant such as a pump.
Discharge regulator	Structure regulating the flow from one canal to another.
Diversion structure	Structure in a river or canal to divert all or some of the water into a (diversion) canal.
Drawdown curve	Water surface profile, when water surface slope is larger than bottom slope.
Drop	A rapid change of bed elevation, also called a step.
Dry density	Mass of soil per unit of volume on dry weight basis.
Dunes	Types of bed form indicating significant sediment transport over a sandy bed.
Dynamic equilibrium	Short-term morphological changes that do not affect the morphology over a long period.
Dynamic viscosity	The ratio between the shear stress acting along any plane between neighbouring fluid elements and the rate of deformation of the velocity gradient perpendicular to this plane.
Eddy	A vortex type of water motion, partly flowing opposite to the main current; small whirlpool; movement of flowing water in a circular direction, caused by irregularities or obstructions in canals, rivers or streams.
Eddy viscosity	Name for the momentum exchange coefficient; also called 'eddy coefficient'.
Elevation head	The vertical distance to a point above a reference level.
Energy (grade) line	Plot of the total energy head in the flow direction.
Energy gradient	Difference in total energy per unit of horizontal distance in the flow direction.
Energy head, Total-	Sum of the elevation of the free water surface above a horizontal datum in a section and the velocity head at that section.
Energy loss/head loss	Difference in total energy between two cross-sections.

Energy, Specific-	Sum of the elevation of the free water surface above the bed and the velocity head at that section.
Equity	Criterion of the share for each individual or group that is considered fair by all system members; the measure can be defined as the delivery of a fair share of water to users throughout a system; the spatial uniformity of the ratio of the delivered amount of water to the required (or scheduled) amount.
Erodible	Used for the material (soil) prone to erosion.
Erosion	The process by which soil is washed or otherwise moved by natural factors from one place to another; the gradual wearing away of canal beds by flowing water.
Erosion and scour	The detachment and transport of sediment particles because of flowing water. The processes can occur over land or within rivers and canals and ultimately result in the deposition of transported sediment at downstream locations. The movement of sediment can lead to the loss of significant soil volumes, the instability of canal beds and banks, the undercutting of bridge pier and abutment foundations, the reduction of conveyance and storage capacity, and the damaging of aquatic habitat.
Erosive	Used for the mechanism causing erosion.
Error	The difference of a measured value from its known true or correct value (or sometimes from its predicted value).
Euler	Leonhard Euler (1707–1783) – Swiss mathematician and physicist.
Event	An occurrence, which meets specified conditions, e.g. damage, a threshold rainfall, water level or discharge.
Extreme	A value expected to be exceeded once, on average, in a given (long) period of time.
Fall	A sudden drop in bed level of a stream.
Fixed-bed channel	The bed and sidewalls are non-erodible; neither erosion nor accretion occurs.
Flow	Movement of a volume of water; not to be confused with ‘rate of flow’ or ‘discharge’.
Flow control method	In general, a regulation method for irrigation structures to maintain a specific flow condition in the irrigation system.
Flow, steady-	Flow in which the depth and velocity remain constant with respect to time.
Flow, uniform-	Flow in which the depth and velocity remain constant with respect to space.
Free flow	Flow through a canal, which is not affected by the level of the downstream water.
Free water level	Level or surface of a body of water in free contact with the atmosphere, meaning at atmospheric pressure.
Freeboard	The difference in elevation of the maximum (normal) flow line and the ground surface or bank at a canal or drain section. Also the vertical distance between the maximum water surface elevation in design and the top of retaining banks or structures, provided to prevent overtopping because of unforeseen conditions.
Free-surface	Interface between a liquid and a gas. More generally a free surface is the interface between the fluid (at rest or in motion) and the atmosphere.

Friction	Boundary shear resistance of the wetted surface of a channel, which opposes the flow of water; process by which energy is lost through shear stress.
Friction coefficient	Coefficient used to calculate the energy gradient by friction.
Froude	William Froude (1810–1879) – English naval architect and hydro-dynamicist who used the law of similarity to study the resistance of model ships.
Froude number	A dimensionless number representing the ratio of inertia forces and gravity forces acting upon water. $Fr^2 = \bar{v}^2/g y$. It is used to differentiate open channel flow regimes and to distinguish between sub-critical and super-critical flow.
Gauge	Device for measuring water level, discharge, velocity, pressure, etc, relative to a datum.
Gauge datum	Fixed plane to which the water level is related; the elevation of the zero of the gauge is related to this plane.
Gauge height	Elevation of water surface measured by a gauge.
Gradient	Measure of slope in metre of rise or fall per metre of horizontal distance; dimensionless.
Gradually varied flow	Flow characterized by relatively small changes in velocity and pressure distributions over a short distance.
Head	Potential energy of water due to its height above a datum or reference level, usually expressed in m.
Head works	The main intake structure of an irrigation system, often equipped with a weir or barrage, an intake sluice, sediment excluder or sand trap.
Head-discharge relationship	Curve or table which gives the relation between the head and the discharge in an open channel at a given cross-section for a given flow condition, e.g. steady, rising or falling.
Hydraulic	Relating to the flow or conveyance of liquids, especially water through pipes or channels.
Hydraulic jump	Abrupt, sudden change from supercritical to subcritical flow; flow transition from a rapid (supercritical flow) to a slow flow motion (subcritical flow). Giorgio Bidone published the first investigations in 1820. The present theory was developed by Bélanger (1828) and has been verified experimentally by many researchers (Bakhmeteff and Matzke 1936).
Hydraulic radius	Quotient of the wetted cross-sectional area and the wetted perimeter.
Hydrostatic pressure	Also known as the gravitational pressure, it is the pressure at a point due to the weight of the fluid above it.
Ideal fluid	Frictionless and incompressible fluid; fluid has zero viscosity: it can't sustain shear stress at any point.
International System of Units	SI = <i>Système International d'Unités</i> ; system of units adopted in 1960 based on the metre-kilogram-second (MKS) system. It is commonly called the SI unit system. The basic seven units are: for length, mass, time, electric current, luminous intensity, amount of substance and temperature.
Irregular waves	Waves with random wave periods (in practice also heights), which are typical for natural wind-induced waves.
Karman constant	'Universal' constant of proportionality between the Prandtl mixing length and the distance from the boundary. Experimental results indicate that $\kappa = 0.40$.

Karman, von	Theodore von Karman (1881–1963) – Hungarian expert on fluid-dynamics, who studied the vortex shedding behind a cylinder (Karman vortex street).
Kinematic viscosity	Dynamic viscosity divided by the fluid density.
Lagrange	Joseph-Louis Lagrange (1736–1813) – French mathematician and astronomer.
Laminar flow	Flow characterized by fluid particles moving along smooth paths in thin layers (laminas), with one layer gliding smoothly over an adjacent layer and not influenced by adjacent layers perpendicular to the flow direction. Laminar flows follow Newton’s law of viscosity that relates shear stress to the rate of angular deformation: $\tau = \mu(\delta v/\delta y)$.
Level-top canal	A canal with horizontal embankments between cross-regulators to meet zero flow condition for downstream control.
Longitudinal section	Vertical section along the centre line of a canal, it shows the original and the final levels.
Main canal	Is the irrigation canal taking water from the supply (source) and conveying the water to the lateral or secondary canals.
Maintenance	Operations performed in preserving irrigation or drainage canals and drain pipes, hydraulic structures, service roads and works in good or near original conditions. Repairs are part of maintenance; the regular, continuous inspection and repair of irrigation and drainage systems.
Manning	Robert Manning (1816–1897); Chief Engineer of Public Works, Ireland. In 1889, he presented two formulae, but he preferred to use the second formula.
Mathematical model	Model that simulates a system’s behaviour by a set of equations, perhaps together with logical statements, by expressing relationships between variables and parameters.
Mean depth	Average depth of a canal, being the cross sectional area divided by the surface or top width.
Mean velocity	Average velocity in a canal, being the discharge divided by the cross sectional (wetted) area.
Meandering	Single channel having a pattern of successive deviations in alignment that results in a more or less sinusoidal course.
Mixing length	The mixing length is the characteristic distance travelled by a fluid particle before its momentum is changed by the new environment; the mixing length theory is a turbulence theory developed by Prandtl (1925).
Modelling	Simulation of some physical phenomenon or system with another system believed to obey the same physical laws or rules in order to predict the behaviour of the former by experimenting with the latter.
Momentum exchange coefficient	Apparent kinematic (eddy) viscosity in turbulent flows; analogous to the kinematic viscosity in laminar flows. Momentum exchange coefficient is proportional to the shear stress divided by the strain rate. Also called eddy viscosity or eddy coefficient (Boussinesq, 1877).
Navier	Louis Marie Henri Navier (1785–1835) – French engineer who extended Euler’s equations of motion (Navier 1823).

Navier-Stokes equation	Momentum equation applied to a small control volume of incompressible fluid; usually written in vector notation. Navier first derived the equation by a different method. De Saint-Venant in 1843 and Stokes in 1845 derived it in a more modern manner.
Negative surge	A negative surge results from a sudden change in flow that decreases the flow depth. It is a retreating wave front moving upstream or downstream.
Newton	Sir Isaac Newton (1642–1727) – English mathematician and physicist. His contributions in optics, mechanics and mathematics were fundamental.
Nikuradse	J. Nikuradse – German engineer who investigated the flow in smooth and rough pipes (1932).
Non uniform flow	Flow that varies in depth, cross-sectional area, velocity and hydraulic slope from section to section.
Normal depth	Uniform equilibrium open channel flow depth; depth at a given point in a canal corresponding to uniform flow, water surface and bed are parallel.
Numerical modelling	Refers to the analysis of physical processes (e.g. hydraulic) using computational models.
Off-take	Structure with or without gates, that conveys water to a secondary canal or tertiary unit.
One-dimensional flow	Neglects the variations and changes in velocity and pressure transverse to the main flow direction.
One-dimensional model	Model defined with one spatial coordinate, the variables being averaged in the other two directions.
Open canal	Natural or man-made structure that contains, restricts and directs the flow of water. The surface of the water is open to the atmosphere, and therefore, the flow is referred to as free flow. The design of canals includes the solution of relationships between bed and bank roughness, channel geometry, and flow velocity. Free surface flows are driven by gravity and they can vary in both time and space.
Open channel	Channel in which the water surface is in free contact with the air (free surface).
Overflow structure	Structure with water flowing over its crest.
Particle size distribution	The fractions of clay, silt and sand particles in a soil.
Pascal	Blaise Pascal (1623–1662) – French mathematician, physicist and philosopher, who developed the modern theory of probability. Between 1646 and 1648, he formulated the concept of pressure and showed that the pressure in a fluid is transmitted through the fluid in all directions. The unit of pressure is named after Pascal: one Pascal equals a Newton per square-metre.
Physical modelling	Investigations of hydraulic processes using a (physical) scale model.
Porosity	The ratio of the volume of pores filled by air and/or water and the total volume of a soil sample.
Positive surge	Positive surge results from a sudden change in flow that increases the depth. It is an abrupt wave front. The unsteady flow conditions may be solved as a quasi-steady flow situation.
ppm	Abbreviation for parts per million.

Prandtl	Ludwig Prandtl (1875–1953) – German physicist who introduced the concept of the boundary layer and developed the turbulent, mixing length’ theory.
Precision	The degree of mutual agreement among a series of individual measurements. Precision is often, but not necessarily, expressed by the standard deviation of the measurements.
Primary canal	Canal that conveys water from the head works to the secondary canals and tertiary units.
Probability	The chance that a prescribed event will occur, represented as a pure number (p) in the range $0 < p < 1$. It can be estimated empirically from the relative frequency (i.e. The number of times the particular event occurs, divided by the total count of all events in the class considered).
Prototype	Actual structure or condition being simulated in a numerical or physical model.
Rapidly varied flow	A flow characterized by large changes over a short distance (e.g. weirs, gates, hydraulic jump).
Rating curve	Graphic or tabular presentation of the discharge or flow through a structure or channel section as a function of water stage (depth of flow).
Rayleigh	John William Strutt, Baron Rayleigh (1842–1919) – English scientist in acoustics and optics. His works are the basis of wave propagation theory in fluids.
Regression analysis	Statistical technique applied to paired data to determine the degree or intensity of mutual association of a dependent variable with one or more independent variables.
Regular waves	Waves with a single height, period and direction.
Regulator	Structure to set (regulate) water levels and/or discharges in an irrigation network.
Relative density	Density of soil material with reference to its maximum possible density for a given compaction effort. Can be expressed as a percentage of the maximum possible density, or using descriptive terms such as ‘loose’, ‘medium’ or ‘dense’.
Response time	Time-lag, i.e. The time needed for a canal network to reach a new steady state after a change in water level or discharge.
Reynolds	Osborne Reynolds (1842–1912) – British physicist and mathematician who expressed the Reynolds number and stress (i.e. turbulent shear stress).
Reynolds number	Dimensionless number representing the ratio of the inertia force over the viscous force: $Re = \bar{v}D/\nu$
Roughness coefficient	Factor in formulae for computing the average flow velocity in open channels that represents the effect of roughness and other geometric characteristics of the channel upon the energy losses; e.g. the de Chézy, Manning or Strickler coefficients.
Roughness factor	See roughness coefficient.
Saltation	In sediment transport, particle motion by jumping and bouncing along the bed.
Sand	Sediment particles, mainly quartz, with a diameter of between 0.062 mm and 2 mm, generally classified as fine, medium, coarse or very coarse.
Sand trap	Enlargement in a channel where the velocity drops so that any sand that it carries can settle and be removed.
Scalar	A quantity that has a magnitude described by a real number and no direction. A scalar means a real number rather than a vector.

Scour	Removal of bed material by the eroding power of a flow of water; erosive action, particularly, pronounced local erosion by fast flowing water that excavates and carries away material from the bed and banks.
Sediment	Any material carried in suspension by the flow or as bed load that would settle to the bottom in the absence of fluid motion; particles transported by, suspended in or deposited by a flow.
Sediment concentration	The ratio of the mass (or volume) of the dry sediment in a water/sediment mixture to the total mass (or volume) of the suspension.
Sediment load	The amount of sediment carried/transported by running water.
Sediment transport	Movement of sediment transported in any way by a flow; from the point of transport it is the sum of suspended and bed load transported; from the point of origin it is the sum of bed material load and the wash load.
Sediment transport capacity	Ability of a stream to carry a certain volume of sediment per unit time for given flow conditions. Also called the sediment transport potential.
Sediment yield	Total sediment outflow including bed-load and suspension.
Sedimentation	Deposition of sediments in channels due to a decrease in velocity and corresponding reduction in the size and amount of sediment that can be carried.
Sedimentation basin	Basin placed at selected points along a canal to collect sand and silt.
Sequent depth	In open channel flow, the solution of the momentum equation at a transition between supercritical and subcritical flow gives two flow depths (upstream and downstream flow depths). They are called sequent depths.
Set point	The target value or desired output.
Settling basin	Small basin placed at selected points along an open channel to collect sand and silt.
Shear strength	Ability of a material to resist forces tending to cause movement along an interior smooth surface.
Side slope	Slope of the side of a channel with the horizontal; tangent of the angle with the horizontal; the ratio of the horizontal and vertical components of the slope.
Silt	Sediment particles with a grain size between 0.004 mm and 0.062 mm, i.e. coarser than clay particles but finer than sand.
Silt basin	Small basin placed at selected points along a channel to collect sand and silt.
Silt clearance	Removal of silt deposited in a channel section above the design bed levels; the general term also includes bank trimming in the case of constriction of width by silting.
Silting	Process of accretion or rising of the channel bed by depositing of sediment in the flow. Also called 'accretion of silt. Building of silt layers on channel sides is referred to as silting, but not as accretion.
Similitude	The correspondence between the behaviour of a model and that of its prototype, with or without geometric similarity. Scale effects usually limit the correspondence.
Simulation	Representation of a physical system by a computer or a model that imitates the behaviour of the system; a simplified version of a situation in the real world.
Slope	Inclination of the canal side from the horizontal; e.g. 1 vertical to 2 horizontal; inclination of the channel bottom from the horizontal.

Soil specific gravity	Ratio of the weight of water-free soil to its volume; bulk density; N/m^3 .
Soil structure	Clustering of soil particles into units called peds or aggregates; arrangement of soil particles into aggregates that occur in a variety of recognized shapes, sizes and strengths.
Soil texture	Characterization of soils in respect of particle size and distribution; the relative proportion of the three soil fractions (sand, silt, and clay).
Specific discharge	The flow rate per unit of cross-sectional area.
Specific energy	Quantity proportional to the energy per unit mass, measured with the channel bottom as datum and expressed in meter of water.
Specific volume	The volume of a unit mass of dry soil in an undisturbed condition, equalling the reciprocal of the dry bulk density of the soil.
Steady flow	Flow that occurs when conditions at any point of the fluid do not change with the time.
Steady state	Fluid motion in which the velocity at every point of the field is independent of time in either magnitude or direction; flow condition in which the input energy equals the output energy.
Stochastic	Having random variation in statistics.
Stream function	Vector function of space and time which is related to the velocity field. The stream function exists for steady and unsteady flow of incompressible fluid as it satisfies the continuity equation. Lagrange introduced the stream function.
Streamline	A line drawn so that the velocity vector is always tangential to it (no flow across a streamline); in steady flow the line coincides with the trajectory of the fluid particles.
Subcritical flow	The flow in an open channel is subcritical if the flow depth is larger than the critical depth. A flow for which the Froude number is less than unity; surface disturbances can travel upstream.
Super-critical flow	The flow in an open channel is super-critical if the flow depth is smaller than the critical depth. A flow for which the Froude number is larger than one; surface disturbances will not travel upstream.
Surge	A surge in an open channel is a sudden change of flow depth (i.e. Abrupt increase or decrease in depth). An abrupt increase in flow depth is called a positive surge while a sudden decrease in depth is termed a negative surge. A positive surge is also called (improperly) a 'moving hydraulic jump' or a 'hydraulic bore'.
Suspended concentration	The in time-average ratio of the mass (or volume) of the dry sediment in a water/sediment mixture to the total mass (or volume) of the mixture; also average of the mean (time average) suspended concentration over the entire area.
Suspended load	Transported sediment material maintained into suspension by turbulence of the flow for considerable periods and without contact with the bed; the velocity of the load is almost the same as that of the flow; it is part of the total sediment transport.
Suspension	A two-phase system, which may consists of solid particles suspended in water.
Tertiary off-take	A discharge regulator on the secondary or primary canal to supply a tertiary unit.
Textural class	The name of a soil group with a particular range of sand, silt and clay percentages of which the sum is 100% (e.g. sandy clay: 45–65% sand, 0–20% silt, 35–55% clay).

Threshold of motion	Value at which the forces imposed on a sediment particle overcome its inertia and it starts to move.
Time lag	Time needed for a canal network to reach a new steady state after a change in water level or discharge.
Top width	Width of the channel measured across it at the water surface.
Total load (origin)	Total load comprises the 'bed material load' (including suspended load) and the 'wash load'.
Total load (transport)	The total load consists of the 'bed load' and 'suspended load' (including wash load).
Tractive force	The force exerted by flowing water on the bed and banks of a channel and tangential to the flow direction.
Tractive stress	The force per unit of wetted area that acts on the bed and bank material, trying to dislodge the material against cohesion, internal repose and gravity.
Turbulence	Flow motion characterized by its unpredictable behaviour, strong mixing properties and a broad spectrum of length scales.
Turbulent flow	Fluid particles move in very irregular paths, causing exchange of momentum from one part of the flow to another. The flow has great mixing potential and a wide range of eddy length scales. The flow is agitated by cross-currents and eddies; any particle may move in any direction with respect to any other particle and the energy loss is almost proportional to the square of the velocity.
Two-dimensional flow	All particles are assumed to flow in parallel planes along identical paths in each of these planes. There are no changes in flow normal to the planes. An example is the flow in a wide, rectangular channel.
Uniform equilibrium flow	Flow for which the velocity is the same at every point, in magnitude and direction, at any given instant; steady uniform and unsteady uniform flow.
Uniform flow	Flow with no change in depth or any other flow characteristic (wetted area, velocity or hydraulic gradient) along a canal.
Unsteady flow	Flow in which the velocity changes, with time, in magnitude or direction.
Validation	The comparison between model results and prototype data, to validate a physical or numerical model. Validation is carried out with prototype data that are different from those used for calibration and verification of the model.
Velocity	The rate of movement at a certain point in a specified direction.
Velocity head	The energy per unit weight of water in view of its flow velocity; square of the mean velocity divided by twice the acceleration due to gravity.
Velocity, mean-	The discharge at a given cross-section divided by the wetted area at that section.
Velocity, surface-	Velocity at the water surface at a given point of a channel.
Viscosity	Property that characterizes the resistance of a fluid to shear: i.e. resistance to a change in shape or movement of the surroundings.
Void ratio	Ratio of the volume of pores to the volume of solids in a soil.
Voids	Pores or small cavities between the particles in a rock or soil mass, may be occupied by air, water or both; the spaces between stones or gravel in river structures.
Volume control	Flow control method with the set point in the middle of the downstream or upstream canal section.

Wash load	Portion of the suspended load with particle sizes smaller than those found in the bed; in near-permanent suspension and transported without deposition; the amount of wash load transported through a section is independent of the transport capacity of the flow.
Washout or washing-out	Erosion of earth from canal banks or below structures, caused by excessive flow velocity and turbulence, accumulation of debris, burrowing animals, or bad drainage, leading to a complete breakdown of banks, structures, or lining.
Water-level	Elevation of the free water surface relative to a datum; also called stage or gauge height.
Water-level regulator	Structure to regulate the water level.
Water-surface slope	Difference in elevation of the water surface per unit horizontal distance in the flow direction.
Wave amplitudes	The magnitude of the greatest departure from equilibrium of the wave disturbance
Wave celerity	The speed of wave propagation.
Wave frequency	The inverse of wave period.
Wave height	The vertical distance between the trough and the following crest.
Wave period	Time taken for two successive wave crests to pass the same point.
Wavelength	The straight-line distance between two successive wave crests.
Weber	Moritz Weber (1871–1951) – German Professor.
Weber number	Dimension less number characterizing the ratio of inertial forces over surface tension forces. It is relevant in problems with gas-liquid or liquid-liquid interfaces.
Wetted perimeter	The length of wetted contact between water and the solid boundaries of a cross-section of an open channel; usually measured in a plane normal to the flow direction.
Wetted surface	The surface area in contact with the flowing water in an open channel.
Width	Dimension of a channel measured normal to the flow direction.

Index

- accuracy 80, 118
- Ackers–White sediment transport
 - predictor 108, 146
- actual bottom slope 28
- actual sediment concentration 125, 131
- actual sediment load 147
- actual sediment transport 118
- adaptation length 115
- adaptation time 115
- Airy's theory 33
- allowable shear stress 65
- alluvial friction predictor 68
- alternate water depths 20
- angle of repose 66
- area or wetted area 14
- average energy dissipation 69
- average velocity 15, 20

- backwater curve 28, 136, 150
- backwater profile 121
- Bakhmeteff B. A. 19
- bed features 78
- bed forms 77
 - dunes 78
 - flat bed 78
 - particle parameter 81
 - ripples 78
- bed load 99, 103
- bed load transport 70
- bed material 65
- bed roughness 82
- Bernoulli D. 18
- bottom level
 - relative change in 143
 - variation in 131, 144
- bottom slope 27, 61
- boundary conditions 116, 124

- Boussinesq coefficient 17
- Brownlie sediment transport predictor 104, 108

- canal
 - canal capacity 33, 59
 - canal dimensions 130
 - canals in regime 62
 - canal network 33
 - canal operation 60
 - canal with a rigid boundary 61
 - canal with an erodible boundary 61
- celerity of a disturbance 76
- celerity of a wave 33
- change of momentum 16, 24
- channel slope 33, 36
- characteristic lines 43
- coefficient of Boussinesq 17, 24
- coefficient of Coriolis 23
- command 59, 187
- command level 143
- composite roughness 77, 86, 87, 125
 - movable bed 87
 - in rectangular canal 95
 - rigid boundaries 86
- concentration 57
 - actual concentration 124, 136, 148, 149, 150, 151, 152
 - equilibrium concentration 125, 136, 141, 147, 150, 152
 - initial concentration 125
 - of sediment by mass 58
- conservation of mass 15, 34
- conservation of momentum 15
- continuity equation 15, 37, 38, 73, 123
 - for sediment transport 73, 124
- continuity principle 15

- continuous flow 147
- controlled deposition 139
- control sections 130, 131
- control structure 143
- control volume 17
- conveyance concept 33
- conveyance of non-suspended sediments 71
- conveyance of sediment in suspension 71
- Coriolis coefficient 18
- correction factor 108
- coupled solution 74
- Courant number 118
- critical boundary shear stress 66
- critical depth 20
- critical flow 19
- critical mobility parameter 121
- critical shear stress 66
- critical slope 28
- cross section 61
- cumulative size distribution 52
- cumulative size-frequency curve 52

- Darcy-Weisbach friction factor 82, 177
- de Chézy coefficient 26, 77
- de Chézy equation 23, 25
- deepening 139, 141
- density 49
- dependent variables 34, 43
- depth-averaged concentration 113
- depth-averaged equilibrium concentration 125
- depth integrated models 112, 113
 - Galappatti's model, 124, 134
- de St. Venant equations 35, 38
- diameter
 - mean diameter 52
 - median diameter 52
 - nominal diameter 51
- dimensionless numbers 12
 - Froude number 13
 - Reynolds number 13
- dimensionless parameters 49
- discharge 15
- downstream boundary 117
- downstream control 59
- drawdown curve 28, 150
- drawdown profile 121
- dry bulk density 50
- dunes 78
- dynamic equation 35, 38, 73, 124
- dynamic viscosity 13

- earthen canal 63
- effective de Chézy coefficient 91
- effective hydraulic roughness 91
- effective roughness 122
- energy equation 17
- energy head 18
- energy losses 17
- energy principle 17
- Engelund-Hansen sediment transport predictor 104, 108
- entrainment 121
- equilibrium sediment concentration 125, 131, 147
- equilibrium sediment transport 118
- equilibrium transport rate 112
- erodible boundary 61
- erosion 59
- excess bed shear stress 57

- fall velocity 49, 53
- finite difference method
 - coupled solution 74
 - uncoupled solution 74
- flat bed 78
- flow control 59
 - downstream control 59
 - upstream control 60
- flow profile 116
- form resistance 83
- freeboard 67
- friction factor 77, 82, 121, 129
- friction factor predictor 73, 122
- friction slope 35
- Froude number 13

- Galappatti's depth-integrated model 112, 113, 124, 134
- geometric mean diameter 52
- gradually varied flow 27, 32, 135
- gradually varied flow equation 116
- gradually varied unsteady flow 36
 - continuity equation 37
 - dynamic equation 35

- grain related shear stress 83
 gravity wave 32
- hydraulically optimal cross-section 67
 hydraulically rough boundary 22
 hydraulically smooth boundary 22
 hydraulic aspects 126
 hydraulic depth 14
 hydraulic design 33
 hydraulic radius 14
 hydraulic resistance 77, 82
 hydraulic structure 34
- imposed boundary condition 105
 independent variables 34
 inflow 130
 inflow storage capacity 33
 initial bottom level 131
 initial concentration 125
 initiation of motion 99, 100
 initiation of suspension 101
 in regime canals 62
 irrigation aspects 129
 irrigation canals 33, 34, 59
 irrigation flows 131
 irrigation requirements 59, 60
 irrigation season 59, 130
 irrigation supply 135
- kinematic viscosity 13
 kinetic energy 18, 23
- Lacey
 Lacey equations 63
 Lacey regime theory 62
 Lacey silt factor 63
 Lagrange equation 33
 Lagrange wave speed 40
 laminar flow 13
 laminar sub-layer 26
 law of continuity 36
 length scale 113
 lined canal 71
 lower flow regime 81
- maintenance, type of 130
 Manning equation 26
- Manning's roughness coefficient 64, 89
 mass balance, for the total sediment transport 116
 mass sediment balance 134
 maximum boundary shear stress 65
 maximum flow velocity 67
 maximum permissible velocity 65, 68
 maximum velocity 61
 of the sediment particles 131
 mean sediment concentration 131
 method of characteristics 43, 47
 minimum permissible velocity 68
 mobility parameter 121
 modified Lax method 117, 118, 119
 morphological changes 75
 of the bottom 116
 movable bed 87
- negative characteristic 42
 negative waves 33, 47
 net deposition 134
 net entrainment 134
 net flux of sediment 116
 Nikuradse J. 22, 26
 no motion of particles 83
 non-equilibrium, suspended sediment transport 112
 non-wide channels 105
 non-wide irrigation canal 23, 85, 92, 93
- one-dimensional flow 10, 16, 74
 one-dimensional sediment equations 124
 open channel flow 10, 24, 34
 operation scenarios 71
 optimal canal design 71
 optimal cross-section 67
 oscillatory waves 32
 outflow 130
 outflow storage capacity 33
- particle mobility parameter 56
 particle parameter 56, 81, 101
 particle Reynolds number 57, 100
 particle size 49, 52
 permissible velocity method 62, 68

- piezometric head 19
- porosity 49
- positive characteristic 42
- positive waves 33, 47
- potential energy 23
- ppm 58, 129, 134, 176
- predictability 79
- pressure energy 23
- principle of Bernoulli 18
- prismatic cross section 16
- prism storage 37

- qualitatively assessment, of sediment deposition 154
- quasi-steady flow 76, 123

- rapidly varied flow 11, 12
- rapidly varied unsteady flow 11, 32
- rational method 62, 68
- real fluid 18
- rectangular canal 95, 122
- regime method 62
- relative change in bottom level 143
- relative density 50
- relative deposition 137, 138, 141
- relative discharge 135
- relative median sediment size 138
- relative sediment deposition 151
- relative sediment load 138
- relative sediment size 138
- relative transport capacity 69
- required supply level 33
- required water level 60
- response time 75
- Reynolds number 13
- rigid boundaries 61, 86
- ripples 78
- roughness 77
 - type of 125
- roughness coefficient 83
- roundness 53

- section depth 14
- sediment aspects 129
- sedimentation 54, 59
- sediment concentration 129
- sediment data 131
- sediment mass balance 118

- sediment predictors 143
- sediments 49
 - cohesive 49
 - non-cohesive 49
- sediment size 129
- sediment transport 33, 83
 - equilibrium conditions 98
 - non-equilibrium conditions 71, 99, 112, 115
- sediment transport capacity 99, 103, 136
- sediment transport equation 70, 73
 - initiation of motion 100
 - initiation of suspension 101
- sediment transport load 70
- sediment transport per unit width 106, 125
- sediment transport predictors 68, 99, 103, 108, 122, 125
 - of Ackers-White 108
 - of Brownlie 108
 - of Engelund-Hansen 108
 - of van Rijn 52, 103, 104
 - of Yang 103
- sediment transport rates 121
- sediment transport theories 33, 56
 - bed load 99
 - suspended load 99
- sediment trap 99
- set point 135
- SETRIC 123
- shape 49
- shape factor 53
- shear stress 13, 25, 56
- shear velocity 21, 25, 70
- Shields' diagram 100
- short wave 33
- side slope 11, 67, 68, 92, 191, 205
- sieve diameter 51
- silt factor 63
- simple wave 46, 47
- simulation period 130, 137
- single roughness 125
- size distribution 49, 50
- size frequency 51
- skin resistance 83
- skin roughness 86
- slope of the energy line 27, 36, 124
- slope stability 67

- smoothness factor 69
 solitary wave 33
 spatially varied flow 12
 specific density 50
 specific energy 15, 19
 specific weight 50
 sphericity 53
 stability 118
 stable canal design 68
 stable irrigation canals 62
 steady flow 10, 16, 17, 33
 steady uniform flow 11, 36
 Stokes law 54
 storage capacity 33
 storage concept 33
 stream power 68
 stream tubes 86
 Strickler equation 26
 structure, type of 130
 subcritical flow 20, 44
 sub-sections 88
 supercritical flow 20, 44
 surface or top width 14
 suspended load 99, 103
 in equilibrium condition 114
 suspended sediment transport
 predictor 103
 suspension 54
- three-dimensional flow 10
 threshold condition 65
 time scale 33, 113
 top width 67
 total energy 15
 total friction factor 84
 total resistance 83
 total sediment concentration 116
 total sediment transport 103, 106,
 107, 125
 in non-wide canals 110
 total sediment transport capacity 103
 total shear stress 83, 84
 tractive force 25, 65
 tractive force method 62, 64
 translatory wave 32
 transport of sediment, *see* sediment
 transport
 transport rate parameter 57
- trapezoidal cross section 105
 turbulent flow 14, 25
 two-dimensional flow 10, 16
- uncontrolled sediment deposition 138
 uncoupled solution 74
 uniform flow 11, 16, 24, 28
 unsteady flow 11, 27, 32, 33, 35
 conveyance concept 33
 oscillatory waves 32
 storage concept 33
 translatory waves 32
 unsteady varied flow 11
 upstream boundary 117, 130
 upstream control 60
- van Rijn method 122
 varied flow 11
 varying water depth 105
 vegetation on the sidewall 87
 velocity distribution 110
 velocity gradient 12
 velocity head 15, 23
 velocity profile 21, 22
 viscous sub-layer 22
 volumetric concentration 57
- wall roughness 26
 water delivery method 59, 75
 water depth 14
 actual water depth 28
 critical water depth 28
 normal water depth 28
 water level 34
 rate of rise 37
 water supply 59, 74, 130
 wave height 78
 wave length 33, 78
 wedge storage 37
 weed growth 130
 weighted roughness 77
 wetted area 14, 189
 wetted perimeter 14
 White and Colebrook expression, for
 de Chézy coefficient 26
 widening 139, 141
 wide rectangular canal 45